



Universidad de Granada
Departamento de Ecología

Exopolymer particles in the ocean:

*Production by microorganisms, carbon export and
mesopelagic respiration*

Tesis Doctoral

Ignacio Pérez Mazuecos

Granada, a 3 de Noviembre 2015

Editor: Universidad de Granada. Tesis Doctorales
Autor: Ignacio Pérez Mazuecos
ISBN: 978-84-9125-422-5
URI: <http://hdl.handle.net/10481/41752>



Universidad de Granada



Programa oficial de *Doctorado en Biología Fundamental y de Sistemas*

Título de la Tesis:

Exopolymer particles in the ocean: production by microorganisms, carbon export and mesopelagic respiration

(Partículas exopoliméricas en el océano: producción por microorganismos, exportación de carbono y respiración mesopelágica)

Tesis doctoral presentada por el Licenciado Ignacio Pérez Mazuecos para obtener el grado de Doctor por la Universidad de Granada.

Fdo.: Ignacio Pérez Mazuecos

Dirigida por:

Dra. Dña. **Isabel Reche Cañabate**, Departamento de Ecología e Instituto del Agua, *Universidad de Granada*, Granada

Dr. D. **Javier Aristegui Ruiz**, Departamento de Biología e Instituto de Oceanografía y Cambio Global (IOCAG), *Universidad de Las Palmas de Gran Canaria*, Las Palmas de Gran Canaria

Dr. D. **Josep Maria Gasol Piqué**, Departamento de Biología y Oceanografía, Institut de Ciències del Mar, *Consejo Superior de Investigaciones Científicas (CSIC)*, Barcelona

Granada, a 3 de Noviembre 2015

Dra. Isabel Reche Cañabate

Profesora titular del departamento de Ecología de la Universidad de Granada

Dr. Javier Arístegui Ruiz

Catedrático del departamento de Biología de la Universidad de las Palmas de Gran Canaria

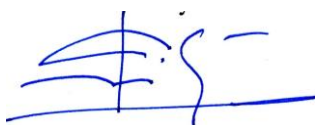
Dr. Josep Maria Gasol Piqué

Profesor de Investigación del departamento de Biología Marina y Oceanografía del Instituto de Ciencias del Mar (ICM, CSIC)

Certifican:

Que los trabajos de investigación desarrollados en la memoria de la tesis doctoral titulada "*Exopolymer particles in the ocean: production by microorganisms, carbon export and mesopelagic respiration*" son aptos para ser presentados por el Licenciado Ignacio Pérez Mazuecos ante el tribunal designado para optar al grado de Doctor por la Universidad de Granada.

Para que así conste, en cumplimiento de las disposiciones vigentes, se extiende el presente certificado a 3 de Noviembre de 2015.



Fdo.: Isabel Reche Cañabate

Fdo.: Javier Arístegui Ruiz

Fdo.: Josep M. Gasol Piqué

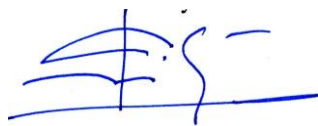
El doctorando Ignacio Pérez Mazuecos y los directores de la tesis Isabel Reche Cañabate, Javier Arístegui Ruíz y Josep M. Gasol Piqué garantizamos, al firmar esta tesis doctoral, que el trabajo ha sido realizado por el doctorando bajo la dirección de los directores de la tesis y hasta donde nuestro conocimiento alcanza, en la realización del trabajo, se han respetado los derechos de otros autores a ser citados cuando se han utilizado sus resultados o publicaciones.

A Granada, a 3 de Noviembre de 2015

Director/es de la Tesis



Fdo.: Isabel Reche Cañabate

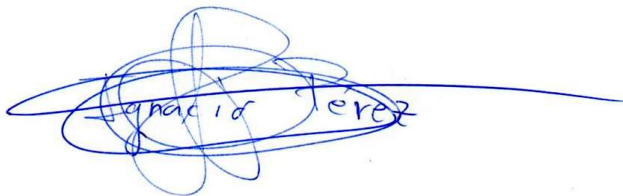


Fdo.: Javier Arístegui Ruíz



Fdo.: Josep M. Gasol Piqué

Doctorando



Fdo.: Ignacio Pérez Mazuecos

Durante el desarrollo de esta tesis doctoral (2010-2014), Ignacio Pérez Mazuecos disfrutó de una beca de formación JAE BBVA-CSIC otorgada por el Ministerio de Ciencia e Innovación.

Fundación **BBVA**



El trabajo de investigación que engloba esta tesis doctoral ha sido desarrollada en el marco de dos proyectos: La Expedición Malaspina 2010 financiada por el Ministerio de Ciencia e Innovación a través del programa Consolider-Ingenio 2010 (proyecto CSD2008-00077) y el proyecto Hotmix financiado por el Plan Nacional 2008-2012 (proyecto CTM2011-30010-C02/MAR).



HotMix-2014

A mi familia,

Acknowledgements/Agradecimientos

...y al final llegué a la meta. ¡Menuda carrera de obstáculos!

Esta es la única parte de la tesis en la que puedo escribir libremente lo que me apetezca... ¡No me lo creo!

Durante todo este tiempo muchísima gente me ha ayudado de forma desinteresada, a quienes deberé agradecer infinitamente.

Desde mi familia, mis padres y hermanos, agradezco su máximo apoyo y paciencia para que todo llegase a buen puerto. A Diana gracias por tu espera.

Mis compañeros del instituto del agua, con los que he compartido muchas horas de trabajo en el laboratorio. A Tere, Gema, Mohammad, Gaetano, Eli y muchos/as más que han arrimado el hombro para que mis análisis en el laboratorio saliesen genial. Sin ellos esta tesis no habría sido posible, así que mi más sincero agradecimiento. Espero que sus tesis finalicen exitosamente y en un futuro próximo nos encontremos trabajando juntos de nuevo. A Eva por zambullirme en el mundo de los TEPs, gracias por tu dedicación.

Durante las campañas oceanográficas en las que participé (Malaspina y Hotmix), mejor dicho eternas campañas oceanográficas y con jornadas de trabajo interminables, también en aquellas visitas al Instituto de Ciencias del Mar de Barcelona y la Facultad de Ciencias del Mar de Las Palmas de Gran Canaria, multitud de compañeros (seniors, predoctorales, postdoctorales, técnicos, etc) me echaron una mano para que las muestras que han permitido escribir esta tesis dieran óptimos resultados, a todos ellos gracias, gracias y millones de veces gracias.

A mis directores de tesis, Isabel, Javier y Pep os expreso mi más sincero agradecimiento. Me habeis permitido zambullirme en la oceanografía y he aprendido mucho de la gradísima experiencia de cada uno de vosotros. Isabel, que desde mi último año de carrera me has soportado, disculpas por ser tan cabezota y creer en mí aún cuando ni yo mismo creía en mí. Javier y Pep gracias por haber estado en los momentos que he necesitado de vuestra experiencia.

Thanks to my colleagues of the Mina and Everard Goodman Faculty of Life Sciences (Bar Ilan University, Israel), and especially to Ilana and Dina for a productive and nice stay with them.

Y, por último, a todos/as que me habeis hecho reír y disfrutar durante todo este tiempo. Porque solo con buen ánimo se llega a hacer un buen trabajo, gracias por ayudarme a realizar esta tesis sin hablarme de ciencia.

"I do not know what I may appear to the world, but to myself I seem to have been only like a boy playing on the sea-shore, and diverting myself in now and then finding a smoother pebble or a prettier shell than ordinary, whilst the great ocean of truth lay all undiscovered before me."

(Sir Isaac Newton)



Index/ Índice

<i>Summary/ Resumen (in Spanish)</i>	17
<i>Chapter 1: Introduction and basic methodology</i>	21
1.1. <i>Introduction</i>	23
1.2. <i>General objectives</i>	31
1.3. <i>Methodology</i>	32
1.4. <i>References</i>	38
<i>Chapter 2: Exopolymer particles distribution and contribution to the biological carbon pump in the global ocean</i>	43
2.1. <i>Abstract</i>	45
2.2. <i>Introduction</i>	47
2.3. <i>Material and methods</i>	49
2.4. <i>Results</i>	60
2.5. <i>Discussion</i>	77
2.6. <i>References</i>	87
<i>Chapter 3: Exopolymer particles production by heterotrophic prokaryotes at the carbon export and sequestration layers</i>	93
3.1. <i>Abstract</i>	95
3.2. <i>Introduction</i>	97
3.3. <i>Material and methods</i>	99
3.4. <i>Results</i>	105
3.5. <i>Discussion</i>	120
3.6. <i>References</i>	127
<i>Chapter 4: Temperature control of microbial respiration and growth efficiency in the mesopelagic zone of the South Atlantic and Indian Oceans</i>	133
4.1. <i>Abstract</i>	135
4.2. <i>Introduction</i>	137
4.3. <i>Material and methods</i>	139
4.4. <i>Results</i>	146
4.5. <i>Discussion</i>	155
4.6. <i>References</i>	161
<i>Chapter 5: Distribution and contribution of exopolymer particles to carbon exports in the Mediterranean Sea</i>	165
5.1. <i>Abstract</i>	167
5.2. <i>Introduction</i>	169

5.3. <i>Material and methods</i>	171
5.4. <i>Results</i>	178
5.5. <i>Discussion</i>	195
5.6. <i>References</i>	204
Chapter 6: High heterotrophic production of exopolymer particles in the Levantine Intermediate Waters of the Mediterranean Sea	209
6.1. <i>Abstract</i>	211
6.2. <i>Introduction</i>	213
6.3. <i>Material and methods</i>	215
6.4. <i>Results</i>	220
6.5. <i>Discussion</i>	232
6.6. <i>References</i>	237
Conclusions/Conclusiones (in Spanish)	241
ANNEXES/ANEXOS	247
ANNEX I/ANEXO I: <i>Abbreviation Index/Índice de Abreviaturas</i>	249
ANNEX II/ANEXO II: <i>Figure Index/Índice de Figuras</i>	253
ANNEX III/ANEXO III: <i>Table Index/Índice de Tablas</i>	257
ANNEX IV/ANEXO IV: LIBRO BLANCO DE MÉTODOS Y TÉCNICAS DE TRABAJO OCEANOGRÁFICO	259
ANNEX V/ANEXO V: <i>artículo en Deep-Sea Research I</i>	277

Summary/ Resumen (in Spanish)

Las partículas exopoliméricas son sustancias de naturaleza polisacáridica producidas principalmente por fitoplancton y procariotas heterotróficos. Éstas pueden autoensamblarse en partículas de mayor tamaño y, cuando su flotabilidad es negativa, son exportadas hacia el océano profundo contribuyendo con ello a la bomba biológica de carbono. En esta tesis hemos descrito la distribución de partículas exopoliméricas en los océanos Atlántico, Índico y Pacífico y en el mar Mediterráneo, y hemos valorado su papel en la exportación de carbono hacia el océano profundo. Por otro lado, hemos determinado la producción de partículas exopoliméricas por procariotas heterotróficos tanto en aguas superficiales como en aguas profundas así como la respiración de la materia orgánica en la zona mesopelágica (200-1000 m de profundidad). Esta región es clave en la mineralización del carbono orgánico que transita desde la superficie hacia las profundidades del océano.

Se han realizado dos campañas oceanográficas: una primera circumnavegación a lo largo de los océanos Atlántico, Índico y Pacífico ("*Expedición Malaspina-2010*") y otra a lo largo del mar Mediterráneo ("*Hotmix-2014*"). En la primera campaña oceanográfica observamos que las concentraciones máximas de partículas exopoliméricas aparecían recurrentemente por encima de la profundidad del máximo de clorofila y que geográficamente aparecían en las zonas próximas a los afloramientos (por ejemplo Benguela, Domo de Costa Rica, Gran Bahía Australiana y en las zonas de divergencia ecuatorial). Consecuentemente, el mejor predictor de la distribución de partículas exopoliméricas fue la producción primaria. Nuestro estudio también indica que el flujo descendente de partículas exopoliméricas es la vía principal de entrada de éstas hacia el océano profundo. Sin embargo, también debe existir síntesis *de novo* por procariotas heterotróficos en el océano profundo que justifique los elevados valores de transferencia de exopolímeros estimados entre la zona mesopelágica y batipelágica (>1000 m de profundidad). Por tanto, los procariotas heterotróficos no sólo participan activamente mineralizando la materia orgánica durante su tránsito por la zona mesopelágica

hacia el fondo sino que también pueden generar sustratos polisacáridicos y partículas exopoliméricas en aguas profundas. Esto explicaría los tiempos de residencia cortos (de meses a años) encontrados y que sugieren una naturaleza semilábil. La estimas del contenido de carbono en forma de partículas exopoliméricas en el océano global es de 4.8 Pg C, es decir, entre un 25% y un 40% del carbono orgánico particulado. El flujo global de partículas exopoliméricas a profundidades superiores a los 1000 m se estimó en 0.4 Pg C año⁻¹, comparable a las estimas medias globales de flujo de carbono orgánico particulado hacia la zona batipelágica.

En la segunda campaña oceanográfica nuevamente encontramos que las concentraciones máximas de partículas exopoliméricas aparecían por encima del máximo de clorofila en la cuenca oeste del Mar Mediterráneo y en la región Noreste del océano Atlántico, particularmente cerca del estrecho de Gibraltar. La distribución geográfica de partículas exopoliméricas pudo explicarse mayoritariamente por la actividad del fitoplancton, aunque los procariontes heterotróficos también resultaron ser relevantes en determinar su distribución, no sólo en superficie sino también en las zonas profundas, particularmente en el agua Levantina Intermedia. Por lo tanto, la distribución de partículas exopoliméricas en el Mediterráneo profundo está controlada, en parte, por el flujo descendente de partículas, siendo mayor en la cuenca oeste y en la región Noreste del océano Atlántico.

Esta tesis contribuye a arrojar luz sobre el papel crucial de las partículas exopoliméricas en la bomba biológica del océano y sobre el papel desempeñado por los procariontes heterotróficos en su dinámica.

"The ocean remains one of the least explored and understood environments on the planet – a frontier for discoveries that could provide important benefits Ocean science and technology will play an increasingly central role in the multidisciplinary study and management of the whole-Earth system."

U.S. Commission on Ocean Policy,
An Ocean Blueprint for the 21st Century (2004)

Chapter 1:
Introduction and basic methodology



“Basic to the understanding of any ecosystem is knowledge of its food web, through which energy and materials flow. If microorganisms are major consumers in the sea, we need to know what kinds are the metabolically important ones and how they fit into the food web.”

Lawrence Pomeroy

1.1. Introduction

1.1.1. *Role of the prokaryotes in the oceanic carbon cycle: respiration, exudation and growth*

Marine ecosystems are globally estimated to harbor more than 10^{29} prokaryotes (Whitman et al., 1998), which exceeds the total biomass of the higher trophic groups (Pomeroy, 2007). The dominance of prokaryotes is even greater in terms of metabolism (Pomeroy, 2001), so these microscopic organisms are regarded as the core drivers of the recycling of biologically relevant chemical elements and energy fluxes in the oceanic waters.

Prokaryotes act as a trophic link through the microbial loop responsible for transforming dissolved organic matter (DOM) into particulate organic matter (POM), supplying organic matter to higher trophic levels of the food web (Pomeroy, 1974; Azam et al., 1983). From the food web point-of-view, the organic carbon proportion used for new biomass production in relation to the total carbon assimilated by prokaryotes determines the microbial loop's efficiency, which is commonly indicated as prokaryotic growth efficiency (PGE) (del Giorgio and Cole, 1998). The knowledge of this index is imperative for constraining carbon fluxes in marine ecosystems since PGE provides an estimate of the organic carbon percentage susceptible to be transferred to higher trophic levels (Sherr and Sherr, 1991). However, a variable proportion of organic carbon assimilated by prokaryotes is not incorporated into biomass (Figure 1.1.). These organic carbon either is respired to CO_2 (del Giorgio et al., 1997) or released to the environment as a huge variety of organic compounds: dissolved rich-polysaccharide exudates, which end up generating exopolymer particles (EP) (Stoderegger and Herndl, 1999; Passow 2002; Ortega-Retuerta et al., 2010), extracellular enzymes (Arnosti, 2003), refractory organic material persistent to further microbial mineralization (Jiao et al., 2010; Jorgensen et al., 2014), etc. Therefore, to a better understand and to constrain carbon fluxes is imperative to progress in the knowledge of these processes.

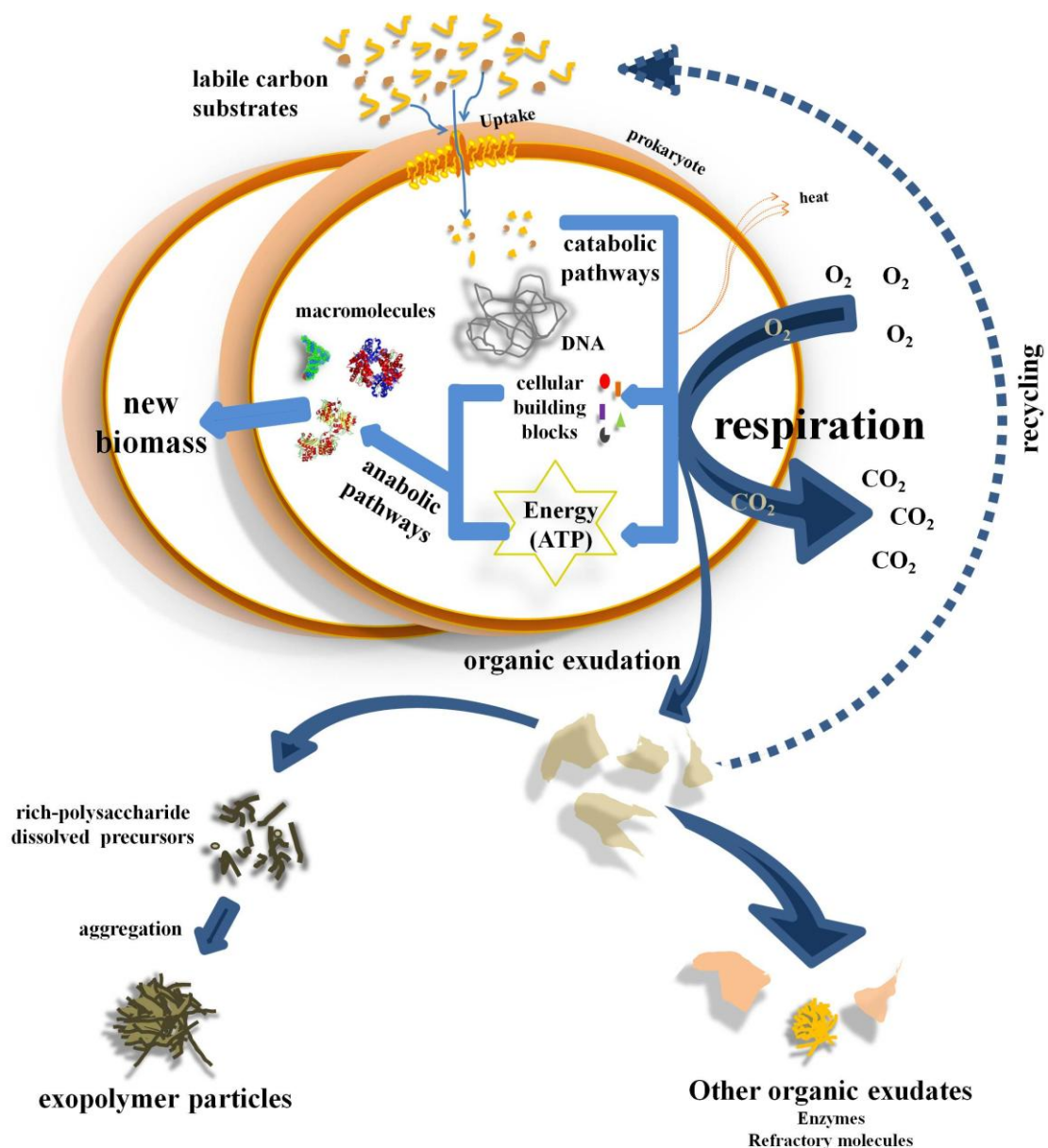


Figure 1. 1. Simplified depiction of the organic carbon fate through three major prokaryotic metabolic pathways: respiration, organic exudation and new biomass production.

In the global ocean, around 80% of the net primary production in the ocean surface (ca. 50 Pg C yr⁻¹; but see Arístegui et al., 2005a) occurs in the open waters (Hedges, 1992; Field et al., 1998). Half or more of the carbon fixed by the algal community is processed by heterotrophic microbes directly in the epipelagic ocean (Azam, 1998; Ducklow, 2000; Robinson, 2008), and only a low percentage of ~ 10% of the organic carbon produced in the ocean surface is

Introduction and basic methodology

exported to the mesopelagic zone and, even lower amount of carbon is sequestered in waters of more than 1000 m depth (Robinson et al., 2010).

This vertical export of organic matter from surface to deep waters is the main substrate for deep-ocean prokaryotic metabolism respiration (R) and production (PHP) (Arístegui et al., 2009). Both R and PHP, thereby, decrease gradually with depth, although more subtly for R (Arístegui et al., 2009). The annual global R estimates in surface waters (< 200 m), about 37 Pg C, are higher than the annual R rates in the whole dark ocean, ~24 Pg C yr⁻¹ in the mesopelagic and ~1.5 Pg C yr⁻¹ in the bathypelagic waters (Figure 1.2.; del Giorgio and Duarte, 2002). Similarly, about 50% of the total water column PHP takes place in the epipelagic waters, ~ 30 % at mesopelagic depths and ~20 % in the deep ocean (Figure 1.2.; Arístegui et al., 2009). The average growth rates of the prokaryotes are higher in the epipelagic waters (0.157 d⁻¹), intermediate at mesopelagic depths (0.090 d⁻¹) and lower in the deep ocean (0.061 d⁻¹). In addition, there is a reduction of the carbon use efficiencies from ~ 15 % in the epipelagic zone to approximately ~ 4 % in the dark ocean (Figure 1.2.; Arístegui et al., 2009).

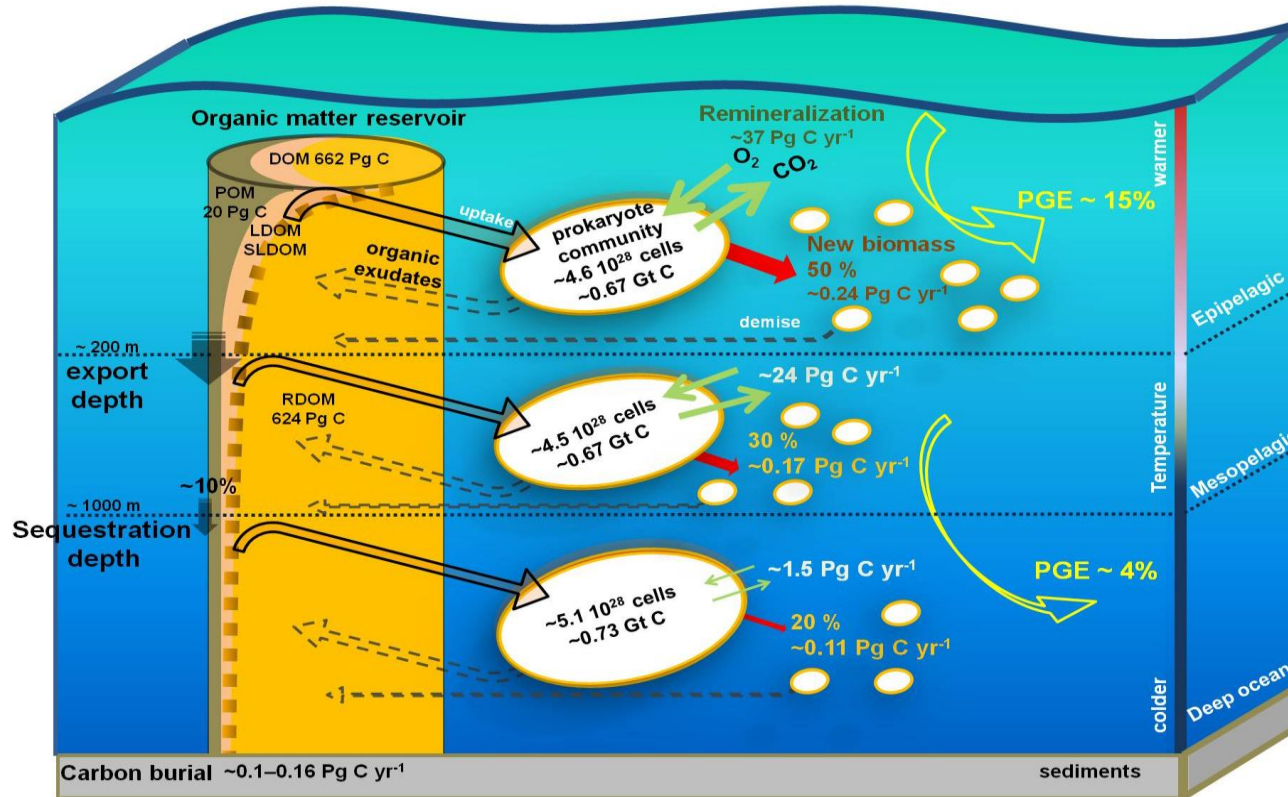


Figure 1. 2. Illustration indicating the global estimates for organic matter reservoirs [POM (particulate organic matter) and DOM (dissolved organic matter) = LDOM (labile DOM) + SLDOM (semilabile DOM) + RDOM (refractory DOM)] and prokaryotic mineralization, new biomass generation and growth efficiencies (PGE) in the epipelagic (from surface to 200 m depth), mesopelagic (200 – 1000 m depth) and deep ocean (> 1000 m). The global data of the organic matter reservoirs are from Hansell et al. (2009) and Jiao et al. (2010), and the global data of the prokaryotic metabolic rates and biomass from del Giorgio and Duarte (2002) and Aristegui et al. (2005a and 2009).

1.1.2. *Respiration in the mesopelagic zone*

It is widely accepted that POM flux attenuation from the photic zone to the deep ocean is mostly driven by remineralization of the mesopelagic heterotrophic prokaryotes (del Giorgio and Duarte, 2002; Arístegui et al., 2005a). Due to the methodological difficulties for estimating the R rates by using direct O₂ consumption measurements with the Winkler technique, most direct R estimates are restricted to the photic zone (Robinson, 2008) and there are still very few direct R estimates in the mesopelagic waters. These few data correspond to the North Atlantic Ocean and the Mediterranean Sea (Biddanda and Benner, 1997; Arístegui et al., 2005b; Reinthaler et al., 2006; Baltar et al., 2010; Weinbauer et al., 2013). Many more direct R estimates, and consequently data of growth efficiencies (PGE), must be obtained to test the idea that the mesopelagic is a key layer in the transit of POM from the photic zone to the deep ocean.

Additionally, there is little knowledge about the environmental factors that control prokaryotic carbon metabolism in mesopelagic depths. Indeed, temperature must be an important factor affecting prokaryotic metabolism in the dark ocean (Pomeroy and Wiebe, 2001), although there is little information published on this respect. Mesopelagic prokaryotic assemblages are exposed to a broad range of temperatures throughout the mesopelagic zone along distant oceanic regions. Thus, POM flux attenuation from surface to the deep ocean, due to remineralization by mesopelagic prokaryotes, would presumably vary according to temperature changes across the mesopelagic zone of the world's ocean (Buesseler et al., 2007; Marsay et al., 2015).

In this dissertation, new direct estimates of R rates and PGE were determined in the mesopelagic waters of unexplored regions of the global ocean. The R and PGE dependence on mesopelagic temperature was also assessed.

1.1.3. Exopolymer particles and carbon export

The non-living organic matter in the ocean is a heterogeneous collection of compounds with diverse origins: algal extracellular exudates, viral lysis, cellular senescence, predation and abiotic or biotic transformations (Volkman and Tanoue, 2002). These organic compounds cover a wide size spectrum from colloidal (nanometers) to macroscopic particles (millimeters) (Verdugo et al., 2004) (Figure 1.3.).

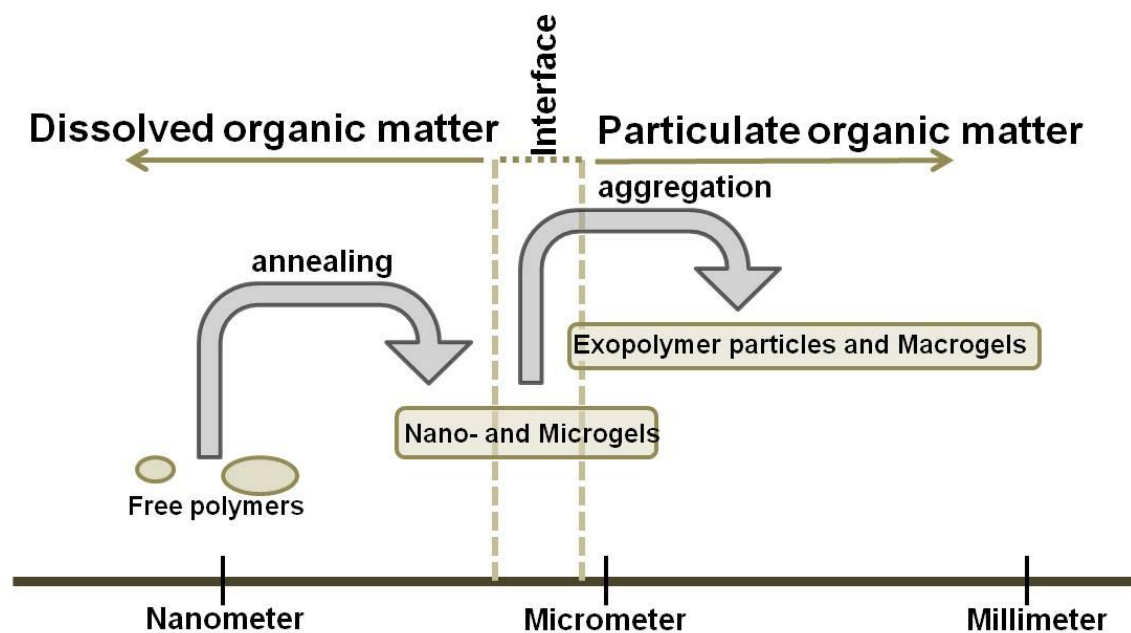


Figure 1. 3. Size continuum of marine organic matter from dissolved (DOM) to particulate (POM) organic matter, adapted from Verdugo et al. (2004).

The distinction between DOM and POM is only operational. The organic matter passing through filters with effective pore sizes between 0.2 and 0.7 μm is considered the DOM pool and the organic matter retained on the filter is considered the POM pool.

Exopolymer particles (EP, Alldredge et al., 1993) are ubiquitous particles in all marine ecosystems (Passow et al., 2002). The ecological relevance of EP lies in their sticky nature and low density that affect different oceanic processes. These particles can accumulate in the surface microlayer of the ocean when they have positive buoyancy affecting gases exchange with the atmosphere (Azetsu-Scott and Passow, 2004; Wurl et al., 2011). They can also

stay suspended in the water column when they have neutral buoyancy or be ballasted and exported downward when they have negative buoyancy, contributing to the “oceanic biological carbon pump” (Volk and Hoffert, 1985) (Figure 1.4.). EP production is determined by the abiotic aggregation of polysaccharide-rich dissolved precursors released into the marine environment by heterotrophic and autotrophic organisms of several trophic levels (mainly microorganisms) under diverse physiological conditions (Figure 1.4.).

1.1.4. *Exopolymer particles contribution to the biological pump*

EP ballasted with fecal pellets, algal debris, clay, calcium carbonate, etc. is termed “marine snow” and can sink down into the deep ocean increasing the efficiency of the biological pump and mineral exports (Turley, 2002; De la Rocha and Passow, 2007). These organic aggregates can be mineralized during their transit to the deep ocean defining two boundary depths (Lampitt et al., 2008; Passow and Carlson, 2012; Turner, 2015): The “export depth” is the bottom of the euphotic zone or the maximum mixed layer, and the “sequestration depth” is the bottom of the mesopelagic zone (or twilight zone). The mesopelagic zone is the layer where most of the exported organic matter remineralization takes place with a consequent relevant attenuation of the carbon flux. Therefore, this layer is key in determining the biological pump efficiency (Passow and Carlson, 2012). Finally, the carbon exported below the sequestration depth is usually considered to become sequestered, and would stay in the deep ocean for more than 100 years.

The core of this PhD dissertation is the description of EP distribution in the profile from the surface to the deep waters in the Atlantic, Indian and Pacific Oceans and in the Mediterranean Sea. We also explored the main biological drivers determining the distribution patterns observed and we determined experimentally the EP production rates by heterotrophic prokaryotes. We believe that our results will contribute to understand the role of EP in the ocean carbon cycle at a global scale.

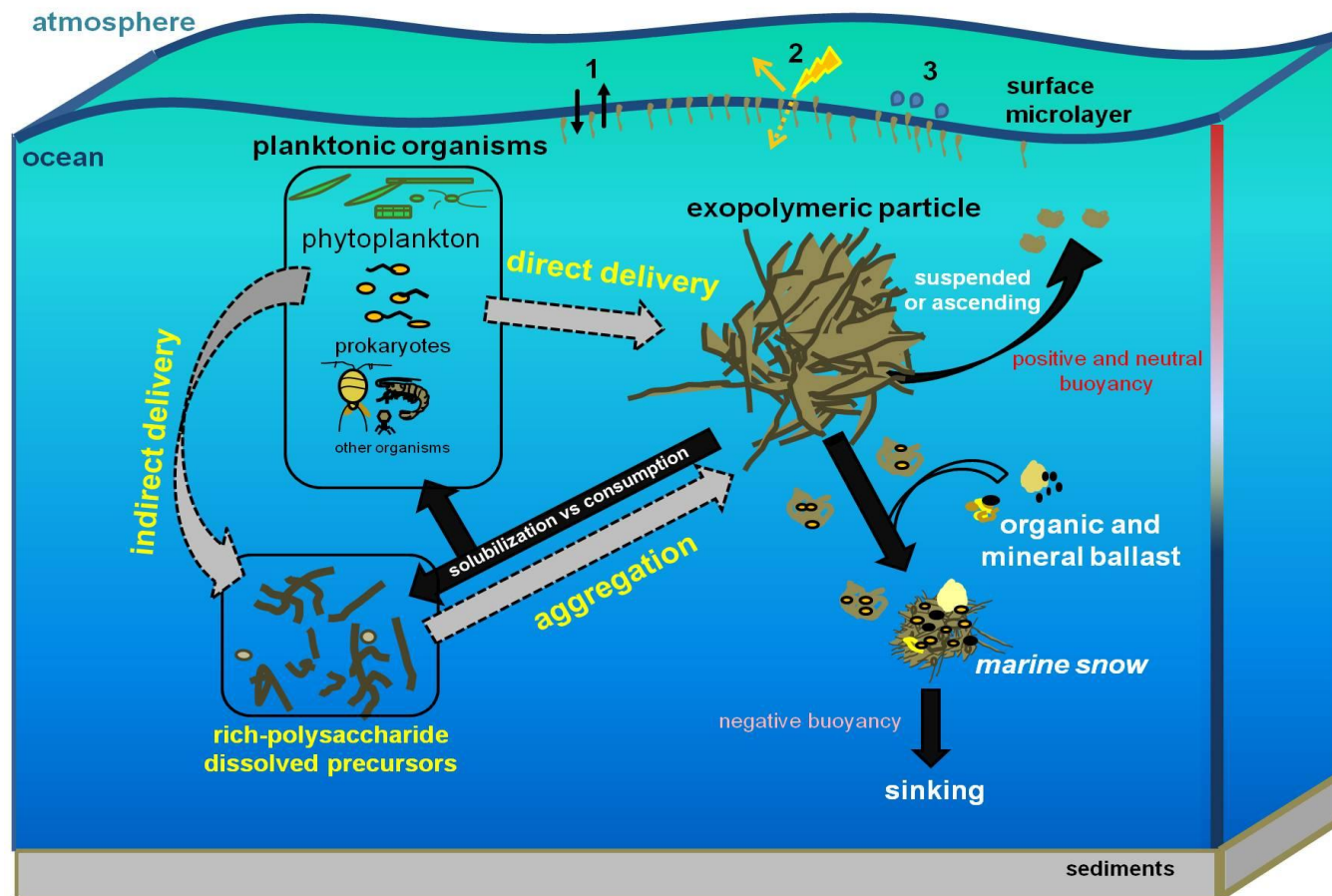


Figure 1. 4. Schematic depiction showing the organisms (mainly phytoplankton and prokaryotes) and routes (gray arrows) involved in the EP formation and described in the literature (taken from Passow, 2002a; Verdugo et al., 2004). Additionally, the fate of EP in the oceanic water column is also illustrated (black arrows): mineralization (consumption or solubilization) mostly by heterotrophic microbes, sinking down to the deep ocean as ballasted aggregates, persistence in the water column as suspended particles or ascending to the surface as buoyant particles. The numbers from 1 to 3 represent the processes affected by EP accumulation at the surface microlayer: 1) ocean-atmosphere gases exchange, 2) light penetration in the water column and 3) injection to atmosphere via bubble bursting.

1.2. General objectives

The main objectives of this dissertation are:

1. To describe the distribution of exopolymer particles, from the surface to deep waters, in the Atlantic, Indian and Pacific Oceans and in the Mediterranean Sea.
2. To determine the main biological drivers affecting the geographical distribution of exopolymer particles both in the epipelagic and the deep ocean.
3. To estimate the contribution of exopolymer particles to the total carbon export from surface to deep waters in the Atlantic, Indian and Pacific Oceans and in the Mediterranean Sea.
4. To determine experimentally the production rates of exopolymer particles by heterotrophic prokaryotes in surface (above the “export depth”) and deep (below the “sequestration depth”) waters.
5. To provide estimates of both, direct respiration rates and prokaryotic growth efficiency, at mesopelagic depths in two underexplored regions, the South Atlantic and the Indian Oceans.

1.3. Methodology

1.3.1. Sampling and study sites

Sampling was carried out during two oceanographic cruises: the circumnavigation Malaspina 2010 and the cruise Hotmix in the Mediterranean Sea.

1.3.1.1. Malaspina cruise:

During this cruise, the oceanographic vessel *R/V Hespérides* crossed the Atlantic, Indian and Pacific Oceans in 7 legs (Figure 1.5.). The cruise departed from Cadiz (Spain) on 16th December 2010 and finished in Cartagena (Spain) on 10th July 2011 (Figure 1.5.).

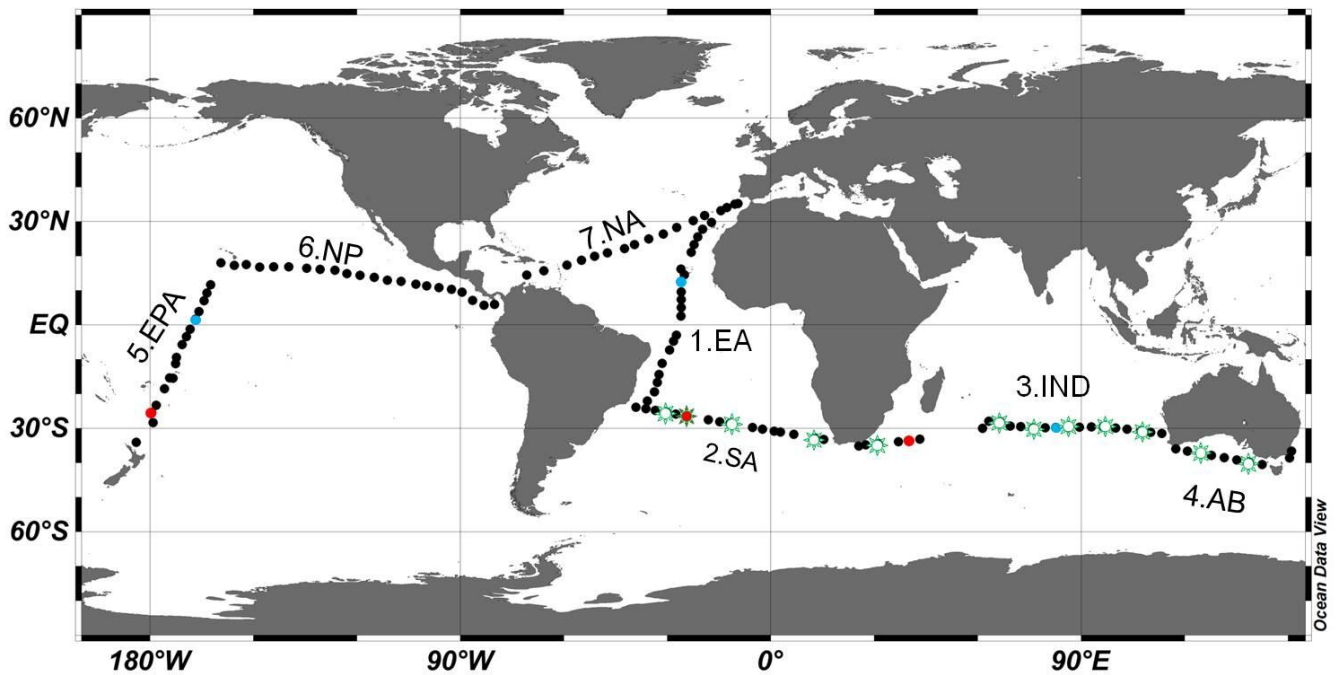


Figure 1. 5. Map of the Malaspina 2010 cruise showing the stations (filled circles) where the samples were collected for both the epipelagic and the deep ocean. The cruise was divided into 7 legs: Equatorial Atlantic (EA), South Atlantic (SA), Indian (IND), Great Australian Bight (AB), Equatorial Pacific (EPA), North Pacific (NP) and North Atlantic (NA). Numbers 1 to 7 indicate the temporal order of the legs. The asterisks represent the stations where mesopelagic respiration experiments were conducted and colored filled circles correspond to stations where samples of the epipelagic (blue circles) or deep (red circles) waters were collected to perform the prokaryotic EP production experiments.

Introduction and basic methodology

Samples for both vertical profiles and experiments (respiration and prokaryotic EP production) were collected using a rosette of 24 Niskin bottles (12 L) coupled to a conductivity-temperature-pressure probe (CTD) (Seabird SBE 911Plus) (Figure 1.6.) in different casts, covering surface waters up to 200 m depth and dark waters from 200 m down to 4000 m depth. In the vertical profiles, a total of 10 depths were sampled, up to 5 depths above the 200 m depth and other 5 depths in the deep ocean (> 200 m). Samples for experiments were taken in 20 L carboys and processed immediately after sampling.

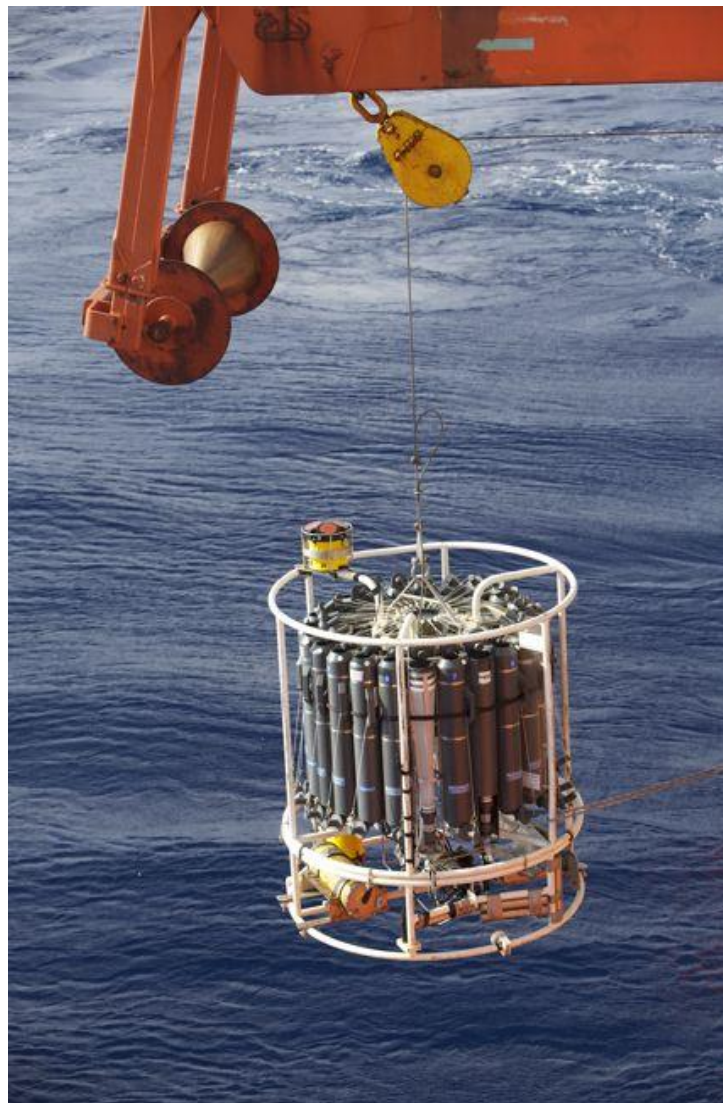


Figure 1. 6. Launching of a 24 Niskin bottles rosette coupled to a CTD sensor (at the bottom) from on board the oceanographic R/V Hespérides.

1.3.1.2. Hotmix cruise:

During this cruise, the oceanographic vessel *B/O Sarmiento de Gamboa* crossed the Mediterranean Sea and Northeast Atlantic Ocean, from the eastern Mediterranean basin starting on 29th April 2014 to the northeastern Atlantic Ocean ending on 28th May 2014 (Figure 1.7.).

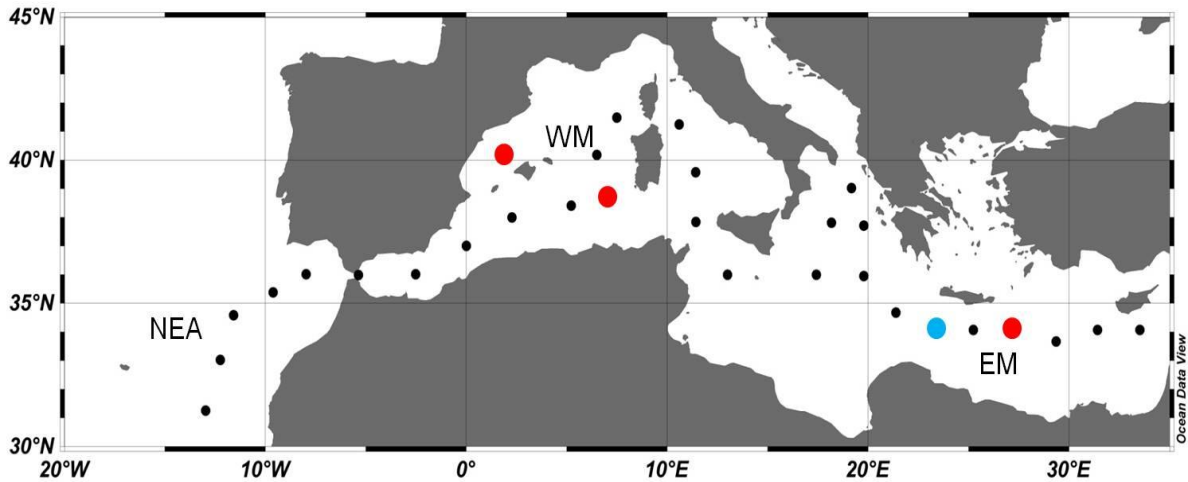


Figure 1. 7. Map of the Hotmix cruise showing the sampling stations (filled circles) where the samples were collected both in the epipelagic and in the dark ocean. The cruise was divided into 3 regions: Eastern Mediterranean (EM), Western Mediterranean (WM) and Northeast Atlantic (NEA). The colored circles indicate stations where samples of the epipelagic (blue circles) or deep waters > 200 m depth (red circles) were taken to perform the prokaryotic EP production experiments. The station between Majorca and the Barcelona coast corresponds to the Hotmix-test station where an initial test experiment of prokaryotic EP production was carried out.

Water samples for both vertical profiles and prokaryotic EP production experiments were collected using a rosette of 24 Niskin bottles (12 l each) coupled to a conductivity and Seabird Seacat SBE21 temperature–pressure probe (CTD). Casts covered three zones: epipelagic waters down to 200 m depth, mesopelagic waters from 200 to 1000 m depth and bathypelagic waters up to 10 m above the bottom depth. In vertical profiles, a total of 13 depths were sampled covering the entire water column, 4 depths above 200 m depth and other 9 depths in the deep waters (> 200 m). Water for experiments was taken in 25 L carboys and processed immediately after sampling. An additional sampling station was included in our study, between Barcelona and the Majorca coasts,

that corresponded to the *Hotmix*-test station where water for initial prokaryotic EP production experiments was collected (2th October 2013).

1.3.2. Chemical and biological analyses

Several techniques have been used to reach the objectives of this PhD dissertation. The detailed procedures are described in the corresponding chapter and here I present a brief summary (Figure 1.8.).

1.3.2.1. Organic matter characterization:

Particulate organic carbon (POC) in the *Malaspina* cruise was measured in a Carlo-Erba CHN analyzer according to the Vidal and Galindo (2012) protocol.

Total organic carbon (TOC) and **dissolved organic carbon (DOC)**, after filtration, samples in the *Hotmix* experiments were analyzed by high-temperature catalytic oxidation on a Shimadzu TOC-V CSH total organic carbon analyzer.

Exopolymer particles (EP) were analyzed using the colorimetric alcian blue method (Passow and Alldredge, 1995). For more details see the protocol in Mazuecos et al. (2012) (details in *Annex IV*).

Dissolved acidic polysaccharides (dAPS) in the *Malaspina* experiments were analyzed following the alcian blue method, after a dialysis step, according to Thornton et al. (2007).

Dissolved neutral total carbohydrates (DTCHO) analysis. Mono- (DMCHO) and polysaccharides (DPCHO, previously hydrolyzed), in the *Malaspina* experiments were determined by the spectrophotometric method using the alkaline ferricyanide reaction with 2, 4, 6-tripyridyl-s-triazine (Myklestad et al., 1997).

1.3.2.2. Inorganic nutrients:

Nitrate (N) and phosphate (P) concentrations were analyzed simultaneously and automatically by segmented continuous flow in a colorimetric detection SAN ++ analyzer in the vertical profiles of the *Hotmix* cruise. In *Hotmix* experiments, P and N concentrations, after oxidation with potassium persulfate (Valderrama, 1981), were determined with the modified method of Murphy and Riley (1962) and by the ultraviolet spectrophotometric method (Rice et al., 2012), respectively.

1.3.2.3. *Planktonic microorganisms:*

Pigment analyses, chlorophyll *a* concentration (*chl a*) and phaeophytin *a*, were measured fluorometrically after acetone extraction and subsequent acidification (Yentsch and Menzel, 1963).

Identification of phytoplankton groups

Picophytoplankton abundances (*Synechococcus* sp., *Prochlorococcus* sp. and picoeukaryote populations) were quantified by flow cytometry (Collier, 2000) using a cytometer fitted with a laser emitting at 488 nm. The different groups were identified based on the red and orange fluorescence and side scatter signals.

Larger algal groups were quantified using an inverted microscope (Utermöhl, 1958) in the *Malaspina* cruise and by flow cytometry discriminating the different algal groups based on fluorescence and scatter signals in the *Hotmix* cruise.

Heterotrophic prokaryotic abundance (PHA) was determined by flow cytometry (Gasol and del Giorgio, 2000), using a cytometer fitted with a laser emitting at 488 nm. Prokaryotes were identified by their signatures in a plot of side scatter versus green fluorescence.

Viral abundance (VA) was determined by flow cytometry fitted with a laser emitting at 488 nm following Brussaard (2004). Viruses were identified by their signatures in a plot of side scatter versus green fluorescence.

1.3.2.4. *Planktonic metabolism:*

Primary production (PP) was determined using the ¹⁴C technique in the *Malaspina* cruise (Steeman-Nielsen, 1952; Marañón et al., 2001) and was obtained from the standard product of the Ocean Productivity website (<http://www.science.oregonstate.edu/ocean.productivity/>), based on the Vertically Generalized Production Model (Behrenfeld and Falkowski, 1997), in the *Hotmix* cruise.

Prokaryotic heterotrophic production (PHP) was measured by ³H-Leucine incorporation into proteins (Kirchman et al., 1985) using the microcentrifugation protocol proposed by Smith and Azam (1992). Leucine incorporation rates were converted into carbon by using a theoretical factor of 1.55 kg C mol Leu⁻¹ (Simon

and Azam, 1989), assuming no internal isotope dilution (Kirchman and Ducklow, 1993).

Respiration (R) measurements in the *Malaspina* cruise were performed by automated microWinkler titrations using a Dissolved Oxygen Analyser (DOA; SiS®) with photometric end-point detection (Williams and Jenkinson, 1982). For more details see the protocol in Arístegui et al. (2012) (details in *Annex IV*).

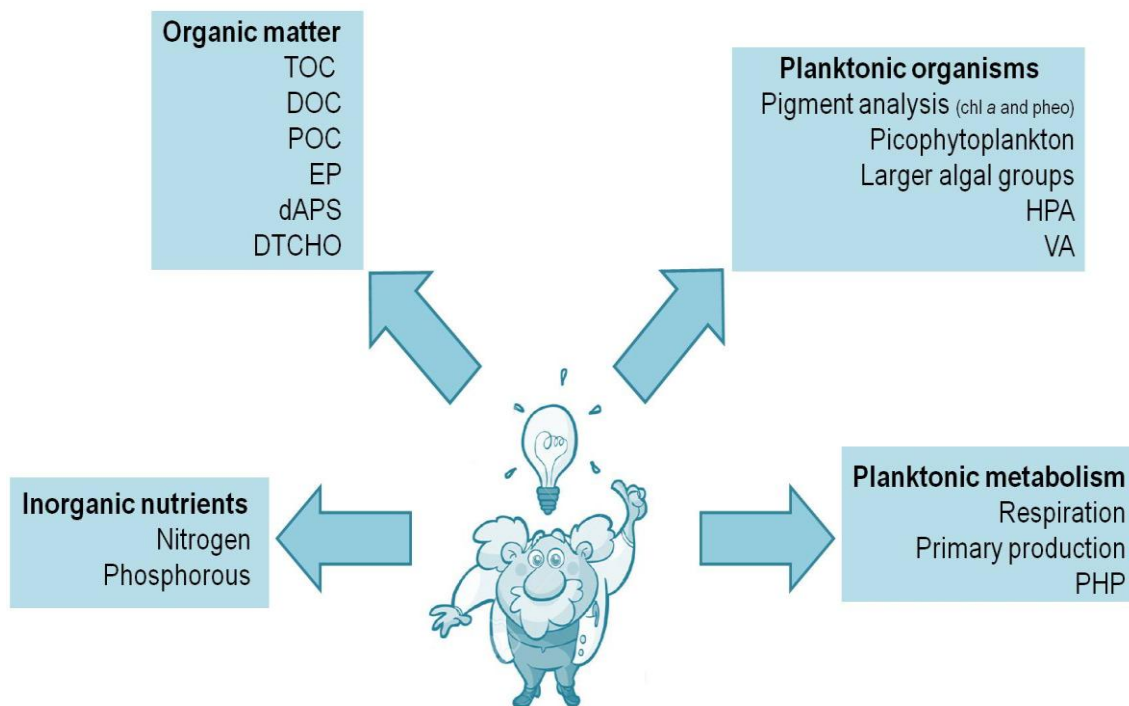


Figure 1. 8. Scheme of the used chemical and biological analysis for this dissertation.

1.4. References

- Allredge A. L., Passow U., Logan B. E. 1993. The abundance and significance of a class of large, transparent organic particles in the ocean. *Deep-Sea Research I*, 40 (6): 1131 – 1140.
- Aristegui J., Gasol J. M., Duarte C. M., Herndl G. J. 2009. Microbial oceanography of the dark ocean's pelagic realm. *Limnology and oceanography*, 54(5): 1501 – 1529.
- Aristegui J., Agustí S., Middelburg J., Duarte C.M. 2005a. Respiration in the mesopelagic and bathypelagic zones of the oceans. In: P. Del Giorgio, P.J. LeB Williams (eds). *Respiration in Aquatic Ecosystems*. Oxford Univ. Press. p.p. 182 – 206.
- Aristegui J., Duarte C. M., Gasol J. M., Alonso-Sáez L. 2005b. Active mesopelagic prokaryotes support high respiration in the subtropical northeast Atlantic Ocean. *Geophys. Res. Lett.* 32, L03608. <http://dx.doi.org/10.1029/2004GL021863>.
- Aristegui J., Mazuecos I. P., Vázquez-Domínguez E. 2012. Medida de la respiración mediante cambios *in vitro* de la concentración de O₂, in: *EXPEDICIÓN DE CIRCUNNAVEGACIÓN MALASPINA 2010: CAMBIO GLOBAL Y EXPLORACIÓN DE LA BIODIVERSIDAD DEL OCEANO GLOBAL. LIBRO BLANCO DE MÉTODOS Y TÉCNICAS DE TRABAJO OCEANOGRÁFICO*. CSIC, Enrique Moreno-Ostos (eds.), p. p. 565 - 573.
- Arnosti C. 2003. Microbial extracellular enzymes and their role in dissolved organic matter cycling, In: *Aquatic ecosystems: interactivity of dissolved organic matter*. (Findlay S. E. G., Sinsabaugh R. L. eds.) Academic Press, San Diego. P.p. 315 – 342.
- Azam F. 1998. Microbial control of oceanic carbon flux: The plot thickens. *Science* 280: 694 – 696.
- Azam F., Fenchel T., Field J. G., Gray J. S., Meyer-Reil L. A., Thingstad F. 1983. The ecological role of water column microbes in the sea. *Marine Ecology Progress Series*, 10: 257 - 263.
- Azetsu-Scott K., Passow U. 2004. Ascending marine particles: Significance of transparent exopolymer particles (TEP) in the upper ocean. *Limnology and Oceanography*, 49(3): 741 – 748.
- Baltar, F., Aristegui, J., Gasol, J.M., Herndl, G.J., 2010. Prokaryotic carbon utilization in the dark ocean: growth efficiency, leucine-to-carbon conversion factors, and their relation. *Aquat. Microb. Ecol.* 60, 227-232. <http://dx.doi.org/10.3354/ame01422>
- Biddanda, B., Benner, R., 1997. Major contribution from mesopelagic plankton to heterotrophic metabolism in the upper ocean. *Deep-Sea Research I*, 44 (12): 2069-2085.
- Behrenfeld M. J., Falkowski P. G. 1997. Photosynthetic rates derived from satellite-based chlorophyll concentration. *Limnology and Oceanography*, 42: 1 – 20.
- Buesseler K. O., Lamberg C. H., Boyd P. W., Lam P. J., Trull T. W., Bidigare R. R., Bishop J. K. B., Casciotti K. L., Dehairs F., Elskens M., Honda M., Karl D. M., Siegel D. A., Silver M. W., Steinberg D. K., Valdes J., Van Mooy B., Wilson S. 2007. Revisiting carbon flux through the ocean's twilight zone. *Science* 316 (5824): 567 – 570.
- Brussaard C. P. D. 2004. Optimisation of procedures for counting viruses by flow cytometry. *Applied Environmental Microbiology*. 70: 1506 - 1513.
- De la Rocha C., Passow U. 2007. Factors influencing the sinking of POC and the efficiency of the biological carbon pump. *Deep-Sea Research II*, 54: 639 – 658.
- Carlson C. A., del Giorgio P. A., Herndl G. J. 2007. Microbes and the Dissipation of Energy and Respiration: From Cells to Ecosystems. *Oceanography*, 20 (2): 89 - 100.
- Collier J. L. 2000. Flow cytometry and the single cell in phycology. *Journal of Phycology*, 36 (4): 628 - 644.
- Del Giorgio P. A., Cole J. J. 1998. Bacterial growth efficiency in natural aquatic ecosystems. *Annual Review Ecology Systems*, 29: 503 – 41.
- Del Giorgio P. A., Duarte C. M. 2002. Respiration in the open ocean. *Nature*, 420: 379 – 384.
- Del Giorgio P. A., Cole J. J., Cimperis A. 1997. Respiration rates of bacteria exceed phytoplankton in unproductive aquatic systems. *Nature* 385: 148 – 51.
- Gasol J. M., del Giorgio P. A. 2000. Using flow cytometry for counting natural planktonic bacteria and understanding the structure of planktonic bacterial communities. *Scientia Marina*, 64: 197 – 224.
- Ducklow H. 2000. Bacterial production and biomass in the oceans. In: Kirchman D. L. (ed.) *Microbial ecology of the oceans*. Wiley-Liss, New York, p 85 -120.
- Field B. B., Behrenfeld M. J., Randerson J. T., Falkowski P. 1998. Primary Production of the Biosphere: Integrating Terrestrial and Oceanic Components. *Science*, 281: 237 – 240.

- Hansell D. A., Carlson C. A., Repeta D. J., Schlitzer R. 2009. Dissolved organic matter in the ocean. *Oceanography*, 22 (4): 202 – 211.
- Hedges, J. I. 1992. Global biogeochemical cycles: progress and problems. *Marine Chemistry*, 39: 67 – 93.
- Jiao N., Herndl G. J., Hansell D. A., Benner R., Kattner G., Wilhelm S. W., Kirchman D. L., Weinbauer M. G., Luo T., Chen F., Azam F. 2010. Microbial production of recalcitrant dissolved organic matter: long-term carbon storage in the global ocean. *Nature*, 8: 593 – 599.
- Jorgensen L., Stedmon C. A., Granskog M. A., Middelboe M. 2014. Tracing the long-term microbial production of recalcitrant fluorescent dissolved organic matter in seawater. *Geophysical Research Letters*, 41 (7): 2481 – 2488.
- Kirchman D. L., Ducklow H. W. 1993. Estimating conversion factors for thymidine and leucine methods for measuring bacterial production. In: Kemp P. F., Sherr B. F., Sherr E. B., Cole J. J. (eds) *Handbook of methods in aquatic microbial ecology*. Lewis Publishers, Boca Raton, p. p. 513 - 517.
- Kirchman D. L., K'nees E., Hodson R. E. 1985. Leucine incorporation and its potential as a measure of protein synthesis by bacteria in natural aquatic systems. *Applied Environmental Microbiology*, 49: 599 - 607.
- Lampitt R. S., Achterberg E. P., Anderson T. R., Hughes J. A., Iglesias-Rodriguez M. D., Kelly-Guerreyn B. A., Lucas M., Popova E. E., Sanders R., Shepherd J. G., Smythe-Wright D. and Yool A. 2008. Ocean fertilization: a potential means of geoengineering? *Phil. Trans. R. Soc. A*, 366: 3919 – 3945.
- Marañón E., Holligan P. M., Barciela R., González N., Mouriño B., Pazó M. J., Varela M. 2001. Patterns of phytoplankton size structure and productivity in contrasting open-ocean environments. *Marine Ecology Progress Series*, 216: 43 - 56.
- Marsay C. M., Sanders R. J., Henson S. A., Pabortsava K., Achterberg E. P., Lampitt R. S. 2015. Attenuation of sinking particulate organic carbon flux through the mesopelagic ocean. *PNAS*, 112(4): 1089 – 1094.
- Mazuecos I. P., Ortega-Retuerta E., Reche I. 2012. Medida de Partículas Exopoliméricas Transparentes (TEP) en agua marina, in: *EXPEDICIÓN DE CIRCUNNAVEGACIÓN MALASPINA 2010: CAMBIO GLOBAL Y EXPLORACIÓN DE LA BIODIVERSIDAD DEL OCÉANO GLOBAL. LIBRO BLANCO DE MÉTODOS Y TÉCNICAS DE TRABAJO OCEANOGRÁFICO*. CSIC, Enrique Moreno-Ostos (eds.), p. p. 515 - 520.
- Murphy J., Riley J. P. 1962. A Modified Single Solution Method for the Determination of Phosphate in Natural Waters. *Analytica Chimica Acta*, 27: 31 – 36.
- Myklestad S., Skanoy E., Hestmann S. 1997. A sensitive and rapid method for analysis of dissolved mono- and polysaccharides in seawater. *Marine Chemistry*, 56 (3–4): 279–286.
- Ortega-Retuerta E., Duarte C. M., Reche I. 2010. Significance of Bacterial Activity for the distribution and dynamics transparent exopolymer particles in the Mediterranean sea. *Microbial Ecology*, 59: 808 – 818.
- Passow U. 2002a. Transparent exopolymer particles (TEP) in aquatic environments. *Progress in Oceanography*, 55: 287 – 333.
- Passow U. 2002b. Production of transparent exopolymer particles (TEP) by phyto- and bacterioplankton. *Marine Ecology Progress Series*, 236: 1 - 12.
- Passow U., Alldredge A. L. 1995. A dye-binding assay for the spectrophotometric measurement of transparent exopolymer particles (TEP). *Limnology and Oceanography*, 40 (7): 1326 – 1335.
- Passow U., Carlson C. A. 2012. The biological pump in a high CO₂ world. *Marine Ecology Progress Series*. 470: 249 – 271.
- Pomeroy L. R. 1974. The ocean's food web, a changing paradigm. *BioScience* 24: 499 - 504.
- Pomeroy L. R., Wiebe W. J. 2001. Temperature and substrates as interactive limiting factors for marine heterotrophic bacteria. *Aquatic Microbial ecology*, 23: 187–204
- Pomeroy L.R., Williams P. J. le B, Azam F., Hobbie J. E. 2007. The microbial loop. *Oceanography*, 20 (2): 28 – 33.
- Pomeroy, L.R. 2001. Caught in the food web: Complexity made simple? *Scientia Marina*, 65: 31 – 40.

- Reinthalder, T., van Aken, H., Veth, C., Arístegui, J., Robinson, C., Williams, P.J.B., Lebaron, P., Herndl, G.J. 2006. Prokaryotic respiration and production in the meso- and bathypelagic realm of the eastern and western North Atlantic basin. *Limnol. Oceanogr.* 51 (3): 1262-1273.
- Rice E. W., Baird R. B., Eaton A. D., Clesceri L. S. 2012. *Standard Methods for the Examination of Water and Wastewater*, 22nd Edition. 4500-Ultraviolet Spectrophotometric Screening Method. APHA, AWWA, WEF.
- Robinson C. 2008. Heterotrophic bacterial respiration. In: Kirchman DL (ed) *Microbial Ecology of the Oceans*, 2nd edition. John Wiley and Sons, Hoboken, N. J., p 299 – 334.
- Robinson C., Williams P. J. le B. 2005. Chapter 9: Respiration and its measurements in surface marine waters. In: Williams P. J. le B. & del Giorgio P. A. (eds) *Respiration in Aquatic Ecosystems*. pp 147 – 180. Oxford University Press, New York.
- Sherr E. B., Sherr B. F. 1991. Planktonic microbes: Tiny cells at the base of the ocean's food webs. *Trends in Ecology and Evolution*, 6(2): 50 – 54.
- Sherr E. B., Sherr B. F. 1996. Temporal offset in oceanic production and respiration processes implied by seasonal changes in atmospheric oxygen: the role of heterotrophic microbes. *Aquatic Microbial Ecology*, 11: 91 – 100.
- Simon M., Azam F. 1989. Protein content and protein synthesis rates of planktonic marine bacteria. *Marine Ecology-Progress Series*, 51: 201 – 213.
- Smith D. C., Azam F. 1992. A simple economical method for measuring bacterial protein synthesis rates in seawater using ³H-leucine. *Marine Microbial Food Webs*, 6: 107 – 114.
- Steeman-Nielsen E. 1952. The use of radioactive carbon (C¹⁴) for measuring organic production in the sea. *J. Cons. Int. Explor. Mer.*, 18: 117-140.
- Stoderegger K. E., Herndl G. J. 1999. Production of exopolymer particles by marine bacterioplankton under contrasting turbulence conditions. *Marine Ecology Progress Series*, 189: 9 – 16.
- Thornton D. C. O., Fejes E. M., Dimarco S. F., Clancy K. M. 2007. Measurement of acid polysaccharides in marine and freshwater samples using alcian blue. *Limnology and Oceanography Methods*, 5: 73 – 87.
- Turley C. 2002. The importance of “marine snow”. *Microbiology Today*, 29: 177 – 179.
- Turner J. T. 2015. Zooplankton fecal pellets, marine snow, phytodetritus and the ocean's biological pump. *Progress in Oceanography*, 130: 205 – 248.
- Utermöhl H. 1958. Zur Vervollkommung der quantitativen Phytoplankton-Methodik. *Mitt. Int. Verein. Theor. Angew. Limnol.*, 9: 1 - 38.
- Valderrama J. C. 1981. The simultaneous analysis of total Nitrogen and total phosphorus in natural waters. *Marine chemistry*, 10: 109 – 122.
- Verdugo P., Alldredge A. L., Azam F., Kirchman D. L., Passow U., Santschi P. H. 2004. The oceanic gel phase: a bridge in the DOM-POM continuum. *Marine Chemistry* 92: 67 – 85.
- Vidal M., Galindo M. 2012. Determinación de carbono y nitrógeno orgánico particulados mediante analizador elemental, in: *EXPEDICIÓN DE CIRCUNNAVEGACIÓN MALASPINA 2010: CAMBIO GLOBAL Y EXPLORACIÓN DE LA BIODIVERSIDAD DEL OCÉANO GLOBAL. LIBRO BLANCO DE MÉTODOS Y TÉCNICAS DE TRABAJO OCEANOGRÁFICO*. CSIC, Enrique Moreno-Ostos (eds.), p. p. 139 - 141.
- Volkman J. K., Tanoue E. 2002. Chemical and Biological Studies of Particulate Organic Matter in the Ocean. *Journal of Oceanography*, 58: 265 – 279.
- Volk T., Hoffert M. I. 1985. Ocean carbon pumps: analysis of relative strengths and efficiencies in ocean-driven atmospheric CO₂ changes. In *The Carbon Cycle and Atmospheric CO₂: Natural Variations Archean to Present* (eds. E. T. Sundquist and W. S. Broecker). American Geophysical Union, Washington DC, pp. 99-110.
- Weinbauer, M.G., Liu, J., Motegi, C., Maier, C., Pedrotti, M.L., Dai, M., Gattuso, J.P., 2013. Seasonal variability of microbial respiration and bacterial and archaeal community composition in the upper twilight zone. *Aquat. Microb. Ecol.* 71, 99-115.
- Whitman W. B., Coleman D. C., Wiebe W. J. 1998. Prokaryotes. The unseen majority. *PNAS*, 95: 6578 – 6583.

Introduction and basic methodology

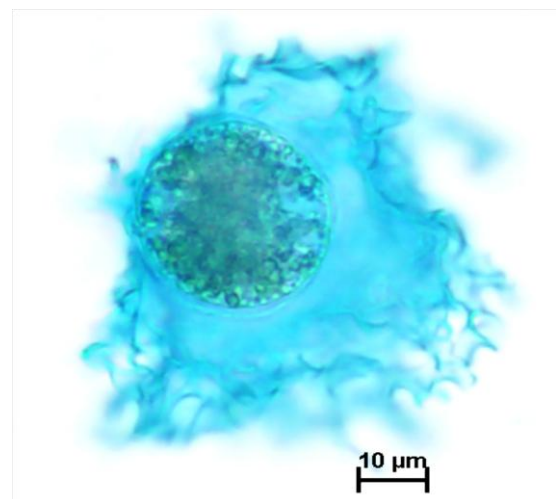
- Williams P. J. LeB., Jenkinson N. W. 1982. A transportable microprocessor- controlled precise Winkler titration suitable for field station and siphboard use. *Limnology and Oceanography*, 27 (3): 2843 - 2855.
- Wurl O., Miller L., Svein S. 2011. Production and fate of transparent exopolymer particles in the ocean. *Journal of Geophysical Research*, 116: 1 - 16.
- Yentsch C. S., Menzel D. W. 1963. A method for the determination of phytoplankton chlorophyll and phaeophytin by fluorescence. *Deep-Sea Research*, 10: 221 - 231.

Chapter 2:

Exopolymer particles distribution and contribution to the biological carbon pump in the global ocean



Abbreviated title: **Global distribution of exopolymer particles**



*Exopolymer particles stained with alcian blue and excreted by *Lepidodinium chlorophorum*.
Photo: P. Claquin
Reference: Claquin et al., 2008*

2.1. Abstract

Exopolymer particles (EP), derived from acidic polysaccharides released by microorganisms, can affect the biological pump by promoting the carbon export towards the deep ocean. Here, we performed a detailed inventory of EP concentrations from the surface to 4,000 m depth across the tropical and subtropical regions of the Atlantic, Indian and Pacific Oceans. In the epipelagic waters, the EP concentrations ranged from undetectable to 173.6 $\mu\text{g XG eq l}^{-1}$ with maximum values above the deep chlorophyll maxima. The highest EP concentrations were observed in upwelling regions of the Benguela, Costa Rica Dome, Great Australian Bight and in the equatorial zones. In fact, primary production (PP) was the best predictor of EP concentration in these waters. In the meso- and bathypelagic waters, the EP concentrations mirrored the epipelagic pattern indicating that the vertical export is a major process determining the EP pool in the interior ocean. In the mesopelagic zone, besides the EP exported from the epipelagic waters (< 200 m), EP concentrations were also positively related to the *in situ* prokaryotic heterotrophic activity suggesting a *de novo* EP synthesis in this zone. This mesopelagic synthesis could explain the EP transfer efficiencies towards the bathypelagic zone higher than 100%. We speculate that this EP synthesis in the deep ocean might be related to the lifestyle of the heterotrophic prokaryotes, predominantly attached to particles. Our estimation of EP fluxes below the sequestration depth (> 1000 m) averaged 1.2 $\text{g C m}^{-2} \text{ year}^{-1}$ (based on the most conservative conversion factor to carbon). This estimation provides an EP global export below the sequestration depth of 0.4 Pg C year^{-1} . The global pool of EP, in terms of carbon, obtained in this study was 4.8 Pg C or 8.4 Pg C (depending on the conversion factors) accounting for one quarter or two fifths of the global POC.

2.2. Introduction

Exopolymer particles (EP), or transparent exopolymer particles (TEP, Alldredge et al., 1993), are polysaccharide-enriched and organic gel-like particles with a sticky nature generated by aquatic microorganisms (Passow, 2002a). The origin of EP and their precursors is complex, involving microorganisms of several trophic levels and physiological conditions (Prieto et al., 2001; Passow, 2002a, b; Ortega-Retuerta et al., 2010; Vardi et al., 2012). In the epipelagic zone, phytoplankton are considered the main source of the EP precursors, i.e. dissolved polysaccharides, usually released under stress conditions (Berman-Frank and Dubinsky, 1999; Berman-Frank et al., 2007, Van Oostende et al., 2013). Exudation of EP precursors by phytoplankton is determined by phytoplankton abundance (Passow, 2002a), species composition (Passow and Alldredge, 1994; Passow, 2002b; Fukao et al., 2010) and physiological status (Hong et al., 1997; Passow, 2002a). More recently, EP production mediated by viral infection has been also reported (Vardi et al., 2012; Lønborg et al., 2013). Vardi et al. (2012) showed that stressed phytoplankton could produce a mucilage EP-rich barrier againsts viral infection, although the cellular materials released by viral lysis also can, by themselves, contribute to the development of the EP pool (Shibata et al., 1997; Lønborg et al., 2013; Sheik et al., 2014).

Prokaryotes also actively release EP precursors (Passow, 2002b; Ortega-Retuerta et al., 2010) and participate in EP production from detritus (Ramaiah et al., 2001; Thornton, 2004). Moreover, they can also modify the aggregation properties of the algal exudates (Rochelle-Newall et al., 2010; Van Oostende et al., 2013) or directly act as physical bonds among polymers (Sugimoto et al., 2007). Therefore, EP-prokaryote interactions are really intricate. EP have been considered both, as a food substrate or as a metabolic byproduct. On the one hand, EP can provide a three-dimensional biopolymeric network that can be colonized by bacteria (Passow and Alldredge, 1994, Verdugo et al., 2012), becoming carbon-rich hot spots (Azam and Long, 2001). On the other hand, EP can just constitute a physical support that facilitates prokaryotic life in suspended aggregates (Bar-Zeev et al., 2012).

EP distribution in marine systems has been mostly studied in coastal and surface waters (e. g. Engel, 2004; Corzo et al., 2005; Ortega-Retuerta et al., 2009, 2010), generally during algal blooms (e. g. Kiørboe et al., 1996; Ramaiah et al., 2001; Harlay et al., 2009; Leblanc et al., 2009; Van Oostende et al., 2012) or mucus events (Radic et al., 2005; Scoullou et al., 2006). Therefore, the information on EP distribution in the open and the deep ocean (> 200 m) is scarce. The only few studies in the open ocean have reported low EP concentrations (Engel, 2004; Leblanc et al., 2009; Ortega-Retuerta et al., 2010; Kodama et al., 2014), while EP concentrations in the deep ocean appeared to be similar to those of the surface ocean (Kumar et al., 1998; Bar-Zeev et al., 2011). In addition, there is little knowledge on the biological drivers shaping EP distribution in the epipelagic zone, where phytoplankton is present, versus those drivers involucrated in the deep ocean (> 200 m) where prokaryotes are dominant.

Since EP are sticky gel-like particles, they can act as agglutinating glue (Engel, 2000) easily ballasted by organic and mineral components (e.g. fecal pellets, algal debris, clay, calcium carbonate) generating larger aggregates of higher density known as “marine snow” (Alldredge and Silver, 1988; Logan et al., 1995). The ballasted-EP can sink down into the deep ocean increasing the magnitude of the “oceanic biological pump” and mineral exports (Passow et al., 2001; Turley, 2002; De la Rocha and Passow, 2007). In this context, two boundary depths have been defined in the ocean (Lampitt et al., 2008; Passow and Carlson, 2012; Turner, 2015). The “export depth” identified as the bottom of the euphotic zone or as the maximum mixed layer, and the “sequestration depth” defined as the bottom of the mesopelagic zone, where most of the organic matter remineralization takes place and, consequently, a dramatic attenuation of export carbon flux. The carbon exported below sequestration depth is usually considered as carbon sequestered in the deep ocean for more than 100 years. Exports mediated by EP can, therefore, be another relevant via of carbon accumulation in the deep ocean, but there is no information on EP contribution to carbon export in large oceanographic surveys. In fact, these EP fluxes can account for up to approximately 50% of total particulate organic carbon (POC)

exported to mesopelagic depths (Passow, 2002a; Ramaiah et al., 2005; Martin et al., 2011).

We provide here a global inventory of exopolymer particles (EP) from epipelagic to bathypelagic waters across the Atlantic, Indian and Pacific Oceans and evaluate the potential biological drivers of EP distribution. We also estimated EP fluxes at the export (200 m) and sequestration (1000 m) depths and assessed the EP contribution to POC fluxes.

2.3. Material and methods

2.3.1. Study site and Sampling

Sampling was carried out from on board R/V Hespérides during the circumnavigation expedition Malaspina 2010 (www.expedicionmalaspina.es) crossing the N and S Atlantic, Pacific and Indian oceans from December 16th 2010 to July 10th 2011. A total of 125 stations were sampled in 7 different legs (Figure 2.1.). Water samples were collected using a rosette of 24 Niskin bottles (12 l each) coupled to a conductivity and Seabird SBE 9 temperature–pressure probe (CTD). Casts included surface waters (down to 200 m depth), which we consider the zone where phytoplankton develops, and meso- and bathypelagic waters from 200 m down to 4,000 m depth where most biotic activity is driven by prokaryotes. A total of 10 depths were sampled, including 3-m, the depths receiving 20% and 7% of surface photosynthetically active radiation (PAR), the depth of the deep chlorophyll maximum (DCM) and at 20 meters below the DCM. Samples below the surface layer (> 200 m depth) were collected at the Deep Scattering Layer, the depth of the oxygen minimum, the depth of the maximum salinity and at 4,000 m depth, trying to cover the maximum variability of the deep ocean.

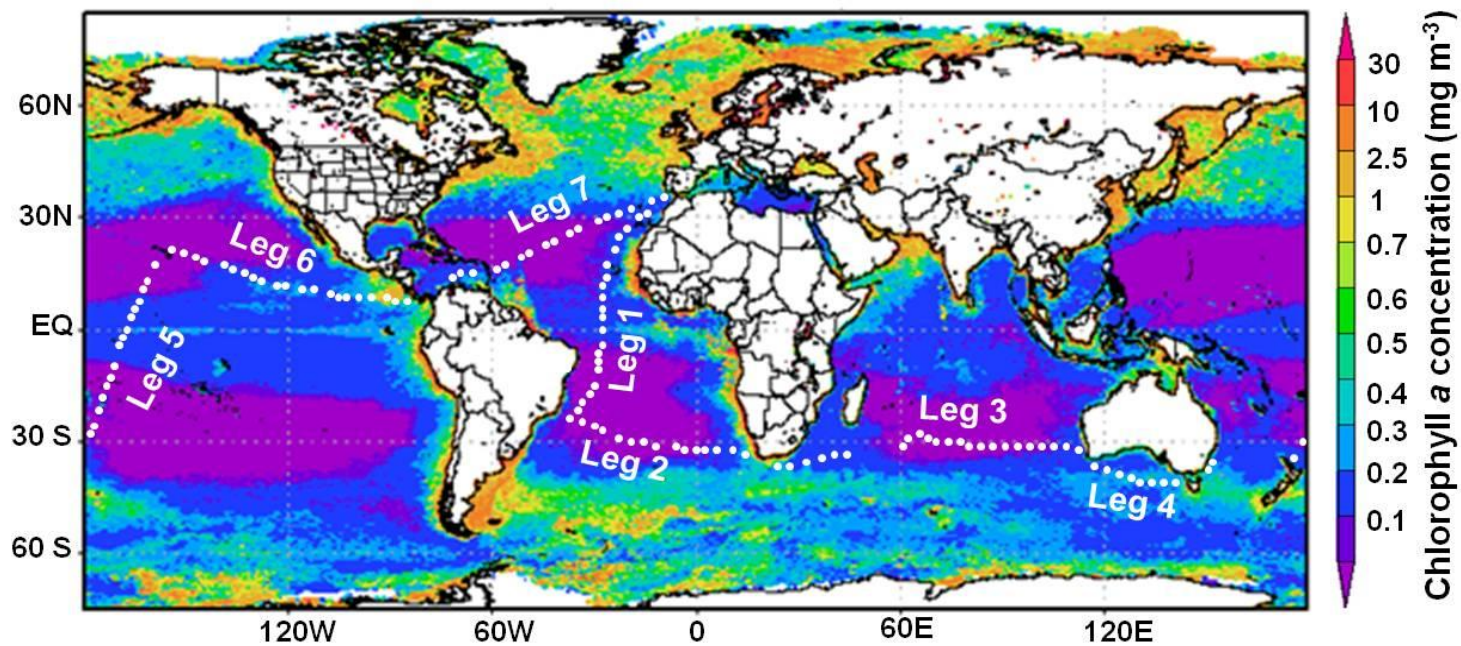


Figure 2. 1. Map of the circumnavigation expedition Malaspina 2010 showing the 125 sampling stations (white dots) distributed in seven legs where EP samples were collected at 10 depths from surface (3 m) and deep (down to 4,000 m) waters. Leg 1 from Cádiz, Spain to Rio de Janeiro, Brazil (23 stations), leg 2 from Rio de Janeiro to Cape Town, South Africa (15 stations), leg 3 from Cape Town to Perth, Australia (23 stations), leg 4 from Perth to Sydney, Australia (10 stations), leg 5 from Auckland, New Zealand to Honolulu, USA (18 stations), leg 6 from Honolulu to Panama (21 stations) and leg 7 from Cartagena de Indias, Colombia to Cádiz, Spain (15 stations). These stations were superimposed on a Moderate Resolution Imaging Spectroradiometer (MODIS) image (Source: <http://modis.gsfc.nasa.gov/>) of chlorophyll a averaged for the whole sampling period from December 16th 2010 to July 10th 2011.

Global distribution of exopolymer particles

2.3.2. *Biological and chemical analyses*

2.3.2.1. *Particulate organic carbon (POC)*

Samples for POC (4-6 L) were filtered through GF/F filters (Whatmann). POC was analyzed in a Carlo-Erba CHN analyzer after thawing the filters in an atmosphere of HCl fumes to remove carbonates. Blanks were determined from filters that have undergone every step in the procedure including the loading into filter holders, and had been washed with distilled water. Only samples for the epipelagic and mesopelagic zone were available.

2.3.2.2. *Concentration of exopolymer particles (EP)*

EP concentrations were determined using the alcian blue method (Passow and Alldredge, 1995). Duplicate or triplicate samples (250- 1500 ml) were gently filtered through 0.4 μm polycarbonate filters (25 mm diameter, Poretics) and the exopolymer particles (EP) retained on the filters were fully covered with 0.5 ml of a 0.02 % solution of alcian Blue (Sigma) in 0.06 % acetic acid (pH 2.5) for 5 seconds (Figure 2.2.). The stained filters were frozen at -80°C on board until analysis in the laboratory.

The alcian blue was extracted from the unfrozen filters adding 5 ml of sulfuric acid (80 % v/v) and the absorbance of the solution was measured at 787 nm in 1 cm-path disposable polystyrene cuvettes using ultrapure water as blanks (Figure 2.2.). Three blanks were performed in each batch of samples (including staining and freezing in parallel to the samples). Each solution of alcian blue was calibrated using a fresh standard solution of xanthan gum (XG). Four or five known volumes of XG solution were filtered through pre-weighed polycarbonate filters and weighted again to determine the exact quantity of the XG solution. Another similar set of filters were stained and analyzed, as described above, to get the correspondence between weights and absorbances. Then, a calibration curve was prepared for each alcian blue solution (Figure 2.3.).

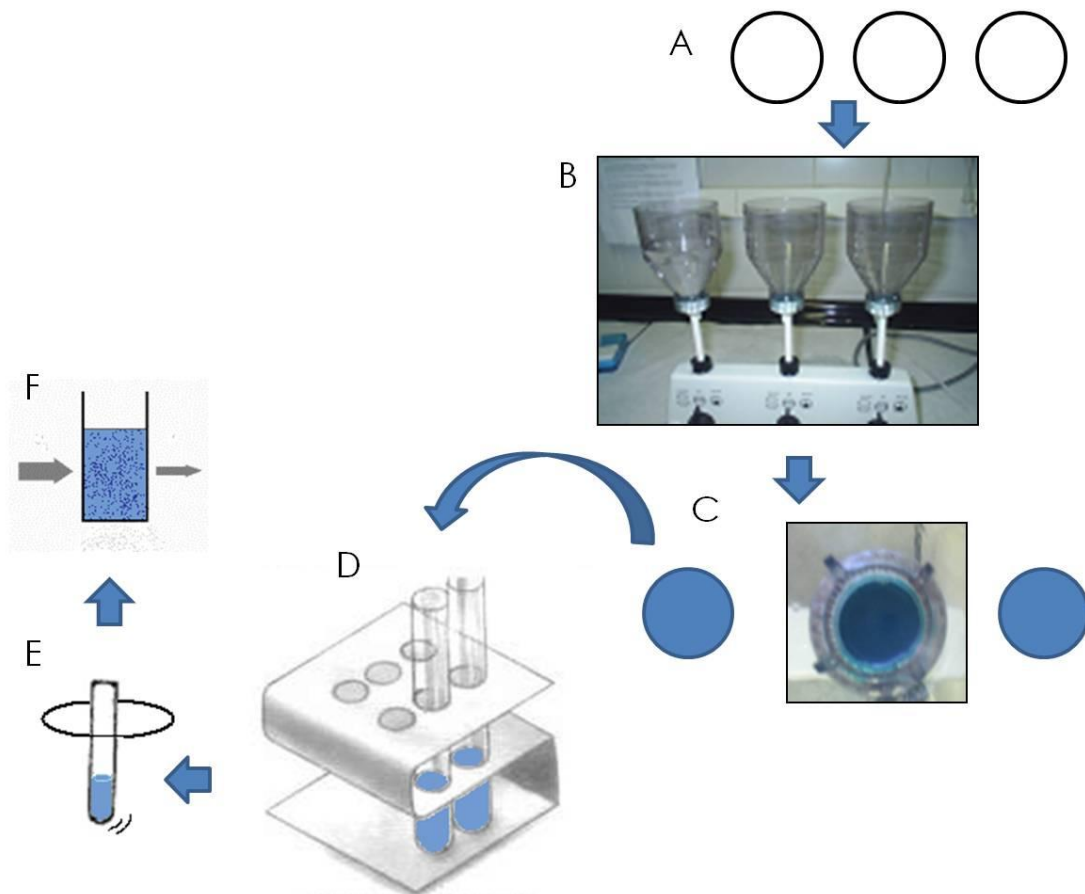


Figure 2. 2. Laboratory procedure to determinate EP concentrations by the colorimetric alcian blue technique. On board, the $0.4 \mu\text{m}$ polycarbonate filters (A) were placed in the filtration system (B) and the retained EP were stained with alcian blue solution (C). Then, the filters were frozen (-80°C). In the laboratory, the unfrozen and stained filters were placed in test tubes and extraction of the alcian blue dye was performed during 2 – 3 hour with sulfuric acid (80 %) (D) shaking several times during extraction (E). In the laboratory, the absorbance of the extracted solution was measured at 787 nm (F). More details in Mazuecos et al. (2012) (details in Annex IV).

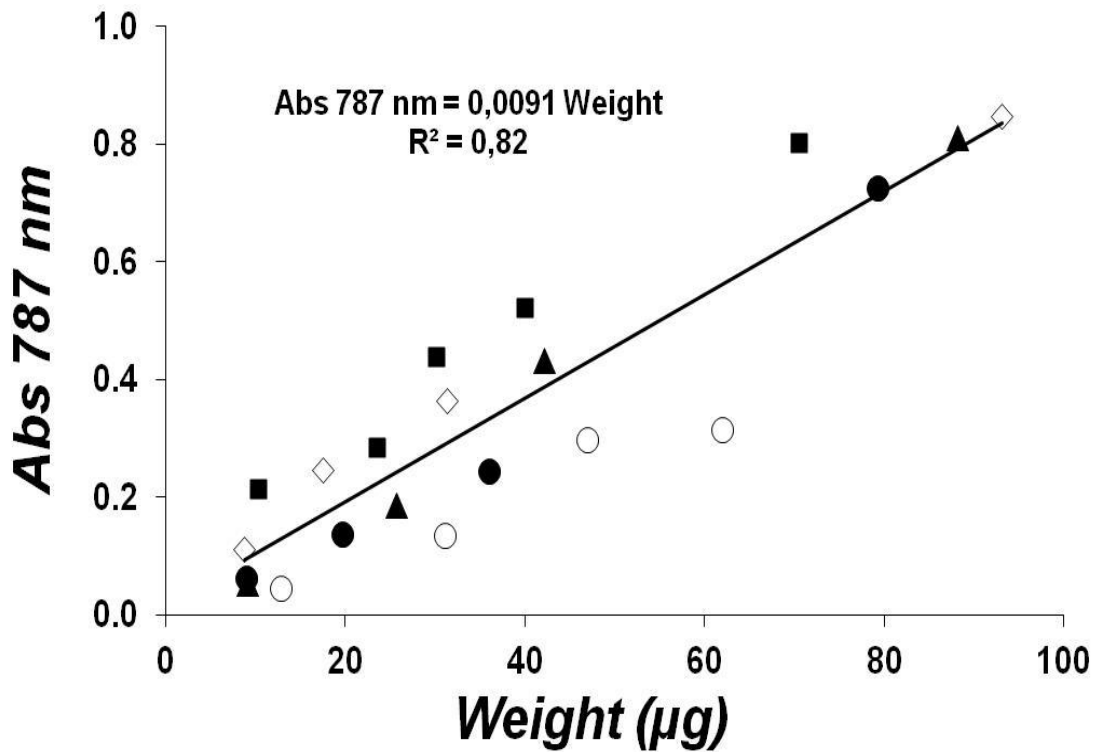


Figure 2. 3. Calibration curve (solid black line) used to relate the absorbance of alcian blue dye at 787 nm with the weight of Xanthan Gum (μg). The Xanthan Gum (XG) weight was obtained as the difference between before and after filtering a known XG solution. Each symbol represents different calibration curves.

The EP concentrations were calculated as:

$$\text{EP concentration } (\mu\text{g XG eq. L}^{-1}) = (A_{\text{sample}} - A_{\text{blank}}) V^{-1} \times f$$

where A_{sample} is the absorption of the sample at 787 nm, A_{blank} is absorption of the blank (filter + alcian blue), V is the filtered volume of seawater sample (L) and f is the calibration factor (1/slope). The results are expressed as μg of XG equivalents per liter ($\mu\text{g XG eq. L}^{-1}$). The detection limit of the technique was $2.2 \mu\text{g XG eq L}^{-1}$ and the average coefficient of variation in replicate samples was $\sim 20 \%$. Although there is not still a standard conversion factor, EP concentrations were converted into carbon units (C-EP) using the lowest and the overall conversion factors found in the literature of 0.51 and $0.75 \mu\text{g C per } \mu\text{g XG eq.}$ (Engel and Passow, 2001) to give an first approximation of carbon contained in the EP pool and the contribution to the global POC pool.

2.3.2.3. Primary production (PP)

The incorporation of carbon into the dissolved and particulate fractions was measured using the ^{14}C technique (Steeman-Nielsen, 1952; Marañón et al., 2001). Five or six depths were systematically sampled from near-surface waters to the DCM depth or in stations with shallow DCM the upper 100 m. Water samples (75 ml) were transferred to one dark and three light bottles at each depth and station. The samples were incubated under artificial light (12 hours) after addition of 10-20 μCi (370 K bq) of sodium bicarbonate ($\text{NaH}^{14}\text{CO}_3$). At the end of the incubations, 5-ml aliquots of each sample were placed into 20 ml scintillation vials for determination of total labelled organic carbon, total primary production (TPP), that includes the dissolved organic carbon (DOC) and the particulate organic carbon (POC) generated. An aliquot of 5 ml of each sample was filtered onto 0.20 μm polycarbonate filters and the water passing the filter was used to estimate DOC production. The remaining 65-ml of the water was filtered through 0.2 μm filters and the filters were collected for determination of the POC production. Filters were placed into vials and exposed to concentrated hydrochloric acid fumes for a minimum of 12 h before the addition of 3.5 ml Packard Ultima Gold liquid scintillation cocktail. Liquid samples (TPP and DOC) were acidified with 100 μl of hydrochloric acid (5 N) and shaken during 24 h before addition of 15 ml Ultima Gold XR scintillation cocktail. Radioactivity (disintegrations per minute, dpm) was measured in a Packard Tri-Carb 4000 scintillation counter. Dissolved or particulate primary production rates ($\mu\text{g C l}^{-1} \text{ d}^{-1}$) were calculated by subtracting the counts per minute of the dark bottles (dpm_{dark}) from the respective light ones ($\text{dpm}_{\text{light}}$) to correct for non-photosynthetic ^{14}C -incorporation. We used a value of 25,700 $\mu\text{g C l}^{-1}$ for the concentration of dissolved inorganic carbon (DIC). The formula used was:

Primary production ($\mu\text{g C l}^{-1} \text{ d}^{-1}$) = [incubated volume (ml) / filtered volume (ml)]
x DIC x [($\text{dpm}_{\text{light}}$ - dpm_{dark})/dpm added x incubation time (days)].

Global distribution of exopolymer particles

2.3.2.4. Chlorophyll *a* concentration (*chl a*)

Chl *a* concentration was determined fluorometrically after acetone extraction (Yentsch and Menzel, 1963). From 200 ml to 500 ml were filtered through 25 mm Whatman GF/F filters. Chl *a* was extracted after addition of 5-7 ml of 90% acetone, during 24 hours in the dark at 4 °C. After measurement of the fluorescence in a Turner Design fluorometer, concentration was calculated as: $\text{Chl } a \text{ } (\mu\text{g l}^{-1}) = F \times (R_s - R_a) \times V_a / V_s$ where *F* is the fluorimeter conversion factor, *R_s* is the fluorescence of the sample and *R_a* is the acetone blank, *V_a* is the 90% acetone volume added and *V_s* is the sample volume filtered.

2.3.2.5. Identification of phytoplankton groups

Abundances of *Synechococcus* sp., *Prochlorococcus* sp. and picoeukaryotes were quantified by flow cytometry (Collier, 2000) using a FACScalibur flow cytometer (BD Biosciences) fitted with a laser emitting at 488 nm. Three replicate samples were measured *in vivo* on board immediately after sampling. A calibrated solution of 1 µm diameter yellow-green fluorescent latex beads (Polysciences) was added as an internal standard for the quantification of cell concentrations. Identification was based on the red (FL3) and orange (FL2) fluorescence and side scatter (SSC) signals. The counts of cells and beads were obtained from the cytograms created by the Cell Quest software (Beckton-Dickinson), and then, converted to cell abundances (cell ml⁻¹) of each picophytoplankton population.

For larger specific algal groups, a volume of about 250 ml of water was introduced into glass bottles, fixed with hexamine-buffered formaldehyde solution at 1% final formalin concentration and stored until microscopic examination. 100 ml composite chambers were filled with sample that was allowed to settle during 48 hours. Two or more transects of the chamber bottom were examined with an inverted microscope (Utermöhl, 1958) under 312 X magnification to count the smaller cells, and the whole chamber bottom was scanned to identify the larger, less frequent forms. When possible, identification was made at the level of species, but many organisms had to be pooled in

categories such as “small dinoflagellates”, “small flagellates” or “small coccolithophorids” (in this case, mainly *Emiliana huxleyi* and *Gephyrocapsa sp.*).

2.3.2.5. Prokaryotic heterotrophic abundance (PHA) and production (PHP)

Prokaryotic heterotrophic abundance (PHA) was determined by flow cytometry (Gasol and del Giorgio, 2000), using a FACScalibur cytometer (BD Biosciences) fitted with a laser emitting at 488 nm. Samples were obtained from the same Niskin bottles and 1.5 ml aliquots were fixed with 1% of paraformaldehyde + 0.05 % glutaraldehyde (final concentrations), deep-frozen in liquid nitrogen and stored at -80 °C until analysis (less than one week after collection). Prokaryotes were stained with SybrGreen I (10x final), detected in a plot of side scatter against green fluorescence, and cyanobacteria were deleted in a plot of green vs red fluorescence. In the surface samples where *Prochlorococcus* could not unambiguously be separated from the other prokaryotes, we run a simultaneous unstained sample and the final concentration of cyanobacteria deleted from the total prokaryotic abundance counts. Flow rate was measured several times per day by measuring the volume acquired per unit of time with a well-calibrated pipette and after removal of the outer sleeve of the sample injection tube. This flow rate ($\mu\text{l min}^{-1}$) was used to convert the events min^{-1} into cellular concentrations. We used 1 μm yellow-green Polysciences beads for reference and to even up the scaling of scatter and fluorescence among samples.

Prokaryotic heterotrophic production (PHP) was estimated from ^3H -Leucine (specific activity=144.2 Ci mmol^{-1}) incorporation into proteins (Kirchman et al., 1985) using the microcentrifugation protocol proposed by Smith and Azam (1992). In the surface and mesopelagic waters, four replicates and two trichloroacetic acid (TCA)-killed blanks in microcentrifuge tubes (1.2 ml) were added L-[4, 5- ^3H] leucine at 20 nM. Samples and blanks were incubated (for 1 to 10 h) at *in situ* temperature. Incubations were stopped by addition of TCA to 50%, centrifuged (10 min. and 10000 r.p.m.) and rinsing with TCA 5%. Then, 1 ml scintillation cocktail, Optisafe HiSafe scintillation cocktail (Wallac-Perkin Elmer), was added. In the deep samples (≥ 1000 m depth) we used the filtration instead of centrifugation. L-[4, 5- ^3H] leucine at 5 nM of final concentration was added to

Global distribution of exopolymer particles

four 40 ml-replicates and two blanks (adding 4 ml of 37% formaldehyde) falcon tubes and then incubated for 4 to 12 hours. Incubations of the replicate samples were stopped adding 4 ml of 37% formaldehyde. Replicates and blanks were filtrated through 0.2 μm filters (47 μm diameter) and the filters were washed and rinsed three times with 5 ml TCA to 5% concentration. Dry filters were placed inside of scintillation vials and 9 ml scintillation cocktail (Optisafe FilterCount, Perkin-Elmer) was added. Radioactivity was measured in a liquid scintillation counter (Beckman LL6000) on board after 24 h.

Leucine incorporation rates were converted into carbon by using a theoretical factor of 1.55 kg C mol Leu⁻¹ (Simon and Azam, 1989), assuming that isotope dilution was negligible under the saturating concentration of ³H-Leucine.

2.3.2.6. *Viral abundance (VA)*

Viral abundance (VA) was counted by flow cytometry using a FACScalibur flow cytometer (BD Biosciences) fitted with a laser emitting at 488 nm (Brussaard, 2004). Samples (2 ml) were fixed with 25% glutaraldehyde (0.5 % final concentration), deep-frozen in liquid nitrogen and stored at - 80 °C until analyses in the lab as described in Marie et al (1999). Samples were diluted with TE (1x Tris-ethylenediaminetetraacetic acid) buffer such the event rate were between 100 to 800 viruses s⁻¹ and stained with SybrGreen I. Then, samples were run at a medium flow speed, rates ranging from 61 to 77 $\mu\text{l min}^{-1}$. Using these flow rates, VA (virus like particle l⁻¹) was determined from virus-like particle counts obtained in FL1 versus SSC plots.

2.3.3. *Data Analyses*

Statistical analyses were performed in Statistica 6.0 (StatSoft Inc., 1997). The data were log-transformed to fit the regression assumptions of normality and homoscedasticity. Regression analyses were performed to examine the relationships between EP distribution and the potential biological drivers: phytoplankton, heterotrophic prokaryotes and virus. Depth-integrated data were calculated using a conventional trapezoid method (Hornbeck, 1975).

2.3.3.1. Estimations of the EP export (EP F_{200}) and sequestration (EP F_{1000}) fluxes

To estimate the EP export fluxes at 200 m (EP F_{200}) and at 1000 m (EP F_{1000}), which has been called “sequestration” depth (Passow and Carlson, 2012) in $\text{mg C m}^{-2} \text{ d}^{-1}$, we first calculated the corresponding POC fluxes at these depths and then applied the relationship that we obtained between POC and EP in this large-scale oceanographic survey.

To determine the POC fluxes derived from primary production, we used the algorithm of Martin et al. (1987), as described by Yokokawa et al. (2013). First, we calculated the POC fluxes at 100 m depth (F_{100}) with the equation proposed by Berger and Wefer (1990) as:

$$\text{POC } F_{100} (\text{mg C m}^{-2} \text{ d}^{-1}) = 2 \times \text{PP}^{1/2} \times (\text{PP}/100)$$

where PP is the depth-integrated primary production measured during the circumnavigation. Then, we estimated the POC flux (F_z) at the two selected depths (z) of 200 m and 1000 m using the power function of Martin et al. (1987):

$$\text{POC } F_z (\text{mg C m}^{-2} \text{ d}^{-1}) = F_{100} \times (z/100)^{-b}$$

where b the coefficient of flux attenuation estimated with the equation proposed by Marsay et al. (2015). This coefficient is dependent on the median temperature in the upper 500 m (T):

$$b = (0.062 \times T) + 0.303$$

2.3.3.2. Transfer efficiency of exopolymer particles (EP TE) between zones

EP transfer efficiency (EP TE) between adjacent vertical zones (epi-, meso- and bathypelagic) is defined as the EP percentage that represents the EP concentration in top layer with respect the layer immediately below.

The EP transfer efficiency from epipelagic to mesopelagic waters (EP TE_{epi-meso}) was calculated as:

$$EPTE_{epi-meso} = \frac{[EP]_{>200m}^{<1000m} / l_{meso}}{[EP]_{>0m}^{<200m} / l_{epi}} \times 100$$

where $[EP]_{>200m}^{<1000m}$ is the depth-integrated EP concentration between 200 m and 1000 m depth, l_{meso} the length of mesopelagic zone in meters, $[EP]_{>0m}^{<200m}$ is the depth-

Global distribution of exopolymer particles

integrated EP concentration between surface and 200 m depth, l_{epi} is the length of epipelagic zone.

Additionally, the EP transfer efficiency from mesopelagic to bathypelagic waters ($EP\ TE_{meso-bathy}$) was calculated as:

$$EPTE_{meso-bathy} = \frac{[EP]_{>1000m}^{<4000m} / l_{bathy}}{[EP]_{>200m}^{<1000m} / l_{meso}} \times 100$$

where $[EP]_{>1000m}^{<4000m}$ is the depth-integrated EP concentration between 1000 m and 4000 m depth, l_{bathy} the length of bathypelagic zone, $[EP]_{>200m}^{<1000m}$ is the depth-integrated EP concentration between 200 m and 1000 m depth, and l_{meso} is the length of the mesopelagic zone in meters.

Finally, the contribution of EP to the total POC fluxes ($EP\ \%POC\ Flux$) at 200 m and 1000 m depths was calculated as:

$$EP\ \%POC\ Flux = (EP\ Flux / POC\ Flux) \times 100$$

2.4. Results

2.4.1. EP profiles and distribution across the different oceanic basins

EP profiles were very consistent across all the oceanic basins with systematic higher concentrations in the epipelagic zone than in the deep (>200 m) ocean (Figure 2.4.). EP concentrations at the epipelagic waters were very variable, ranging ca. three orders of magnitude from 0.4 to 173.6 $\mu\text{g XG eq l}^{-1}$ and a median value of 14.0 $\mu\text{g XG eq l}^{-1}$. It is noticeable that the highest EP concentrations were observed in surface waters of the South Atlantic Ocean (Figure 2.4.). The EP concentrations in the deep waters were very homogeneous, usually with values below 50 $\mu\text{g XG eq l}^{-1}$ (Figure 2.4.). The median concentration in the mesopelagic zone was of 5.3 $\mu\text{g XG eq l}^{-1}$, with a range from undetectable to 64.7 $\mu\text{g XG eq l}^{-1}$ and the concentrations in the bathypelagic zone ranged from undetectable to 40.6 $\mu\text{g XG eq l}^{-1}$ with a median value of 4.9 $\mu\text{g XG eq l}^{-1}$.

EP concentrations decreased with depth in all the oceanic basins (Figure 2.4.). The exponential fit of the regressions was $\text{EP } (\mu\text{g XG eq l}^{-1}) = 20.30 (\pm 0.73) e^{-2.64(\pm 0.33) \times \text{depth (km)}}$ ($r^2 = 0.15$ and $p\text{-value} < 0.001$), the power fit was $\text{EP } (\mu\text{g XG eq l}^{-1}) = 27.78 (\pm 1.57) \times \text{depth}^{-0.17 (\pm 0.01)}$ with depth expressed in meters ($r^2 = 0.14$ and $p\text{-value} < 0.001$) and the log-log regression was $\text{Log}_{10} \text{EP } (\mu\text{g XG eq l}^{-1}) = -0.25 (\pm 0.01) \text{Log}_{10} \text{depth (m)} + 1.47 (\pm 0.03)$ ($r^2 = 0.27$ and $p\text{-value} < 0.001$).

The regions with the highest EP concentrations in the epipelagic zone were observed in the South Atlantic Ocean close to the Benguela upwelling, in the North Pacific Ocean close to the upwellings of the Costa Rica Dome, in the Great Australian Bight coastal waters and in the equatorial regions (Figure 2.5. A, orange and green color). It is remarkable that the maximum EP concentrations in the epipelagic zone corresponded to regions with comparatively shallow DCM depths (black dashed lines in Figure 2.5. A), resulting in an inverse relationship between depth-integrated EP in epipelagic waters and the DCM depth ($N=118$; $\text{Log}_{10}\text{EP} = -0.46 (\pm 0.12) \text{Log}_{10}\text{DCM depth} + 4.09 (\pm 0.25)$, $r^2 = 0.11$, $p\text{-value} = 0.0003$). The shallower the DCM depth, the higher the epipelagic EP concentrations were. We also observed vast areas with extremely low EP concentrations, particularly important close to the Iberian coasts and in the

Global distribution of exopolymer particles

middle of the South Atlantic and Indian gyres. In the deep waters, the EP distribution reproduced a similar pattern to than observed in the epipelagic zone with maximum values in the upwelling regions (Figure 2.5. B). In fact, we found a significant and positive relationship between the depth-integrated EP concentrations in the epipelagic waters and the depth-integrated EP concentrations in the mesopelagic waters (Figure 2.6. A) as well as between these latter values and the depth-integrated EP concentrations in the bathypelagic waters (Figure 2.6. B). In fact, this mirror pattern between epipelagic and deep waters was statistically significant and suggests a major role of the EP downward exports at the global scale.

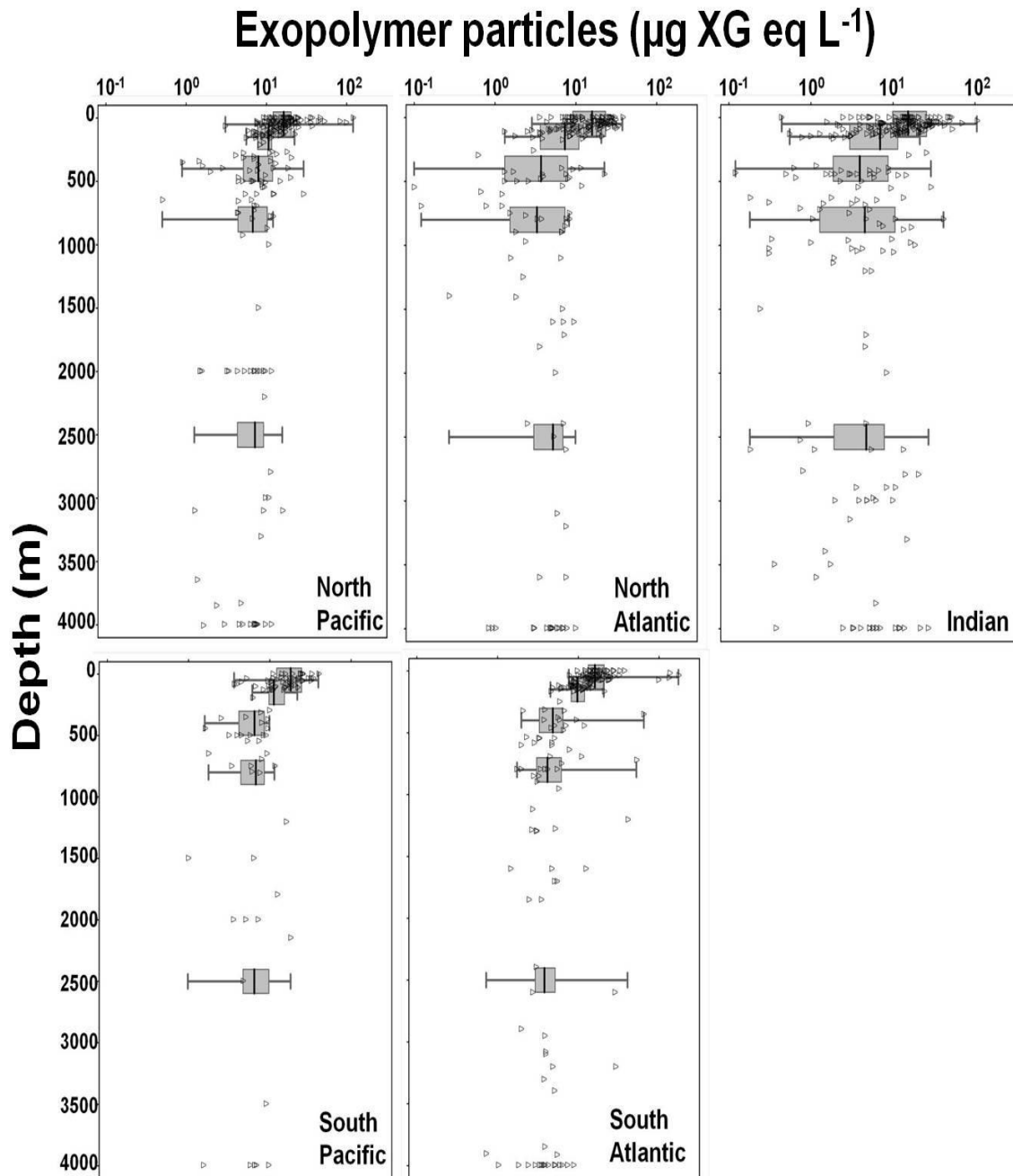


Figure 2. 4. Vertical profiles of exopolymer particles (Log_{10} -transformed) in different oceanic basins (North and South Pacific, North and South Atlantic and Indian Oceans). Gray open triangles correspond to the raw data. Gray boxes are the 25-75% percentiles, black lines inside the boxes represent the median values and the whiskers are the range of EP binned in the next intervals: 0 – 100 m, 100 – 200 m, 200 – 600 m, 600 – 1000 m, 1000 – 4000 m.

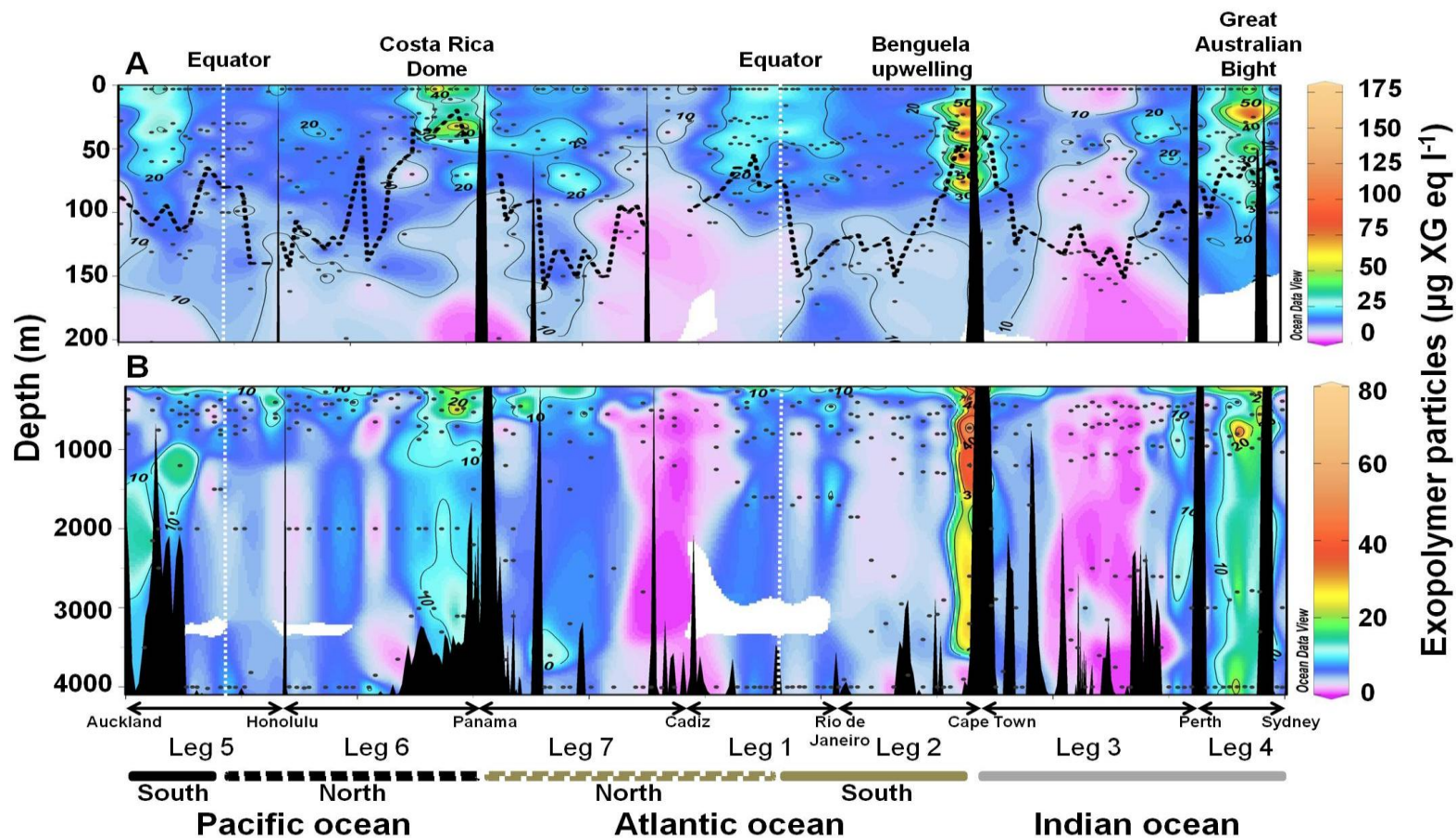


Figure 2. 5. Geographical distribution of the concentration of exopolymer particles in the epipelagic zone (from 3 m to 200 m depth) (A) and in the deep ocean (from 200 m to 4000 m) (B). Black dashed lines correspond to the Deep Chlorophyll Maximum depth and the vertical white dashed lines plot the equator. Note that the EP concentrations in the epipelagic and deep waters have different scales.

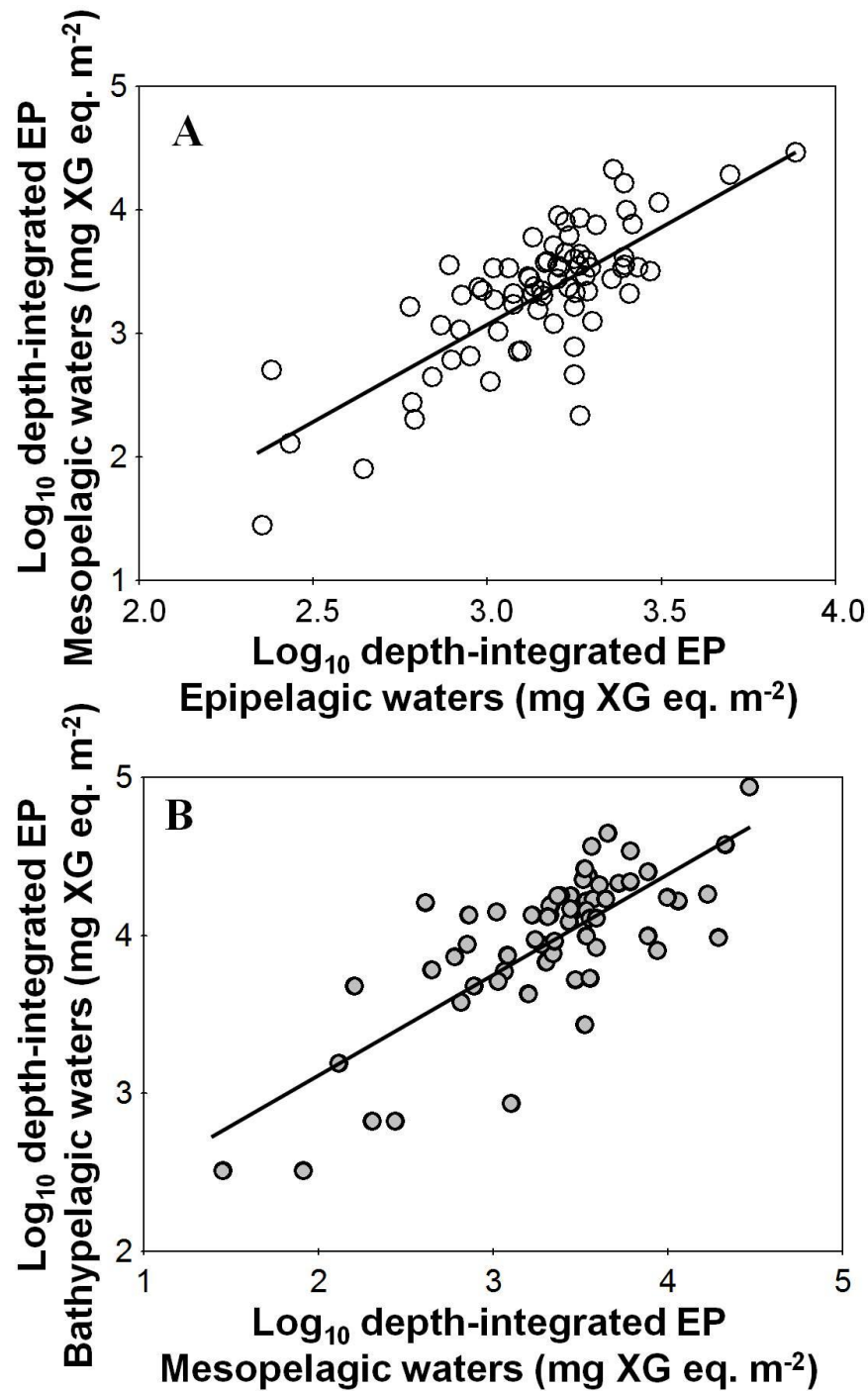


Figure 2. 6. Log-log relationships between depth-integrated EP (A) in the epipelagic (Epi-EP) and mesopelagic (Meso-EP) waters [$n = 74$, $r^2 = 0.58$ and p -value < 0.001 ; Log_{10} Meso-EP = $1.60 (\pm 0.16) \text{Log}_{10}$ Epi-EP - $1.71 (\pm 0.50)$] and (B) between depth-integrated EP in mesopelagic (Meso-EP) waters and depth-integrated EP in the bathypelagic waters (Bathy-EP) [$n = 65$, $r^2 = 0.58$ and p -value < 0.001 ; Log_{10} Bathy-EP = $0.64 (\pm 0.06) \text{Log}_{10}$ Meso-EP + $1.84 (\pm 0.23)$].

2.4.2. EP Contribution to the POC pool

We found a significant and positive correlation between EP and POC concentrations (Figure 2.7.).

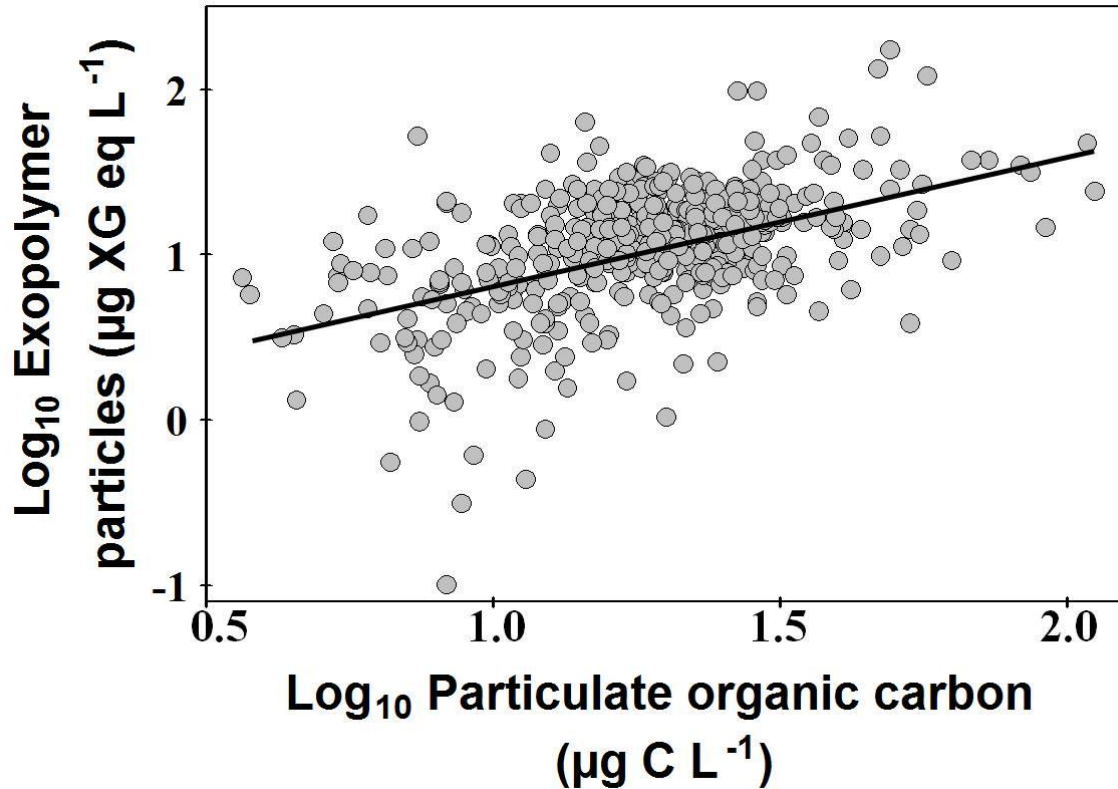


Figure 2. 7. Log-log relationship between exopolymer particles (EP) and particulate organic carbon (POC) including all epipelagic and mesopelagic samples available from this global study ($n = 478$; $\text{Log}_{10} \text{EP} = 0.73 (\pm 0.06) \text{Log}_{10} \text{POC} + 0.11 (\pm 0.08)$, $r^2 = 0.25$ and $p\text{-value} < 0.00001$).

We expressed EP concentration in carbon units (C-EP) to estimate the contribution of EP to the total POC pool (%POC) (Table 2.1.). The contribution of EP as % of POC was slightly higher in the epipelagic waters, and particularly in waters above the DCM depth, than in the mesopelagic waters. This percentage was particularly high at 3-m surface and subsurface depths (Table 2.1.).

Table 2. 1. Carbon content (C-EP) of the exopolymer particles, median and ranges in the epipelagic, mesopelagic and bathypelagic waters, estimated by using the conversion factors (CF) of 0.51 and 0.75 $\mu\text{g C per } \mu\text{g XG eq}$ (Engel and Passow, 2001), and their corresponding percentage of the POC pool [%POC = (C-EP / POC) x 100].

	Carbon content Median (Range) $\mu\text{g C l}^{-1}$	Median %POC		
		CF 0.51	CF 0.75	N
Epipelagic waters	10.5 (0.3-130.2)	33	48	411
Surface (3 m)	12.2 (0.3-89.9)	35	51	110
Subsurface	12.4 (1.1-130.2)	37	55	97
DCM	8.8 (0.4-99.7)	29	42	103
Below DCM	8.2 (0.6-73.8)	30	45	101
Mesopelagic waters	4.0 (0.0-48.5)	28	42	67
Bathypelagic waters	3.7 (0.0-30.4)	-	-	-

2.4.3. Biological factors driving EP distribution

We assessed the relevance of various biological factors shaping EP distributions both in the epipelagic zone and in the deep ocean by using regression analysis. Significant log-log relationships between EP concentration (as dependent variable) and different biological drivers (independent variables) in the epipelagic waters are shown in Table 2.2. (phytoplanktonic variables) and in Table 2.3. (heterotrophic variables).

We found a positive and significant relationship between EP concentration and primary production (PP), in volumetric terms, in all the oceanic basins except in the South Pacific (Table 2.2.). In addition, the depth-integrated EP concentration was also significantly related to the depth-integrated PP (Figure 2.8.), which underlines the main role of the phytoplanktonic exudates in determining EP concentration in surface waters. However, this positive relationship was not equally robust for the concentration of chlorophyll *a* in volumetric terms (Table 2.2.) or in depth-integrated values ($n = 118$; $r^2 = 0.09$, $p\text{-value} = 0.0009$ and $\text{slope} = 0.45 \pm 0.13$).

Global distribution of exopolymer particles

A detailed exploration of the influence of the different phytoplanktonic groups, showed that cyanobacteria (*Prochlorococcus* sp., *Synechococcus* sp.) were significant and positively related to EP concentration, although the explained variances were low, always below 36% (Table 2.2.). Despite these low variances, these relationships were consistent in all ocean basins with similar slopes among them (close to 0.20) and the slopes were also similar for both cyanobacteria types, *Prochlorococcus* sp. and *Synechococcus* sp., underlining the consistency of this pattern (Table 2.2.). Unexpectedly, we did not find any significant relationship between EP concentration and diatom abundances (Table 2.2.).

In relation to the role of heterotrophic prokaryotes and viruses in the epipelagic zone, we found positive relationships in volumetric terms, but with low explained variance (with values lower than 0.35) (Table 2.3.). The production by heterotrophic prokaryotes (PHP) and virus abundance (VA) were weakly correlated to EP concentration. However, PHA was more consistently correlated to EP concentration, except in the South Pacific. The slopes of these last relationships varied greatly between 0.14 in the North Pacific Ocean and 1.14 in the North Atlantic Ocean (Table 2.3.). The depth-integrated PHP and PHA in the epipelagic waters were not significantly correlated to the depth-integrated EP concentration (p-value > 0.05).

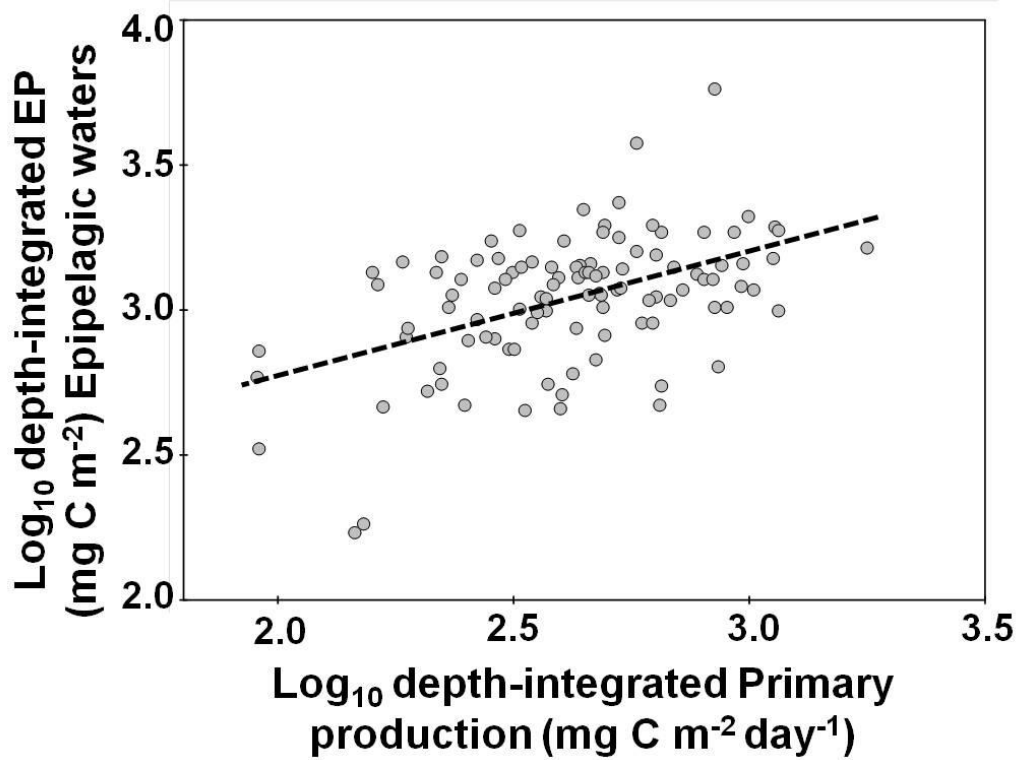


Figure 2. 8. Log-log relationship between depth-integrated exopolymer particles concentration (Epi-EP) and depth-integrated primary production (PP) in the epipelagic zone [n= 107, $r^2 = 0.23$ and p -value < 0.001; $\text{Log}_{10} \text{Epi-EP} = 0.42 (\pm 0.08) \text{Log}_{10} \text{PP} + 1.92 (\pm 0.20)$]. Depth-integrated EP concentrations are converted to carbon units using the overall conversion factor of $0.75 \mu\text{g C per } \mu\text{g XG eq.}$

Global distribution of exopolymer particles

Table 2. Results of the log-log regression analyses in the epipelagic waters between exopolymer particles and phytoplankton. * means significant regressions (p -value < 0.05) and n.s. indicates non-significant regressions. Other algal groups refer to the algal taxa that were not consistently visualized at all sampling stations.

Dependent var.	Independent var.	Geographical region	Slope (\pm SE)	Intercept. (\pm SE)	r^2	p -value	N
Exopolymer particles ($\mu\text{g XG eq l}^{-1}$)	Primary production ($\text{mg C m}^{-3} \text{ day}^{-1}$)	Global*	0.29 (\pm 0.04)	1.40 (\pm 0.03)	0.14	< 0.001	426
		South Pacific	-	-	-	n.s.	36
		North Pacific*	0.20 (\pm 0.05)	1.36 (\pm 0.04)	0.16	< 0.001	90
		North Atlantic*	0.39 (\pm 0.08)	1.40 (\pm 0.06)	0.19	< 0.001	94
		South Atlantic*	0.21 (\pm 0.08)	1.39 (\pm 0.07)	0.06	< 0.05	91
		Indian*	0.48 (\pm 0.09)	1.55 (\pm 0.10)	0.19	< 0.001	115
	Chlorophyll <i>a</i> ($\mu\text{g L}^{-1}$)	Global*	0.10 (\pm 0.04)	1.19 (\pm 0.03)	0.01	< 0.05	561
		South Pacific*	-0.43 (\pm 0.13)	0.90 (\pm 0.10)	0.18	< 0.05	49
		North Pacific	-	-	-	n.s.	122
		North Atlantic	-	-	-	n.s.	126
		South Atlantic	-	-	-	n.s.	115
		Indian*	0.36 (\pm 0.10)	1.31 (\pm 0.08)	0.07	< 0.001	149
	<i>Prochlorococcus</i> sp. (cell ml^{-1})	Global*	0.25 (\pm 0.03)	-0.08 (\pm 0.12)	0.15	< 0.001	586
		South Pacific*	0.30 (\pm 0.11)	-0.18 (\pm 0.52)	0.12	< 0.05	55
		North Pacific*	0.17 (\pm 0.05)	0.37 (\pm 0.24)	0.08	< 0.05	127
		North Atlantic*	0.14 (\pm 0.05)	0.47 (\pm 0.24)	0.07	< 0.05	120
		South Atlantic*	0.27 (\pm 0.06)	-0.24 (\pm 0.30)	0.14	< 0.001	125
		Indian*	0.36 (\pm 0.05)	-0.62 (\pm 0.24)	0.24	< 0.001	159
	<i>Synechococcus</i> sp. (cell ml^{-1})	Global*	0.20 (\pm 0.01)	0.52 (\pm 0.04)	0.26	< 0.001	589
		South Pacific	-	-	-	n.s.	55
		North Pacific*	0.15 (\pm 0.02)	0.70 (\pm 0.07)	0.32	< 0.001	127
North Atlantic*		0.23 (\pm 0.03)	0.36 (\pm 0.11)	0.29	< 0.001	128	
South Atlantic*		0.19 (\pm 0.03)	0.58 (\pm 0.09)	0.26	< 0.001	120	
Indian*		0.27 (\pm 0.03)	0.24 (\pm 0.09)	0.36	< 0.001	159	
Picoeukaryotes (cell ml^{-1})	Global*	0.24 (\pm 0.02)	0.44 (\pm 0.06)	0.17	< 0.001	586	
	South Pacific*	-0.23 (\pm 0.06)	1.77 (\pm 0.15)	0.22	< 0.001	55	
	North Pacific*	0.21 (\pm 0.03)	0.56 (\pm 0.10)	0.25	< 0.001	127	
	North Atlantic*	0.29 (\pm 0.06)	0.27 (\pm 0.18)	0.16	< 0.001	128	
	South Atlantic	-	-	-	n.s.	120	
	Indian*	0.39 (\pm 0.04)	0.00 (\pm 0.11)	0.36	< 0.001	159	
Coccolithophores (cell ml^{-1})	Global*	0.25 (\pm 0.05)	0.23 (\pm 0.18)	0.08	< 0.001	349	
	South Pacific*	-0.32 (\pm 0.12)	2.43 (\pm 0.43)	0.18	< 0.05	32	
	North Pacific	-	-	-	n.s.	72	
	North Atlantic	0.32 (\pm 0.12)	-0.10 (\pm 0.66)	0.05	0.065	77	
	South Atlantic*	0.28 (\pm 0.08)	0.15 (\pm 0.29)	0.17	< 0.001	71	
	Indian*	0.57 (\pm 0.10)	-0.99 (\pm 0.35)	0.27	< 0.001	97	
Diatoms (cell ml^{-1})	Global	0.06 (\pm 0.03)	1.01 (\pm 0.08)	0.01	0.069	349	
	South Pacific	-	-	-	n.s.	32	
	North Pacific	-	-	-	n.s.	72	
	North Atlantic	-	-	-	n.s.	77	
	South Atlantic	-	-	-	n.s.	71	
	Indian	-	-	-	n.s.	97	
Dinoflagellates (cell ml^{-1})	Global*	0.35 (\pm 0.06)	-0.01 (\pm 0.19)	0.04	< 0.001	349	
	South Pacific	-	-	-	n.s.	32	
	North Pacific	-	-	-	n.s.	72	
	North Atlantic*	0.31 (\pm 0.12)	0.09 (\pm 0.41)	0.08	< 0.05	77	
	South Atlantic*	0.26 (\pm 0.07)	0.33 (\pm 0.24)	0.16	< 0.001	71	
	Indian*	0.81 (\pm 0.14)	-1.68 (\pm 0.48)	0.26	< 0.001	97	
Other algal groups (cell ml^{-1})	Global*	0.21 (\pm 0.05)	0.37 (\pm 0.18)	0.06	< 0.001	349	
	South Pacific	-	-	-	n.s.	32	
	North Pacific*	0.21 (\pm 0.07)	0.41 (\pm 0.29)	0.10	< 0.05	72	
	North Atlantic	-	-	-	n.s.	77	
	South Atlantic*	0.25 (\pm 0.08)	0.26 (\pm 0.29)	0.14	< 0.05	71	
	Indian	0.23 (\pm 0.14)	0.28 (\pm 0.48)	0.03	0.096	97	

Table 2. 3. Results of the log-log regression analyses in the epipelagic waters between exopolymer particles and heterotrophic prokaryotes and viruses. * = significant regressions (p -value < 0.05) and n.s. means non-significant regression.

Dependent var.	Independent var.	Geographical region	Slope (\pm SE)	Intercept. (\pm SE)	r^2	p -value	N
Exopolymer particles ($\mu\text{g XG eq l}^{-1}$)	PH production ($\mu\text{g C l}^{-1} \text{d}^{-1}$)	Global*	0.07 (\pm 0.02)	1.16 (\pm 0.02)	0.02	< 0.05	558
		South Pacific	-	-	-	n.s.	51
		North Pacific*	0.08 (\pm 0.03)	1.22 (\pm 0.03)	0.05	< 0.05	128
		North Atlantic	-	-	-	n.s.	122
		South Atlantic*	0.13 (\pm 0.05)	1.23 (\pm 0.03)	0.06	< 0.05	108
		Indian	-	-	-	n.s.	149
	PH abundance (cell ml^{-1})	Global*	0.27 (\pm 0.05)	-0.43 (\pm 0.27)	0.05	< 0.001	573
		South Pacific	-	-	-	n.s.	56
		North Pacific*	0.14 (\pm 0.07)	0.34 (\pm 0.40)	0.03	< 0.05	128
		North Atlantic*	1.14 (\pm 0.14)	-5.55 (\pm 0.82)	0.35	< 0.001	126
		South Atlantic*	0.51 (\pm 0.10)	-1.75 (\pm 0.60)	0.18	< 0.001	113
		Indian*	0.40 (\pm 0.11)	-1.24 (\pm 0.66)	0.08	< 0.001	150
	Viral abundance (vir. ml^{-1})	Global*	0.18 (\pm 0.04)	-0.12 (\pm 0.28)	0.04	< 0.001	554
		South Pacific	-	-	-	n.s.	56
		North Pacific*	0.24 (\pm 0.08)	-0.46 (\pm 0.53)	0.08	< 0.05	119
North Atlantic*		0.28 (\pm 0.07)	-0.76 (\pm 0.50)	0.10	< 0.001	127	
South Atlantic		-	-	-	n.s.	93	
Indian*		0.31 (\pm 0.11)	-1.08 (\pm 0.76)	0.05	< 0.05	159	

In Table 2.4. we present the results of the regressions analysis in the mesopelagic zone. The EP concentrations were weakly correlated to PHA and PHP, while we did not find any relationship with VA. The relationships between EP concentrations and PHA were significant only in the Indian Ocean, while these relationships with the PHP rates were inconsistent with negative slopes in the Pacific basins, positive in the Atlantic basins and absent in the Indian basin (Table 2.4.). Interestingly, and unlike the epipelagic zone, the depth-integrated PHP was significant and positively related to the depth-integrated EP concentration (Figure 2.9.), and the depth-integrated PHA in mesopelagic waters was weakly and positively related to depth-integrated EP ($n = 72$; $r^2 = 0.07$, p -value < 0.05 and slope = 0.58 ± 0.25). No significant relationships were observed in the bathypelagic waters either considering the data in volumetric terms or the depth-integrated values.

Global distribution of exopolymer particles

Table 2. 4. Results of the log-log regression analyses in the mesopelagic waters between exopolymer particles and biological variables. * = significant regressions (p -value < 0.05) and n.s. means non-significant regression.

Dependent var.	Independent var.	Geographical region	Slope (\pm SE)	Intercept. (\pm SE)	r^2	p -value	N
Exopolymer particles ($\mu\text{g XG eq l}^{-1}$)	PH production ($\mu\text{g C l}^{-1} \text{d}^{-1}$)	Global*	0.15 (\pm 0.06)	0.89 (\pm 0.08)	0.04	< 0.05	190
		South Pacific*	-0.29 (\pm 0.11)	0.46 (\pm 0.12)	0.27	< 0.05	22
		North Pacific*	-0.20 (\pm 0.09)	0.59 (\pm 0.13)	0.08	< 0.05	55
		North Atlantic*	0.35 (\pm 0.13)	1.04 (\pm 0.19)	0.22	< 0.05	30
		South Atlantic	-	-	-	n.s.	32
		Indian	0.28 (\pm 0.16)	1.06 (\pm 0.30)	0.06	0.080	51
	PH abundance (cell l^{-1})	Global*	0.21 (\pm 0.11)	-0.43 (\pm 0.55)	0.02	< 0.05	203
		South Pacific	-	-	-	n.s.	23
		North Pacific	-	-	-	n.s.	56
		North Atlantic	-	-	-	n.s.	36
		South Atlantic	0.43 (\pm 0.22)	-1.44 (\pm 1.08)	0.11	0.057	34
		Indian*	0.96 (\pm 0.39)	-4.47 (\pm 2.03)	0.11	< 0.05	54
	Viral abundance (vir. ml^{-1})	Global	-	-	-	n.s.	194
		South Pacific	-	-	-	n.s.	23
		North Pacific	-	-	-	n.s.	54
North Atlantic		-	-	-	n.s.	37	
South Atlantic		-	-	-	n.s.	29	
Indian		-	-	-	n.s.	51	

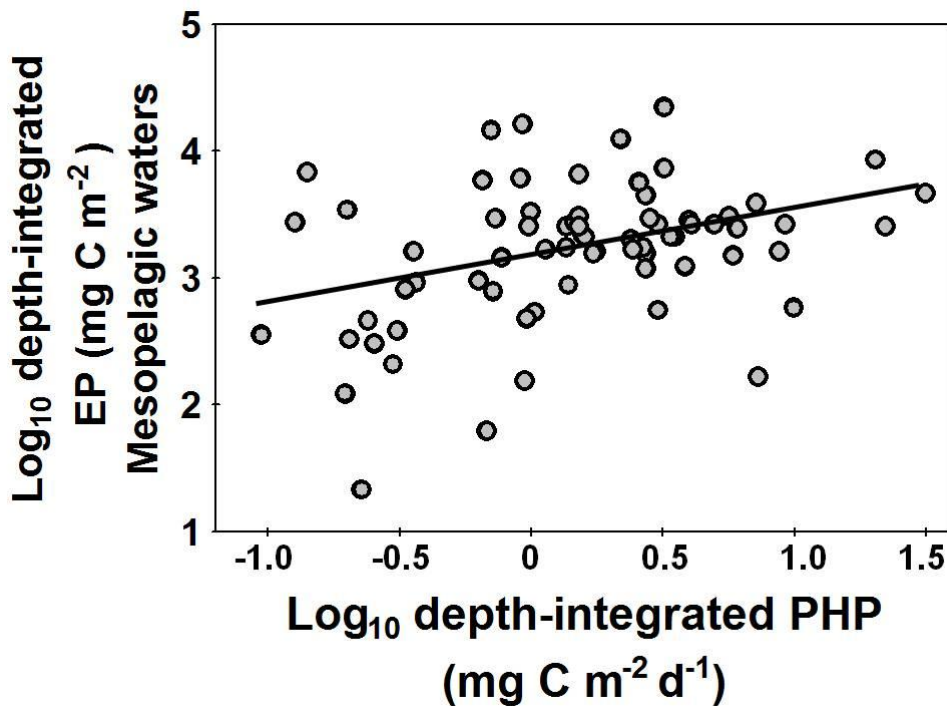


Figure 2. 9. Log-log relationship between depth-integrated EP concentrations and PHP in the mesopelagic zone [$n= 71$, $r^2 = 0.13$ and p -value < 0.001; $\text{Log}_{10} \text{Meso-EP} = 0.37 (\pm 0.11) \text{Log}_{10} \text{PHP} + 3.15 (\pm 0.06)$]. Depth-integrated EP concentrations are converted to carbon units using the overall conversion factor of $0.75 \mu\text{g C per } \mu\text{g XG eq}$.

2.4.4. EP export and sequestration fluxes

Estimates of the EP export fluxes (EP F_{200}) using the lowest and the overall carbon conversion factors are shown in the Table 2.5., with the highest values in the North Pacific and North Atlantic basins (Figure 2.10. A). EP transfer efficiency from epipelagic to mesopelagic waters (EP $TE_{\text{epi-meso}}$) showed that approximately one third of the epipelagic EP reached the mesopelagic waters. The average EP $TE_{\text{epi-meso}}$ was 35% ranging from 3 to 86 % (Table 2.5.), with the highest values in the North Pacific Ocean (Figure 2.10. B). Similarly, EP fluxes were about one third of the total POC flux at 200 m depth (EP % POC Flux₂₀₀) (Table 2.5.). The highest EP contributions to POC fluxes were observed in the Indian Ocean (Figure 2.10. C). The depth-integrated EP concentration in the mesopelagic waters (Meso-EP) was positive and significantly related to EP exports from 200 m [$n = 65$, $r^2 = 0.30$ and $p\text{-value} < 0.001$; $\text{Log}_{10} \text{Meso-EP} = 1.06 (\pm 0.20) \text{Log}_{10} \text{EP } F_{200} + 1.84 (\pm 0.27)$] (Figure 2.10. D) and to the EP transfer efficiency from epipelagic to mesopelagic waters [$n = 71$, $r^2 = 0.55$ and $p\text{-value} < 0.001$; $\text{Log}_{10} \text{Meso-EP} = 1.39 (\pm 0.15) \text{Log}_{10} \text{EP } TE_{\text{epi-meso}} + 1.14 (\pm 0.23)$] (Figure 2.10. E). However, EP contribution to the total POC flux from the epipelagic to the mesopelagic zone was significant but inversely related to the depth-integrated EP concentration in the mesopelagic waters [$n = 65$, $r^2 = 0.30$ and $p\text{-value} < 0.001$; $\text{Log}_{10} \text{Meso-EP} = -2.87 (\pm 0.55) \text{Log}_{10} \text{EP } \% \text{POC Flux}_{200} + 7.53 (\pm 0.83)$] (Figure 2.10. F).

Estimates of the EP fluxes at sequestration depth (EP F_{1000}) are also shown in Table 2.5. The highest values were observed in the North Pacific and North Atlantic basins, like the EP export fluxes (Figure 2.11. A). EP transfer efficiency from mesopelagic to bathypelagic waters (EP $TE_{\text{meso-bathy}}$) ranged from 25 to 245% (Table 2.5.), with values above 100 % in the South Pacific and North Atlantic Oceans (Figure 2.11. B) revealing that most of EP that reached the mesopelagic waters should be exported towards the bathypelagic zone along with other EP from different sources located in the mesopelagic zone. EP fluxes accounted for about half of the total POC flux at 1000 m depth (EP % POC Flux₁₀₀₀) (Table 2.5.). The highest EP contributions to POC fluxes were observed in the Indian Ocean

Global distribution of exopolymer particles

(Figure 2.11. C). The depth-integrated EP concentration in the bathypelagic waters (Bathy-EP) was positive and significantly related to the EP fluxes from 1000 m [$n = 60$, $r^2 = 0.31$ and $p\text{-value} < 0.001$; $\text{Log}_{10} \text{Bathy-EP} = 0.97 (\pm 0.19) \text{Log}_{10} \text{EP F}_{1000} + 3.27 (\pm 0.13)$] (Figure 2.11. D) and to the EP transfer efficiency from mesopelagic to bathypelagic waters, but more weakly [$n = 65$, $r^2 = 0.08$ and $p\text{-value} = 0.028$; $\text{Log}_{10} \text{Bathy-EP} = 0.60 (\pm 0.26) \text{Log}_{10} \text{EP TE}_{\text{meso-bathy}} + 2.70 (\pm 0.52)$] (Figure 2.11. E). In contrast, EP contribution to the total POC flux from the mesopelagic to the bathypelagic zone was significant but inversely related to the depth-integrated EP concentration in the bathypelagic waters [$n = 60$, $r^2 = 0.31$ and $p\text{-value} < 0.001$; $\text{Log}_{10} \text{Bathy-EP} = -2.61 (\pm 0.51) \text{Log}_{10} \text{EP \%POC Flux}_{1000} + 8.45 (\pm 0.90)$] (Figure 2.11. F).

Table 2. 5. Mean and range (in brackets) of the transfer efficiencies (TE) of exopolymer particles (EP) from epipelagic to mesopelagic waters (EP TE_{epi-meso}; %) and from mesopelagic to bathypelagic waters (EP TE_{meso-bathy}; %), as well as the estimated EP fluxes (EP F) and their percentages relative to the total POC fluxes [EP %POC Flux = (EP Flux/POC Flux) x 100] at 200 m (EP F₂₀₀ and EP % POC Flux₂₀₀) and 1000 m (EP F₁₀₀₀ and EP % POC Flux₁₀₀₀) depths, obtained with the algorithm of Martin et al. (1987) and using the lowest and the overall conversion factor from XG equivalent to carbon (CF), 0.51 and 0.75 µg C per µg XG eq reported by Engel and Passow (2001).

	EP F ₂₀₀ (mg C m ⁻² d ⁻¹)		EP TE _{epi-meso} (%)	EP % POC Flux ₂₀₀		EP F ₁₀₀₀ (mg C m ⁻² d ⁻¹)		EP TE _{meso-bathy} (%)	EP % POC Flux ₁₀₀₀	
	CF 0.51	CF 0.75		CF 0.51	CF 0.75	CF 0.51	CF 0.75		CF 0.51	CF 0.75
Global	17.0(2.3-56.5)	25.0 (3.4-83.0)	35 (3-86)	22 (13-41)	32 (19-60)	3.3 (0.4-10.4)	4.9 (0.6-15.3)	97 (25-245)	39 (24-78)	58 (35-114)
South Pacific	15.6 (5.0-33.6)	22.9 (7.4-49.3)	33 (11-55)	22 (15-31)	32 (23-46)	2.8 (0.9-5.9)	4.2 (1.4-8.6)	113 (63-168)	41 (29-58)	61 (43-85)
North Pacific	20.6 (7.8-56.5)	30.3 (11.4-83.0)	50 (12-86)	19 (13-26)	29 (19-39)	4.1 (1.6-10.4)	6.0 (2.3-15.3)	86 (32-173)	35 (24-48)	52 (35-70)
North Atlantic	22.5 (6.4-49.8)	33.1 (9.3-73.2)	26 (3-41)	19 (13-28)	27 (19-42)	4.1 (1.2-9.4)	6.0 (1.7-13.8)	115 (70-214)	35 (25-53)	52 (36-78)
South Atlantic	15.9 (9.1-31.7)	23.4 (13.3-46.6)	32 (18-56)	21 (16-25)	31 (23-37)	3.3 (2.0-8.1)	4.8 (2.9-11.9)	92 (29-174)	37 (26-44)	55 (38-64)
Indian	10.1 (2.3-35.5)	14.9 (3.4-52.2)	33 (5-85)	26 (15-41)	39 (22-60)	2.2 (0.4-6.6)	3.3 (0.6-9.7)	95 (25-245)	47 (28-78)	69 (41-114)

Global distribution of exopolymer particles

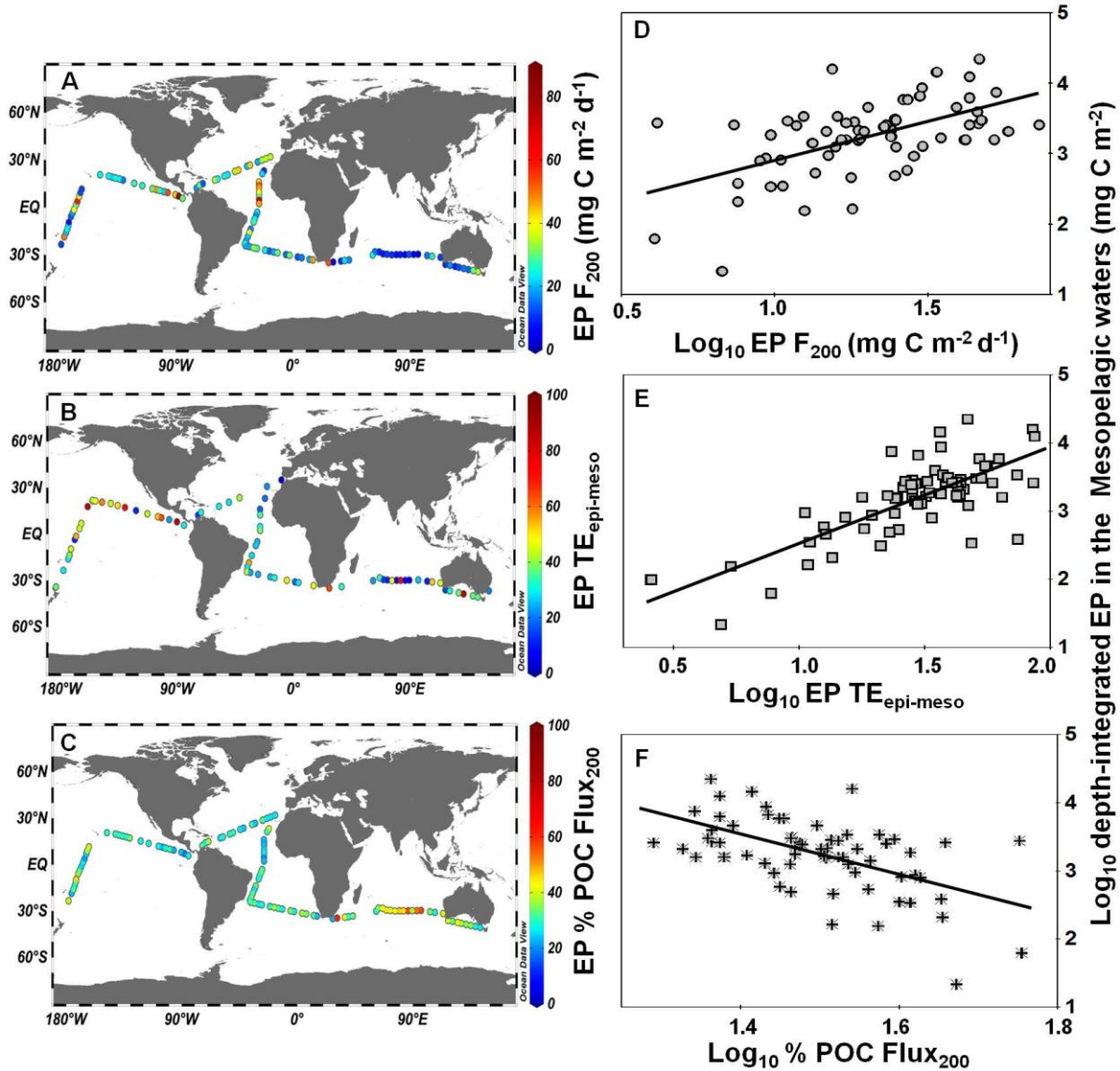


Figure 2. 10. Distribution along the circumnavigation Malaspina 2010 of the exopolymer particles (EP) fluxes at 200 m ($EP F_{200}$) (A), EP transfer efficiency to mesopelagic waters ($EP TE_{epi-meso}$) (B) and EP contribution to total POC ($EP \% POC Flux_{200}$) (C). Log-log relationships between depth-integrated EP in the mesopelagic waters (Meso-EP) and the estimated EP fluxes at 200 m (D), EP transfer efficiency from epipelagic to mesopelagic waters (E) and EP contribution to the total POC fluxes at 200 m ($EP \% POC Flux_{200}$) (F). EPF_{1000} fluxes and depth-integrated EP concentrations are converted to carbon units using the overall conversion factor of $0.75 \mu g C$ per $\mu g XG eq$.

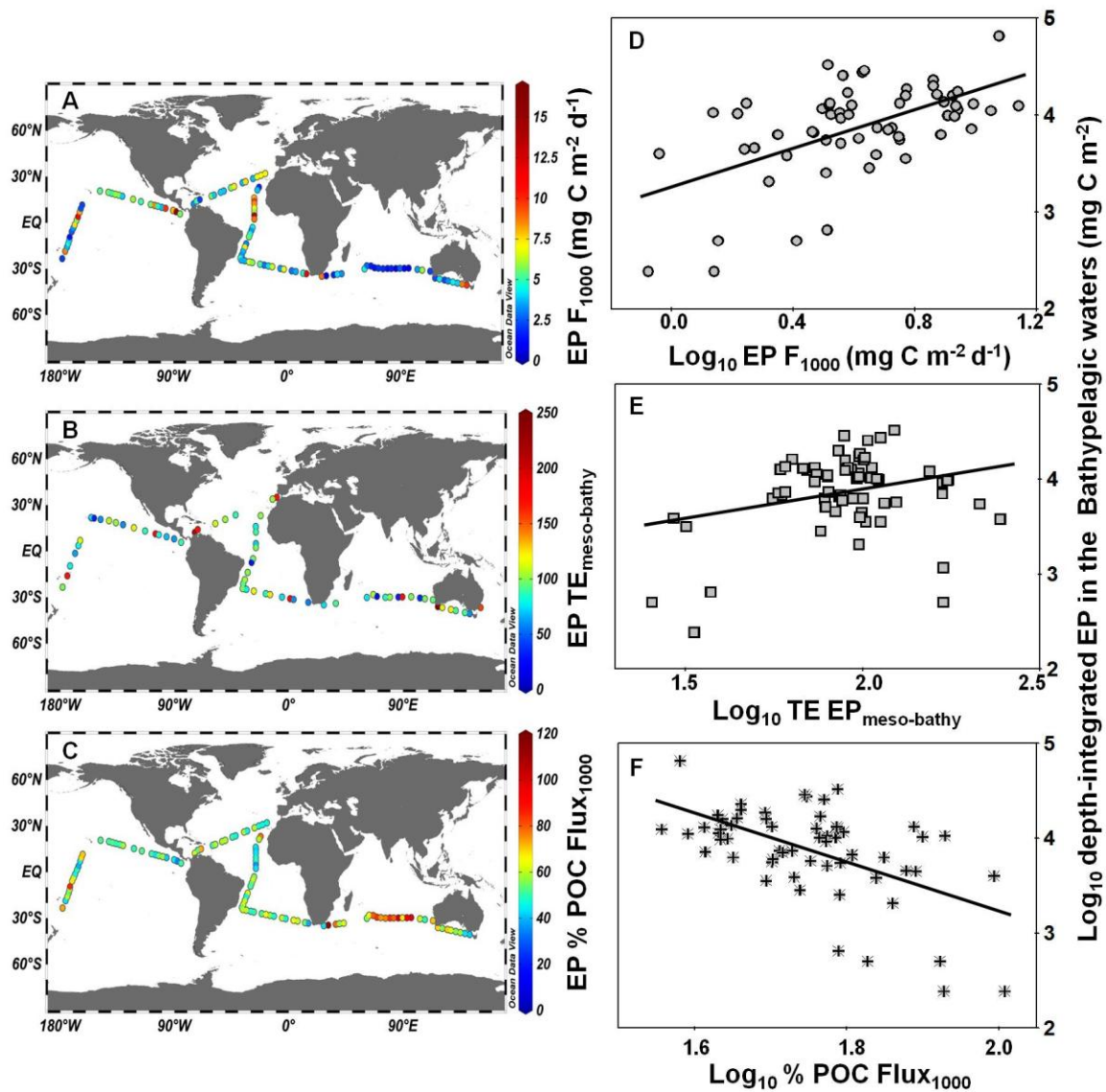


Figure 2. 11. Distribution along the circumnavigation Malaspina 2010 of the exopolymer particles (EP) fluxes at 1000 m ($EP F_{1000}$) (A), EP transfer efficiency to bathypelagic waters ($EP TE_{meso-bathy}$) (B) and EP contribution to total POC ($EP \% POC Flux_{1000}$) (C). Log-log relationships between depth-integrated EP in the bathypelagic waters (Bathy-EP) and the estimated EP fluxes at 1000 m (D), EP transfer efficiency from mesopelagic to bathypelagic waters (E) and EP contribution to the total POC fluxes at 1000 m ($EP \% POC Flux_{200}$) (F). $EP F_{1000}$ fluxes and depth-integrated EP concentrations are converted to carbon units using the overall conversion factor of $0.75 \mu\text{g C per } \mu\text{g XG eq}$.

2.5. Discussion

We provide here a first inventory of exopolymer particles (EP) from surface to deep waters in all the oceanic basins and have assessed their contribution to carbon export and sequestration into the deep ocean. We report a recurrent vertical pattern, irrespectively of the oceanic basins, with higher EP concentrations in the epipelagic waters above the depth of the chlorophyll *a* maximum and the EP geographical distribution was mainly related to primary production. In the mesopelagic and bathypelagic waters, EP concentrations were lower and mirrored, to some extent, the concentrations in the epipelagic waters suggesting the importance of exopolymer particles in export (on average, 32 %) and sequestration (on average, 58 %) fluxes of particulate carbon.

2.5.1. Global distribution of exopolymer particles

Compared to coastal waters, data on EP concentration in the open ocean are scarce, with values in the literature for the North Atlantic Ocean (Engel, 2004; Harlay et al., 2009; Leblanc et al., 2009), the Mediterranean Sea (Ortega-Retuerta et al., 2010; Bar-zeev et al., 2011) or the North Pacific Ocean (Kodama et al., 2014). Even more limited are the studies on EP concentration in deep waters (Kumar et al., 1998; Ramaiah et al., 2000; Prieto et al., 2006; Bar-Zeev et al., 2009, 2011; Kodama et al., 2014), and there are basically no data (Passow and Alldredge, 1995; Prieto et al., 2007) below the sequestration depth (i.e. 1000 m after Passow and Carlson, 2012).

The values previously reported for the epipelagic waters in the open ocean (Table 2.6.) are comparable to the values obtained in this study, only Bar zeev et al. (2011) in the Eastern Mediterranean Sea and Wurl et al. (2011) in the North Pacific Ocean observed values higher than the EP range obtained in this study. The maximum EP concentrations are generally found in the first meters of the water column well above the deep chlorophyll maximum (DCM). Ortega-Retuerta et al. (2009) and Wurl et al. (2011) also reported higher EP concentrations in the mixed layer or above the fluorescence maxima. Bar-Zeev et al. (2011), during the thermal stratification period in the Eastern Mediterranean Sea, observed that EP concentrations at the DCM were about 40% lower than in

the near-surface waters. Similarly, Kodama et al. (2014) in the oligotrophic region of the western North Pacific Ocean also reported that the EP subsurface maximum occurred immediately above the chlorophyll maximum. This net accumulation of low density EP in the first meters of the water column appears to be related to phytoplankton activity, although chl *a* concentration do not appear to be a relevant predictor of the global EP distribution. It is known that the highest rates of primary production are usually found above the DCM layer (e. g. Marañón et al., 2000; Pérez et al., 2006; Moreno-Ostos et al., 2011). Indeed, in our study EP concentration was better predicted by primary production than chlorophyll *a* concentration, both in volumetric terms and with depth-integrated data. The net accumulation of low density EP in the first meters of the water column seems related to the environmental conditions that affect phytoplankton activity. Phytoplankton stressed by high solar radiation and low inorganic nutrient availability would excrete EP and their dissolved precursors (Hong et al., 1997; Berman-Frank and Dubinsky, 1999; Corzo et al., 2000; Mari et al., 2005).

In relation to the regional EP distribution, we observe that the maximum EP concentrations in surface waters appeared in regions with shallow DCM depths, usually located in upwelling areas. Prieto et al. (2006) already detected that maximum EP concentrations were closely coupled to regions with favorable growing conditions for phytoplankton such as upwellings, fronts and regions of mixing, where nutrients increased in the photic zone (zones with shallower nutricline and DCM). Therefore, the DCM depth can also be considered a valuable proxy for EP distribution.

Exploring in detail the different phytoplankton groups, we observed that the most robust (higher significant variance values) and recurrent (in all the oceanic basins) relationships were obtained between EP concentration and the *Prochlorococcus* sp. and *Synechococcus* sp. abundances (Table 2.2.). Although it is known that cyanobacteria release extracellular dissolved organic carbon (Bertilsson et al., 2005; López-Sandoval et al., 2013; Becker et al., 2014) and these compounds might aggregate to form EP (Arrigo, 2007), most observations in specific areas such as the Adriatic Sea (Radic et al., 2005), the Strait of Gibraltar

(Macías et al., 2009) or the Celtic Sea (Van Oostende et al., 2012) had suggested that these algal species were not relevant in EP production. However, indirect evidences of aggregation and downward export of cyanobacteria-rich aggregates have also been detected (Lomas and Moran, 2011). Paradoxically, we found a good relationship between primary production and EP concentration in the epipelagic zone, but it was not associated to the major phytoplankton species in upwelling regions (i.e. diatoms), but with *cyanobacteria sp.* This apparent controversy might be related to most sampling stations are located in the open ocean and the planktonic community structure in this vast region is dominated by pico-autotrophs. Unlike the algal blooms, the picophytoplankton-dominated populations do not release large amounts of exopolymers, precursors of EP, but their contribution compared to the whole primary production would increase in the open ocean (Teira et al., 2001). In fact, in relation to the depth-integrated primary production corresponding to different algal groups classified by size, we observed that the depth-integrated EP concentrations in the epipelagic zone were differently related to depth-integrated primary production corresponding to micro-, nano- and picophytoplankton. The best positive relationship was for picophytoplankton ($r^2 = 0.13$ and $p\text{-value} < 0.001$), while nanophytoplankton was very weakly related ($r^2 = 0.05$ and $p\text{-value} < 0.05$) and microphytoplankton was unrelated ($p\text{-value} > 0.05$). This suggests that the epipelagic EP pool in the open ocean mostly depends on picophytoplankton activity.

The role of heterotrophic prokaryotes on EP abundance in the epipelagic zone appears to be very weak at this global scale (Table 2.3.). Despite some previous studies have evidenced that heterotrophic prokaryotic assemblages in surface waters can either directly generate EP or indirectly interact with the release of algal exudates and another detrital material, promoting accumulation and persistence of EP in surface waters (Radic et al., 2003; Rochelle-Newall et al., 2010; Ortega-Retuerta et al., 2010; Bar-Zeev et al., 2011; Van Oostende et al., 2013), we do not obtain strong relationships with prokaryotic heterotrophic production and they are very weak with abundance. Although EP production by phytoplankton can be also mediated by viral infection (Vardi et al., 2012), the

observed relationships between virus abundance and EP concentration are very weak in this study.

In spite of the lack of studies on EP concentration below the epipelagic zone (Table 2.6.), the few values published in the Gulf of Cadiz and the Strait of Gibraltar (Prieto et al., 2006), in the western North Pacific (Kodama et al., 2014) and in the Santa Barbara Channel (Passow and Alldredge, 1995) are in accordance with the EP ranges obtained in this study for meso- and bathypelagic waters. Exceptionally, higher EP concentrations in relation to those in the surface waters have been reported by Kumar et al. (1998) and Ramaiah et al. (2000) in the Arabian Sea, by Prieto et al. (2007) in a deep-sea hydrothermal system or by Bar-Zeev et al. (2009, 2011) in the Gulf of Aqaba and in the eastern Mediterranean Sea. In relation to the main biotic factors determining EP concentration in the deep waters, we observe that mesopelagic heterotrophic prokaryotic production was a significant predictor, although the low and contrasting values of the slopes (from -0.29 to 0.35) and the low explained variances (only up to 27%) suggest that other factors such as, for instance, the exports from epipelagic waters should contribute to the EP concentration in the deep ocean.

Global distribution of exopolymer particles

Table 2. 6. Compilation of the exopolymer particles concentrations (mean and ranges; given in $\mu\text{g XG eq l}^{-1}$) reported from the literature.

Geographic area	Conditions	Sampling date	Depth (m)	Mean (ranges)	Reference
<i>Atlantic Ocean</i>					
Open Northeast Atlantic	Bloom and post-bloom	1996	Open ocean surface (10 - 50)	28.5 (max. 124)	Engel, 2004
Northeast Atlantic	Bloom	Summer 2005	0 - 100	b.d. - 450 < 100 open ocean	Leblanc et al., 2009
English channel	Time series	Autumn and spring	Surface	281 (37 - 1735) 452 (26 - 3604)	Klein et al., 2011
Northeast Atlantic (Bay of Biscay)	Bloom	Spring 2006	Coastal surface open ocean surface	< 100 - 3000 40 - 120	Harlay et al., 2009
Northeast Atlantic (Bay of Biscay)	Blooms	Spring 2006 - 2008	0 - 100	22 - 1101	Van Oostende et al., 2012
Gulf of Cadiz	Different bloom phases	Summer 1997	0 - 100	118 (< 28 - 609)	García et al., 2002
		Spring 2001	0 - 200	25 - 205	Prieto et al., 2006
Gulf of Mexico (Guaymas Basin)	Hydrothermal System	Spring 2002	0 ~ 2010	7.8 - 6451	Prieto and Cowen, 2007
<i>Indian Ocean</i>					
Arabian Sea	Monsoon	Summer 1996	0 - 1000	< 50 - 1020	Ramaiah et al., 2000*
Arabian Sea (Dona Paula Bay)	Monsoon period	From 1998 to 2000	0 -1000	< 100 - 600	Kumar et al., 1998*
Bay of Bengal	Monsoon	Summer 1996	Surface	1300 - 149100	Bhaskar and Bhosle, 2006
			0 - 1000	70 - 130	Kumar et al., 1998*
<i>Pacific Ocean</i>					
Santa Barbara channel	Different blooms phases	1993 - 1994	0 - 500	14 - 252	<i>Passow and Alldredge, 1995</i>
Monterey Bay		Summer 1993	0 - 50	43 - 310	
Santa Barbara channel	Sea-surface microlayer	Autumn	Surface	138 - 5600	Wurl et al., 2009
Isahaya Bay (Japan)	Bloom and non-bloom	Spring and autumn 2007 - 2008	Surface	10 - 3490	Fukao et al., 2011
Subarctic Pacific (Otsuchi Bay, Japan)	Spring bloom, time series	Winter - Spring 1998	Surface (0 - 15)	1344 (24 - 2321)	Ramaiah et al., 2001
Great Barrier Reef (Australia)	-	Winter 1999 -2000	5	23 - 791	Wild, 2000
ALOHA off Hawaii	-	Winter 1999	-	253 (max. 477)	Prieto pers. com.
North Pacific and Offshore Hawaii	Open ocean	Summer 2009	Surface	< 50 - 780	Wurl et al., 2011**
East Sound (USA)	Bloom	Spring 1994	Surface (≤ 20 m)	50 - 160	Kjørboe et al., 1996
Sagami Bay (Japan)	Different trophic stages	2004 - 2005	0 - 120	50 - 250	Sugimoto et al., 2007
Western North Pacific	oligotrophic waters	Spring 2013	5-300	18-69	Kodama et al., 2014

<i>Other marine areas</i>					
Mediterranean Sea	Non bloom	Spring 2007	0 - 200	21.4 (4.5 – 94.3)	Ortega-Retuerta et al., 2010
Eastern Mediterranean sea	From different trophic stages to muscus event	2003 - 2004	0.5 - 4	101-748	Scoullos et al., 2006
Eastern Mediterranean sea	oligotrophic waters	2008 - 2009	Surface	116 - 420	<i>Bar-Zeev et al., 2011</i>
Northern Adriatic	mucus event	Summer 2002	DCM	48 - 189	Radíc et al., 2005
Arctic Ocean	Sea ice covered	Autumn and Spring 2009-2010	Deep (300 – 1000)	83 - 386	Wurl et al., 2011**
Gulf of Aqaba (Red Sea)	Time series	Spring 2008	2 - 20	570 (4 – 14800)	<i>Bar-Zeev et al., 2009</i>
Bransfield Strait (Antarctica)	Non bloom	Summer	Surface	80-1400	<i>Bar-Zeev et al., 2009</i>
Gerlache Strait	Non bloom	Summer	5, DCM and 300	23 - 228	Engel et al., 2002
Drake Passage	Non bloom	Summer	0 - 100	56.7 (b.d. – 345.9)	Engel et al., 2000
Anvers Island (Antarctica)	Non bloom	Summer	0 - 100	38 (b.d. - 283)	Jähmlich et al., 1998
Southern Ocean	Different bloom stages	Summer	0 - 100	35 (b.d. - 157)	Riebesell et al., 1995
Ross Sea	Non bloom	Winter 2005	Surface	15 - > 500	Passow et al., 1995
Central Baltic Sea	<i>Phaeocystis</i> bloom, times series	Winter 1994	0 - 200	15.4 (b.d. - 48.9)	Ortega-Retuerta et al., 2009
Western Baltic Sea	Non Bloom	Summer 1999	0 - 150	308 (b.d. - 2800)	Hong et al., 1997
Mecklenburg bight (Western Baltic Sea)	Bloom	Spring	0 - 20	200 (145 - 322)	Engel et al., 2002
Norwegian Fjords	-	Autumn 1994	Surface	1300 (max. 5300)	Engel et al., 2000
Norwegian fjords	Bloom	Spring 1992	Bottom (16 - 26)	267 - 471	Jähmlich et al., 1998
	Different trophic stages	Spring 1992	0 - 63	100 - 255	Riebesell et al., 1995
Global subtropical Atlantic, Indian and Pacific Oceans	Non bloom	Dec 2010 - Jul 2011	Epipelagic 0-200	< 1 - 173	<i>This study</i>
			Mesopelagic 200 - 1000	b.d. - 65	
			Bathypelagic 1000 - 4000	b.d. - 41	

References in **bold** show EP concentrations in the open ocean and references in italics refer to EP values in the deep ocean (≥ 200 m). *References: Ramaiah et al. (2000) and Kumar et al. (1998), EP concentrations were given as mg of alginic acid equivalents per liter. For transformation into xanthan gum units, the Engel and Passow (2001) conversion factor of 1 mg alginic acid equivalents $l^{-1} = 10 \mu g$ XG eq l^{-1} was used. **Reference: Wurl et al. (2011), the EP concentrations were given in μmol C L^{-1} . For transformation into xanthan gum units, the Engel (2004) conversion factor of 0.63 was applied. b.d. = values below detection.

Global distribution of exopolymer particles

2.5.2. Export and sequestration fluxes of exopolymer particles

The robust correlations found among the depth-integrated EP concentrations in the epipelagic, mesopelagic and bathypelagic waters (Figure 2.6.) confirmed that the EP distribution in the deep ocean was, to a relevant extent, mostly dependent on the sinking of exopolymer particles from epipelagic waters. In fact, the estimated (using *in situ* primary production and temperature) fluxes of exopolymer particles at 200 m (EP F₂₀₀) and 1000 m (EP F₁₀₀₀) predicted the depth-integrated EP concentrations in their corresponding mesopelagic and bathypelagic zones (Figures 2.10. and 2.11.). Martin et al. (2011), during a sub-polar North Atlantic spring phytoplankton bloom, determined that between 25% and 43% of the EP-containing particulate carbon at 100 m depth was exported below 750 m. Similarly, Bar-Zeev et al. (2009) observed an export of EP from surface waters to deeper waters (down to 300 m) during a diatom bloom in the Gulf of Aqaba. However, other authors did not observe a relevant link between a high concentration of diatom-rich aggregates in an upwelling bloom in surface waters and the vertical aggregates flux (Kiørboe et al., 1998).

Although the sinking EP fraction could be variable, our predicted EP fluxes at 200 m and 1000 m depths (Table 2.5.) were in accordance with the measured EP fluxes at different intermediate depths reported by Passow (2002a) (from 7 to 70 mg C m⁻² d⁻¹), Ramaiah et al. (2005) (from 29 to 62 mg C m⁻² d⁻¹), Waite et al. (2005) (up to 25 mg C m⁻² d⁻¹), Reigstad and Wassmann (2007) (up to 390 mg C m⁻² d⁻¹) or Martin et al. (2011) (from undetectable to 120 mg C m⁻² d⁻¹). The highest EP fluxes both at 200 m and 1000 m were observed in the equatorial waters of the Pacific and Atlantic Oceans coincident with the equatorial upwelling (Figures 2.10. and 2.11.).

If we assume constant rates over the year and we use the most conservative CF to carbon (0.51 µg C per µg XG eq), the annual global rates of EP F₂₀₀ and EP F₁₀₀₀ in our study would average 6.2 g C m⁻² yr⁻¹ at 200 m and 1.2 g C m⁻² yr⁻¹ at 1000 m depth. Considering an ocean surface at 3.6 × 10¹⁴ m², the contribution of EP to C export below sequestration depth (>1000 m) would be

estimated to be 0.4 Pg C yr^{-1} . This global EP flux below the sequestration depth would be of the same magnitude that the estimated range of POC sequestration from 0.2 to 0.7 Pg C yr^{-1} (Sarmiento and Gruber, 2002; Dunne et al., 2007; Honjo et al., 2008; Henson et al., 2012; Guidi et al., 2015). Therefore, these calculations and the high EP percentages relative to POC fluxes at sequestration depths (between 24 and 78% of POC fluxes) emphasize the role of EP in the biological carbon pump.

Since EP concentrations in the deep ocean were systematically lower than in the epipelagic waters and only 35 % of the epipelagic EP are sunk to the mesopelagic waters ($EP \text{ TE}_{\text{epi-meso}}$), likely a significant fraction of the organic material has to be rapidly either remineralized or dispersed during its transit from epipelagic waters to the mesopelagic waters (Buesseler et al., 2007). The aggregate settling rate depends on its size and density (Burd and Jackson, 2009). Polymeric self-assembly (the physico-chemical process that brings polymers together to form gel particles, i.e. microgels) or coagulation (the physical process that bring particles together) occur under conditions of high particle concentration, such as in phytoplankton blooms (Chin et al., 1998; Burd and Jackson, 2009; Verdugo, 2012). Therefore, these density-dependent processes may be insignificant in the deep ocean, where polymer and particle concentrations are low and exopolymer dispersion and particle disaggregation might be the prevailing processes. In fact, the very limited data on the abundance of self-assembled microgels (Verdugo et al., 2008) indicated a clear decline with depth from 1.8×10^9 microgels l^{-1} at 50 m to 3.4×10^8 microgels l^{-1} at 1100 m in the BATS station or from 3.5×10^8 microgels l^{-1} at 100 m to 1.4×10^8 microgels l^{-1} at 4,000 m in the ALOHA station.

However, the estimated transfer efficiency between mesopelagic and bathypelagic zones ($EP \text{ TE}_{\text{meso-bathy}}$), in some areas, had values higher than 100% (Figure 2.11.). This fact suggests a *de novo* EP synthesis or lateral exports inside the mesopelagic zone. Prokaryotes in the deep ocean appear to be better adapted to a particle-attached lifestyle (Herndl and Reinthaler, 2013), releasing EP precursors under favorable conditions to form suspended “*protobiofilms*”

Global distribution of exopolymer particles

(referred to EP with extensive microbial outgrowth and colonization; Bar-Zeev et al., 2012). Indeed, several studies (Lauro and Barlett, 2007; Lauro et al., 2009) have shown that deep water prokaryotes possess larger genomes than their surface water counterparts, that they use in a more versatile and opportunistic life mode.

The global carbon content of EP was estimated using the average carbon content in the epipelagic, mesopelagic and bathypelagic zones. We then, knowing the total area of the global ocean (Eakins and Sharman, 2010), calculated the global EP in term of carbon in each layer and integrated them to yield a first rough estimate of the EP carbon content in the global ocean of 4.8 Pg C, using the most conservative CF.

The global carbon estimates resulted in 0.6 Pg C for the epipelagic zone and 4.2 Pg C for the deep ocean (using the lowest conversion factor of 0.51). Comparatively, this estimated global EP carbon would represent between one quarter and two fifths (considering the lowest 0.51 and highest 0.88 conversion factors reported in the literature; Engel and Passow, 2001) of the total POC of the epipelagic zone, ~ 2.3 Pg C (Stramska, 2009). Our global EP calculations also account for approximately between one quarter and two fifths of the global POC estimations (~ 20 Pg C) reported by Cauwet (1978).

Acknowledgements

We thank our scientific colleagues and C. M. Duarte for the coordination of the Malaspina expedition, as well as the technical staff and crew members on board the BIO Hespérides, for their support in the field sampling during the different legs of the Malaspina cruise. This paper is a contribution to the INGENIO 2010 CONSOLIDER program (CDS2008-00077). IPM was supported by a JAE Pre-doc fellowship, from the Spanish National Research Council (CSIC) and the BBVA Foundation, Spain. IPM, JA and JMG were partly supported by project HotMix (CTM2011-30010-C02/MAR).

2.6. References

- Allredge A. L., Silver M. W. 1988. Characteristics, dynamics and significance of snow marine. *Progress in Oceanography*, 20 (1): 41 - 82.
- Allredge A. L., Passow U., Logan B. E. 1993. The abundance and significance of a class of large, transparent organic particles in the ocean. *Deep-Sea Research I*, 40 (6): 1131 - 1140.
- Arrigo K. R. 2007. Carbon cycle: Marine manipulations. *Nature*, 450: 491 - 492.
- Azam F., Long R. A. 2001. Sea snow microcosms. *Nature*, 414: 495 -497.
- Bar-Zeev E., Berman T., Rahav E., Dishon G., Herut B., Kress N. and Berman-Frank I. 2011. Transparent exopolymer particle (TEP) dynamics in the eastern Mediterranean sea. *Marine Ecology Progress Series*, 431: 107 - 118.
- Bar-Zeev E., Berman-Frank I., Stambler N., Vazquez E. D., Zohary T., Capuzzos E., Meeder E., Suggests D. J., Iluz D., Dishon G. and Berman T. 2009. Transparent exopolymer particles (TEP) link phytoplankton and bacterial production in the Gulf of Aqaba. *Aquatic Microbial Ecology*, 56: 217 - 225.
- Bar-Zeev E., Berman-Frank I., Girshevitz O., Berman T. 2012. Revised paradigm of aquatic biofilm formation facilitated by microgel transparent exopolymer particles. *PNAs*, 109 (23): 9119 - 9124.
- Becker J. W., Berub P. M., Follet C. L., Waterbury J. B., Chisholm S. W., DeLong E. F. and Repeta J. 2014. Closely related phytoplankton species produce similar suites of dissolved organic matter. *Frontiers in Microbiology*, doi: 10.3389/fmicb.2014.00111
- Berger W. H., Wefer G. 1990. Export production: Seasonality and intermittency, and paleoceanographic implications. *Paleogeogr. Paleoclimatol. Paleoecol.* 89: 245 - 254. doi:10.1016/0031-0182(90)90065-F
- Berman-Frank I., Dubinsky Z. 1999. Balanced growth in aquatic plants: Mith or reality? Phytoplankton uses the imbalance between carbon assimilation and biomass production to their strategic advantage. *Bioscience*, 49 (1): 29 - 37.
- Berman-Frank I., Rosenberg G., Levitan O., Haramaty L., Mari X. 2007. Coupling between autocatalytic cell death and transparent exopolymeric particle production in the marine cyanobacterium *Trichodesmium*. *Environmental Microbiology*, 9(6): 1415 - 1422.
- Bertilsson, S., Berglund, O., Pullin, M. J., and Chisholm, S. W. 2005. Release of dissolved organic matter by *Prochlorococcus*. *Vie et Milieu* 55, 225-232.
- Bhaskar P. V., Bhosle N. B. 2006. Dynamics of transparent exopolymeric particles (TEP) and particle-associated carbohydrates in the Dona Paula bay, west coast of India. *Journal of Earth System Science*, 115: 403 - 413.
- Brussaard C. P. D. 2004. Optimisation of procedures for counting viruses by flow cytometry. *Applied Environmental Microbiology*. 70: 1506 - 1513.
- Buesseler, K. O., Lamborg C. H., Boyd P. W., Lam P J., Trull T. W., Bidigare R. R., Bishop K. B., Casciotti K. L., Dehairs F., Elskens M., Honda M., Karl D. M., Siegel D. A., Silver M. W., Steinberg D. K., Valdes J., Van Mooy B., Wilson S. 2007. Revisiting carbon flux through the ocean's twilight zone. *Science*, 316: 567 - 570.
- Burd A. B., Jackson G. A. 2009. Particle Aggregation. *Annual review of Marine Science*, 1: 65-90.
- Cauwet G. 1978. Organic chemistry of seawater particulates. Concepts and developments. *Oceanologica Acta*, 1(1): 99 - 105.
- Chin W.-C., Orellana M. V., Verdugo P. 1998. Spontaneous assembly of marine dissolved organic matter into polymer gels. *Nature*, 391: 568 - 572.
- Claquin P., Probert I., Lefebvre S., Veron B. 2008. Effects of temperature on photosynthetic parameters and TEP production in eight species of marine microalgae. *Aquatic Microbial Ecology*, 51: 1 - 11.
- Collier J. L. 2000. Flow cytometry and the single cell in phycology. *Journal of Phycology*, 36 (4): 628 - 644.
- Corzo A., Morillo J. A., Rodríguez S. 2000. Production of transparent exopolymer particles (TEP) in cultures of *Chaetoceros calcitrans* under nitrogen limitation. *Aquatic Microbial Ecology*, 23: 63 - 72.
- Corzo A., Rodríguez-Gálvez S., Lubian L., Sangrá P., Martínez A., Morillo J.A. 2005. Spatial distribution of transparent exopolymer particles in the Bransfield Strait. *Antarctica Journal Plankton Research*, 27 (7): 635 - 646.

- Dunne J. P., Sarmiento J. L., Gnanadesikan A. 2007. A synthesis of global particle export from the surface ocean and cycling through the ocean interior and on the seafloor. *Global Biogeochemical Cycles*, 21, GB4006. doi:10.1029/2006GB002907.
- De la Rocha C., Passow U. 2007. Factors influencing the sinking of POC and the efficiency of the biological carbon pump. *Deep-Sea Research II*, 54: 639 – 658.
- Eakins B.W., Sharman G.F. 2010. *Volumes of the World's Oceans from ETOPO1*, NOAA National Geophysical Data Center, Boulder, CO.
- Engel A. 2004. Distribution of transparent exopolymer particles (TEP) in the northeast Atlantic Ocean and their potential significance for aggregation processes. *Deep-Sea Research I*, 51: 83 – 92.
- Engel A. 2000. The role of transparent exopolymer particles (TEP) in the increase in apparent particle stickiness (a) during the decline of a diatom bloom. *Journal of Plankton Research*, 22 (3): 485 – 497.
- Engel A., Passow U. 2001. Carbon and nitrogen content of transparent exopolymer particles (TEP) in relation to their Alcian Blue adsorption. *Marine Ecology Progress Series*, 219: 1 – 10.
- Engel A., Thoms S., Riebesell U., Rochelle-Newall E., Zondervan I. 2004. Polysaccharide aggregation as a potential sink of marine dissolved organic carbon. *Nature*, 428: 929 – 932.
- Engel A., Meyerhofer M., von Brockel K. 2002. Chemical and biological composition of suspended particles and aggregates in the Baltic Sea in summer (1999). *Estuarine, coastal and Shelf Sciences*, 55: 729 – 741.
- Fukao T., Kimoto K., Kotani Y. 2010. Production of transparent exopolymer particles by four diatom species. *The Japanese Society of Fisheries Science*, 76: 755 – 760.
- Fukao T., Kitahara S., Karino N., Yamatogi T., Kimoto K., Kotani Y. 2011. Dynamics of transparent exopolymer particles in spring and autumn in Isahaya Bay, Japan. *Nippon Suisan Gakkaishi*, 77 (6): 1027 – 1033.
- Gasol J. M., del Giorgio P. A. 2000. Using flow cytometry for counting natural planktonic bacteria and understanding the structure of planktonic bacterial communities. *Scientia Marina*, 64: 197 – 224.
- García C. M., Prieto L., Vargas M., Echevarría F., García-LaFuente J., Ruíz J., Rubín J. P. 2002. Hydrodynamics and the spatial distribution of plankton and TEP in the Gulf of Cadiz. (SW Iberian Peninsula). *Journal of Plankton Research*, 24: 817 – 833.
- Guidi L., Legendre L., Reygondeau G., Uitz J., Stemann L., Henson S. A. 2015. A new look at ocean carbon remineralization for estimating deep-water sequestration. *Global Biogeochemical Cycles*, doi: 10.1002/2014GB005063
- Harlay J., De Bodt C., Engel A., Jansen S., d'Hoop Q., Piontek J., Van Oostende N., Groomd S., Sabbe K., Chou L. 2009. Abundance and size distribution of transparent exopolymer particles (TEP) in a coccolithophorid bloom in the northern Bay of Biscay. *Deep-Sea Research I*, 56: 1251 – 1265.
- Henson S. A., Sanders R., Madsen E. 2012. Global patterns in efficiency of particulate organic carbon export and transfer to the deep ocean. *Global Biogeochemical Cycles*, 26: GB1028, doi:10.1029/2011GB004099
- Herndl G. J., Reinthaler T. 2013. Microbial control of the dark end of the biological pump. *Nature Geoscience* 6 (9), 718–724.
- Hong Y., Smith W. O., White A.-M. 1997. Studies of transparent exopolymer particles (TEP) produced in the Ross Sea (Antarctica) and by *Phaeocystis antarctica* (Prymnesiophyceae). *Journal of Phycology*, 33: 368 – 376.
- Honjo S., Manganini S. J., Krishfield R. A., Francois R. 2008. Particulate organic carbon fluxes to the ocean interior and factors controlling the biological pump: A synthesis of global sediment trap programs since 1983. *Progress in Oceanography*, 76(3): 217 – 285. doi:10.1016/j.pocean.2007.11.003.
- Hornbeck, R. W. 1975. *Numerical methods*. New York: Quantum Publishers, 465 pp.
- Jähmlich S., Thomsen L., Graf G. 1998. Factors controlling aggregate formation in the benthic boundary layer of the Mecklenburg Bight (western Baltic Sea). *Journal of Sea Research*, 41: 245 – 254.

Global distribution of exopolymer particles

- Kjørboe T., Hansen J., Alldredge A.L., Jackson G. and others. 1996. Sedimentation of phytoplankton during a spring diatom bloom: rates and mechanisms. *Journal of Marine Research*, 54: 1123 – 1148.
- Kjørboe T., Tiselius P., Mitchell-Innes B., Hansen J. L. S., Visser A. W. and Mari X. 1998. Intensive aggregate formation with low vertical flux during an upwelling-induced diatom bloom. *Limnology and Oceanography*, 43 (1): 104 – 116.
- Kirchman D. L., K'nees E., Hodson R. E. 1985. Leucine incorporation and its potential as a measure of protein synthesis by bacteria in natural aquatic systems. *Applied Environmental Microbiology*, 49: 599 - 607.
- Klein C., Claquin P., Pannard A., Napoléon C., Le Roy B. and Véron B. 2011. Dynamics of soluble extracellular polymeric substances and transparent exopolymer particle pools in coastal ecosystems. *Marine Ecology Progress Series*, 427: 13 – 27.
- Kodama T., Kurogi H., Okazaki M., Jinbo T., Chow S., Tomoda T., Ichikawa T. and Watanabe T. 2014. Vertical distribution of transparent exopolymer particle (TEP) concentration in the oligotrophic western tropical North Pacific. *Marine Ecology Progress Series*, 513: 29-37.
- Kumar M. D., Sarma V. V. S. S., Ramaiah M., Gauns M., de Sousa S. N. 1998. Biogeochemical significance of transparent exopolymeric particles in the Indian Ocean. *Geophysical Research Letters*, 25 (1): 81 – 84.
- Lauro F. M., Bartlett D. H. 2007. Prokaryotic lifestyles in deep sea habitats. *Extremophiles* 12: 15 – 25.
- Lauro F. M., McDougald D., Thomas T., Williams T. J., Egan S., Rice S., DeMaere M. Z., Ting L., Ertan H., Johnson J., Ferriera S., Lapidus A., Anderson I., Kyrpides N., Munk A. C., Detter C., Han C. S., Brown M. V., Robb F. T., Kjelleberg S., Cavicchioli R. 2009. The genomic basis of trophic strategy in marine bacteria. *PNAs*, 106 (37): 15527 – 15533.
- Leblanc K., Hare C. E., Feng Y., Berg G. M., DiTullio G. R., Neeley A., Benner I., Sprengel C., Beck A., Sanudo-Wilhelmy S. A., Passow U., Klinck K., Rowe J. M., Wilhelm S. W., Brown C. W., Hutchins D. A. 2009. Distribution of calcifying and silicifying phytoplankton in relation to environmental and biogeochemical parameters during the late stages of the 2005 North East Atlantic Spring Bloom. *Biogeosciences*, 6: 2155 – 2179.
- Lønborg C., Middelboe M. and Brussaard C. P. D. 2013. Viral lysis of *Micromonas pusilla*: impacts on dissolved organic matter production and composition. *Biogeochemistry*, DOI 10.1007/s10533-013-9853-1.
- Logan B. E., Passow U., Alldredge A. L., Grossart H-P., Simon M. 1995. Rapid formation and sedimentation of large aggregates is predictable from coagulation rates (half-lives) of transparent exopolymer particles (TEP). *Deep-Sea Research II*, 42 (1): 203 – 214.
- Lampitt R. S., Achterberg E. P., Anderson T. R., Hughes J. A., Iglesias-Rodriguez M. D., Kelly-Guerreyn B. A., Lucas M., Popova E. E., Sanders R., Shepherd J. G., Smythe-Wright D. and Yool A. 2008. Ocean fertilization: a potential means of geoengineering? *Phil. Trans. R. Soc. A*, 366: 3919 – 3945.
- Lomas M. W., Moran S. B. 2011. Evidence for aggregation and export of cyanobacteria and nano-eukaryotes from the Sargasso Sea euphotic zone. *Biogeosciences*, 8: 203 – 216.
- López-Sandoval D. C., Rodríguez-Ramos T., Cermeño P., Marañón E. 2013. Exudation of organic carbon by marine phytoplankton: dependence on taxon and cell size. *Marine Ecology Progress Series*, 477: 53 – 60.
- Marañón E., Holligan P. M., Barciela R., González N., Mouriño B., Pazó M. J., Varela M. 2001. Patterns of phytoplankton size structure and productivity in contrasting open-ocean environments. *Marine Ecology Progress Series*, 216: 43 - 56.
- Marañón E., Holligan P. M., Varela M., Mouriño B. and Bale A. J. 2000. Basin-scale variability of phytoplankton biomass, production and growth in the Atlantic Ocean. *Deep Sea Research Part I: Oceanographic Research Papers*, 47 (5): 825 - 857.
- Macías D., Navarro G., Bartual A., Echevarría F. and Huertas E. 2009. Primary production in the Strait of Gibraltar: Carbon fixation rates in relation to hydrodynamic and phytoplankton dynamics. *Estuarine, Coastal and Shelf Science*, 83: 197 – 210.
- Mari X., 2008. Does ocean acidification induce an upward flux of marine aggregates? *Biogeosciences*, 5: 1023 – 1031.

- Mari X., Rassoulzadegan F., Brussaard C. P. D., Wassmann P. 2005. Dynamics of transparent exopolymeric particles (TEP) production by *Phaeocystis globosa* under N- or P-limitation: a controlling factor of the retention/export balance. *Harmful Algae*, 4: 895 – 914.
- Marie D., Brussaard C. P. D., Thyrhaug R., Bratbak G., Vaultot D. 1999. Enumeration of marine viruses in culture and natural samples by flow cytometry. *Applied Environmental Microbiology*, 65: 45 – 52.
- Marsay C. M., Sanders R. J., Henson S. A., Pabortsava K., Achterberg E. P., Lampitt R. S. 2015. Attenuation of sinking particulate organic carbon flux through the mesopelagic ocean. *PNAS*, 112(4): 1089 – 1094.
- Martin J. H., Knauer G. A., Karl D. M., Broenkow W. W. 1987. Vertex-carbon cycling in the Northeast Pacific. *Deep-Sea Research*, 34: 267–285.
- Martin P., Lampitt R. S., Perry M. J., Sanders R., Lee C., D’Asaro E. 2011. Export and mesopelagic particle flux during a North Atlantic spring diatom bloom. *Deep-Sea Research I*, 58: 338 – 349.
- Mazuecos I. P., Ortega-Retuerta E., Reche I. 2012. Medida de Partículas Exopoliméricas Transparentes (TEP) en agua marina, in: Expedición of Circunnavegación Malaspina 2010: Cambio global y Exploración de la Biodiversidad del Océano Global. Libro blanco de Métodos y Técnicas de Trabajo Oceanográfico. CSIC, Enrique Moreno-Ostos (eds.), p. p. 515 - 520.
- Moreno-Ostos E., Fernández A., Huete-Ortega M., Mouriño-Carballido B., Calvo-Díaz A., Morán X. A. G., Marañón E. 2011. Size-fractionated phytoplankton biomass and production in the tropical Atlantic. *Scientia Marina*, 75 (2): 379- 389.
- Ortega-Retuerta E., Duarte C. M., Reche I. 2010. Significance of Bacterial Activity for the distribution and dynamics transparent exopolymer particles in the Mediterranean sea. *Microbial Ecology*, 59: 808 – 818.
- Ortega-Retuerta E., Reche I., Pulido-Villena E., Agustí S., Duarte C. M. 2009. Uncoupled distributions of transparent exopolymer particles (TEP) and dissolved carbohydrates in the Southern Ocean. *Marine Chemistry*, 115: 59 - 65.
- Passow U. 2002a. Transparent exopolymer particles (TEP) in aquatic environments. *Progress in Oceanography*, 55: 287 – 333.
- Passow U. 2002b. Production of transparent exopolymer particles (TEP) by phyto- and bacterioplankton. *Marine Ecology Progress Series*, 236: 1 - 12.
- Passow U., Alldredge A. L. 1994. Distribution, size and bacterial colonization of transparent exopolymer particles (TEP) in the ocean. *Marine Ecology Progress Series*, 113: 185 – 198.
- Passow U., Alldredge A. L. 1995. A die-binding assay for the spectrophotometric measurement of transparent exopolymer particles (TEP). *Limnology and Oceanography*, 40 (7): 1326 - 1335.
- Passow U., Carlson C. A. 2012. The biological pump in a high CO₂ world. *Marine Ecology Progress Series*, 470: 249 – 271.
- Passow U., Kozłowski W. and Vernet M. 1995. Palmer LTER: temporal variability of transparent exopolymeric particles in Arthur Harbor during the 1994–95 growth season. *Antarctic Journal-Review*, 1995, 265–266.
- Passow U., Shipe R. F., Murray A., Pak D. K., Brzezinski M. A., Alldredge A. L. 2001. The origin of transparent exopolymer particles (TEP) and their role in the sedimentation of particulate matter. *Continental Shelf Research*, 21: 327 – 346.
- Pérez V., Fernández E., Marañón E., Morán X. A. G., Zubkov M. V. 2006. Vertical distribution of phytoplankton biomass, production and growth in the Atlantic subtropical gyres. *Deep Sea Research Part I: Oceanographic Research Papers*, 53 (10): 1616 – 1634.
- Prieto L., Sommer F., Stibor H., Koeve W. 2001. Effects of planktonic copepods on transparent exopolymeric particles (TEP) abundance and size spectra. *Journal of Plankton Research*, 23 (5): 515 – 525.
- Prieto L., Cowen J. P. 2007. Transparent exopolymer particles in a deep-sea hydrothermal system: Guaymas Basin, Gulf of California. *Marine Biology*, 150 (6): 1093 – 1101.

Global distribution of exopolymer particles

- Prieto L., Navarro G., Cózar A., Echebarría F., García C. M. 2006. Distribution of TEP in the euphotic and upper mesopelagic zones of the Southern Iberian coasts. *Deep-Sea Research II*, 53: 1314 – 1328.
- Radic T., Kraus R., Fuks D., Radic J., Pecar O. 2005. Transparent exopolymeric particles' distribution in the northern Adriatic and their relation to microphytoplankton biomass and composition. *Science of the Total Environment*, 353: 151 -161.
- Radic T., Radic J., Nadjek M., Fucks D., Blazina M. 2003. Potential of the Northern Adriatic bacterioplankton for the production of the transparent exopolymer particles. *Periodicum Biologorum*, 105(4): 381-387.
- Ramaiah N., Sarna VVSS, Gauns M., Kumar M. D., Madhupratap M. 2000. Abundance and relationship of bacteria with transparent exopolymer particles during the 1996 summer monsoon in the Arabian Sea. *Indian Academy Science, Proceedings (Earth Planetary Science)*, 109: 443 – 451.
- Ramaiah N., Takeda S., Furuya K., Yoshimura T., Nishioka J., Aono T., NOjiri Y., Imai K., Kudo I., Saito H., Tsuda A. 2005. Effect of iron enrichment on the dynamics of transparent exopolymer particles in the western subarctic Pacific. *Progress in Oceanography*, 64: 253 – 261.
- Ramaiah N., Yoshikawa T., Furuya K. 2001. Temporal variations in transparent exopolymer particles (TEP) associated with a diatom spring bloom in a subarctic ria in Japan. *Marine Ecology Progress Series*, 212: 79 – 88.
- Reigstad M., Wassmann P. 2007. Does *Phaeocystis* spp. contribute significantly to vertical export of organic carbon? *Biogeochemistry*, 83: 217 – 234.
- Riebesell U., Reigstad M., Wassmann P., Noji T., Passow U. 1995. On the trophic fate of *Phaeocystis pouchetii* (Hariot): VI. Significance of *Phaeocystis*-derived mucus for vertical flux. *Netherlands Journal of Sea Research*, 33: 193 – 203.
- Rochelle-Newall E. J., Mari X., Pringault O. 2010. Sticking properties of transparent exopolymeric particles (TEP) during aging and biodegradation. *Journal of Plankton Research*, 32 (10): 1433 – 1442.
- Sarmiento J. L., Gruber N. 2002. Sinks for anthropogenic carbon. *Physics Today*, 55(8), 30 - 36.
- Scoullou M., Plavsic M., Karavoltos S., Sakellari A. 2006. Partitioning and distribution of dissolved copper, cadmium and organic matter in Mediterranean marine coastal areas: The case of a mucilage event. *Estuarine, Coastal and Shelf Science*, 67: 484 – 490.
- Shibata A., Kogure K., Koike I., Ohwada K. 1997. Formation of submicron colloidal particles from marine bacteria by viral infection. *Marine Ecology Progress Series*, 155: 303 – 307.
- Sheik A. R., Brussaard C. P. D., Lavik G., La, P., Musat N., Krupke A., Littmann S., Strous M., Kuypers M. M. M. 2014. Responses of the coastal bacterial community to viral infection of the algae *Phaeocystis globosa*. *The ISME Journal*, 8, 212 – 225.
- Simon M., Azam F. 1989. Protein content and protein synthesis rates of planktonic marine bacteria. *Marine Ecology-Progress Series*, 51: 201 – 213.
- Smith D. C., Azam F. 1992. A simple economical method for measuring bacterial protein synthesis rates in seawater using ³Hleucine. *Marine Microbial Food Webs*, 6: 107 – 114.
- StatSoft Inc. 1997. *Statistica for Windows* (computer program manual). Tulsa, Oklahoma, USA.
- Steeman-Nielsen E. 1952. The use of radioactive carbon (C¹⁴) for measuring organic production in the sea. *J. Cons. Int. Explor. Mer.*, 18: 117-140.
- Stramska M.. 2009. Particulate organic carbon in the global ocean derived from SeaWiFS ocean color. *Deep Sea Research*, I 56 (9): 1459 – 1470.
- Sugimoto K., Fukuda H., Baki M. A., Koike I. 2007. Bacterial contributions to formation of transparent exopolymer particles (TEP) and seasonal trends in coastal waters of Sagami Bay, Japan. *Aquatic Microbial Ecology*, 46: 31 – 41.
- Teira E., Pazó M. J., Serret P., Fernández E. 2001. Dissolved organic carbon production by microbial populations in the Atlantic Ocean. *Limnology and Oceanography*, 46(6): 1370-1377.
- Thornton D. C. O. 2004. Formation of transparent exopolymeric particles (TEP) from macroalgal detritus. *Marine ecology Progress Series*, 282: 1 – 12.
- Turley C. 2002. The importance of “marine snow”. *Microbiology Today*, 29: 177 – 179.

- Turner J. T. 2015. Zooplankton fecal pellets, marine snow, phytodetritus and the ocean's biological pump. *Progress in Oceanography*, 130: 205 – 248.
- Utermöhl H. 1958. Zur Vervollkommung der quantitativen Phytoplankton-Methodik. *Mitt. Int. Verein. Theor. Angew. Limnol.*, 9: 1 - 38.
- Van Oostende N., Harlay J., Vanelslander B., Chou L., Vyverman W., Sabbe K. 2012. Phytoplankton community dynamics during late spring coccolithophore blooms at the continental margin of the Celtic Sea (North East Atlantic, 2006–2008). *Progress in Oceanography*, 104: 1 – 16.
- Van Oostende N., Moerdijk-Poortvliet T. C. W., Boschker H. T. S., Vyverman W., Sabbe K. 2013. Release of dissolved carbohydrates by *Emiliana huxleyi* and formation of transparent exopolymer particles depend on algal life cycle and bacterial activity. *Environmental Microbiology*, 15(5): 1514 – 1531.
- Vardi A., Haramaty L., Van Mooy B. A. S., Fredricks H. F., Kimman S. A., Larsen A., Bidle K. D. 2012. Host-virus dynamics and subcellular controls of cell fate in a natural coccolithophore population. *PNAS*, 109 (47): 19327 - 19332.
- Verdugo P. 2012. Marine Microgels. *Annual Review of Marine Science*, 4: 375 – 400.
- Verdugo P., Orellana M. V., Chin W.-C., Petersen T. W., van den Eng G., Benner R., Hedges J. I. 2008. Marine biopolymer self-assembly: implications for carbon cycling in the ocean. *Faraday Discussions*, 139: 393 – 398.
- Waite A. M., Gustafsson O., Lindahl O., Tiselius P. 2005. Linking ecosystem dynamics and biogeochemistry: Sinking fractionation of organic carbon in a Swedish fjord. *Limnology and Oceanography*, 50(2): 658–671.
- Wild C. 2000. Effekte von marine snow - Sedimentation auf Steinkorallen (Hexacorallia, Scleractinia) des Great Barrier Reef, Australien. *Dipl. Universität Bremen Biologie/Chemie Bremen*.
- Wurl O., Miller L., Röttgers R., Vagle S. 2009. The distribution and fate of surface-active substances in the sea-surface microlayer and water column. *Marine Chemistry*, 115: 1 – 9.
- Wurl O., Miller L., Svein S. 2011. Production and fate of transparent exopolymer particles in the ocean. *Journal of Geophysical Research*, 116: 1 – 16.
- Yentsch C. S., Menzel D. W. 1963. A method for the determination of phytoplankton chlorophyll and phaeophytin by fluorescence. *Deep-Sea Research*, 10: 221 - 231.
- Yokokawa T., Yang Y., Motegi C., Nagata T. 2013. Large-scale geographical variation in prokaryotic abundance and production in meso- and bathypelagic zones of the central Pacific and Southern Ocean. *Limnology and Oceanography*, 58 (1): 61 -73.

Chapter 3:

Exopolymer particles production by heterotrophic prokaryotes at the carbon export and sequestration layers



Abbreviated title: EP production by heterotrophic prokaryotes

3.1. Abstract

Exopolymer particles (EP) production by prokaryotes has been scantily studied particularly in open and deep waters, and the influence of viral lysis on this process is basically unknown. We performed six experiments in open waters of the Atlantic, Indian and Pacific oceans to quantify EP production by prokaryotes under contrasted viral loads. Three experiments were performed with epipelagic waters (< 200 m depth), containing fresh and recently produced dissolved and particulate organic carbon (DOC and POC), and other three experiments with bathypelagic waters (> 1000 m), containing aged DOC and exported POC. Each experiment consisted of a control treatment, with prokaryotes growing without predators and normal viral load, and a treatment with prokaryotes growing with a viral load manipulation (virus-free). EP production in epipelagic experiments ranged from 2.5 ± 0.2 to 11.4 ± 3.2 $\mu\text{g XG eq. L}^{-1} \text{ day}^{-1}$, while in bathypelagic experiments between 0.3 ± 0.1 and 4.2 ± 0.3 $\mu\text{g XG eq. L}^{-1} \text{ day}^{-1}$, usually with higher EP production in epipelagic experiments. These results suggest, therefore, that the different available organic substrates in these contrasting marine zones led generally to produce more EP in the epipelagic waters than in the bathypelagic waters. In the experiments performed with epipelagic waters, the cell-specific EP production was below $15 \text{ fg XG eq. cell}^{-1} \text{ day}^{-1}$ in all the control treatments, whereas in the treatments with viral load manipulation, production reached up to $130 \text{ fg XG eq. cell}^{-1} \text{ day}^{-1}$, indicating that the different viral stress or manipulation of the treatments (control vs. virus-free) affected the prokaryotic EP production. In the experiments performed with bathypelagic waters, however, the cell-specific EP production was between 2.4 and $48.7 \text{ fg XG eq. cell}^{-1} \text{ day}^{-1}$ and without relevant differences between treatments. The estimated *in situ* EP production in epipelagic waters ranged from 0.01 to $6.59 \mu\text{g XG eq. L}^{-1} \text{ day}^{-1}$ corresponding to an average residence time of 71 days. However, the estimated EP production in bathypelagic waters resulted substantially lower, ranging from 0.01 to $0.17 \mu\text{g XG eq. L}^{-1} \text{ day}^{-1}$, and led to longer EP residence times that ranged from 260 days in the North Atlantic Ocean to 504 days in the North Pacific Ocean.

3.2. Introduction

The pool of exopolymer particles in aquatic ecosystems is composed of a continuum of sizes from colloids of a few nanometers to aggregates of several hundred micrometers with diverse composition that includes proteins, polysaccharides or nucleic acids (Long and Azam, 1996; Passow, 2002; Verdugo et al., 2004). A well-known type of these polymers is the acidic-polysaccharides that can be stained with alcian blue, termed generically as transparent exopolymer particles or just exopolymer particles (EP) (Alldredge et al., 1993). Since EP are sticky and gel-like particles, the EP pool plays an important role in the aggregation process during marine snow formation (Burd and Jackson, 2009) and, consequently, in the vertical export of particulate organic carbon (POC) towards the deep ocean, contributing to the oceanic biological pump (Logan et al., 1995; Passow, 2002; Mazuecos et al., Chapter 2).

Despite the major producers of exopolymers in the photic zone are the phytoplanktonic cells when submitted to nutrient or light stress (Berman-Frank and Dubinsky, 1999; Passow, 2002; Berman-Frank et al., 2007), the role of heterotrophic prokaryotes appears to also be relevant in some areas such as, for instance, the Mediterranean Sea (Bar-Zeev et al., 2011; Ortega-Retuerta et al., 2010). Heterotrophic prokaryotes can also directly release polymeric substances (Decho, 1990; Bhaskar and Bhosle, 2005; Radic et al., 2006, Ding et al., 2008; Koch et al., 2014), particularly under stress by ultraviolet B radiation (Ortega-Retuerta et al., 2009). They also promote the aggregation of preexisting polymers by modifying the stickiness of the algal exudates (Grossart et al., 2006; Gärdes et al., 2010; Rochelle-Newall et al., 2010; Van Oostende et al., 2013) or by inducing the formation of microscopic EP condensation nuclei (so-called "*protobiofilms*" previous to biofilm formation) induced by quorum sensing signals (Bar-Zeev et al., 2012; Tan et al., 2014).

The microbial epipelagic realm contrasts considerably with the deep ocean (Ducklow et al., 2001; Buesseler et al., 2007; Arístegui et al., 2009; Herndl and Reinthaler, 2013). In the epipelagic zone (0-200 m depth), phytoplankton produce fresh, high quality exudates that promote bacterial growth (Cole et al.,

1982; Moran et al., 2002; Ortega-Retuerta et al., 2008; Fouilland et al., 2014), whereas in the mesopelagic zone (200-1000 m) the prokaryotic assemblages use the dissolved or particulate organic carbon (DOC or POC) exported from the upper layers (Baltar et al., 2009; Robinson et al., 2010). Operatively, the borderline between epipelagic and mesopelagic zones is considered the “*carbon export depth*” located between 100 and 200 m depth (Passow and Carlson, 2012; Turner, 2015). The organic carbon flux is dramatically attenuated, mostly due to bacterial mineralization (Aristegui et al., 2009), in its downward transit across the mesopelagic zone down to about 1000 m (the so-called “*carbon sequestration depth*”) (Turner, 2015). Below this layer, carbon is assumed to remain sequestered for time scales longer than centuries, contributing significantly to the biological pump (Passow and Carlson, 2012; Turner, 2015). Although EP generation by heterotrophic prokaryotes has been scantily studied in epipelagic and coastal waters, there is no knowledge about prokaryotic EP production in deep waters. In addition, the fact that the POC pool in the deep ocean is younger and with higher nutritive value than the corresponding DOC pool appears to have promoted a life strategy in prokaryotes mostly associated to particles (Herndl and Reinthaler, 2013). Prokaryotes from the deep ocean overexpress, in comparison with their surface counterparts, genes for the synthesis of pili that allow them to adhere to particles, and genes for polysaccharide degradation (DeLong et al., 2006; Martin-Cuadrado et al., 2007). These microorganisms tend to harbor comparatively larger genomes and be opportunistic maintaining very diverse enzymatic machinery (Lauro et al., 2009).

In this complex context of interactions among POC, DOC and prokaryotes, the role of viruses might be critical by releasing labile organic components from the planktonic cells during lysis (Wilhelm and Suttle, 1999; Suttle, 2007) both in surface and deep waters. However, how viral lysis can affect EP production has not been studied in these two contrasting scenarios. In the case of phytoplanktonic cells, recent studies have connected lytic viral infection with programmed cell death and a concomitant enhancement of

EP production by heterotrophic prokaryotes

exopolymer production in cultures of the coccolithophorid *Emiliana huxleyi* (Bidle et al., 2007; Vardi et al., 2012) and of the Chlorophyta *Micromonas pusilla* (Lønborg et al., 2013). However, to the best of our knowledge, the influence of bacteriophage lysis on EP production is unknown. Lysis products may also act as glue enhancing aggregation processes and might serve as condensation nuclei for the exopolymer aggregates (Shibata et al., 1997) or, by contrast, inhibit EP formation as in their presence the organic matter pool would be more efficiently remineralized by the prokaryotes (Bonilla-Findji et al., 2008).

We performed several experiments to elucidate the influence of viruses on the production of exopolymer particles by heterotrophic prokaryotes in two contrasting oceanic zones. The experiments were set up using waters from above the *carbon export depth* or epipelagic zone (with fresh DOC and POC) and waters from below the *carbon sequestration depth* or bathypelagic zone (with aged DOC and exported POC) in open areas of the Atlantic, Indian and Pacific Oceans.

3.3. Material and methods

3.3.1. Study area

The experiments were conducted on board the *R/V Hespérides* vessel during the circumnavigation “*Malaspina 2010*”. Water samples were collected from different stations above export depths (< 200 m) and below sequestration depths (> 1000 m) in the open waters of the Atlantic, Indian and Pacific Oceans (Table 1). We used a rosette sampler with 24 Niskin bottles (12 l) coupled to a conductivity and temperature–pressure (CTD) probe (Seabird 911Plus).

3.3.2. Experimental set-up

Natural prokaryotic populations, with variable viral loadings were monitored to assess the influence of viral lysis on extracellular release of dissolved carbohydrates and production of exopolymeric particles (EP). All *in vitro* incubations were carried out on board in Nalgene HDPE bottles (2L) by triplicate, at *in situ* temperature in a temperature-controlled chamber and in the dark. All material used was previously acid-washed and rinsed with ultrapure water.

Three experiments were performed with waters from above the *export depths* (*ExpW*) and other three using waters from below the *sequestration depths* (*SeqW*) (Table 3.1.). Water samples were sequentially filtered as shown in Figure 3.1. First, water samples were filtered by 1 μm (through 0.1N HCl pre-washed Preflow capsule filters, Pall Corporation) to remove large particles and grazers that were used as inoculum of natural microbial populations. Then, the filtrate was filtered again by 0.2 μm (through sterile Whatman Polycap cartridge filters) to exclude the microbial populations. Finally, in all the treatments submitted to a manipulation of the initial viral load (virus-free seawater), seawater was ultrafiltered using a 0.1N NaOH-prewashed tangential flow system (30 KDa Sartorius Vivaflow 200 filtration system) except for the epipelagic experiment of the Atlantic Ocean (*At-ExpW*; Table 3.1.) in which viruses were microwave-inactivated as in the protocol proposed by Bonilla-Findji et al. (2008). These fractions of filtered waters were mixed, and homogenized, to carry out the two treatments by triplicate. *Control* treatments consisted of 75% of 0.2 μm filtrated seawater and 25% of the prokaryotic inoculum, and the treatments with a *viral load manipulation* consisted of 75% of ultrafiltered or microwave-inactivated seawater and 25% of inoculum, which represented a reduction (in average ca. 35 %) of the *in situ* viral abundance at the onset of the treatments (Table 3.1.) allowing the prokaryotes to grow exponentially. The incubation time was 10 days for the Indian and Atlantic experiments (both in *ExpW* and *SeqW* experiments), 7 days for the *Pac-ExpW* experiment and 12 days for the *Pac-SeqW* experiment.

During the course of the experiments, three replicates in every sampling time were collected for characterization of the microbial community by measuring virus abundance (VA), prokaryotic heterotrophic abundance (PHA) and production (PHP), as well as changes in the concentrations of exopolymer particles (EP) and their dissolved precursors, i.e. neutral total carbohydrates (DTCHO) and acidic polysaccharides (dAPS).

EP production by heterotrophic prokaryotes

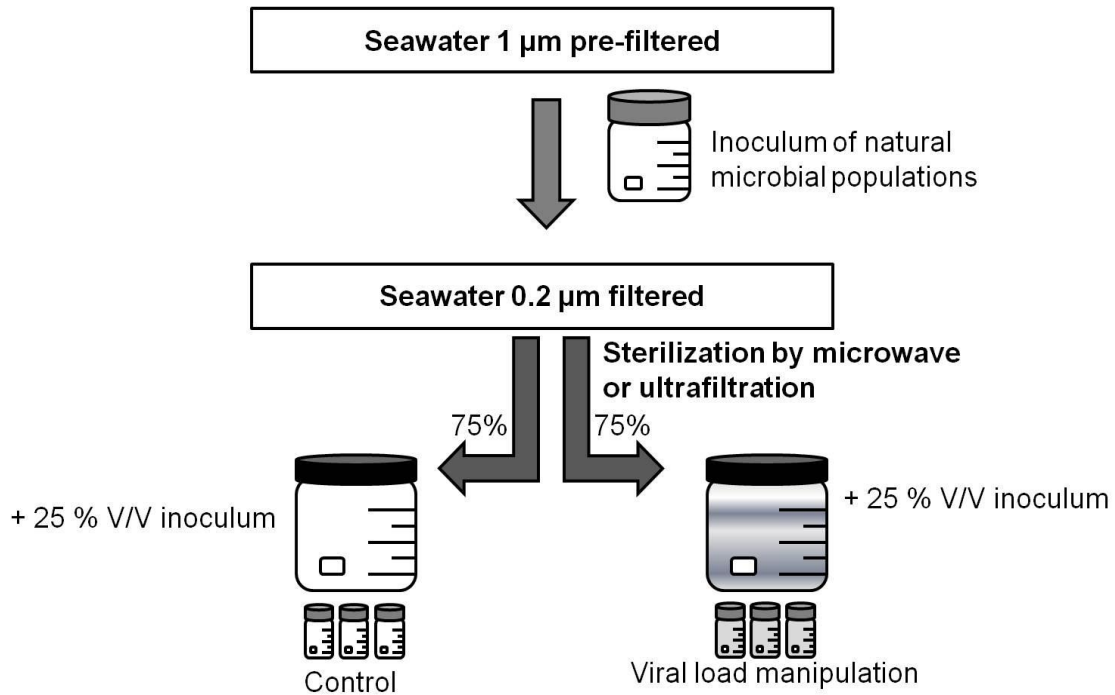


Figure 3. 1. Scheme of the experimental set-up and the different sequential filtrations.

3.3.3. Biological and chemical analyses

3.3.3.1. Concentration of exopolymer particles (EP)

EP concentrations were measured by using the alcian blue colorimetric method proposed by Passow and Alldredge (1995). Samples (25 - 1500 ml) were gently filtered through 0.4 µm polycarbonate filters. EP retained on the filters were fully covered with 0.5 ml of a 0.02 % solution of alcian Blue (Sigma) in 0.06 % acetic acid (pH 2.5) and frozen at -80°C on board until analysis in the laboratory. Three or four blanks (with ultrapure water) were also stained and frozen in parallel in each batch of samples. The alcian blue was extracted from the unfrozen filters adding 5 ml of sulfuric acid 80% and absorbance was measured at 787 nm in 1-cm path disposable polystyrene cuvettes using ultrapure water as blank. A calibration curve with a standard solution of xanthan gum (25 mg l⁻¹) was used to relate absorbance values with EP concentrations. The EP concentration is expressed as micrograms of xanthan gum equivalents per liter (µg XG eq l⁻¹) and the coefficient of variation for the replicates averaged ca. 20%.

3.3.3.2. Concentration of dissolved neutral carbohydrates and acidic polysaccharides

Samples for dissolved acidic polysaccharides (dAPS), neutral monosaccharides (DMCHO) and polysaccharides (DPCHO) were pre-filtered through 0.4 μm polycarbonate membrane filters (Sartorius) and stored in 15 ml sterile polyethylene flasks at $-20\text{ }^{\circ}\text{C}$ until analysis.

The concentration of dAPS was determined following the alcian blue method according to Thornton et al. (2007). Briefly, the filtered extracts were dialyzed, to removed salts, in 8 ml dialysis tubes with a molecular weight cutoff of 500-1000 Da (with cellulose ester membrane, Spectrum Laboratories) for approximately 24 h in a bath of ultrapure water (milli-Q). A few drops of a sodium azide solution (0.02% final concentration) were added to suppress prokaryotic growth. Samples were analyzed immediately after dialysis, transferring 5 ml of sample into a glass tube with 1 ml of alcian blue solution (similar concentration as used in the analysis of EP). After mixing, the total 6 ml were again filtered through a 0.4 μm pore-size SFCA syringe filter (Sartorius) and the absorbance of the filtrate, collected directly into a 1-cm-path semi-micropolystyrene cuvette, was measured at 610 nm on a spectrophotometer (Perkin Elmer). We used standard solutions of xathan gum (with 0, 5, 10, 15 and 20 mg l^{-1}) to relate absorbance values with dPAS concentrations and to be able to compare with the EP concentrations. The units are also given in xathan gum (XG) equivalents l^{-1} .

The concentration of DMCHO and DPCHO (previously hydrolyzed by oxidation of the free reduced sugars with 1N HCl and $150\text{ }^{\circ}\text{C}$ during 1 h) were determined by the spectrophotometric method using the alkaline ferricyanide reaction with 2, 4, 6-tripyridyl-s-triazine (Myklestad et al., 1997). A standard curve made with D-glucose at concentrations at 0.25, 0.5, 1.0 and 2.0 mg l^{-1} was used to calibrate the carbohydrate concentrations. Triplicate reagent blanks in ultrapure (Milli-Q) water were subtracted daily. The total concentration of carbohydrates (DTCHO in $\mu\text{g l}^{-1}$) is the sum of DMCHO and DPCHO.

3.3.3.3. Viral abundance (VA)

EP production by heterotrophic prokaryotes

VA was determined by flow cytometry using a FACScalibur flow cytometer (BectonDickinson) fitted with a laser emitting at 488 nm (Brussaard, 2004). Samples (2 ml) were fixed with 0.5% glutaraldehyde, deep-frozen in liquid nitrogen and stored at -80°C until analyses. Then, SYBR Green I (Molecular Probes; 10 X diluted with sterilized ultrapure water) was used to stain the genetic material of the virus particles, and samples were run at flow rates between 60 and 75 $\mu\text{l min}^{-1}$ after being diluted with TE buffer (1x Tris-ethylenediaminetetraacetic acid) such that the event rate was between 100 and 800 particles s^{-1} . VA was gated and counted (viruses ml^{-1}) in the SSC vs. FL1 plot using the Cell-Quest software (BectonDickinson).

3.3.3.4. Prokaryotic heterotrophic abundance (PHA) and production (PHP)

PHA was also measured by using flow cytometry (Gasol and del Giorgio, 2000). Aliquots of 1.5 ml were fixed with 1% of paraformaldehyde + 0.05 % glutaraldehyde, deep-frozen in liquid nitrogen and stored at -80°C until analysis. Triplicate samples were stained with Syto13 (5 μM) and run through a FACSCanto cytometer (BectonDickinson) equipped with an argon laser emitting at 488 nm. Abundance (cell ml^{-1}) was calculated from a bivariate plot of light scatter and green fluorescence using the CellQuest software (BectonDickinson). Molecular Probes latex beads (0.92 μm) were always used as internal standards. Flow rate was calculated from the difference of volume running a sample with known volume for 10 min.

The PHP rates were estimated by ^3H -Leucine (specific activity = 144.2 Ci mmol^{-1}) incorporation into proteins (Kirchman et al., 1985) using the microcentrifugation protocol proposed by Smith and Azam (1992). Briefly, three replicates (1.2 ml) and two trichloroacetic acid (TCA)-killed blanks in microcentrifuge tubes were added L-[4, 5- ^3H] leucine at 20 nM. Samples and blanks were incubated (for 4 to 15 h) at in situ temperature. Incubations were stopped by adding 50% TCA, centrifuged (10 min. and 14000 rpm) and rinsed with 5% TCA and again centrifuged. Scintillation cocktail (1 ml Optisafe HiSafe) was added, and after 24 h, the emitted radioactivity was counted in a liquid scintillation counter on board. Leucine incorporation rates ($\text{pmol Leu l}^{-1} \text{h}^{-1}$)

were converted into carbon ($\mu\text{g C l}^{-1} \text{ d}^{-1}$) by using a theoretical factor of 1.55 kg C mol Leu⁻¹ (Simon and Azam, 1989), which assumes that isotope dilution was negligible under this saturating concentration of 20 nM of ³H-Leucine.

3.3.3.5. Data analysis

PHP rates were integrated (PHP_{int}) during the experiments as the area obtained from initial time to final time and expressed as $\mu\text{g C L}^{-1} \text{ day}^{-1}$. Daily increase rates for PHA, AV, dAPS, DTCHO and EP were calculated using the expression:

$$\Delta_x = (X_{t_f} - X_{t_0}) / t$$

where X_{t_f} and X_{t_0} are the variable at the final and initial times, respectively, and t ($t_f - t_0$) is the time elapsed in days.

We explored the relationship between the daily increase rate of EP (ΔEP) and the other variables which were log-transformed to fit the assumptions of normality and homocedasticity. The slopes of the regressions between ΔEP and PHP_{int} gave experimental estimates of intrinsic EP production rates (i.e. the quantity of EP produced per day normalized by PHP). We used these experimental EP production rates to calculate *in situ* EP production rates by the heterotrophic prokaryotes using the PHP data measured in the natural environment. EP residence times (in days) were estimated by dividing *in situ* EP concentration by the *in situ* EP production rate.

ANOVA analyses were performed to test for the differences in EP production by prokaryotic populations in different treatments (control vs manipulation of the viral load) over time in the six experiments. This analysis also allowed testing if there was interaction between the factors “time” and “treatment” on the dependent variable (production of EP). Subsequently, significant differences between times were determined by using the Tukey HSD test. All statistical analyses were performed using Statistica 6.0 (StatSoft Inc., 1997).

3.4. Results

3.4.1. Changes of the microbial community during the experiments

At the onset of the experiments, prokaryotic heterotrophic abundance (PHA T_0) and virus abundance (VA T_0) were higher in the control than in the treatments submitted to a viral load manipulation (Table 3.1.). Initial conditions of DTCHO and dAPS (EP precursors) were above 10 times and from three to five times, respectively, higher in the experiments performed with epipelagic waters (< 200 m) than in bathypelagic waters (200 - 1000 m)(Table 3.1.).

In the epipelagic experiments (*ExpW*) (Figure 3.2.), the virus abundance (VA) was very homogeneous over time regardless of the treatments (control vs. viral load manipulation) or locations with the exception of the experiment performed in the Pacific Ocean. PHA increased consistently in all the *in vitro* cultures, up to 3-fold in the control treatments and in the treatments with viral load manipulation increased at final incubation time from 3 (Ind-*ExpW*) to 10 fold (At-*ExpW*). The increment of PHA (Δ PHA) ranged between 0.90 and 8.02×10^7 cell L⁻¹ day⁻¹, being Δ PHA higher in the control treatments than in the treatments with manipulation of the viral load with the exception of the experiment performed in the Atlantic Ocean (Table 3.2.). The prokaryotic heterotrophic production (PHP) increased over time fitting to logistic growth in both treatments and reaching the plateau after three days of incubation. The integrated heterotrophic production (PHP_{int}) ranged from 4.23 - 33.77 μ g C L⁻¹ day⁻¹ (Table 3.2.).

Table 3. 1. Location of the sampling stations, environmental conditions of the water collected to perform the experiments and conditions at the onset of experiments (T_0). The experiments had two treatments: “Control” with viral abundances similar to the in situ values and another treatment including a “viral load manipulation”. The acronym “ExpW” corresponds to experiments performed with waters from above the carbon export depths in the epipelagic waters (< 200 m) and the acronym “SeqW” corresponds to experiments performed with waters from below sequestration depths or in bathypelagic waters (> 1000 m). Standard errors in brackets.

Sampling information							
Ocean		Atlantic [At-]		Indian [Ind-]		Pacific [Pac-]	
Latitude		14.3°N	26.5°S	29.9°S	33.6°S	5.8°S	25.5°S
Longitude		26.0°W	21.4°W	76.1°E	39.9°E	170.7°W	179.5°E
Date (day/month/year)		26/12/2010	24/01/2011	01/03/2011	18/02/2011	28/04/2011	19/04/2011
Sampling depth (m)		65	3200	140	4000	80	2150
Parameters <i>in situ</i> ¹							
Temperature (°C)		20.1	2.3	16.5	1.2	27.8	2.2
Salinity (psu)		36.26	34.91	35.60	34.74	35.52	34.65
[O ₂] (μmol kg ⁻¹)		133	231	217	199	186	139
Chl <i>a</i> (μg l ⁻¹)		0.66	-	0.27	-	0.31	-
EP (μg XG eq L ⁻¹)		29.6	1.5	5.5	2.6	16.6	18.0
PHA (x 10 ⁵ cell ml ⁻¹)		7.94	0.18	6.71	0.52	3.55	0.39
PHP (ng C l ⁻¹ h ⁻¹)		6.08	0.26	5.92	0.08	91.38	1.08
VA (x 10 ⁶ particles ml ⁻¹)		4.12	0.08	9.22	0.22	17.50	0.04
Experiments ¹							
Experiment code		At-ExpW	At-SeqW	Ind-ExpW	Ind-SeqW	Pac-ExpW	Pac-SeqW
DTCHO T_0 (μg C l ⁻¹)		71.3 (6.2)	8.3 (4.2)	83.9 (12.4)	10.9 (1.1)	110.4 (25.3)	9.2 (3.5)
dAPS T_0 (μg XG eq L ⁻¹)		1126 (24.0)	515 (13.0)	913 (45.0)	312 (25.0)	2133 (123.0)	412 (30.0)
PHA T_0 (x 10 ⁵ cell ml ⁻¹)	Control	6.21 (0.03)	0.16 (0.02)	3.99 (0.12)	0.41 (0.01)	2.98 (0.03)	0.31 (0)
	Viral load manipulation	0.50 (0.02)	0.09 (0.01)	0.45 (0.03)	0.07 (0.02)	0.47 (0.06)	0.08 (0.03)
PHP T_0 (ng C l ⁻¹ h ⁻¹)	Control	10.50 (0.87)	1.60 (0.35)	0.91 (0.33)	0.51 (0.43)	442.07 (28.09)	1.27 (0.45)
	Viral load manipulation	3.22 (0.25)	0.62 (0.1)	33.87 (4.89)	3.09 (0.56)	177.98 (15.68)	2.22 (0.33)
VA T_0 (x 10 ⁶ vir ml ⁻¹)	Control	3.49 (0.78)	0.06 (0.01)	7.72 (0.33)	0.20 (0.04)	12.17 (0.23)	0.03 (0.01)
	Viral load manipulation	1.10 (0.45)	0.02 (0)	0.21 (0.01)	0.01 (0)	1.06 (0.12)	< 0.01

¹Data from Mazuecos et al. (Chapter 1). [O₂] = O₂ concentration; Chl *a* = chlorophyll *a* concentration; EP = exopolymer particles; PHA = heterotrophic prokaryotic abundance; PHP = prokaryotic heterotrophic production; VA = viral abundance; DTCHO = dissolved total polysaccharides; dAPS = dissolved acidic polysaccharides.

EP production by heterotrophic prokaryotes

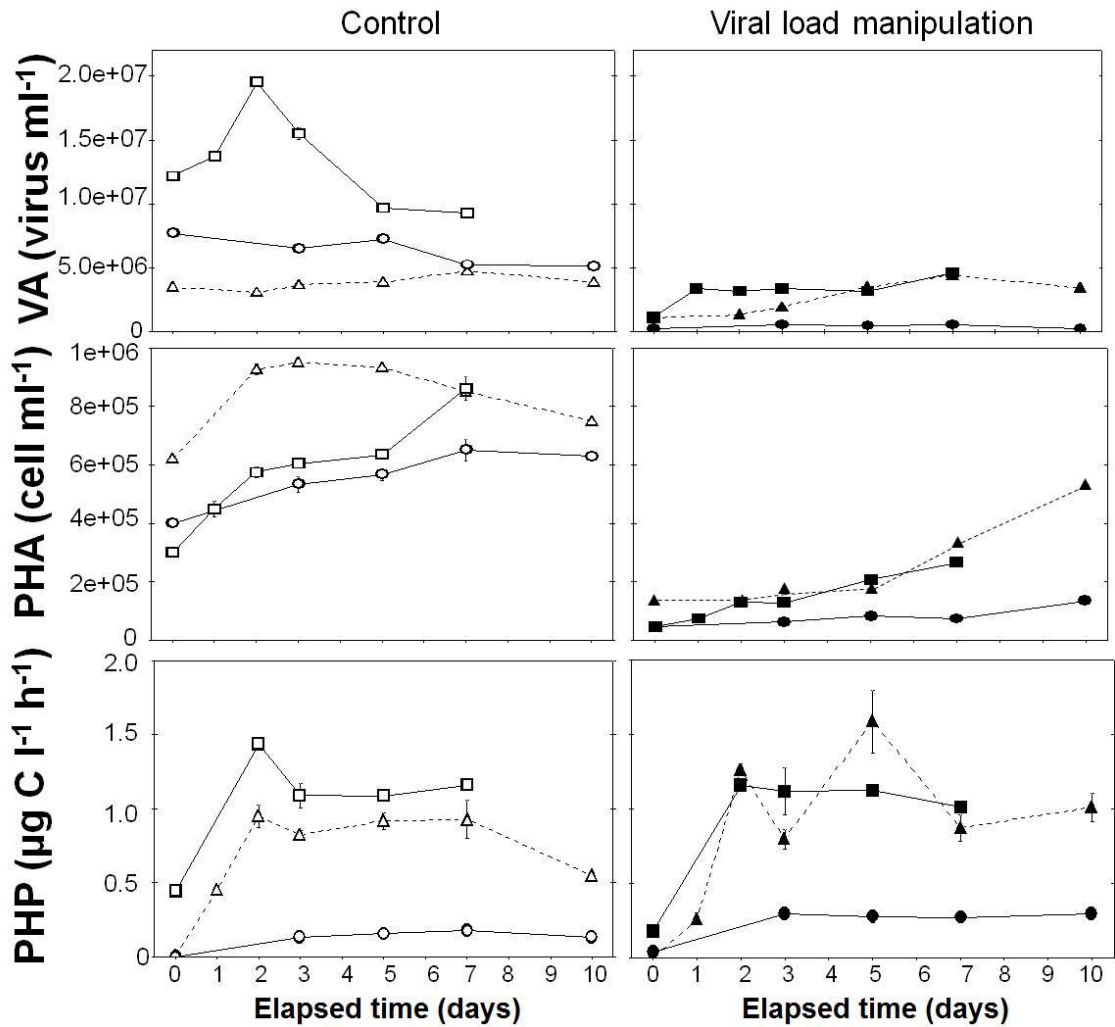


Figure 3. 2. Time changes of the virus abundance (VA), prokaryotic heterotrophic abundance (PHA) and production (PHP) in control treatments (open symbols) and in the treatments with a manipulation of the viral load (filled symbols) for the three experiments conducted with waters located above the export depths (ExpW experiments) in the Atlantic (At-ExpW, triangles), in the Indian (Ind-ExpW, circles) and in the Pacific (Pac-ExpW, squares) Oceans. Error bars represent the standard deviation (SD) of three replicates. When errors bars do not appear is because the SD is smaller than the symbol.

Table 3. 2. Mean values (\pm standard deviations) of the daily increments in viral abundance (ΔVA), prokaryotic heterotrophic abundance (ΔPHA), integrated prokaryotic heterotrophic production (PHP_{int}), dissolved acidic polysaccharides ($\Delta dAPS$), dissolved neutral carbohydrates ($\Delta DTCHO$), exopolymer particles (ΔEP), and mean VA:PHA ratios in the experiments.

Treatments		ΔVA ($\times 10^7$ virus L^{-1} day^{-1})	ΔPHA ($\times 10^7$ cells L^{-1} day^{-1})	PHP_{int} ($\mu g C L^{-1}$ day^{-1})	$\Delta dAPS$ ($\mu g XG eq. L^{-1}$ day^{-1})	$\Delta DTCHO$ ($\mu g C L^{-1}$ day^{-1})	ΔEP ($\mu g XG eq. L^{-1}$ day^{-1})	VA:PHA (virus prok. $^{-1}$)
At-ExpW	Control	4.38 (\pm 0.33)	1.29 (\pm 0.09)	24.25	65 (\pm 17)	12.7 (\pm 0.8)	2.8 (\pm 0.5)	4.7 (\pm 0.9)
	Viral load manipulation	23.63 (\pm 0.14)	4.86 (\pm 0.93)	33.77	97 (\pm 25)	7.9 (\pm 1.2)	3.4 (\pm 0.7)	15.2 (\pm 6.6)
Ind-ExpW	Control	-25.97 (\pm 1.19)	2.30 (\pm 0.17)	4.23	181 (\pm 41)	10.7 (\pm 2.4)	2.5 (\pm 0.2)	12.1 (\pm 4.3)
	Viral load manipulation	0.23 (\pm 0.09)	0.90 (\pm 0.12)	7.09	68 (\pm 17)	1.9 (\pm 1.0)	2.9 (\pm 0.6)	5.7 (\pm 2.6)
Pac-ExpW	Control	-41.43 (\pm 1.56)	8.02 (\pm 0.42)	31.39	169 (\pm 24)	21.6 (\pm 3.6)	11.4 (\pm 3.2)	25.4 (\pm 10.3)
	Viral load manipulation	50.26 (\pm 3.53)	3.13 (\pm 0.08)	27.82	72 (\pm 10)	5.6 (\pm 0.5)	6.5 (\pm 1.2)	25.9 (\pm 10.6)
At-SeqW	Control	-0.02 (\pm 0.03)	3.58 (\pm 0.10)	2.17	11 (\pm 5)	0.5 (\pm 0.3)	1.0 (\pm 0.4)	2.2 (\pm 1.6)
	Viral load manipulation	1.25 (\pm 0.09)	1.14 (\pm 0.02)	0.87	-18 (\pm 6)	1.3 (\pm 0.4)	1.0 (\pm 0.2)	3.4 (\pm 3.3)
Ind-SeqW	Control	1.92 (\pm 0.19)	0.11 (\pm 0.03)	0.67	3 (\pm 2)	0.2 (\pm 0.2)	0.5 (\pm 0.8)	6.0 (\pm 1.5)
	Viral load manipulation	2.83 (\pm 0.29)	5.54 (\pm 0.15)	8.06	35 (\pm 13)	-0.4 (\pm 0.5)	4.2 (\pm 0.3)	0.8 (\pm 0.6)
Pac-SeqW	Control	0.005 (\pm 0.003)	1.03 (\pm 0.37)	1.05	15 (\pm 7)	-1.0 (\pm 0.4)	1.0 (\pm 0.3)	0.8 (\pm 0.3)
	Viral load manipulation	0.55 (\pm 0.05)	1.94 (\pm 0.13)	1.51	-6 (\pm 3)	0.5 (\pm 0.5)	0.3 (\pm 0.1)	0.4 (\pm 0.3)

EP production by heterotrophic prokaryotes

In the bathypelagic experiments (*SeqW*) (Figure 3.3.), VA remained almost stable in the control treatments of the Atlantic and Pacific Ocean and increased from 5 to 20 fold in the treatments with viral load reduction. Then, the ΔVA values were higher in these last treatments ranging from 0.55 to 2.83×10^7 virus $L^{-1} day^{-1}$ than in the control treatments that ranged from -0.02 to 1.92×10^7 virus $L^{-1} day^{-1}$ (Table 3.2.). PHA in control treatments remained very stable until the last time of incubation, whereas in the treatments with viral load reduction, PHA increased up to 75 fold in the Indian Ocean (Figure 3.3.). The ΔPHA varied between 0.11 and 5.54×10^7 cells $L^{-1} day^{-1}$ and PHPint ranged from 0.67 to $8.06 \mu g C L^{-1} day^{-1}$ (Table 3.2.). These values were higher in the treatments with a viral load reduction except in the experiment of the Atlantic Ocean (*At-SeqW*) (Table 3.2.).

The virus to prokaryote (VA:PHA) ratios, indicative of the potential viral infection or lysis on prokaryotes, were in general higher in the *ExpW* experiments than in the *SeqW* experiments (Table 3.2.).

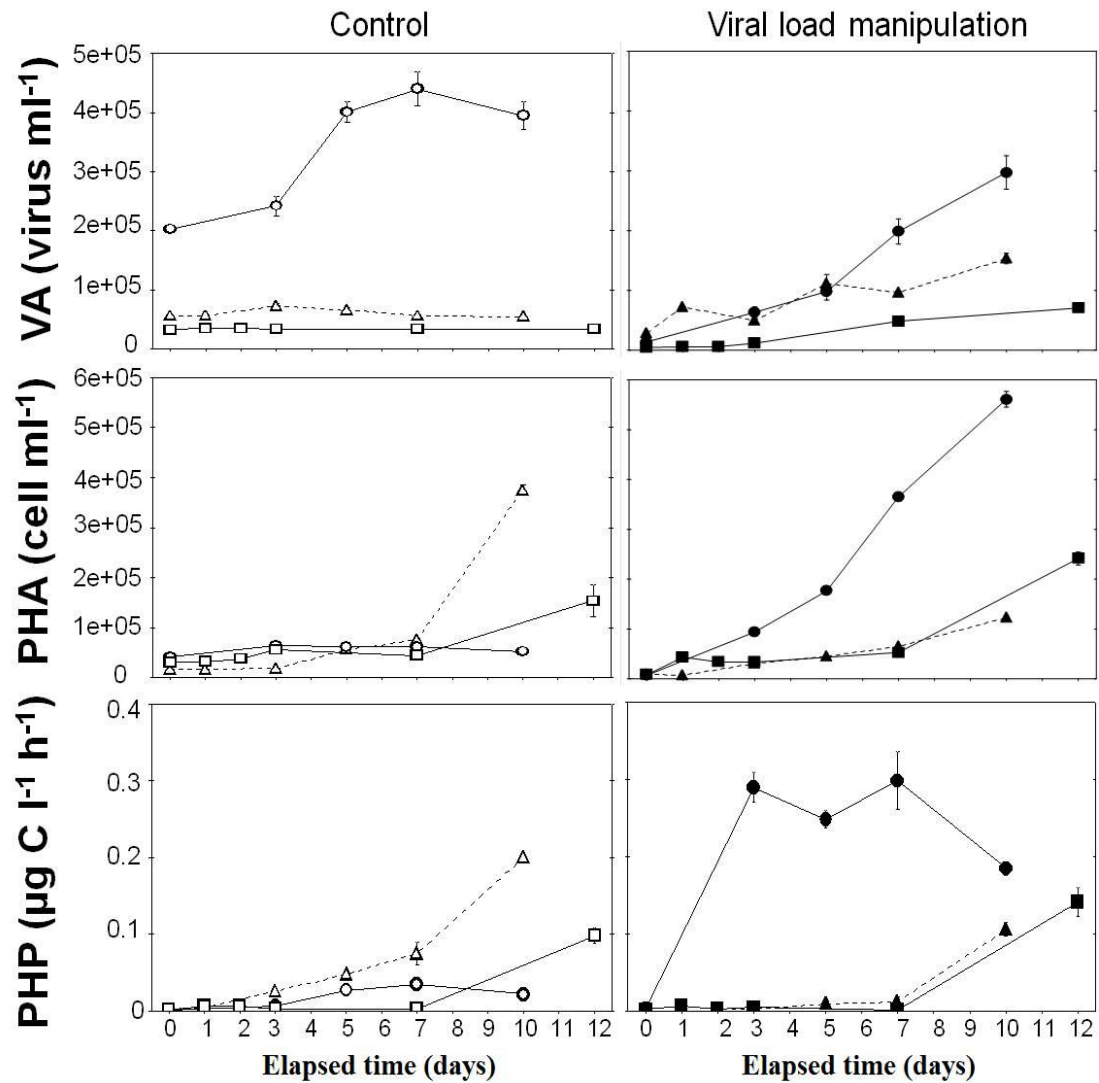


Figure 3. 3. Time changes of the virus abundance (VA), prokaryotic heterotrophic abundance (PHA) and production (PHP) in control treatments (open symbols) and in the treatments with a manipulation of the viral load (filled symbols) for the three experiments conducted with waters located below the sequestration depths (SeqW experiments) in the Atlantic (At-SeqW, triangles), in the Indian (Ind-SeqW, circles) and in the Pacific (Pac-SeqW, squares) Oceans. The error bars represent the standard deviation (SD) of the three replicates. When errors bars do not appear is because the SD is smaller than the symbol.

EP production by heterotrophic prokaryotes

3.4.2. EP production by heterotrophic prokaryotes

In the epipelagic experiments, the increment of dissolved acidic polysaccharides (Δ dAPS) ranged from 65 to 181 $\mu\text{g XG eq. L}^{-1}$, with higher values in the control treatments with exception of the experiment performed in the Atlantic Ocean (Table 3.2.). Total carbohydrates (Δ DTCHO = Δ DMCHO + Δ DPCHO) increased from 1.9 to 21.6 $\mu\text{g C L}^{-1}\text{ day}^{-1}$, being higher the increases in the control treatments in comparison with the treatments with viral load manipulation (Table 3.2.). EP concentrations also increased over time in all these experiments being particularly accentuated in the Pacific Ocean (Figure 3.4.). The daily EP production (Δ EP) ranged from 2.5 and 11.4 $\mu\text{g XG eq. L}^{-1}\text{ day}^{-1}$ (Table 3.2.).

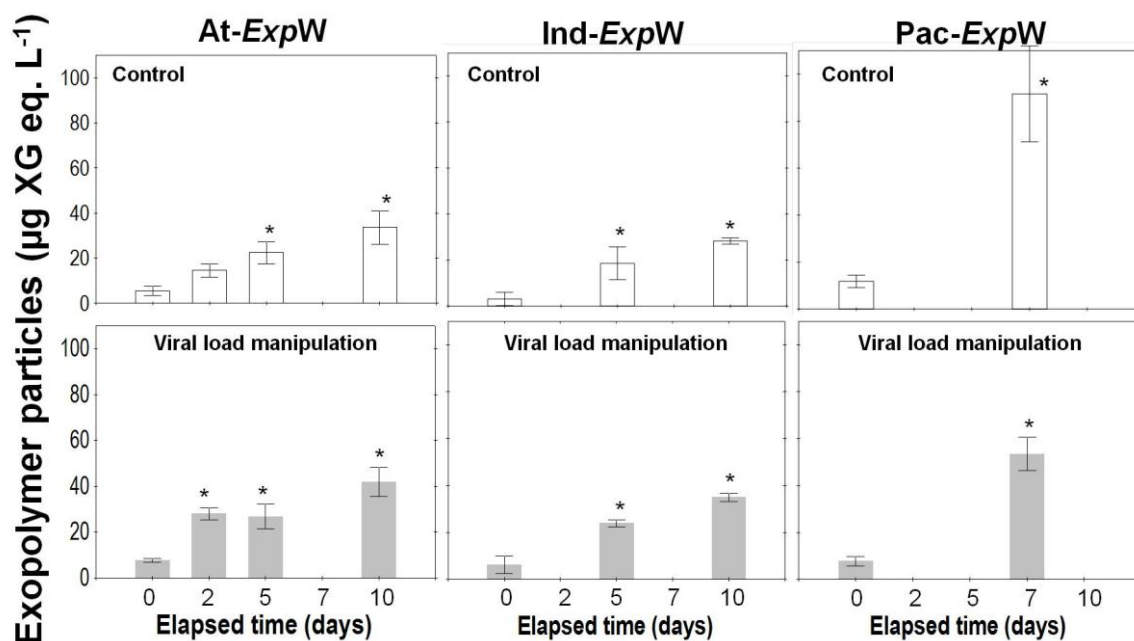


Figure 3. 4. Changes of EP concentrations throughout incubation time in the experiments conducted with waters from above the export depths (ExpW). The asterisks indicate statistically significant differences in comparison with the initial time using Tukey HSD tests.

The daily cell-specific EP production throughout the incubation times was consistently higher in the treatments with a viral load manipulation than in the controls, and these EP production rates decreased with incubation time, especially accentuated in the treatments with viral load reduction (Figure 3.5.). The daily cell-specific EP production in the control treatments were lower than ~ 15 fg XG eq. cell⁻¹ day⁻¹, whereas in the treatments with viral load manipulation (reduction) reached up to 130 fg XG eq. cell⁻¹ day⁻¹ in the Atlantic Ocean.

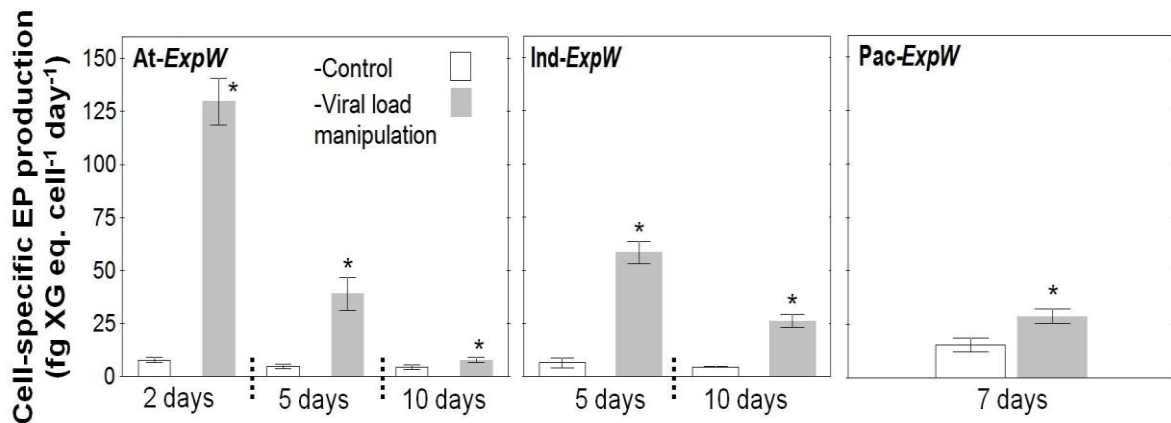


Figure 3. 5. Changes of the cell-specific EP production throughout incubation time in the experiments conducted with waters from above the export depths (ExpW). The asterisks indicate statistically significant differences in comparison with the control using Tukey HSD tests.

In the bathypelagic experiments (*SeqW*), the Δ dAPS values varied from a decrease of 18 μ g XG eq. L⁻¹ to an increase of 35 μ g XG eq. L⁻¹ and the Δ DTCHO values were very stable with only minor changes during the incubation time (Table 3.2.). In contrast, in these experiments EP concentrations increased over incubation time, particularly in the treatment with manipulation of the viral load in the Indian Ocean (Figure 3.6.). The EP production ranged between 0.3 and 4.2 μ g XG eq. L⁻¹ day⁻¹ (Table 3.2.).

EP production by heterotrophic prokaryotes

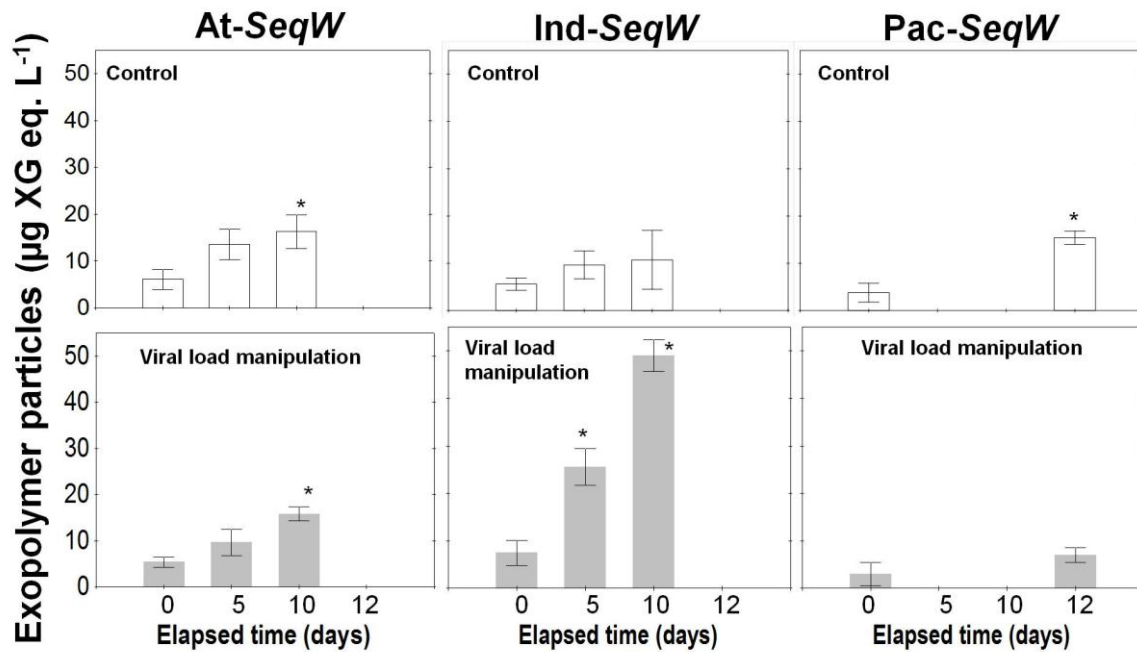


Figure 3. 6. Changes of EP concentrations throughout incubation time in the experiments conducted with waters from below the sequestration depths (*SeqW*). The asterisks indicate statistically significant differences in comparison with the initial time using Tukey HSD tests.

The cell-specific EP production in the control treatments ranged from 4.3 fg XG eq. cell⁻¹ day⁻¹ to 48.7 fg XG eq. cell⁻¹day⁻¹ and from 2.4 to 42.9 in the treatments with manipulated load of viruses (Figure 3.7.). It is remarkable that the values in the control treatments of these experiments were usually higher than those values in the *ExpW* experiments.

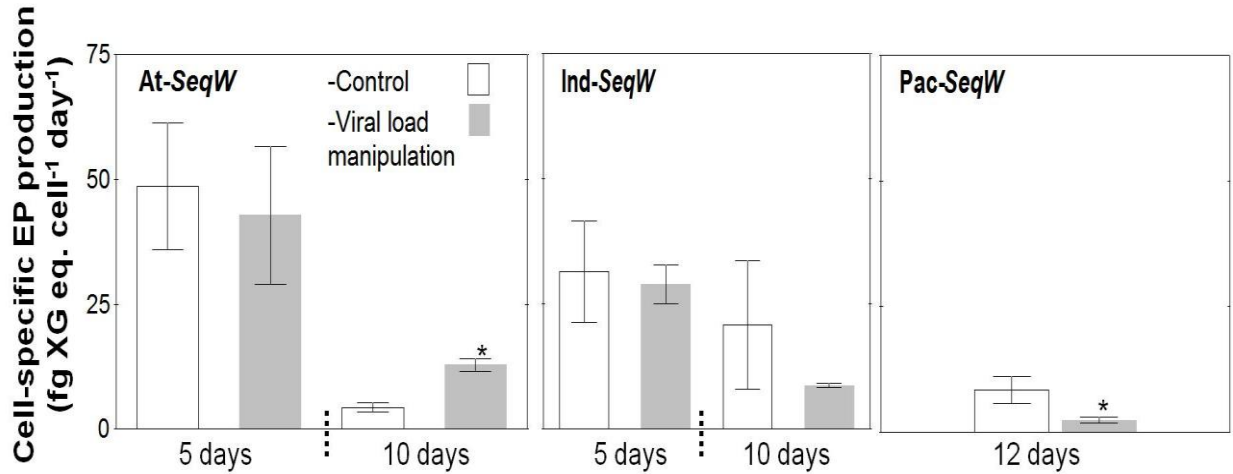


Figure 3. 7. Changes of the cell-specific EP production throughout incubation time in the experiments conducted with waters from below the sequestration depths (SeqW). The asterisks indicate statistically significant differences in comparison with the control treatments using the Tukey HSD test.

To explore the contribution of the heterotrophic prokaryotes to the dissolved precursors (dAPS and dTCHO) and EP production we performed regression analysis. In all cases, we found significant and positive relationships between the daily production of dissolved precursors (Δ dAPS and Δ dTCHO) or the exopolymer particles (Δ EP) and the integrated heterotrophic prokaryotic production (PHP_{int}) (Figure 3.8). The higher the PHP_{int} , the higher the daily precursor or EP production was. It is remarkable that the slopes of these three regression lines were statistically similar being 0.89 ± 0.19 for Δ dTCHO, 0.72 ± 0.19 for Δ dAPS, and 0.61 ± 0.11 for Δ EP.

EP production by heterotrophic prokaryotes

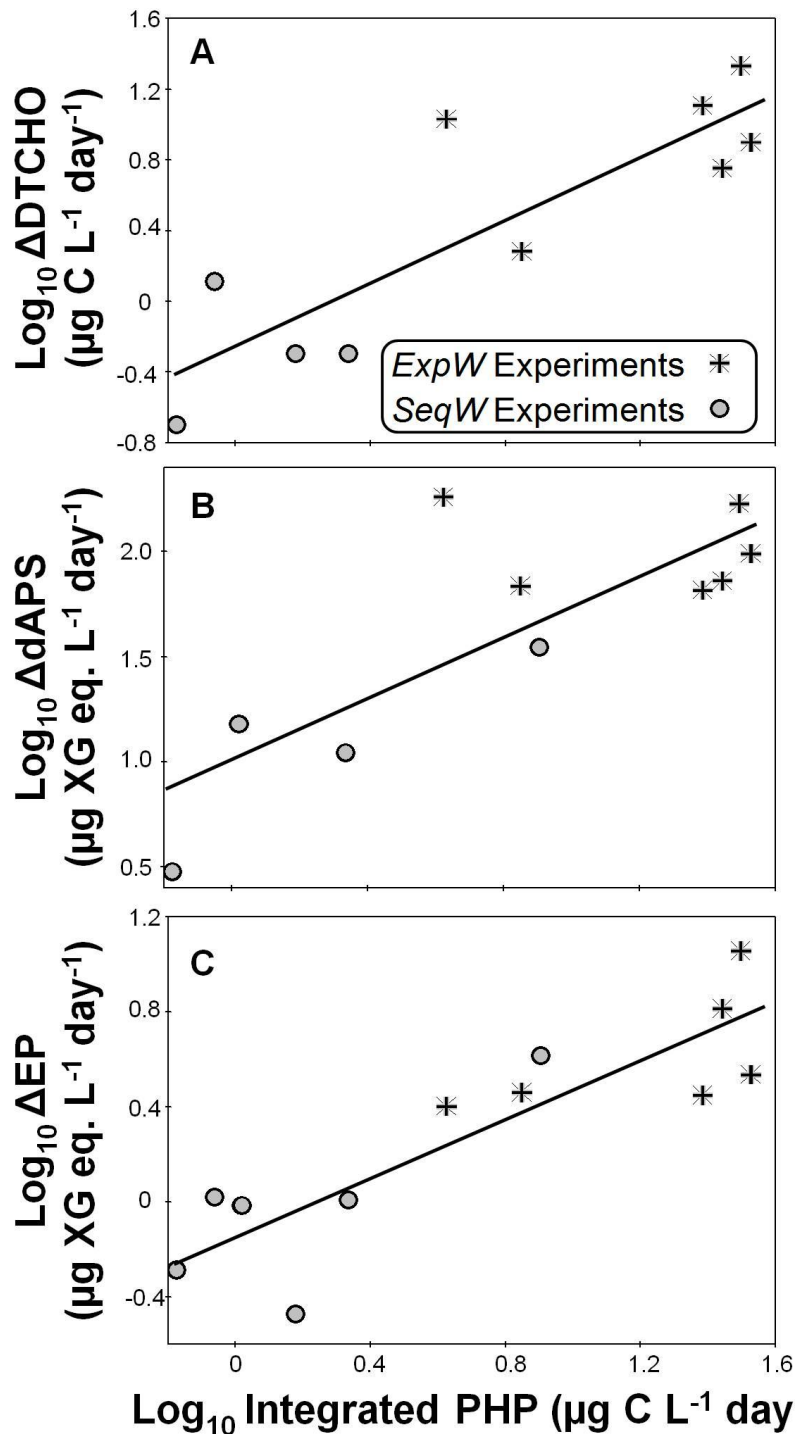


Figure 3. 8. Log-log relationships between integrated PHP (PHP_{int}) and (A) production of neutral polysaccharides ($\Delta DTCHO$) [$n= 10$; $r^2 = 0.73$ and p -value = 0.0017; $\text{Log}_{10} \Delta DTCHO = 0.89 (\pm 0.19) \text{Log}_{10} PHP_{int} - 0.26 (\pm 0.19)$], (B) production of dissolved acidic polysaccharides ($\Delta dAPS$) [$n= 10$; $r^2 = 0.64$ and p -value = 0.0053; $\text{Log}_{10} \Delta dAPS = 0.72 (\pm 0.19) \text{Log}_{10} PHP_{int} + 1.01 (\pm 0.20)$] and (C) production of exopolymer particles (ΔEP) [$n= 12$; $r^2 = 0.76$ and p -value = 0.0002; $\text{Log}_{10} \Delta EP = 0.61 (\pm 0.11) \text{Log}_{10} PHP_{int} - 0.14 (\pm 0.10)$].

We observed significant and positive relationships between ΔEP and their dissolved precursors the $\Delta dAPS$ [$\text{Log}_{10} \Delta EP = 0.61 (\pm 0.13) \text{Log}_{10} \Delta dAPS - 0.58 (\pm 0.23)$; $n = 10$, $r^2 = 0.72$ and $p\text{-value} < 0.01$] and the $\Delta DTCHO$ [$\text{Log}_{10} \Delta EP = 0.61 (\pm 0.12) \text{Log}_{10} \Delta DTCHO - 0.03 (\pm 0.10)$; $n = 10$, $r^2 = 0.75$ and $p\text{-value} < 0.01$] and their corresponding slopes were similar.

These regressions for ΔPHA were also significant but with lower explained variance (r^2): ΔPHA - $\Delta DTCHO$ regression ($n = 10$ and $p\text{-value} < 0.05$) with $r^2 = 0.40$ and slope = $0.86 (\pm 0.37)$; ΔPHA - $\Delta dAPS$ regression ($n = 10$ and $p\text{-value} < 0.05$) with $r^2 = 0.46$ and slope = $0.71 (\pm 0.27)$; ΔPHA - ΔEP regression ($n = 12$ and $p\text{-value} < 0.05$) with $r^2 = 0.39$ and slope = $0.57 (\pm 0.22)$.

To test if the differences in the EP concentrations in the experiments were significant over time and between treatments we performed repeated measure ANOVA analyses (Table 3.3.). Although time had a positive effect in all experiments, the effect of viral load manipulation was more dependent on the nature of the manipulation throughout the time (increase or decrease of the viral load).

EP production by heterotrophic prokaryotes

Table 3.3. Results of repeated measures ANOVA in the experiments to determine if the differences in EP concentrations over time and between treatments (control vs. viral load manipulation) were significant. *n.s.* = not significant effect and * = significant effect (*p*-value < 0.05).

Experiment	Effect	F	p-value	
At-ExpW	Time*	46.22	< 0.001	positive
	Viral load manipulation *	13.57	< 0.01	positive
	Interaction	1.71	n.s.	
Ind-ExpW	Time*	85.72	< 0.001	positive
	Viral load manipulation *	8.59	< 0.05	positive
	Interaction	0.51	n.s.	
Pac-ExpW	Time*	116.18	< 0.001	positive
	Viral load manipulation *	13.12	< 0.01	negative
	Interaction*	8.65	< 0.05	
At-SeqW	Time*	23.71	< 0.001	positive
	Viral load manipulation	1.89	n.s.	n.s.
	Interaction	0.83	n.s.	n.s.
Ind-SeqW	Time*	59.32	< 0.001	positive
	Viral load manipulation *	114.32	< 0.001	positive
	Interaction*	36.65	< 0.001	
Pac-SeqW	Time*	50.44	< 0.001	positive
	Viral load manipulation *	17.02	< 0.01	negative
	Interaction*	11.90	< 0.01	

The viral load manipulation had a significant effect on EP concentration in all the experiments, with exception of the *At-SeqW* (Table 3.3.). In most experiments, this effect was positive, but for the Pacific Ocean experiments (*ExpW* and *SeqW*) the effect of the manipulation of the viral load was negative (Table 3.3.).

We also performed ANOVA analyses to test if the differences in the cell-specific EP production (fg XG eq cell⁻¹ day⁻¹) in the experiments were significant over time and between treatments (Table 3.4.). We observed that in all the epipelagic experiments (*ExpW*), the manipulation (reduction) of the virus abundance had a significant and positive effect on the cell-specific EP production. However, we did not detect any significant effect, or this effect was negative, in the experiments performed with bathypelagic waters (*SeqW*). In both types of experiments (*ExpW* and *SeqW*), the cell-specific EP production was significant and negatively affected by incubation time.

Table 3. 4. Results of ANOVAs in the experiments to determine if the differences in the cell-specific EP concentrations over time and between treatments (control vs. viral load manipulation) were significant. n.s. = not significant effect and * = significant effect (p -value < 0.05).

Experiment	Factor	F	p-value	Effect
At-ExpW	Time*	205.84	< 0.001	negative
	Viral load manipulation *	410.03	< 0.001	positive
	Interaction*	183.14	< 0.001	
Ind-ExpW	Time*	84.13	< 0.001	negative
	Viral load manipulation *	389.79	< 0.001	positive
	Interaction*	65.44	< 0.001	
Pac-ExpW	Viral load manipulation *	49.95	< 0.001	positive
At-SeqW	Time*	46.59	< 0.001	negative
	Viral load manipulation	0.06	n.s.	n.s.
	Interaction	1.72	n.s.	n.s.
Ind-SeqW	Time*	10.14	< 0.05	negative
	Viral load manipulation	2.28	n.s.	n.s.
	Interaction	0.97	n.s.	n.s.
Pac-SeqW	Viral load manipulation *	14.99	< 0.05	negative

We explored the role of viral lysis on the production of dissolved precursors (dAPS and DTCHO) and EP (Δ EP) using the VA:PHA ratio as surrogate of potential viral infection. We observed positive and significant relationships between the VA:PHA ratio and the production of DTCHO [$n = 12$; $r^2 = 0.50$ and p -value = 0.01; Δ DTCHO = 0.53 (± 0.17) virus:prokaryote ratio + 0.58 (± 2.08)], dAPS [$n = 12$; $r^2 = 0.50$ and p -value = 0.; Δ dAPS = 5.04 (± 1.61) virus:prokaryote ratio + 14.83 (± 19.56)], and EP [$n = 12$; $r^2 = 0.68$ and p -value = 0.001; Δ EP = 0.29 (± 0.06) virus:prokaryote ratio + 0.70 (± 0.75)].

3.4.3. *In situ* EP production and residence time

Finally, to estimate the *in situ* EP production rates we used the *in situ* values of prokaryotic heterotrophic production (data as in Mazuecos et al. chapter 1) and the regression equation between PHP_{int} and daily EP production in the experiments (Figure 3.8. C). The *in situ* EP residence time (days) was obtained as the division of *in situ* EP concentration (Table 3.1. and Mazuecos et al., Chapter 2) and the *in situ* EP production.

EP production by heterotrophic prokaryotes

In the epipelagic experiments (*ExpW*) the EP residence time ranged from 14 to 132 days in the Pacific and Atlantic Ocean, respectively. The EP residence times in the bathypelagic experiments (*SeqW*) ranged from 46 to 231 days (Table 3.5.). The estimations of the *in situ* production and residence time for all the ocean basins are also summary in Table 3.5. Residence times were substantially longer in the bathypelagic waters (> 1000 m) than in the epipelagic waters (< 200 m) increasing from the North Atlantic (260 days), through the Indian (354 days) to the North Pacific Ocean (504 days).

Table 3. 5. Estimations of in situ EP production rates and residence times at the depths of the different experiments and in the different ocean basins. Mean values and ranges (in brackets) are shown.

Experiments		<i>In situ</i> EP	
		production ($\mu\text{g XG eq. L}^{-1} \text{ day}^{-1}$)	EP residence time (days)
At-ExpW		0.22	132
Ind-ExpW		0.22	25
Pac-ExpW		1.17	14
At-SeqW		0.03	46
Ind-SeqW		0.02	163
Pac-SeqW		0.08	231
oceanic regions			
North Atlantic	< 200	0.58 (0.06 - 2.34)	39 (1 - 346)
	>1000	0.03 (< 0.01 - 0.16)	260 (14 - 1415)
South Atlantic	< 200	0.48 (0.08 - 1.98)	56 (7 - 473)
	>1000	0.05 (< 0.01 - 0.13)	177 (21 - 1576)
Indian	< 200	0.28 (0.01 - 1.39)	121 (1 - 1996)
	>1000	0.03 (0.01 - 0.11)	354 (2 - 1901)
South Pacific	< 200	0.73 (0.09 - 6.59)	53 (3 - 250)
	>1000	0.06 (0.01 - 0.17)	192 (31 - 645)
North Pacific	< 200	0.58 (0.04 - 5.54)	63 (2 - 625)
	>1000	0.03 (< 0.01 - 0.12)	504 (26 - 3616)
Global	< 200	0.49 (0.01 - 6.59)	71 (1 - 1996)
	>1000	0.04 (< 0.01 - 0.17)	333 (2 - 3616)

3.5. Discussion

Our experiments showed that prokaryotes contribute to the EP pool both in the epipelagic waters (< 200 m; *ExpW*) using the fresh phytoplankton-derived DOC and in the bathypelagic waters (> 1000 m; *SeqW*) using the aged DOC. In fact, the initial concentration of dissolved acidic polysaccharides and carbohydrates, taken as dissolved EP precursors (Thornton et al., 2007; Skoog et al., 2008), in the experiments was substantially higher in the *ExpW* experiments than in *SeqW* experiments (Table 3.1.). The viral influence (or the different manipulation in treatments) on EP production, however, was significant only in the epipelagic waters but not in the bathypelagic waters.

3.5.1. Methodological considerations

Our results were obtained using two treatments with water samples previously filtered (1 μm , 0.2 μm pore-size and ultrafiltered through 30 KDa) or microwaved and incubated in bottles for 7-12 days. The filtration approach has been used in previous studies for the experimental determination of EP production by heterotrophic prokaryotes in surface and coastal waters (Stoderegger and Herndl, 1999; Sugimoto et al., 2007; Ortega-Retuerta et al., 2010). Although it is obvious the role of prokaryotes on EP production, the different procedures in the treatments may have introduced uncertainties in relation to the reproduction of the natural marine environments, and thus, our results must be interpreted with caution. A microwave treatment (in the *At-ExpW* experiment) was used to inactivate the viruses, but this procedure did not physically disintegrate (and likely did not inactivate) all the viruses (Winter et al., 2004), as indicated in the Figure 3.3. In addition, the possibility that microwaving modified the DOC composition of the treatment with a viral load manipulation cannot be ruled out, since the PHA reduction in these treatments suggests that microwaves likely caused prokaryotic lysis and the intracellular content was released into the environment. On the other hand, the ultrafiltration through 30 KDa in the rest of experiments used to

EP production by heterotrophic prokaryotes

reduce the viral abundance (Bonilla-Findji et al., 2008) may also undergo physical (conformational or structural) alteration of the dissolved organic matter (Zsolnay, 2003). Then, the procedures to perform the viral load reduction may introduce artifacts that hamper the interpretation of the results. The alteration of the initial organic matter, after above pre-treatments, would cause that dissolved organic matter become more available for microbial uptake which would explain that PHP T_0 values were similar in both treatments or higher in the treatments of the viral load manipulation than the control treatments (Table 3.1.). Except in the *At-ExpW* experiment (data not available), an analysis of the optical properties of initial dissolved organic matter showed similar spectra in both treatments (control vs. viral load manipulation), but with different fluorescence and absorbance intensities (data not shown). This fact suggest that a portion of the molecules with similar optical properties were retained on the filters, changed its conformation (and optical properties) or both processes.

3.5.2. EP production in the epipelagic and bathypelagic waters

In the experiments performed with epipelagic waters (*ExpW*), EP production rates in absolute terms ($2.5 - 11.4 \mu\text{g XG eq. L}^{-1} \text{ day}^{-1}$) were consistently higher than the rates obtained in the experiments with bathypelagic waters (*SeqW*). The *ExpW* rates were similar to the rates obtained by Ortega-Retuerta et al. (2010) in the open Mediterranean Sea ($4.8 - 19.0 \mu\text{g XG eq. L}^{-1} \text{ day}^{-1}$) and slightly lower than the rates obtained by other authors, in coastal waters, that reached up to $267 \mu\text{g XG eq. L}^{-1} \text{ day}^{-1}$ (Stoderegger and Herndl, 1999; Prieto et al., 2002; Sugimoto et al., 2007). Koch et al. (2014) demonstrated experimentally that EP were produced during the degradation of bioavailable organic matter (i.e. glucose). Therefore, the different initial pool of dissolved organic matter in the epipelagic waters, with more bioavailable organic carbon (Table 3.1.), can contribute to explain to some extent the higher rates in this layer. The temperature of these layers and in the *ExpW* and *SeqW* experiments (ca. *in*

situ temperature) was also very different (Table 3.1.) and the strong influence of temperature on microbial metabolism, both in respiration and in growth is well recognized (White et al., 1991, López-Urrutia and Morán, 2007; Vázquez-Domínguez et al., 2007; Mazuecos et al., 2015 in Chapter 4). Recently, several works highlighted that EP production is a temperature-dependent process (Piontek et al., 2009; Fukao et al., 2012). The higher the temperature, the higher EP production was. Piontek et al. (2009) pointed out that the stimulating effect of temperature on bacterial growth was the ultimate factor producing the increase in EP production.

In fact, in this study prokaryotic heterotrophic production, integrated over the incubation time, was the best predictor of EP production considering all the data (Figure 3.8. C). Previous studies have also reported a tight relationship between these two processes (Sugimoto et al., 2007; Ortega-Retuerta et al., 2010). The similarity of the slope (0.61 ± 0.11) obtained in this study and the slopes obtained by Ortega-Retuerta et al. (2010) for experimental data (0.43 ± 0.14) indicates the robustness of this relationship. Therefore, an increase of temperature and organic matter bioavailability would promote the microbial growth and simultaneously would affect EP production.

Unlike EP production in absolute terms, the cell-specific EP production (i.e. EP production normalized by cell abundance) was usually higher in the controls of experiments performed with bathypelagic waters (*SeqW*) ($4.3 - 48.7$ fg XG eq. cell⁻¹ day⁻¹) than in the controls with epipelagic waters (*ExpW*) ($4.5 - 15.2$ fg XG eq. cell⁻¹ day⁻¹) (white bars in Figures 3.5. and 3.7.). The cell-specific EP production in the *ExpW* experiments was similar to the rates obtained in surface waters in previous studies (Stoderegger and Herndl, 1999; Ortega-Retuerta et al., 2010), but we have not found data for the deep ocean. The higher cell-specific EP production rate in the bathypelagic waters suggests that in this depth the prokaryotes produced more EP per cell despite the extremely less favorable conditions

EP production by heterotrophic prokaryotes

with low bioavailable DOC and lower temperatures than the conditions of their counterparts from the epipelagic waters.

This major synthesis of EP per cell may be a life strategy for the dark ocean prokaryotes to resist adverse conditions (Poli et al., 2010). Several lines of evidence have pointed out a preference of the deep ocean prokaryotes for living associated to particles (Baltar et al., 2009; Herndl and Reinthaler, 2013). These prokaryotes have large genomes to harbor a diverse enzymatic potential, genes for the synthesis of pili and polysaccharides degradation (DeLong et al., 2006; Martin-Cuadrado et al., 2007) and seem to have a preferential opportunistic life (Lauro et al., 2009). In fact, the average EP residence time in the bathypelagic waters estimated in this study was of ca. one year (Table 3.5.), being part of the semi-labile organic carbon fraction (with a residence time of months to years; Carlson, 2002), considerably shorter than the DOC residence time of 370 years (Hansell et al., 2009), that is mostly of refractory nature (with a residence time of centuries to millennia; Hansell, 2013). This result corroborates previous studies that have shown, using radiocarbon, that the particulate organic matter in the deep ocean is considerably younger than the dissolved pool (Druffel and Williams, 1990; Druffel and Robinson, 1999). Therefore, it is expected that POC is a better substrate to prokaryotic life than the dissolved organic substances.

3.5.3. The complex role of viruses in EP production

Previous works have empirically evidenced that viral lysis induced EP production, preceded by programmed cell death in phytoplanktonic species (Bidle et al., 2007; Vardi et al., 2012), but these connections in prokaryotes have not been documented yet. It is known that viral lysis releases submicron particles (Shibata et al., 1997; Uitz et al., 2010) that might self-assemble over time into larger particles (Chin et al., 1998; Verdugo et al., 2004) promoting aggregation and coagulation (Uitz et al., 2010). These submicron particles as well as the capsular material released by bacteria (Stoderegger and Herndl, 1999) may be considered as

condensation nuclei for EP formation. However, Lønborg et al. (2013) concluded that, despite a higher EP concentration were experimentally produced under an intense viral stress, viral lysis has multiple and opposite implications in the oceanic organic matter cycle.

In the epipelagic experiments, the treatments with a viral load manipulation involved its effective reduction over the incubation time (Figure 3.2.) and showed constantly higher cell-specific EP production than control treatments (Figure 3.5.). As we mentioned above, a tight relationship between PHP and EP production has been documented in previous studies (Sugimoto et al., 2007; Ortega-Retuerta et al., 2010) and in our work (Figure 3.8. C). Several authors have also demonstrated a significant effect of viral infection on prokaryotic metabolism (Middelboe and Lyck, 2002; Bonilla-Findji et al., 2008), with a relevant increase of prokaryote growth under less viral stress (less viral load). Viral lysis also involves the release of inorganic and organic nutrients (Wilhelm and Suttle, 1999; Middelboe and Lyck, 2002) that potentially could induce growth of other prokaryotes (Shelford et al., 2014). Any promotion of PHP, therefore, would induce a stimulus of EP production (increasing cell-specific EP production). Certainly, prokaryotes under more favorable conditions, with more available DOC (after ultrafiltration or microwave procedure) and less viral load, can directly increase PHP. The prokaryotic outgrowth, consequently, induces a rapid formation of microscopic EP condensation nuclei (within minutes) that are aggregated in larger EP and, in turn, extensively colonized by heterotrophic prokaryotes (Bar-Zeev et al., 2012). Indeed, increases in EP concentration have been observed previous to the increase of bacterial abundance in experiments analyzing processing of the organic matter (Koch et al., 2014) suggesting that EP release was a process prior to bacterial replication itself. Stoderegger and Herndl (1999) in microbial regrowth cultures also observed a rapid increment of EP in the exponential growth phase (in aprox. 48 h).

EP production by heterotrophic prokaryotes

However, the influence of viral load in the experiments performed with bathypelagic waters (*SeqW*), considering the cell-specific EP production, was not significant in Atlantic and Indian experiments and even negative in the Pacific experiment (Figure 3.7. and Table 3.4.). This contrasting effect of viral manipulation on cell-specific EP production in the *SeqW* experiments suggest that the main role of viruses might be indirect through alleviation of stress or promotion of prokaryote growth although all these interactions are very imbricated and likely are different in the epipelagic waters and in the bathypelagic waters (Weitz and Wilhelm, 2012).

Acknowledgements

We thank our scientific colleagues and C. M. Duarte for the coordination of the Malaspina expedition, as well as the technical staff and crew members on board BIO Hespérides, for their support in the field sampling during the different legs of the Malaspina cruise. This paper is a contribution to the INGENIO 2010 CONSOLIDER program (CDS2008-00077). IPM was supported by a JAE Pre-doc fellowship, from the Spanish National Research Council (CSIC) and the BBVA Foundation, Spain. IPM, JA and JMG were partly supported by project HotMix (CTM2011-30010-C02/MAR).

3.6. References

- Allredge A. L., Passow U., Logan B. E. 1993. The abundance and significance of a class of large, transparent organic particles in the ocean. *Deep-Sea Research I*, 40 (6): 1131 - 1140.
- Arístegui J., Gasol J. M., Duarte C. M., Herndl G. J. 2009. Microbial oceanography of the dark ocean's pelagic realm. *Limnology and Oceanography*, 54(5): 1501 - 1529.
- Baltar F., Arístegui J., Gasol, J. M., Sintes, E., and Herndl, G. J. 2009. Evidence of prokaryotic metabolism on suspended particulate organic matter in the dark waters of the subtropical North Atlantic. *Limnol. Oceanogr.*, 54: 182-193.
- Bar-Zeev E., Berman-Frank I., Girshevitz O., Berman T. 2012. Revised paradigm of aquatic biofilm formation facilitated by microgel transparent exopolymer particles. *PNAS*, 109 (23), 9119 - 9124.
- Bar-Zeev E., Berman T., Rahav E., Dishon G., Herut B., Kress N., Berman-Frank I. 2011. Transparent exopolymer particle (TEP) dynamics in the eastern Mediterranean sea. *Marine Ecology Progress Series*, 431: 107 - 118.
- Berman-Frank I., Dubinsky Z. 1999. Balanced growth in aquatic plants: Myth or reality? Phytoplankton use the imbalance between carbon assimilation and biomass production to their strategic advantage. *Bioscience*, 49 (1): 29 - 37.
- Berman-Frank I., Rosenberg G., Levitan O., Haramaty L. and Mari X. 2007. Coupling between autocatalytic cell death and transparent exopolymer particle production in the marine cyanobacterium *Trichodesmium*. *Environmental Microbiology*, 9 (6): 1415 - 1422.
- Bhaskar P. V., Bhosle N. B. 2005. Microbial extracellular polymeric substances in marine biogeochemical processes. *Current Science*, 88(1): 45-53.
- Bidle K. D., Haramaty L., Ramos J. B., Falkowski P. 2007. Viral activation and recruitment of metacaspases in the unicellular coccolithophore, *Emiliana huxleyi*. *PNAS*, 104(14): 6049 - 6054.
- Bonilla-Findji O., Malitsa A., Lefèvre D., Rochelle-Newall E., Leméa R., Weinbauer M. G., Gattuso J.-P. 2008. Viral effects on bacterial respiration, production and growth efficiency: Consistent trends in the Southern Ocean and the Mediterranean Sea. *Deep-Sea Research II*, 55: 790 - 800.
- Brussaard C. P. D. 2004. Optimisation of procedures for counting viruses by flow cytometry. *Applied Environmental Microbiology*. 70: 1506-1513.
- Buesseler K. O., Lamborg C. H., Boyd P. W., Lam P. J., Trull T. W., Bidigare R. R., Bishop J. K. B., Casciotti K. L., Dehairs F., Elskens M., Honda M., Karl D. M., Siegel D. A., Silver M. W., Steinberg D. K., Valdes J., Van Mooy B., Wilson S. 2007. Revisiting carbon flux through the ocean's twilight zone. *Science* 316 (5824): 567 - 570.
- Burd A. B., Jackson G. A. 2009. Particle Aggregation. *Annual Review of Marine Science*, 1: 65 - 90.
- Carlson C. A. 2002. Production and removal processes. In: Hansell D. A., Carlson C. A. (Eds.), *Biogeochemistry of Marine Dissolved Organic Matter*. Elsevier, San Diego, p. p. 91-151.
- Chin W.-C., Orellana M. V., Verdugo P. 1998. Spontaneous assembly of marine dissolved organic matter into polymer gels. *Nature*, 391: 568 - 572.
- Cole J. J., Likens G. E., Strayer D. L. 1982. Photosynthetically produced dissolved organic-carbon: an important carbon source for planktonic bacteria. *Limnol Oceanogr* 27: 1080 - 1090.
- Decho A. W. 1990. Microbial exopolymer secretions in ocean environments: their role(s) in food webs and marine processes. *Oceanogr. Mar. Biol. Annu. Rev.*, 28: 73 - 153.
- DeLong E. F., Preston C. M., Mincer T., Rich V., Hallam S. J., Frigaard N.-U. Martínez A., Sullivan M. B., Edwards R., Brito B. R., Chrisholm S. W. and Karl D. M. 2006. Community genomics among stratified microbial assemblages in the ocean's interior. *Science*, 311: 496 - 503.

- Ding Y.-X., Chin W.-C., Rodriguez A., Hung C.-C., Santschi P. H., Verdugo P. 2008. Amphiphilic exopolymers from *Sagittula stellata* induce DOM self-assembly and formation of marine microgels. *Marine chemistry*, 112(1-2): 11 - 19.
- Druffel E. R. M., Williams P.W. 1990. Identification of a deep source of particulate organic carbon using bomb ^{14}C . *Nature*, 347: 172 - 174.
- Druffel E. R. M., Robinson B. H. 1999. Is the deep sea on a diet? *Science*, 284: 1139.
- Ducklow H. W., Steinberg D. K. Buesseler K. O. 2001. Upper Ocean Carbon Export and the Biological Pump. *Oceanography*, 14 (4): 50 - 58.
- Fouilland E., Tolosa I., Bonnet D., Bouvier C., Bouvier T., Bouvy M., Got P., Le Floc'h E., Mostajir B., Roques C., Semper R., Sime-Ngand T., Vidussi F. 2014. Bacterial carbon dependence on freshly produced phytoplankton exudates under different nutrient availability and grazing pressure conditions in coastal marine waters. *FEMS Microbiology Ecology*, 87: 757-769.
- Fukao T., Kimoto K., Kotami Y. 2012. Effect of temperature on cell growth and production of transparent exopolymer particles by the diatom *Coscinodiscus granii* isolated from marine mucilage. *Journal of Applied Phycology*, 24(2): 181 - 186.
- Gasol, J. M., Del Giorgio. P. A. 2000. Using flow cytometry for counting natural planktonic bacteria and understanding the structure of planktonic bacterial communities. *Sci. Mar.* 64: 197-224.
- Gärdes A., Iversen M. H., Grossart H.-P., Passow U., Ullrich M. S. 2010. Diatom-associated bacteria are required for aggregation of *Thalassiosira weissflogii*. *The ISME Journal*, 5: 436 - 445.
- Grossart H.-P., Czub G., Simon M. 2006. Algae-bacteria interactions and their effects on aggregation and organic matter flux in the sea. *Environmental Microbiology*, 8(6): 1074 - 1084.
- Hansell, D. A. (2013) Recalcitrant dissolved organic carbon fractions. *Annu. Rev. Mar. Sci.* 5, 421-445.
- Hansell D. A., Carlson C. A., Repeta D. J., Schlitzer R. 2009. Dissolved organic matter in the ocean. A controversy stimulates new insights. *Oceanography* 22, 202-211.
- Herndl G. J., Reinthaler T. 2013. Microbial control of the dark end of the biological pump. *Nature Geoscience*, 6 (9): 718 - 724.
- Kirchman D. L., K'nees E., Hodson R. E. 1985. Leucine incorporation and its potential as a measure of protein synthesis by bacteria in natural aquatic systems. *Appl. Environ. Microbiol.* 49: 599-607.
- Koch B. P., Kattner G., Witt M., Passow U. 2014. Molecular insights into the microbial formation of marine dissolved organic matter: recalcitrant or labile? *Biogeosciences*, 11: 4173 - 4190.
- Lauro F. M., McDougald D., Thomas T., Williams T. J., Egan S., Rice S., DeMaere M. Z., Ting L., Ertan H., Johnson J., Ferriera S., Lapidus A., Anderson I., Kyrpides N., Munk A. C., Detterg C., Hang C. S., Browna M. V., Robb F. T., Kjelleberg S., Cavicchioli R. 2009. The genomic basis of trophic strategy in marine bacteria. *PNAS*, 106 (37): 15527 - 15533.
- Long R. A., Azam F. 1996. Abundant protein-containing particles in the sea. *Aquatic Microbial ecology*, 10: 213 - 221.
- Martin-Cuadrado A.-B., López-García P., Alba J.-C. Moreira D., Monticelli L., Strittmatter A., Gottschalk G., Rodríguez-Valera F. 2007. Metagenomics of deep Mediterranean, a warm bathypelagic habitat. *PLoS One*, 9: e914.
- Middelboe M., Lyck P. G. 2002. Regeneration of dissolved organic matter by viral lysis in marine microbial communities. *Aquatic Microbial Ecology* 27, 187-194.
- Moran X. A. G., Estrada M., Gasol J. M., Pedrós-Alió C. 2002. Dissolved primary production and the strength of phytoplankton-bacterioplankton coupling in contrasting marine regions. *Microb Ecol* 44: 217-223.

EP production by heterotrophic prokaryotes

- Myklestad S., Skanoy E., Hestmann S. 1997. A sensitive and rapid method for analysis of dissolved mono- and polysaccharides in seawater. *Marine Chemistry*, 56 (3-4): 279-286.
- Lauro F. M., McDougald D., Thomas T., Williams T. J., Egan S., Rice S., DeMaere M. Z., Ting L., Ertan H., Johnson J., Ferriera S., Lapidus A., Anderson I., Kyrpides N., Munk A. C., Detter C., Han C. S., Brown M. V., Robb F. T., Kjelleberg S., Cavicchioli R. 2009. The genomic basis of trophic strategy in marine bacteria. *PNAs*, 106 (37): 15527 - 15533.
- Logan B. E., Passow U., Alldredge A. L., Grossart H.-P., Simon M. 1995. Rapid formation and sedimentation of large aggregates is predictable from coagulation rates (half-lives) of transparent exopolymer particles (TEP). *Deep-Sea Research II*, 42 (1): 203 - 214.
- López-Urrutia A., Morán X. A. G. 2007. Resource limitation of bacterial production distorts the temperature dependence of oceanic carbon cycle. *Ecology*, 88(4): 817 - 822.
- Lønborg C., Middelboe M., Brussaard C. P. D. 2013. Viral lysis of *Micromonas pusilla*: impacts on dissolved organic matter production and composition. *Biogeochemistry*, DOI: 10.1007/s10533-013-9853-1.
- Ortega-Retuerta E., Duarte C. M., Reche I. 2010. Significance of Bacterial Activity for the Distribution and Dynamics of Transparent Exopolymer Particles in the Mediterranean Sea. *Microbial Ecology*, 59: 808 - 818.
- Ortega-Retuerta E., Passow U., Duarte C. M. and Reche I. 2009. Effects of ultraviolet B radiation on (not so) transparent exopolymer particles. *Biogeosciences*, 6, 3071 - 3080.
- Ortega-Retuerta E., Reche I. Pulido-Villena E., Agustí S., Duarte C. 2008. Exploring the relationship between active bacterioplankton and phytoplankton in the Southern Ocean Aquatic Microbial Ecology, 52: 99-106.
- Passow U. 2002. Transparent exopolymer particles (TEP) in aquatic environments. *Progress in Oceanography*, 55: 287 - 333.
- Passow U., Alldredge A. L. 1995. A die-binding assay for the spectrophotometric measurement of transparent exopolymer particles (TEP). *Limnology and Oceanography*, 40 (7): 1326 - 1335.
- Passow U., Carlson C. A. 2012. The biological pump in a high CO₂ world. *Marine Ecology Progress Series*. 470: 249 - 271.
- Piontek J., Händel N., Langer G., Wohlers J., Riesebell U., Engel A. 2009. Effects of rising temperature on the formation and microbial degradation of marine diatom aggregates. *Aquatic Microbial Ecology*, 54: 305 - 318.
- Poli A., Anzelmo G., Nicolaus B. 2010. Bacterial Exopolysaccharides from Extreme Marine Habitats: Production, Characterization and Biological Activities. *Marine drugs*, 8(6): 1779-1809.
- Prieto L., Ruiz J., Echevarria F., Garcia C. M., Bartual A., Galvez J. A., Corzo A., Macias D. 2002. Scales and processes in the aggregation of diatom blooms: high time resolution and wide size range records in a mesocosm study. *Deep-Sea Res. I*, 49: 1233 - 1253.
- Radic T., Ivancic I., Fuks D., Radic J. 2006. Marine bacterioplankton production of polysaccharidic and proteinaceous particles under different nutrient regimes. *FEMS Microbiol. Ecol.*, 58: 333 - 342.
- Robinson, C., Steinberg, D.K., Anderson, T.R., Arístegui, J., Carlson, C.A., Frost, J.R., Ghiglione, J.-F., Hernández-León, S., Jackson, J.A., Koppelman, R., Quéguiner, B., Ragueneau, O., Rassoulzadegan, F., Robison, B.H., Tamburini, C., Tanaka, T., Wishner, K.F., Zhang, J., 2010. Mesopelagic zone ecology and biogeochemistry – a synthesis. *Deep Sea Res. II* 57, 1504-1518.
- Rochelle-Newall E. J., Mari X., Pringault O. 2010. Sticking properties of transparent exopolymeric particles (TEP) during aging and biodegradation. *Journal of Plankton Research*, 32(10): 1433 - 1442.

- Shelford E. J., Jørgensen N. O. g., Rasmussen S., Suttle C. A., Middelboe M. 2014. Dissecting the role of viruses in marine nutrient cycling: bacterial uptake of D- and L-amino acids released by viral lysis. *Aquatic Microbial Ecology*, 73: 235 - 243.
- Shibata A., Kogure K., Koike I., Ohwada K. 1997. Formation of submicron colloidal particles from marine bacteria by viral infection. *Marine Ecology Progress Series*, 155: 303 - 307.
- Simon M., Azam F. 1989. Protein content and protein synthesis rates of planktonic marine bacteria. *Marine Ecology Progress Series*, 51: 201 - 213.
- Skoog A., Alldredge A., Passow U., Dunne J., Murray J. 2008. Neutral aldoses as source indicators for marine snow. *Marine Chemistry* 108: 195 - 206.
- Smith D. C., Azam F. 1992. A simple, economical method for measuring bacterial protein synthesis rates in seawater using ³H-leucine. *Marine Microbial Food Webs*, 6: 107 - 114.
- StatSoft Inc, 1997. *Statistica for Windows (Computer Program Manual)*. Tulsa, Oklahoma, USA.
- Stoderegger K., Herndl G. J. 1999. Production of exopolymer particles by marine bacterioplankton under contrasting turbulence conditions. *Marine Ecology Progress Series*, 189: 9 - 16.
- Sugimoto K., Fukuda H., Baki M. A., Koike I. 2007. Bacterial contributions to formation of transparent exopolymer particles (TEP) and seasonal trends in coastal waters of Sagami Bay, Japan. *Aquatic Microbial Ecology*, 46: 31 - 41.
- Suttle C. A. 2007. Marine viruses - Major players in the global ecosystems. *Nature*, 5: 801 - 812.
- Tan C. H., Koh K. S., Xie C., Tay M., Zhou Y., Williams R., Ng W. J., Rice S. A., Kjelleberg S. 2014. The role of quorum sensing signaling in EPS production and the assembly of a sludge community into aerobic granules. *ISME journal* 8: 1186-1197.
- Thornton D. C. O., Fejes E. M., Dimarco S. F., Clancy K. M. 2007. Measurement of acid polysaccharides in marine and freshwater samples using alcian blue. *Limnology and Oceanography Methods*, 5: 73 - 87.
- Turner J. T. 2015. Zooplankton fecal pellets, marine snow, phytodetritus and the ocean's biological pump. *Progress in Oceanography*, 130: 205 - 248.
- Uitz J., Stramski D., Baudoux A. C., Reynolds R. A. , Wright V. M., Dubranna J., Azam F. 2010. Variations in the optical properties of a particle suspension associated with viral infection of marine bacteria. *Limnol. Oceanogr.*, 55(6): 2317 - 2330.
- Vázquez-Domínguez E., Vaqué D., Gasol J. M. 2007. Ocean warming enhances respiration and carbon demand of coastal microbial plankton. *Global Change Biology*, 13: 1327 - 1334.
- Van Oostende N., Moerdijk-Poortvliet T. C. W., Boschker H. T. S., Vyverman W. and Sabbe K. 2013. Release of dissolved carbohydrates by *Emiliana huxleyi* and formation of transparent exopolymers particles depend on algal life cycle and bacterial activity. *Environmental Microbiology*, 15(5): 1514- 1531.
- Vardi A., Haramaty L., Van Mooy B. A. S., Fredricks H. F., Kimmance S. A., Larsen A. and Bidle K. D. 2012. Host-virus dynamics and subcellular controls of cell fate in a natural coccolithophore population. *PNAs*, 109 (47): 19327 -19332.
- Verdugo P., Alldredge A. L., Azam F., Kirchman D. L., Passow U., Satschi P. H. 2004. The oceanic gel phase: a bridge in the DOM-POM continuum. *Marine chemistry*, 92: 67 - 85.
- Weitz J. S., Wilhelm S. W. 2012. Ocean viruses and their effects on microbial communities and biogeochemical cycles. *F1000 Biology Reports*, 4: 17.
- White P. A., Kalf J., Rasmussen J. B., Gasol J. M. 1991. The effect of temperature and algal biomass on bacterial production and specific growth rate in freshwater and marine habitats. *Microbial Ecology*, 21: 99 - 118.

EP production by heterotrophic prokaryotes

- Winter C., Smit A., Herndl G. J., Weinbauer G. 2004. Impact of Virioplankton on Archaeal and Bacterial Community Richness as Assessed in Seawater Batch Cultures. *Applied and Environmental Microbiology*, 70(2): 804 – 813.
- Willhelm S. W., Suttle C. A. 1999. Viruses and Nutrient Cycles in the Sea. *BioScience*, 49 (10): 781 – 788.
- Zsolnay A. 2003. Dissolved organic matter: artefacts, definitions, and functions. *Geoderma* 113:187 – 209.

Chapter 4:

Temperature control of microbial respiration and growth efficiency in the mesopelagic zone of the South Atlantic and Indian Oceans



Ignacio P. Mazuecos, Javier Arístegui, Evaristo Vázquez-Domínguez, Eva Ortega-Retuerta, Josep M. Gasol and Isabel Reche
Deep Sea Research I: vol. 95, p.p. 131 - 138 (2015)
(in Annex V)

Abbreviated title: **Temperature control of R and PGE in the mesopelagic zone**

Temperature control of R and PGE in the mesopelagic zone

4.1. Abstract

We have measured both prokaryotic heterotrophic production (PHP) and respiration (R), then providing direct estimates of prokaryotic growth efficiencies (PGE), in the upper mesopelagic zone (300–600 m) of the South Atlantic and Indian Oceans. Our results showed that *in situ* R ranged 3-fold, from 87 to 238 $\mu\text{mol C m}^{-3} \text{ d}^{-1}$. *In situ* PHP rates were much lower but also more variable than R (ranging from 0.3 to 9.1 $\mu\text{mol C m}^{-3} \text{ d}^{-1}$). The derived *in situ* PGE values were on average $\sim 1.4\%$ (from 0.3% to 3.7%), indicating that most of the organic substrates incorporated by prokaryotes were respired instead of being used for growth. Together with the few previous studies on PGE published before for the Atlantic Ocean and Mediterranean Sea, our findings support the hypothesis that the global mesopelagic zone represents a key remineralization site for export production in the open ocean. We also found a strong correlation between R and PGE with temperature across a gradient ranging from 8.7 to 14.9 °C. The derived Q_{10} value of 3.7 suggests that temperature variability in the mesopelagic zone plays a significant role in the remineralization of organic matter.

Temperature control of R and PGE in the mesopelagic zone

4.2. Introduction

Prokaryotes thriving in the mesopelagic zone (200–1000 m depth) are known to play a key role in the mineralization of organic matter transported to the deep ocean (Arístegui et al., 2009; Anderson and Tang, 2010; Giering et al., 2014). Nevertheless, there is still a great lack of information on the regional variability in the percentage of organic matter that is either mineralized as CO₂ (respiration, R) or used by prokaryotes for growth (prokaryotic heterotrophic production; PHP) in the global mesopelagic zone. This metabolic balance is frequently expressed as “prokaryotic growth efficiency” ($PGE = PHP/(PHP+R)$), a term that provides a proxy of the efficiency in the recycling of organic matter by prokaryotes. Direct estimations of R in the dark ocean, by monitoring oxygen changes inside bottles incubated at *in situ* temperatures, are cumbersome, due to the low microbial rates and the much lower sensitivity of the R methodology, compared with the tracer technique used for PHP. Thus, few studies have provided simultaneous direct estimates of both dark ocean R and PHP, being most of them carried out in waters from the North Atlantic Ocean (Biddanda and Benner, 1997; Arístegui et al., 2005b; Reinthaler et al., 2006; Baltar et al., 2010).

Despite the lack of data of actual R across the world oceans, it has been estimated that mesopelagic microorganisms mineralize up to 90% of the organic matter exported from the photic zone (Robinson et al., 2010), yielding high R at these depths (del Giorgio and Duarte, 2002). This hypothesis is supported by indirect estimates (mostly derived from enzymatic respiratory activities) of global mesopelagic R, ranging between 0.6 and 1.4 Pmol C y⁻¹ (Arístegui et al., 2003 and 2005a), that would contribute 9 – 12% of the global ocean respiration (del Giorgio and Williams, 2005). Arístegui et al. (2009) compiled a large data set on metabolic activities from the dark ocean and found that the decrease in PHP with depth was higher than the decrease in R inferred from ETS activity, leading to a decreasing trend in PGE as the -0.3 power of depth. Assuming a mean PGE in the epipelagic zone of 15% (del Giorgio and Cole, 2000), the predicted PGE in the deep ocean would thus be ~4%. Similarly low PGE (on

average ~2 %) derived from direct R estimates were obtained in the meso- and bathypelagic waters of the central North Atlantic (Reinthal et al., 2006), although higher PGE values have also been reported from the North Atlantic dark ocean (e.g. Arístegui et al., 2005b; Baltar et al., 2010). Nevertheless, in spite of the importance of measuring simultaneously R and PHP for addressing the balance between source and sinks of carbon in the water column, there are still very few PGE estimates using direct R measurements to corroborate the above prediction across the world oceans.

The metabolism of all organisms is affected by many environmental factors, being temperature a key parameter (Brown et al., 2004). In this sense, marine heterotrophic prokaryotes are not an exception (i. e. Pomeroy and Wiebe, 2001; Vázquez-Domínguez et al., 2007; Sarmiento et al., 2010) and temperature changes have been reported to have direct implications for the microbial degradation of organic matter in the surface ocean by modifying PGE (Rivkin and Legendre, 2001; López-Urrutia and Morán, 2007; Vázquez-Domínguez et al., 2007; Wohlers et al., 2009; Kritzberg et al., 2010a and b). As it occurs in the surface ocean, temperature variability in the upper mesopelagic zone would affect the activity of marine microorganisms. Depending on the way in which PGE is modified by temperature in the mesopelagic zone the microbial food web could shift the flow of organic carbon by circulating more C through higher trophic levels or by remineralizing the C as CO₂. Understanding the effects of temperature on PGE and R in the mesopelagic zone would thus help to predict future changes on carbon biogeochemistry in a warmer dark ocean, a region poorly investigated until now (Nagata et al., 2001; Arístegui et al., 2009).

In this study, we provide direct estimates of both R and PHP, and derived PGE values, from the upper mesopelagic zone of two largely unexplored ocean basins: the South Atlantic and the Indian Oceans. We hypothesized that, as reported from the North-Atlantic Ocean (Arístegui et al., 2005b; Reinthal et al., 2006; Baltar et al., 2010; Giering et al., 2014), the prokaryotic assemblages in the upper mesopelagic of these two oceans

Temperature control of R and PGE in the mesopelagic zone

represent active nodes of remineralization of organic matter. We also tested the temperature dependence of R and PGE in our *in situ* data derived from temperature-controlled experiments. Finally, we compiled the existing literature from direct estimates of R and PGE to explore the temperature sensitivity of the dark ocean carbon metabolism.

4.3. Material and methods

4.3.1. Study site and sampling

The study was conducted on board the “*R/V Hesperides*” across the South Atlantic and Indian Oceans (Figure 4.1. and Table 4.1.), during part of the Malaspina Expedition (www.expedicionmalaspina.es) from January to March 2011. A total of 12 stations were sampled crossing the two ocean basins (Figure 4.1.). Water samples for metabolism experiments, as well as for *in situ* measurements, were collected at the same depths in the upper mesopelagic zone (from 330 to 585 m, Table 4.1.) using a rosette sampler (provided with 24 12L-Niskin bottles), implemented with a Conductivity–Temperature–Depth (CTD) instrument (Seabird SBE 9). Before setting up the experiments, water from the Niskin bottle was drawn into a carboy (without any pre-filtration), gently mixed, and left for 2 h inside a temperature-controlled chamber to reach *in situ* temperature. Following, the water was homogeneously distributed into 28 BOD bottles; 7 for each time sampling interval (0, 24, 48 and 72 h) of the experiment. From these, six bottles were used as replicates for oxygen consumption measurement and one bottle for prokaryotic heterotrophic production.

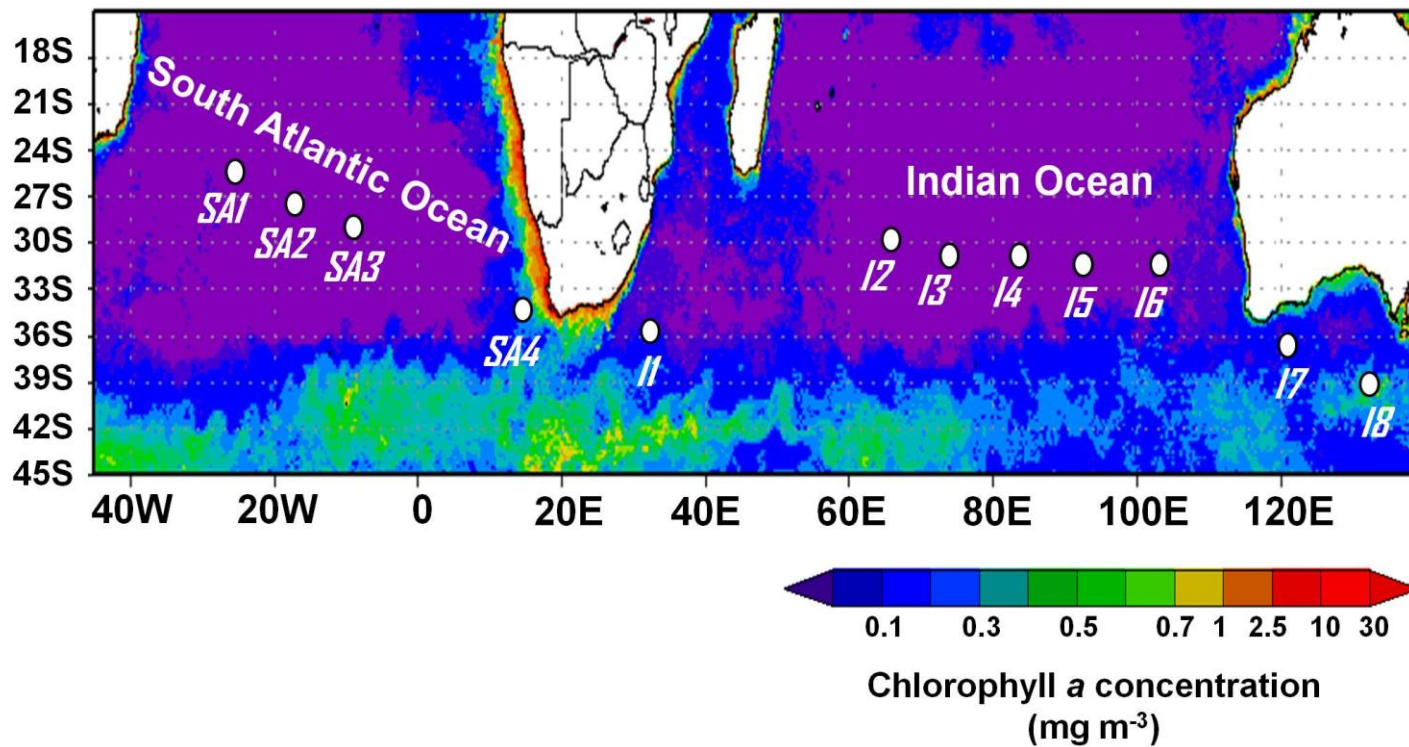


Figure 4. 1. Location of the stations selected for the respiration experiments (white dots), superimposed to a Moderate Resolution Imaging Spectroradiometer (MODIS) image of chlorophyll a averaged for the sampling period (from January to March 2011). Source: <http://modis.gsfc.nasa.gov/>

Temperature control of R and PGE in the mesopelagic zone

Table 4. 1. Stations' location in the South Atlantic (SA) and Indian (I) Oceans and water mass properties at the sampling depths where time-series experiments were performed. AOU = apparent oxygen utilization.

Stations	Date (d/m/y)	Latitude	Longitude	Depth (m)	Temperature (°C)	Salinity (psu)	O ₂ concentration (μmol kg ⁻¹)	AOU (μmol kg ⁻¹)
SA1	22/01/2011	25.9°S	27.6°W	550	9.8	34.78	185.62	94.15
SA2	24/01/2011	27.0°S	21.4°W	450	11.8	35.02	195.81	70.29
SA3	27/01/2011	28.7°S	11.8°W	585	8.7	34.66	178.83	108.43
SA4	04/02/2011	32.8°S	12.8°E	330	11.4	34.95	201.98	64.97
I1	15/02/2011	34.4°S	31.1°E	430	14.9	35.42	189.63	58.16
I2	25/02/2011	28.0°S	63.3°E	450	12.5	35.15	213.54	46.18
I3	28/02/2011	29.6°S	72.4°E	450	11.7	35.03	214.26	50.65
I4	03/03/2011	29.8°S	82.6°E	450	10.9	34.91	222.47	47.23
I5	06/03/2011	29.6°S	93.0°E	450	10.5	34.83	225.67	46.61
I6	09/03/2011	30.3°S	103.3°E	450	9.5	34.71	220.63	57.63
I7	19/03/2011	36.6°S	120.9°E	470	9.5	34.68	227.93	50.85
I8	24/03/2011	39.2°S	135.1°E	400	9.6	34.71	226.81	52.23

4.3.2. Biological analyses

4.3.2.1. Prokaryotic heterotrophic abundance

In situ prokaryotic heterotrophic abundance (PHA) was measured by flow cytometry (Gasol and del Giorgio, 2000), using a FACScalibur Becton Dickinson cytometer equipped with a laser emitting at 488 nm. Samples were obtained from the same Niskin bottles where water was collected for experiments. A 1.5 ml aliquot was fixed with 1% of paraformaldehyde + 0.05 % glutaraldehyde (final concentrations), deep-frozen in liquid nitrogen and stored at -80 °C until analysis (less than one week after collection). Prokaryotic biomass (PB; mg m⁻³) was calculated by transforming relative light side scatter (SSC) to cell diameter, using the linear regression model of Calvo-Díaz and Morán (2006) after staining the samples with SybrGreen I. A spherical shape was assumed to derive cellular volumes, which were later converted to biomass with the allometric equation of Gundersen et al. (2002).

4.3.2.2. Prokaryotic heterotrophic production

Samples for prokaryotic heterotrophic production (PHP) were obtained both directly from the Niskin bottles (*in situ* PHP) and from the BOD bottles used in the time-series experiments at different incubation times (0, 24, 48 and 72 h). PHP was measured by ³H-Leucine (specific activity = 144.2 Ci mmol⁻¹) incorporation into proteins (Kirchman *et al.* 1985), according to the microcentrifugation protocol proposed by Smith and Azam (1992). Four replicates (1.2 ml) and two trichloroacetic acid (TCA)-killed blanks in microcentrifuge tubes were added L-[4, 5-³H] leucine at 20 nM. Samples and blanks for experiments and Niskin bottles were incubated (for 2 to 8 h) at *in situ* temperature. Incubations were stopped by adding 50 % TCA, centrifuged (10 min. and 14000 r.p.m.) and again rinsed with 5 % TCA and centrifuged. Scintillation cocktail (1 ml Optisafe HiSafe, Perkin Elmer) was added and, after 24 h, the emitted radioactivity was counted on board in a liquid scintillation counter (Wallac-Perkin Elmer). Leucine incorporation rates (pmol Leu l⁻¹ h⁻¹) were converted into carbon by using a theoretical factor of 1.55 kg C mol Leu⁻¹ (Simon and Azam 1989), assuming that isotope dilution was negligible under

Temperature control of R and PGE in the mesopelagic zone

this saturating concentration of 20 nM of ^3H -Leucine. PHP rates (average coefficient of variation $\sim 4\%$) were integrated (PHP_{int}) during the experiments as the area obtained from time 0 to the final time (Figure 4.2.), and expressed as daily rates ($\mu\text{mol C m}^{-3} \text{ d}^{-1}$). Prokaryotic biomass turnover times (days) were estimated as PB/PHP for *in situ* samples.

4.3.2.3. Respiration

Water samples for the respiration experiments were homogeneously siphoned into 24 biological oxygen demand (BOD) bottles (nominal volume 125 ml), that were kept in the dark inside temperature-controlled water baths (± 0.1 °C). Six BOD bottles were fixed immediately with Winkler reagents (Figure 4.2.), and left immersed together with the rest of bottles inside the water baths during the dark incubation steps. Other six replicate bottles were fixed at 24, 48 and 72 h. Community respiration was measured at each time series interval (0-24, 24-48 and 48-72 h) from changes in O_2 concentration in the bottles. Finally, like with PHP, integrated respiration rates (R_{int}) were estimated as the area obtained from t_0 to final time and expressed as daily rates ($\mu\text{mol C m}^{-3} \text{ d}^{-1}$). Dissolved oxygen measurements were carried out by automated microWinkler titrations using a Dissolved Oxygen Analyser (DOA; SiS®) with photometric end-point detection (Williams and Jenkinson, 1982). The coefficient of variation of oxygen concentration among replicated bottles was always $<1\%$. A respiratory quotient of 1 was used to convert oxygen consumption into carbon respiration (del Giorgio et al., 2006). To minimize the potential effect of growing prokaryotes inside the BOD bottles along the incubations, experimental R was back-scaled to *in situ* conditions using the power fit obtained between experimentally derived PHP and R, knowing *in situ* PHP (see details in the Results section). For this, we assumed that prokaryotic assemblages were responsible for the whole community respiration. *In situ* specific R rates were obtained as the ratio between *in situ* R and the prokaryotic biomass (R/PB).

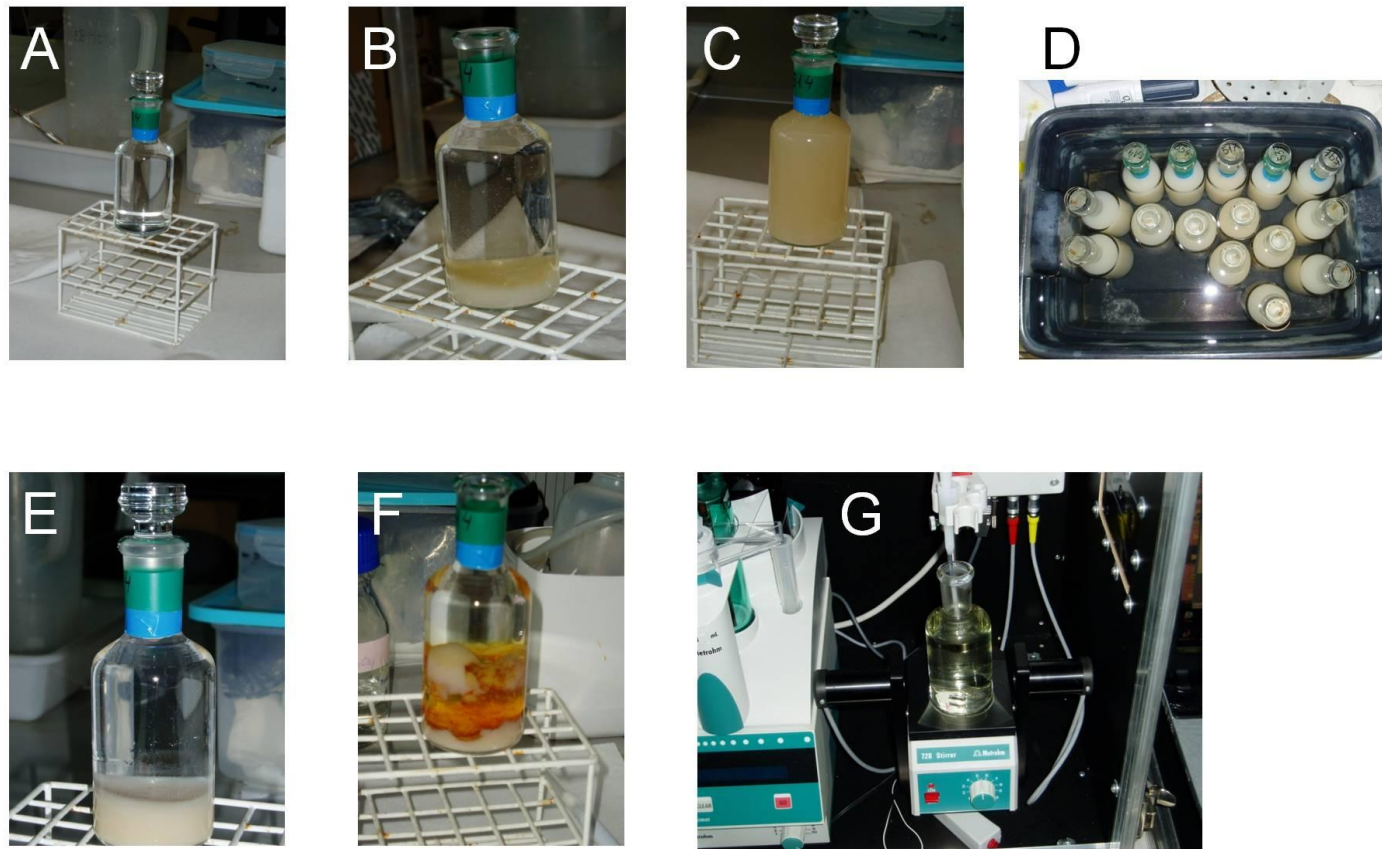


Figure 4. 2. Process of O₂ fixation in BOD bottles and titration with the Dissolved Oxygen Analyzer DOA SiS® titrator. Replicate bottles were taken out the bath before fixation (A); Winkler reagents 1 (manganese sulfate) and 2 (alkaline solution of sodium iodide) were carefully added (B); the BOD bottles were vigorously shaken (C); then the fixed bottles were stored in the dark and covered with water until titration (in less than 24 hours) (D); image of a bottle with the precipitate of manganese hydroxide ready for the titration (E); sulfuric acid solution was added (F); titration (shaking with a magnetic stirrer) was performed with the DOA SiS® titrator (G). More details can be found in Arístegui et al. (2012) (in Annex IV).

Temperature control of R and PGE in the mesopelagic zone

4.3.3. Influence of temperature on respiration

The dependence of R on temperature was tested using the Metabolic Theory of Ecology (MTE) (Brown et al., 2004), assuming that metabolic processes at community-level or ecosystem level depend on ambient temperature (Sarmiento et al., 2010). This temperature dependence was examined in our *in situ* back-scaled R values and also compared to all R data available, derived from direct O₂ consumption, found in the literature.

$$\ln \text{ metabolic rate (R)} = a - b (1 / kT),$$

where k is the Boltzmann's constant $8.62 \cdot 10^{-5} \text{ eV K}^{-1}$ and T is the absolute water temperature in °K. The negative slope (b) in the Arrhenius plot corresponds to the activation energy (E_a , eV). E_a was further transformed to Q_{10} (the change in metabolic rate for a 10 °C temperature increase) using the algorithm proposed by Raven and Geider (1988), $Q_{10} = \text{Exp}(10E_a / rT^2)$, where r is the gas constant ($8.314472 \text{ mol}^{-1} \text{ K}^{-1}$) and T is the mean absolute temperature (°K) across the range over which Q_{10} was measured. E_a was converted to J mol^{-1} using the conversion factor of $96486.9 \text{ J eV}^{-1} \text{ mol}^{-1}$.

4.3.4. Statistical analyses

Statistical analyses were performed using Statistica 6.0 (StatSoft Inc, 1997). The dataset were log-transformed to fit the assumptions of normality and homoscedasticity before performing the regression analysis.

4.4. Results

4.4.1. Respiration, prokaryotic production and growth efficiency in the experiments

In all the experiments ^3H -Leucine incorporation rates increased and O_2 concentrations decreased over time (e. g. Figure 4.3.). Integrated PHP (PHP_{int}) in the experiments ranged from 1.7 to $96.1 \mu\text{mol C m}^{-3} \text{d}^{-1}$, while integrated R (R_{int}) varied ca. 3.5-fold from 131 to $467 \mu\text{mol C m}^{-3} \text{d}^{-1}$ (Table 4.2.), being R and PHP strongly correlated ($N = 10$, $r^2 = 0.79$ and $p\text{-value} = 0.001$). The calculated PGE values from R and PHP in the experiments were low on average ($\sim 5.9\%$), although variable, ranging from 1.3 to 17.1 (Table 4.2.).

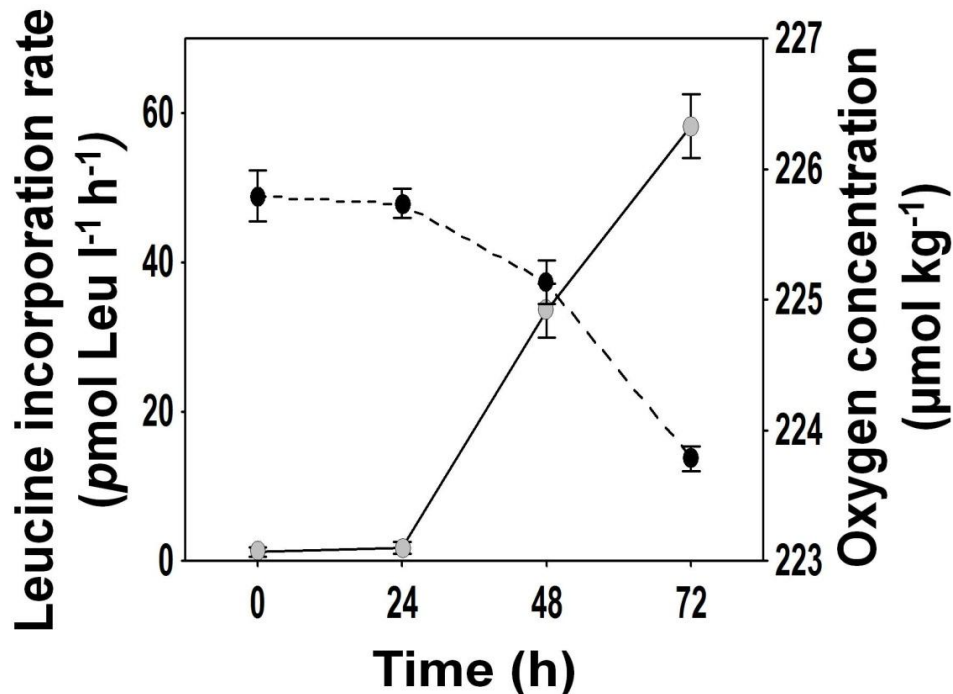


Figure 4. 3. Representative example of the changes in the leucine incorporation rate ($\mu\text{mol Leu l}^{-1} \text{h}^{-1}$, grey dots) and the O_2 concentration ($\mu\text{mol O}_2 \text{kg}^{-1}$, black dots) along the experiment performed at station I1 located in the Indian Ocean at 430 m depth. Bars represent the standard error of 6 replicates.

Temperature control of R and PGE in the mesopelagic zone

Table 4. 2. Integrated community respiration rate (R_{int}) and prokaryotic heterotrophic production (PHP_{int}) estimated over the incubation times (Time, h) in the experiments (see Material and Methods section). The prokaryotic growth efficiencies (PGE) derived from both PHP_{int} and R_{int} are also included. T = Incubation Temperature. *R, and consequently PGE estimates, were not determined in these experiments.

Experiment	Time (h)	T (°C)	PHP_{int} ($\mu\text{mol C m}^{-3} \text{d}^{-1}$)	R_{int} ($\mu\text{mol C m}^{-3} \text{d}^{-1}$)	PGE (%)
SA1	72	9.3	24.2	255	8.7
SA2*	72	9.2	16.9	-	-
SA3	72	9.0	17.7	254	6.5
SA4	24	10.2	7.2	203	3.4
I1	72	15.1	96.1	467	17.1
I2	72	12.6	28.0	340	7.6
I3	72	11.7	12.4	349	3.4
I4	72	11.2	15.4	274	5.3
I5	72	10.6	8.2	297	2.7
I6	72	9.6	4.1	145	2.7
I7*	72	8.6	1.7	-	-
I8	72	8.6	1.7	131	1.3

4.4.2. *In situ* prokaryotic assemblages and metabolism in the upper mesopelagic environment

In situ prokaryotic heterotrophic abundance (PHA) and production (PHP) varied ~ 20-fold (from 0.5 to 11.0 $\times 10^5$ cell ml⁻¹) and 30-fold (from 0.3 to 9.1 $\mu\text{mol C m}^{-3} \text{d}^{-1}$), respectively (Table 4.3.). The highest *in situ* PHA and PHP were found in the western Indian Ocean (stations I1 and I2). However, the highest biomass turnover times were located in the eastern Indian Ocean (stations I6, I7 and I8).

In situ R was estimated by back-scaling experimental R to *in situ* PHP, using the power relationship observed between the integrated experimental PHP and R (Figure 4.4.); where $R_{int} = 127.24 (\pm 22.52) PHP_{int}^{0.283 (\pm 0.053)}$ (N = 10, $r^2 = 0.78$ and p-value = 0.0007). Back-scaled *in situ* R ranged between 87 and 238 $\mu\text{mol C m}^{-3} \text{d}^{-1}$ (Table 4.3.), and represented, on average, about two-fifths of *in vitro* experimentally-derived values. However, both *in situ* and experimental PHP_{int} were significantly correlated (N = 12, slope = 7.65 ± 1.59 , $r^2 = 0.70$ and p-value = 0.0007). The *in situ* R in the studied stations showed a similar

geographical pattern as the experimental R estimates, with the highest values in the western Indian Ocean (stations I1 and I2).

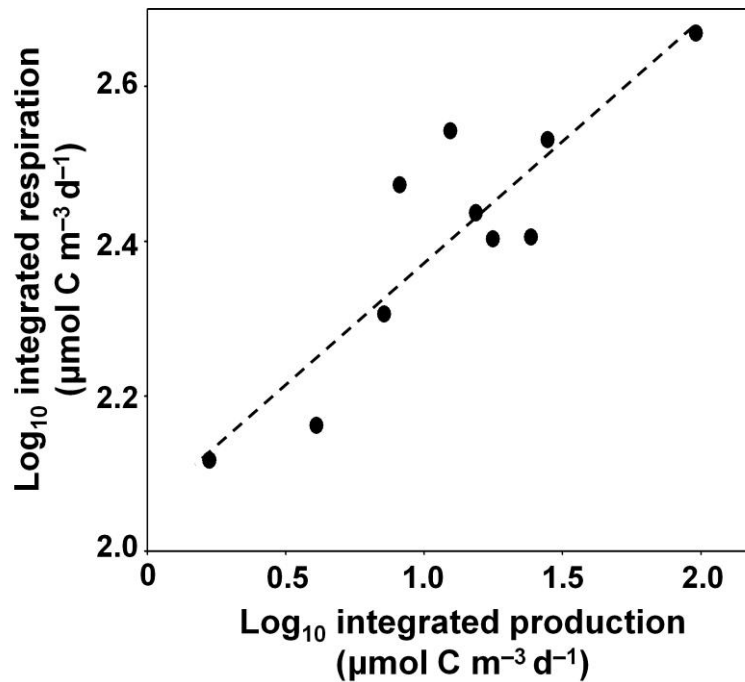


Figure 4. 4. Log-log relationship between integrated prokaryotic heterotrophic production and integrated community respiration in the *in vitro* experiments. The dashed regression line represents the log-log linear transformation of the fitted power function: $R_{int} = 127.24 (\pm 22.52) PHP_{int}^{0.283 (\pm 0.053)}$; $r^2 = 0.78$ and $p\text{-value} = 0.0007$.

The estimated *in situ* PGE values (derived from back-scaled R and *in situ* PHP) were low in all the study stations, but ranged one order of magnitude, from 0.3 to 3.7 % (Table 4.3.), and averaged about 1.4 %. The geographic pattern of the *in situ* PGE was similar to PHP and R, being the highest observed PGE values at stations I1 and I2.

Temperature control of R and PGE in the mesopelagic zone

Table 4. 3. Prokaryotic heterotrophic abundance (PHA) and production (PHP), prokaryotic biomass (PB), turnover time, back-scaled respiration rates (R) and resulting growth efficiencies (PGE) corresponding to the in situ conditions.

Stations	PHA ($\times 10^5$ cell ml ⁻¹)	PB (mg C m ⁻³)	PHP ($\mu\text{mol C m}^{-3} \text{d}^{-1}$)	Turnover time (day)	R ($\mu\text{mol C m}^{-3} \text{d}^{-1}$)	PGE (%)
SA1	0.5	0.30	1.0	24	129	0.8
SA2	0.8	0.47	4.4	9	194	2.2
SA3	0.8	0.44	2.8	13	170	1.6
SA4	3.0	1.62	2.8	48	170	1.6
I1	11.0	6.67	9.1	61	238	3.7
I2	6.0	0.92	6.6	11	218	3.0
I3	1.4	0.86	0.9	80	123	0.7
I4	1.7	0.85	0.8	93	118	0.6
I5	1.7	0.88	1.0	70	129	0.8
I6	1.7	0.88	0.3	278	87	0.3
I7	2.3	1.20	0.3	288	94	0.4
I8	3.0	1.50	1.0	125	127	0.8

4.4.3. Temperature control on R and PGE

Experimental R_{int} was strongly correlated with temperature during the incubations (Figure 4.5.; $N = 10$, $r^2 = 0.79$ and $p\text{-value} = 0.0004$). Figure 4.6. plots the Arrhenius trend for all deep ocean data (derived from O_2 consumption in BOD bottles) found in the literature (see also Table 4.4.) showing a significant temperature dependence ($N = 57$ and $p\text{-value} = 0.000001$) on R across different marine regions. Table 4.5. also shows the results of the Arrhenius plots and Q_{10} values corresponding to this study and all data in the literature. The estimated activation energy (E_a) and fitted Q_{10} value for this study ($E_a = 0.90 \pm 0.29$ eV and $Q_{10} = 3.65$) were consistent with the calculated values from the literature ($E_a = 0.98 \pm 0.16$ eV and $Q_{10} = 4.07$). However, the specific rates of the *in situ* R values (R/PB) were not significantly related to temperature ($p\text{-value} = 0.418$).

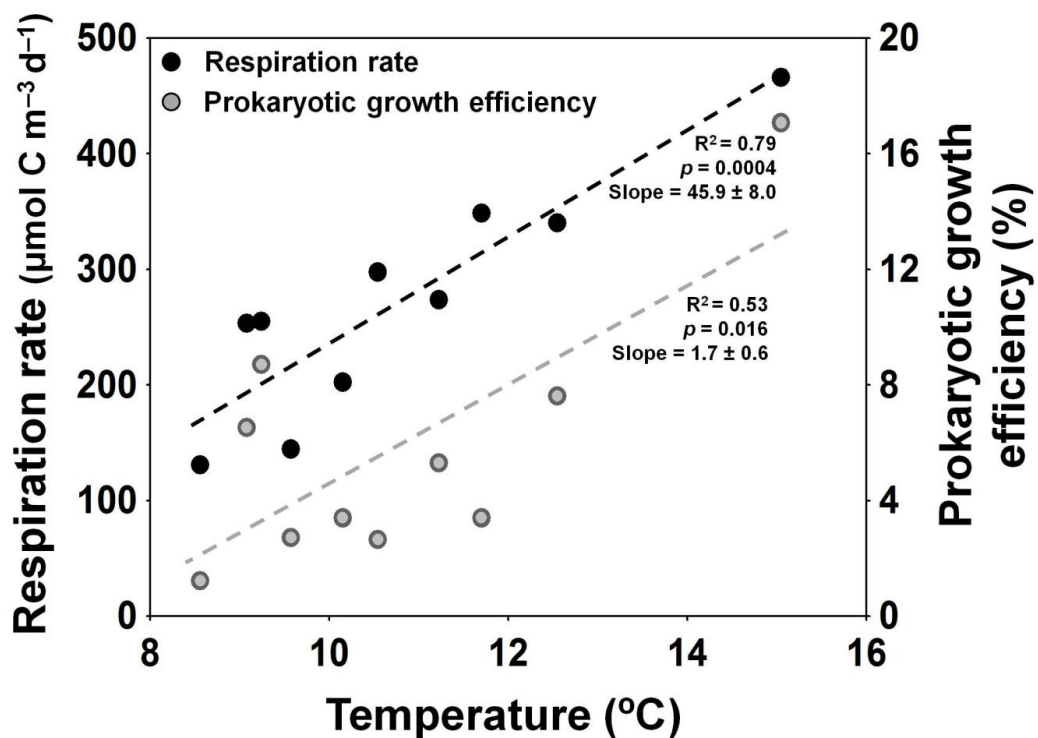


Figure 4. 5. Relationships between temperature and respiration rates (black dots) and prokaryotic growth efficiencies (grey dots) in the *in vitro* experiments. The dashed regression lines plot significant relationships ($p\text{-values} < 0.05$).

Temperature control of R and PGE in the mesopelagic zone

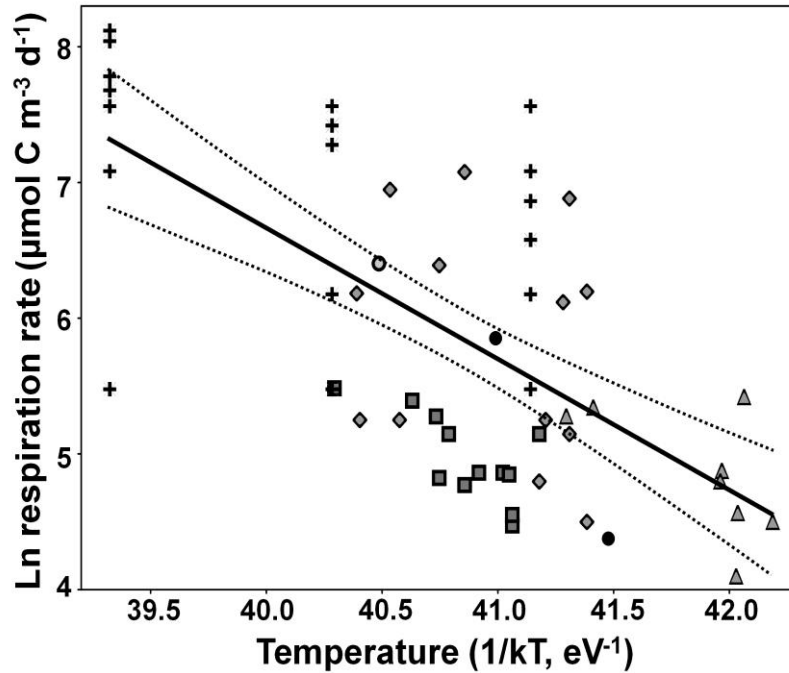


Figure 4. 6. Arrhenius plot showing the effect of temperature ($1/kT$) on the deep ocean R data (derived from O_2 consumption) found in the literature, including also this study data. The black line represents the significant linear relationship (p -value = 0.000001); dashed lines are the 95% confidence interval of the slope. Biddanda and Benner (1997) (crosses), Reinthal et al. (2006) (triangles), Baltar et al. (2010) (diamonds), Aristegui et al. (2005b) (black circles), Weinbauer et al. (2013) (grey circles) and this study (squares).

Table 4. 4. *Reported prokaryotic growth efficiencies (PGE) in the dark ocean, derived from direct measurements of both prokaryotic heterotrophic production (PHP) and respiration (R), indicating the different approaches.*

Location	Depth (m)	PHP approach	R approach	PGE (%)	Reference
Gulf of Mexico	100 - 500	In situ leucine incorporation	Linear regression between time and O ₂ concentration in experiments	8 - 12	Biddanda and Benner, 1997
Subtropical North Atlantic Ocean	600 - 1000	Average of in situ thymidine and leucine incorporation	Difference in O ₂ concentration in experiments. Back-scaling to in situ conditions	13 - 18	Aristegui et al., 2005b
North Atlantic Ocean	100 -4000	In situ leucine incorporation	Difference in O ₂ concentration in experiments	~ 2	Reinthalder et al., 2006
Subtropical North Atlantic Ocean	350 - 1000	In situ leucine incorporation and prokaryotic biomass yield in experiments	Difference in O ₂ concentration in experiments	< 1 - 24	Baltar et al., 2010
South Atlantic and Indian Oceans	300 - 600	In situ leucine incorporation	Difference in O ₂ concentration in experiments. Back-scaling to in situ conditions	< 1 - 17	This study

Temperature control of R and PGE in the mesopelagic zone

Table 4. 5. The slopes of the regression (- activation energy, eV) and the parameters of the Arrhenius plot between Ln of respiration rate (R, $\mu\text{mol C m}^{-3} \text{d}^{-1}$) and inverse of temperature ($1/kT$), $\text{Ln}(R) = a - b(1/kT)$, for *in situ* data in this study and all data in the literature (Figure 4.5.). The Q_{10} temperature coefficients are also shown.

	Temperature range (°C)	Rate	Intercept \pm SE	Slope \pm SE	R ²	p-value	N	Q ₁₀
This study	8.7 - 14.9	R	41.86 \pm 11.98	-0.90 \pm 0.29	0.49	0.012	12	3.65
Literature	1.9 - 22.0	R	45.89 \pm 6.33	-0.98 \pm 0.16	0.42	0.000001	57	4.07

PGE, derived from experimental PHP_{int} and R_{int} , was positive and significantly correlated to temperature (Figure 4.5.; N = 10, $r^2 = 0.53$ and p-value = 0.016), as well as considering the *in situ* conditions (N=12, $r^2 = 0.58$ and p-value = 0.004). However, including all the data found in the literature, we did not obtain a significant relationship between PGE and temperature (Figure 4.7.; p-value > 0.05).

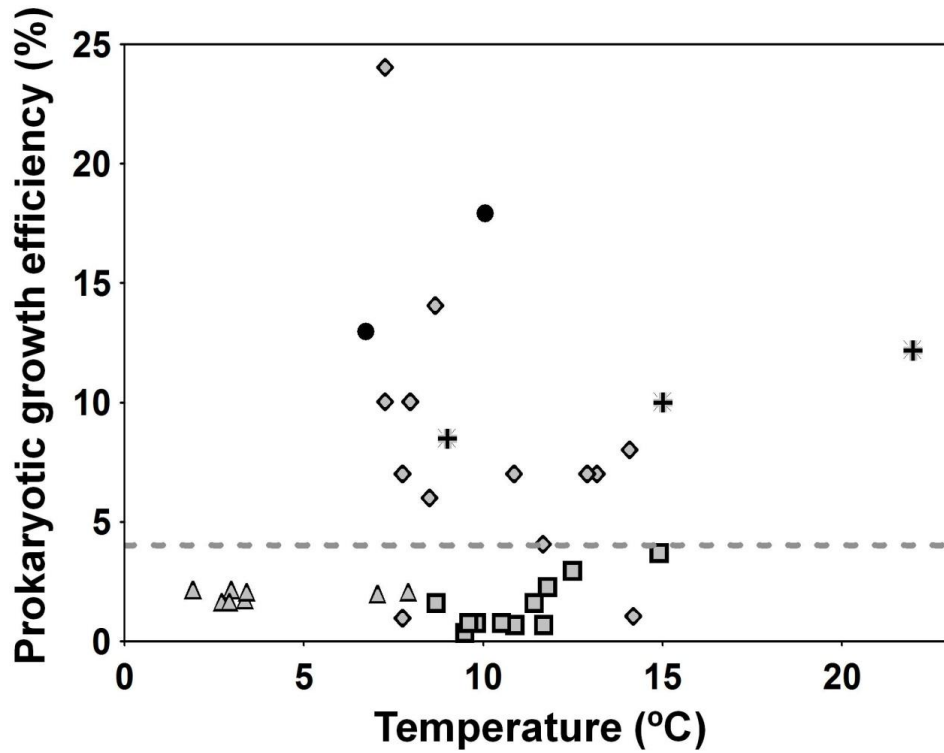


Figure 4. 7. Scatterplot of prokaryotic growth efficiencies (PGE), derived from direct estimates of R and PHP, as function of temperature for deep ocean prokaryotes found in the literature including this study. The grey dashed line represents PGE = 4 %. The symbols correspond to Biddanda and Benner (1997) (crosses), Reinthal et al. (2006) (triangles), Baltar et al. (2010) (diamonds), Arístegui et al. (2005b) (circles) and this study (squares).

Temperature control of R and PGE in the mesopelagic zone

4.5. Discussion

Direct determination of R from O₂ consumption during *in vitro* incubations in the dark ocean requires, in most cases, long-term incubations (> 24 h), to detect significant changes in O₂ concentration. This may lead to the generation of artifacts as consequence of the confinement of microbial populations inside bottles, favoring cell growth after 1-2 days and increasing metabolism. In addition, changes in community structure may also take place during the incubations, shifting the community towards opportunistic populations (Massana et al., 2001). Nevertheless, some studies have shown that, in spite of these changes in community structure during daily incubations, metabolic rates can be maintained constant or directly correlated to the increases in biomass (e. g. Baltar et al., 2012). Despite these drawbacks, some previous studies derived *in situ* R directly from oxygen consumption *in vitro* incubations (Reinthaler et al., 2006; Baltar et al., 2010). Arístegui et al. (2005b) demonstrated, however, that when long incubations (>24 h) are necessary to obtain significant changes in oxygen consumption, the back-scaling of the experimental results to the *in situ* conditions is likely the most accurate approach to infer R in the dark ocean. Thereby, experimental R can be back-scaled to *in situ* conditions when a strong relationship between microbial respiration and production (or biomass) is obtained along the experiment, as it happened in this study (Figure 4.4.).

Few studies have addressed the effect of hydrostatic pressure on prokaryotic metabolism. In spite of the limited information currently available, Tamburini et al. (2013) reviewed these studies, concluding that decompression of deep-water samples underestimates *in situ* activity. This conclusion, however, is based on prokaryotic piezophilic populations from the deep ocean (>1000 m depth), adapted to live under high pressures, low temperatures and very low organic matter concentrations, a situation far different to the mesopelagic realm with lower hydrostatic pressure and higher organic matter content.

To date, the few available estimates of dark R obtained from oxygen consumption have been mostly determined for the North Atlantic Ocean and the Mediterranean Sea (Biddanda and Benner, 1997; Arístegui et al., 2005b;

Reinthal et al., 2006; Baltar et al., 2010; Weinbauer et al., 2013). Our back-scaled *in situ* values of R (ranging from 87 to 238 $\mu\text{mol C m}^{-3} \text{ d}^{-1}$) are comparable to the back-scaled R estimates determined by Arístegui et al. (2005b) in the Canary Current region ($220 \pm 50 \mu\text{mol C m}^{-3} \text{ d}^{-1}$). On the other hand, the experimental R values in this study (from 131 to 467 $\mu\text{mol C m}^{-3} \text{ d}^{-1}$) are more similar to other studies (240 - 3360 $\mu\text{mol C m}^{-3} \text{ d}^{-1}$ in Biddanda and Benner, 1997; 60 - 300 $\mu\text{mol C m}^{-3} \text{ d}^{-1}$ in Reinthal et al., 2006; 90 - 1180 $\mu\text{mol C m}^{-3} \text{ d}^{-1}$ in Baltar et al., 2010; 230 - 1650 $\mu\text{mol C m}^{-3} \text{ d}^{-1}$ in Weinbauer et al., 2013) where the back-scaling approach was not applied.

The largest data set of respiration in the global dark ocean is, however, based on potential respiratory activity derived from enzymatic electron transport system (ETS) measurements. A global average R of 10 $\mu\text{mol C m}^{-3} \text{ d}^{-1}$ was estimated by Arístegui et al. (2003) for the mesopelagic zone assuming a conservative R/ETS ratio of 0.1, characteristic of bacterial populations in senescent state (Christensen et al., 1980). This global rate represents, however, a lower threshold since prokaryotic communities in the mesopelagic zone can be far from being senescent, presenting R/ETS ratios closer to 1 (Arístegui et al., 2005b), typical of bacterial assemblages in exponential growth phase (Christensen et al., 1980). If so the ETS-derived R (using a R/ETS of 1) would be in the range of the back-scaled R obtained in this study.

There are also very few studies in the literature reporting PGE in the dark ocean derived from direct measurements of R and PHP (Table 4.4.). *In situ* PGE in our study were on average $\sim 1.4 \%$. These low PGE are in accordance with estimates reported by Reinthal et al. (2006) in the meso- and bathypelagic region of the North Atlantic Ocean ($\sim 2 \%$), but without any back-scaling procedure in the direct R estimates. Dumont et al. (2011) found similar low PGE in the South of Tasmania using the equation proposed by del Giorgio and Cole (1998) to predict PGE from PHP. Other studies estimated the prokaryotic consumption from empirical equations, which were generated from surface ocean samples (Carlson et al., 2004; Tanaka and Rassoulzadegan, 2004), resulting in higher PGE estimates (5 - 13 % and 19 - 39 %, respectively). Zaccone et al.

Temperature control of R and PGE in the mesopelagic zone

(2003) and Biddanda and Benner (1997) also found high PGE between 6-11 % and 8-12 %, respectively. The methodology used in these later reports, however, could have affected the estimation of *in situ* R. Zacccone et al. used indirect R measurements from ETS activity and Biddanda and Benner only considered 50 % of the measured respiration in the experiments to estimate PGE. Baltar et al. (2010) obtained a wide range of PGE (< 1 - 24 %) from a variety of approaches to estimate PGE from *in vitro* experiments, similar to our experimental range of PGE (1.7 - 17.1 %). Only Arístegui et al. (2005b) used a similar back-scaling procedure to our study to derive R, although PHP was estimated by averaging leucine and thymidine incorporation rates. These authors obtained higher PGE (13 - 18 %), which they attributed, based also on other molecular and metabolic prokaryotic proxies, to the larger organic carbon supply from the continental margins, which likely translated into a more efficient use of carbon for growth in the mesopelagic zone. The low *in situ* PGE values in our study confirm the hypothesis that most of the organic matter transported to the mesopelagic zone in open ocean waters is mineralized, ending up as CO₂; yet more studies reporting direct R estimates are essential for a better knowledge of the regional variability in prokaryotic carbon use throughout the dark ocean.

We observed a strong correlation between water temperature and *in situ* R, suggesting a significant temperature dependence on prokaryotic metabolism also in the mesopelagic ocean. There are several studies describing the influence of temperature on R and PGE. Nagata et al. (2001), in the mesopelagic waters of the subarctic Pacific, observed temperature dependence of prokaryotic growth, reporting positive significant linear regressions in the upper part of the mesopelagic zone. Bendtsen et al. (2002), based on a model of the microbial food web, postulated that the gradient of dissolved organic carbon in the deep North Atlantic could be explained by the temperature dependence of bacterial metabolism. Iversen and Ploug (2013) used results obtained in laboratory experiments to hypothesize that the carbon flux into deep waters would be reduced in warmer environments due to increased remineralization rates. Our results and all these studies suggest that prokaryotic metabolism in the dark

ocean would be affected by rising temperatures. Nevertheless, the influence would be different depending on whether the temperature affects more growth (new biomass generation), being carbon channeled through higher trophic levels, or respiration, being carbon recycled as CO₂ (e. g. Vázquez-Domínguez et al., 2007). The temperature dependence of mineralization rates does not preclude, however, that the concentration and quality of organic matter might also affect oxygen consumption rates in the dark ocean. Indeed, Nagata et al. (2001) concluded that organic matter was more important than temperature in determining the growth of heterotrophic prokaryotes in the upper mesopelagic zone of the Subarctic Pacific.

The metabolic theory of ecology (MTE) establishes an increment of the organisms' metabolism with increasing temperatures (Brown et al., 2004), as has been observed in planktonic communities of the surface ocean (López-Urrutia and Morán, 2007; Regaudie-de-Gioux and Duarte, 2012). Our results show a significant *in situ* R dependence on temperature in the range of 8.7 to 14.9 °C. This temperature dependence is also obtained considering all R data previously reported from the dark ocean (Table 4.5.). In contrast to the expected increase of cell-based metabolism in a warmer environment, we observed in our study a lack of correlation between temperature and specific R (R/PB). Likely a variable fraction of *in situ* prokaryotes were metabolically inactive (Gasol et al., 1995) and, consequently, specific R in our study was not a good proxy to detect temperature changes. The R activation energy value estimated in this study (E_a of 0.90 ± 0.29 eV) was higher than those reported by López-Urrutia and Morán (2007) for specific R in the surface ocean ($E_a = 0.589$ eV), by Yvon-Durocher et al. (2012) for microbial populations in the global ocean ($E_a = 0.57$ eV) or by Arístegui and Montero (1995) for microplankton R derived from ETS activity ($E_a = 0.70$ eV). However, Regaudie-de-Gioux and Duarte (2012) reported comparable E_a values for R in the Atlantic Ocean ($E_a = 0.92 \pm 0.11$ eV). The Q_{10} values determined in this study (Table 4.5.) were also higher than the Q_{10} range of 1 – 3 for R reported by Church (2008).

Temperature control of R and PGE in the mesopelagic zone

Recent forecasts consider a global warming rate per decade between 0.015 and 0.11 °C in the upper 700 m (Intergovernmental Panel on Climate Change; Rhein et al., 2013), which could lead to an increase of R of about 4 % according to our calculations. Since the global-warming slowdown detected in surface ocean during the 21st century is partially a consequence of the heat transfer to deeper depths (Chen and Tung, 2014), prokaryotic mineralization rates at the mesopelagic zone could be influenced by increasing temperatures in the dark ocean. Therefore, the R vs. temperature reported in this study could help to predict future scenarios in the mesopelagic zone.

The positive relationship between PGE and temperature in the experiments (Figure 4.5.) is not consistent with previous studies, which reported a decrease of PGE as temperature increases (Rivkin and Legendre, 2001; Kritzberg et al., 2010a and b). Rivkin and Legendre (2001), in a data compilation study, found a negative relationship between these two parameters for a wide range of temperatures (-1.4 - 29 °C). Likewise, Kritzberg et al. (2010a and b) showed a stronger response of respiration to temperature than production, both in an oligotrophic coastal marine system (with a temperature range of 14.4 - 28 °C) and in Arctic waters (with a temperature range of -0.6 - 5.8 °C). On the contrary, Wohlers et al. (2009) observed in in-door mesocosms' experiments carried out with water from the Baltic Sea, under a gradient of low temperatures (2.5 °C-8.5 °C), that bacterial production was stimulated by temperature increases but community respiration (< 3 µm) remained apparently unaffected; then, BGE increasing with rising temperatures. Reinthaler and Herndl (2005) also found higher PGE during the warmer spring and summer periods than during the cooler winter time in the southern North Sea. Other studies, however, had suggested that R and PHP would respond similarly to temperature changes (López-Urrutia and Morán, 2007; Vázquez-Domínguez et al., 2007), suggesting that differences in the response of PHP and R to environmental factors (and consequently to BGE) would be related to the bioavailability of organic resources (López-Urrutia and Morán, 2007) or, as discussed above, to the co-variation effect between temperature and organic matter.

Acknowledgements

We thank our scientific colleagues and C. M. Duarte for the coordination of Malaspina expedition, as well as the technical staff and crew members on board the BIO Hespérides, for their support in the field sampling during the different legs of the of the Malaspina cruise, and particularly A. Gomes and X.A.G. Morán for providing the in situ PHP data. This paper is a contribution to the INGENIO 2010 CONSOLIDER program (CDS2008-00077). IPM was supported by a JAE Pre-doc fellowship, from the Spanish National Research Council (CSIC) and the BBVA Foundation, Spain. IPM, JA and JMG were partly supported by project HotMix (CTM2011-30010-C02/MAR).

4.6. References

- Anderson T. R., Tang K. W. 2010. Carbon cycling and POC turnover in the mesopelagic zone of the ocean: Insights from a simple model. *Deep-Sea Research II*, 57: 1581 – 1592.
- Aristegui J., Agustí S., Duarte C. M. 2003. Respiration in the dark ocean. *Geophysical Research Letters*, 30(2), 1041, doi: 10.1029/2002GL016227.
- Aristegui J., Agustí S., Middelburg J. J., Duarte C. M. 2005a. Respiration in the mesopelagic and bathypelagic zones of the ocean, in: del Giorgio, P.A. et al. (Eds.). *Respiration in aquatic ecosystems*. p p 181 – 205.
- Aristegui J., Duarte C. M., Gasol J. M., Alonso-Sáez L. 2005b. Active mesopelagic prokaryotes support high respiration in the subtropical northeast Atlantic Ocean. *Geophysical Research Letters*, 32: L03608, Doi: 10.1029/2004GL021863.
- Aristegui J., Gasol J. M., Duarte C. M., Herndl G. J. 2009. Microbial oceanography of the dark ocean's pelagic realm. *Limnology and Oceanography*, 54(5): 1501 – 1529.
- Aristegui J., Mazuecos I. P., Vázquez-Domínguez E. 2012. Medida de la respiración mediante cambios *in vitro* de la concentración de O₂, in: Expedición de circunnavegación Malaspina 2010: Cambio Global y Exploración de la Biodiversidad del Océano Global. Libro Blanco de Métodos y Técnicas de Trabajo Oceanográfico. CSIC. Enrique Moreno-Ostos (eds.), p. p. 565 - 573.
- Aristegui, J., Montero, M. F. 1995. The relationship between community respiration and ETS activity in the ocean. *J. Plankton Res.*, 17, 1563–1571.
- Baltar F., Aristegui J., Gasol J. M., Herndl G. J. 2010. Prokaryotic carbon utilization in the dark ocean: growth efficiency, leucine-to-carbon conversion factors, and their relation. *Aquatic Microbial Ecology*, 60: 227 – 232. Doi: 10.3354/ame01422.
- Baltar F., Lindh M. V., Parparov A., Berman T., Pinhassi J. 2012. Prokaryotic community structure and respiration during long-term incubations. *Microbiologyopen*. 1(2): 214 – 224.
- Bendtsen J., Lundsgaard C., Middelboe M., Acher D. 2002. Influence of bacterial uptake on deep-ocean dissolved organic carbon. *Global Biochemical Cycles*, 16 (4): 1127.
- Biddanda B., Benner R. 1997. Major contribution from mesopelagic plankton to heterotrophic metabolism in the upper ocean. *Deep-Sea Research I*, 44(12): 2069 – 2085.
- Brown J. H., Gillooly J. F., Allen A. P., Savage V. M., West G. B. 2004. Toward a Metabolic Theory of Ecology. *Ecology*, 85: 1771 – 1789.
- Calvo-Díaz A., Morán X. A. G. 2006. Seasonal dynamics of picoplankton in shelf waters of the southern Bay of Biscay. *Aquatic Microbial Ecology*, 42: 159.
- Carlson C. A., Giovannoni S. J., Hansell D. A., Goldberg S. J., Parsons R., Vergin K. 2004. Interactions among dissolved organic carbon, microbial processes, and community structure in the mesopelagic zone of the northwestern Sargasso Sea. *Limnology and Oceanography*, 49: 1073 – 1083.
- Chen X., Tung K.-K. 2014. Varying planetary heat sink led to global-warming slowdown and acceleration. *Science*, 345 (6199): 897 – 903.
- Christensen J. P., Owens T. G., Devol A. H., Packard T. T. 1980. Respiration and physiological state in marine bacteria. *Marine Biology*, 55: 267 – 276.
- Church M. J. 2008. Resource control of bacterial dynamics in the sea, in: *Microbial Ecology of the Oceans*. Kirchman D. L. (eds.), p p 335 - 382.
- Dumont I., Schoemann V., Jacquet S. H. M., Masson F., Becquevort S. 2011. Bacterial abundance and production in epipelagic and mesopelagic waters in the Subantarctic and Polar Front zones south of Tasmania. *Deep-Sea Research II*, 58: 2212 – 2221.
- del Giorgio P. A., Cole J. J. 2000. Bacterial energetics and growth efficiency, in: *Microbial ecology of the oceans*. D. L. Kirchman (eds.), Wiley-Liss. pp 289 – 325.
- del Giorgio P. A., Cole J. J. 1998. Bacterial Growth Efficiency in Natural Aquatic Systems. *Annual Reviews of Ecology Systems*, 29: 503 – 541.
- del Giorgio P. A., Duarte C. M. 2002. Respiration in the open ocean. *Nature*, 420: 379 – 384.
- del Giorgio P. A., Pace M. L., Fischer D. 2006. Relationship of bacterial growth efficiency to spatial variation in bacterial activity in the Hudson River. *Aquatic Microbial Ecology*, 45: 55 – 67.
- del Giorgio P. A., Williams P. J. B. 2005. Chapter 14: The global significance of respiration in aquatic ecosystems: from single cells to the biosphere, in: *Respiration in aquatic ecosystems*. Oxford University Press, New York (eds.), NY. p p 267 – 303.

- Gasol J. M., del Giorgio P. A. 2000. Using flow cytometry for counting natural planktonic bacteria and understanding the structure of planktonic bacterial communities. *Scientia Marina*, 64: 197-224.
- Gasol J. M., del Giorgio P. A., Massana R., Duarte C. D. 1995. Active versus inactive bacteria: size-dependence in a coastal marine plankton community. *Marine Ecology Progress Series*, 128: 91 - 97.
- Giering S. L., Sanders R., Lampitt R. S., Anderson T. R., Tamburini C., Boutrif M., Zubkov M. V., Marsay C. M., Henson S. A., Saw K., Cook K., Mayor D. J. 2014. Reconciliation of the carbon budget in the ocean's twilight zone. *Nature*, 507: 480 - 483.
- Gundersen K., Heldal M., Norland S., Purdie D. A., Knap A. H. 2002. Elemental C, N, and P cell content of individual bacteria collected at the Bermuda Atlantic Time-series Study (BATS) site. *Limnology and Oceanography*, 47 (5): 1525 - 1530.
- Iversen M. H., Ploug H. 2013. Temperature effects on carbon-specific respiration rate and sinking velocity of diatom aggregates - potential implications for deep ocean export processes. *Biogeosciences*, 10: 4073 - 4085.
- Kirchman D. L., K'nees E., Hodson R. E. 1985. Leucine incorporation and its potential as a measure of protein synthesis by bacteria in natural aquatic systems. *Appl. Environ. Microbiol.* 49: 599-607.
- Kritzberg E. S., Arrieta J. M., Duarte C. M. 2010a. Temperature and phosphorous regulating carbon flux through bacteria in a coastal marine system. *Aquatic Microbial Ecology*, 58: 141 - 151.
- Kritzberg E. S., Duarte C. M., Wassmann P. 2010b. Changes in Arctic marine bacterial carbon metabolism in response to increasing temperature. *Polar Biology*, 33: 1673 - 1682.
- López-Urrutia A., Morán X. A. G. 2007. Resource limitation of bacterial production distorts the temperature dependence of oceanic carbon cycle. *Ecology*, 88(4): 817 - 822.
- Massana R., Pedrós-Alió C., Casamayor E. O., Gasol J. M. 2001. Changes in marine bacterioplankton phylogenetic composition during incubations designed to measure biogeochemically significant parameters. *Limnology and Oceanography*, 46:1181 - 1188.
- Nagata T., Fukuda R., Fukuda H., Koike I. 2001. Basin-scale Geographic Patterns of Bacterioplankton Biomass and Production in the Subarctic Pacific, July - September 1997. *Journal of Oceanography*, 57: 301 - 313.
- Pomeroy L. R., Wiebe W. J. 2001. Temperature and substrates as interactive limiting factors for marine heterotrophic bacteria. *Aquatic Microbial Ecology*, 23: 187 - 204.
- Raven J. A., Geider R. J. 1988. Temperature and algal growth. *New Phytologist*, 110: 441 - 461.
- Regaudie-de-Gioux A., Duarte C. M. 2012. Temperature dependence of planktonic metabolism in the ocean. *Global Biogeochemical Cycles*, 26: GB1015.
- Rhein M., Rintoul S.R., Aoki S., Campos E., Chambers D., Feely R.A., Gulev S., Johnson G.C., Josey S.A., Kostianoy A., Mauritzen C., Roemmich D., Talley L.D., Wang F. 2013. Observations: Ocean. In: *Climate Change 2013: The Physical Science Basis. Contribution of Working Group I to the Fifth Assessment Report of the Intergovernmental Panel on Climate Change* [Stocker T.F., Qin D., Plattner G.-K., Tignor M., Allen S.K., Boschung J., Nauels A., Xia Y., Bex V., Midgley P.M. (eds.)]. Cambridge University Press, Cambridge, United Kingdom and New York, NY, USA.
- Reinthal T., Herndl G. J. 2005. Seasonal dynamics of bacterial growth efficiencies in relation to phytoplankton in the southern North Sea. *Aquatic Microbial Ecology*, 39: 7 - 16.
- Reinthal T., van Aken H., Veth C., Arístegui J., Robinson C., Williams P. J. B., Lebaron P., Herndl G. J. 2006. Prokaryotic respiration and production in the meso- and bathypelagic realm of the eastern and western North Atlantic basin. *Limnology and Oceanography*, 51 (3): 1262 - 1273.
- Rivkin R. B., Legendre L. 2001. Biogenic carbon cycling in the upper ocean: Effects of microbial respiration. *Science*, 291: 2398 - 2400.
- Robinson C., Steinberg D. K., Anderson T. R., Arístegui J., Carlson C. A., Frost J. R., Ghiglione J.-F., Hernández-León S., Jackson J. A., Koppelman R., Quéguiner B., Ragueneau O., Rassoulzadegan F., Robison B. H., Tamburini C., Tanaka T., Wishner K. F., Zhang J. 2010. Mesopelagic zone ecology and biogeochemistry - a synthesis. *Deep-Sea Research II*, 57: 1504 - 1518.

Temperature control of R and PGE in the mesopelagic zone

- Sarmento H., Montoya J. M., Vázquez-Domínguez E., Vaqué D., Gasol J. M. 2010. Warming effects on marine microbial food web processes: how far can we go when it comes to predictions? *Philosophical Transactions of The Royal Society B*, 365: 2137 – 2149.
- Simon M., Azam F. 1989. Protein content and protein synthesis rates of planktonic marine bacteria. *Marine Ecology Progress Series*, 51: 201 – 213.
- Smith D. C., Azam F. 1992. A simple, economical method for measuring bacterial protein synthesis rates in seawater using ³H-leucine. *Marine Microbial Food Webs*, 6: 107 – 114.
- StatSoft Inc. 1997. *Statistica for Windows (computer program manual)*. Tulsa, Oklahoma, USA.
- Tamburini C., Boutrif M., Garel M., Colwell R. R., Deming J. W. 2013. Prokaryotic responses to hydrostatic pressure in the ocean- a review. *Environmental Microbiology*, 15(5): 1262 - 1274.
- Tanaka T., Rassoulzadegan F. 2004. Vertical and seasonal variations of bacterial abundance and production in the mesopelagic layer of the NW Mediterranean Sea: bottom-up and top-down controls. *Deep-Sea Research I*, 51: 531 – 544.
- Vázquez-Domínguez E., Vaqué D., Gasol J. M. 2007. Ocean warming enhances respiration and carbon demand of coastal microbial plankton. *Global Change Biology*, 13: 1327 – 1334.
- Weinbauer M. G., Liu J., Motegi C., Maier C., Pedrotti M L., Dai M., Gattuso J. P. 2013. Seasonal variability of microbial respiration and bacterial and archaeal community composition in the upper twilight zone. *Aquatic Microbial Ecology*, 71: 99 – 115.
- Williams P. J. LeB., Jenkinson N. W. 1982. A transportable microprocessor- controlled precise Winkler titration suitable for field station and siphboard use. *Limnology and Oceanography*, 27 (3): 2843 – 2855.
- Wohlers J., Engel A., Zöllner E., Breithaupt P., Jurgens K., Kans-Georg H., Sommer U., Riebesell. 2009. Changes in biogenic carbon flow in response to sea surface warming. *Proc Natl Acad Sci USA*, 106: 7067–7072.
- Yvon-Durocher G., Caffrey J. M., Cescatti A., Dossena M., del Giorgio P., Gasol J. M., Montoya J. M., Pumpanen J., Staehr P. A., Trimmer M., Woodward G., Allen A. P. 2012. Reconciling the temperature dependence of respiration across timescales and ecosystem types. *Nature*, 487: 472 – 476.
- Zaccone R., Monticelli L. S., Seritti A., Santinelli C., Azzaro M., Boldrin A., La Ferla R., Ribera M. D. 2003. Bacterial processes in the intermediate and deep layers of the Ionian Sea in winter 1999: vertical profiles and their relationship to the different water masses. *Journal of Geophysical Research*, 108: 8117 – 8128.

Chapter 5:
Distribution and contribution of
exopolymer particles to carbon exports

in the Mediterranean Sea



Abbreviated title: EP in the Mediterranean Sea

5.1. Abstract

Exopolymer particles (EP) are polysaccharide-enriched particles mostly from microbial origin involved in the formation of large aggregates and mucilages, particularly relevant in the Mediterranean Sea. We performed an extensive survey of EP including the Eastern, the Western Mediterranean Sea and the adjacent Northeast Atlantic Ocean and covering all the depths from surface (3 m) to the bottom depth. EP concentrations decreased markedly with depth, with the highest EP values in the surface waters (from 5.3 to 81.7 $\mu\text{g XG eq l}^{-1}$), normally above the deep chlorophyll maximum depth. The Eastern Mediterranean (EM) basin showed lower EP concentrations than the Western Mediterranean (WM) basin and the Northeast Atlantic (NEA) Ocean, and the highest EP values were observed close to the Strait of Gibraltar. Phytoplankton production (estimated from satellite data), rather than specific phytoplanktonic groups or chlorophyll *a* concentration, was positive and significantly related to EP concentrations in the surface waters. The abundance of heterotrophic prokaryotes was also related to EP concentrations both in surface and deep waters of the Mediterranean Sea, indicating their active influence on the EP pool. EP distribution in the mesopelagic and deep waters mirrored to some extent EP in epipelagic waters suggesting that the downward flux is a significant via of EP transportation into deep waters. The estimated EP fluxes at 200 and 1000 m depth averaged higher values for the WM basin (16.8 and 3.4 $\text{g C m}^{-2} \text{ yr}^{-1}$, respectively) and for the NEA Ocean (14.5 and 5.1 $\text{g C m}^{-2} \text{ yr}^{-1}$, respectively) than for the EM basin (5.5 and 1.1 $\text{g C m}^{-2} \text{ yr}^{-1}$, respectively).

5.2. Introduction

Exopolymer particles (EP), polysaccharide-rich microgels (from ~ 0.4 to $> 200 \mu\text{m}$), are ubiquitous in marine systems (Alldredge et al., 1993). These particles in the open ocean are generated from abiotic aggregation of dissolved polymers released by heterotrophic and autotrophic microorganisms (Passow, 2002; Verdugo et al., 2004). Higher EP concentrations are normally associated with phytoplankton blooms (e. g. Mari and Kiørboe, 1996; Hong et al., 1997) and regions where algal biomass increase due to favorable growth conditions (Prieto et al., 2006). In contrast, relatively elevated EP concentrations may also be expected in oligotrophic zones since a high EP formation per unit cell occurs under nutrient-depleted stresses as a consequence of carbon overflow (Bar-Zeev et al., 2009; 2011). The variable EP accumulation across marine environments is determined by the quantity and quality of the polymers released by microorganisms and the environmental conditions promoting their abiotic self-assembly. The ecological relevance of EP lies in their particular physicochemical properties, with low density and high stickyness (Engel, 2000; Azetsu-Scott and Passow, 2004), that affect the ocean-atmosphere gases exchange (when EP accumulate in the surface microlayer) or downward exports of aggregates towards the deep ocean when they are ballasted (Passow, 2002; Wurl et al., 2011).

The Mediterranean Sea is an oligotrophic ecosystem characterized by surface phosphorous limitation, particularly accentuated in the Levantine basin (Thingstad et al., 2005). This semi-enclosed sea is connected to the Northeast Atlantic Ocean through the highly dynamic and productive region of the Strait of Gibraltar, characterized by a two-layer system with an upper Atlantic layer inflowing into the Mediterranean Sea, and Mediterranean water outflowing at deep (Lacombe et al., 1982; Gascard and Richez, 1985). In this sea, frequent mucilage events with large mucus aggregates, preceded by periods with elevated EP levels, have been described (Radic et al., 2005; Danovaro et al., 2009). A few previous studies have documented the variability of EP concentrations in surface waters (Garcia et al., 2002; Ortega-Retuerta et al., 2010) and in the mesopelagic waters (Bar-Zeev et al., 2011; Prieto et al., 2006; Weinbauer et al., 2103). These

studies showed variable EP accumulations both geographically and vertically, which is well reflected in contrasting regions as the Strait of Gibraltar (García et al., 2002; Prieto et al., 2006) or the Levantine basin (Bar-Zeev et al., 2011). Despite these studies, there is still a gap of knowledge on EP distribution in deep waters of this sea. Here, we designed an extensive survey to describe EP distribution from the Eastern to the Western Mediterranean Sea, including also the closer Northeast Atlantic Ocean. We covered the whole depth profile and we explored the potential biological factors driving their distribution.

5.3. Material and methods

5.3.1. Sampling and study area

A total of 29 stations were sampled from on board *R/V Sarmiento de Gamboa* along a Mediterranean Sea section from East to West also extending to the subtropical Northeast Atlantic (NEA) Ocean reaching the Canary Islands, from 29 April to 28 May 2014 (Figure 5.1.). Water samples were collected using a rosette of 24 Niskin bottles (12 l each) coupled to a conductivity and Seabird SBE 9 conductivity-temperature-pressure probe (CTD). Up to a total of 13 depths were sampled covering the entire water column, from 3 m depth down to 10 m above the seafloor.

Samples from the surface water layer (SW; down to 150 m) were systematically collected at four depths: 3 m, the depth receiving 20% of the surface photosynthetically active radiation, the deep chlorophyll maximum (DCM) depth, and between 10 m and 45 m below the DCM. The depth of the DCM was determined after visual inspection of the vertical profiles of chlorophyll *a* (chl *a*) fluorescence.

On the basis of the temperature-salinity diagrams and previous published information, samples in the aphotic zone (>200 m) were normally taken at depths of the Levantine Intermediate Waters (LIW; two or three sampling depths), from 200 to 400 m depth in the Eastern Mediterranean (EM) basin and between 200 and 600 m depth in Western Mediterranean (WM) basin, and at greater depths of the Eastern and Western Mediterranean Deep Waters (EMDW and WMDW, respectively; up to seven sampling depths). In the NEA Ocean, the deep samples were taken from three water masses: North Atlantic Central Waters (NACW) between 200 to 750 m depth, Mediterranean Waters (MW) from 750 to 1500 m depth and from the North Atlantic Deep Waters (NADW; >1500 m).

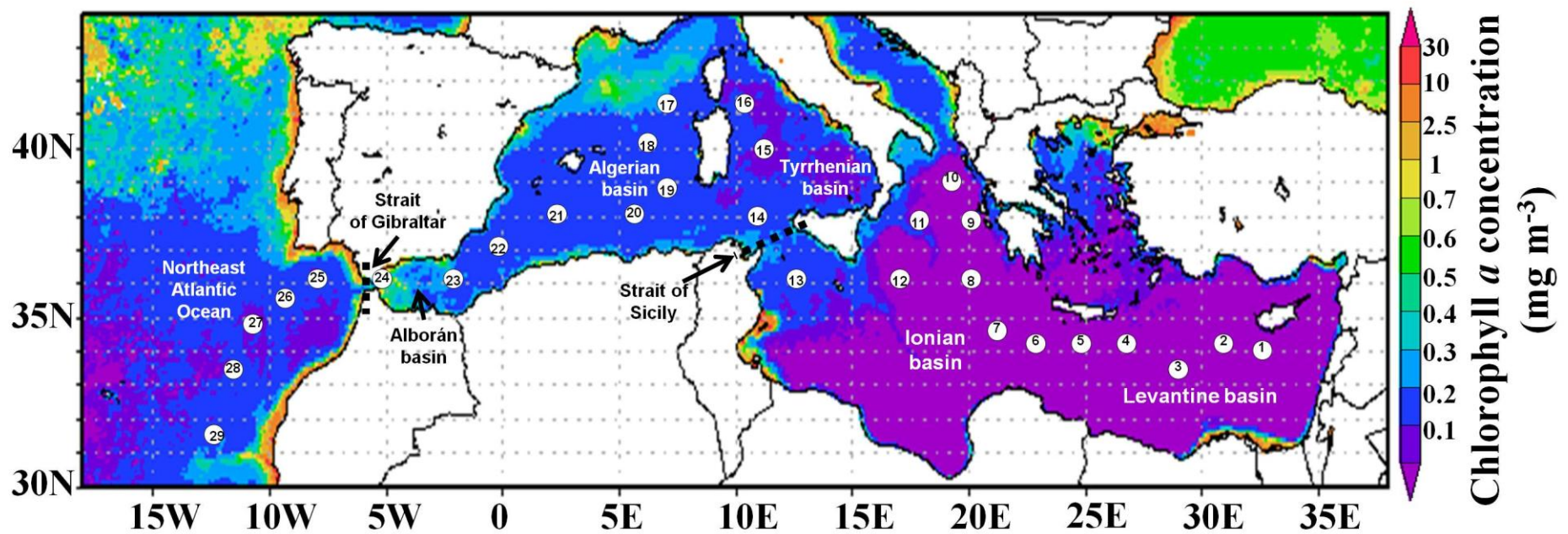


*Figure 5. 1. Map showing the sampling stations (numbers from 1 to 29) during the Hotmix cruise. The stations were superimposed on a Moderate Resolution Imaging Spectroradiometer (MODIS) image of chlorophyll *a* averaged for the whole sampling period (Source: <http://modis.gsfc.nasa.gov/>). Dashed black lines show the separation of the basins in the straits of Sicily (Eastern and Western Mediterranean basins) and Gibraltar (Western Mediterranean and subtropical Northeast Atlantic Ocean).*

5.3.2. Biological and chemical analyses

5.3.2.1. Particulate organic matter

Exopolymer particles (EP) concentrations were measured using the alcian blue method (Passow and Alldredge, 1995). Duplicate or triplicate samples (0.4 – 2 L) were filtered through 0.4 μm polycarbonate filters (25 mm diameter, Poretics) and the exopolymer particles (EP) retained on the filters were stained with 0.5 ml of a 0.02 % solution of alcian blue (Sigma) in 0.06 % acetic acid (pH 2.5). The stained filters were frozen at -80°C until analysis in the laboratory (less than 1 month). The alcian blue was extracted from the thawed filters adding 5 ml of 80 % sulfuric acid and the absorbance was measured at 787 nm in 1 cm path disposable polystyrene cuvettes using ultrapure water as blanks. Three blanks were performed in each batch of samples every day (including staining and freezing in parallel to the samples). Each solution of alcian blue was calibrated using a fresh standard solution of xanthan gum with a concentration of 25 mg l^{-1} . The coefficient of variation of the replicates was $\sim 17\%$. EP concentration was expressed as micrograms xanthan gum equivalents per liter ($\mu\text{g XG eq l}^{-1}$) and converted to carbon units using the lowest and the overall conversion factors of 0.51 and 0.75 $\mu\text{g C per } \mu\text{g XG eq}$ (Engel and Passow, 2001).

Samples for particulate organic carbon (POC) and nitrogen (PON) were determined after filtering 2 L of the water samples through combusted (450°C for 12 h) Whatman GF/F filters (25 mm diameter). These filters were stored frozen (-20°C) until processed. In the laboratory, the filters were thawed and dried overnight at 65°C in a desiccator under HCl fumes to remove carbonates and, then, dried overnight in a desiccator with silica gel. The POC and PON analyses were performed by high-temperature combustion in an elemental analyzer (Perkin Elmer 2400 CHN).

5.3.2.2. Estimation of primary production

Net primary production (PP; $\text{mg C m}^{-2} \text{ day}^{-1}$) at each station, during the sampling period, was obtained from satellite data set in the standard product of the Ocean Productivity website

(<http://www.science.oregonstate.edu/ocean.productivity/>)

which provides PP estimations based on the algorithm Vertically Generalized Production Model (Behrenfeld and Falkowski, 1997).

5.3.2.3. Pigment analysis

Chlorophyll *a* (chl *a*) and phaeophytin *a* (pheo) concentrations were measured by the fluorometric method proposed by Yentsch and Menzel (1963). For each sampling depth, a total volume of 500 ml was filtered through Whatman GF/F filters (25 mm) and stored frozen (- 20 °C) in the dark until analysis. Pigments were extracted in 90% acetone for 24 hours at 4 °C in the dark. The emitted fluorescence of the extracts was read, before and after acidification (with 1N HCl), in a calibrated Turner Design fluorometer (Parsons et al., 1984), expressing the pigment content as $\mu\text{g l}^{-1}$.

5.3.2.4. Identification of phytoplankton groups

Phytoplankton groups were determined immediately after collection from the Niskin bottles, combining a FACScalibur flow cytometer (BD Biosciences), fitted with a laser emitting at 488 nm, and a Cytosense flow cytometer (CytoBuoy b.v.) fitted with a blue (488 nm) and a red (642 nm) laser. This allowed the enumeration of the main algal groups, spanning from pico- to microphytoplankton. Samples from 6-8 depths, down to 200 m, were analyzed immediately after collection. Populations were identified from bivariate plots of forward and side scatter, red, orange and green fluorescence. The cross-check comparison between the two cytometers allowed discriminating more reliably the *in situ* abundances of six algal groups: cyanobacteria (*Phrochlorococcus* sp. and *Synechococcus* sp.), picoeukaryotes, nanoeukaryotes, cryptophytes, and a heterogeneous cluster of microphytoplankton.

5.3.2.5. Heterotrophic prokaryotes

Prokaryotic heterotrophic abundance (PHA, cell ml^{-1}) was determined by flow cytometry (Gasol and del Giorgio, 2000), using a FACScalibur cytometer (BD Biosciences) fitted with a laser emitting at 488 nm. Samples were directly obtained from the Niskin bottles and 1.5 ml aliquots were fixed with 1% of paraformaldehyde + 0.05 % glutaraldehyde (final concentrations), deep-frozen in liquid nitrogen and stored at -80 °C until analysis (less than 24 hours after

collection). Prokaryotes were stained with SybrGreen I, and detected in a plot of side scatter with green fluorescence. We used 1 μm yellow-green Polysciences beads for reference and to even up the scaling of scatter and fluorescence among samples.

Prokaryotic heterotrophic production (PHP) was estimated from ^3H -Leucine (specific activity = 112 Ci mmol^{-1}) incorporation into proteins (Kirchman et al., 1985) and using the microcentrifugation protocol proposed by Smith and Azam (1992). Four replicates (1.2 ml) and two trichloroacetic acid (TCA)-killed blanks in microcentrifuge tubes were added L-[4, 5- ^3H] leucine at 20 nM. Samples and blanks were incubated (for 2 to 8 h) at in situ temperature. Incubations were stopped by addition of 50 % TCA (to 5%), centrifugation (10 min. and 10000 r.p.m.) and rinsing with 5 % TCA. Optisafe HiSafe scintillation cocktail (Perkin Elmer) was added (1 ml), and radioactivity was measured in a liquid scintillation counter (Beckman LL6000) on board. Leucine incorporation rates ($\text{pmol Leu l}^{-1} \text{ h}^{-1}$) were converted into carbon units by using the theoretical conversion factor of 1.55 kg C mol Leu^{-1} (Simon and Azam, 1989), assuming that isotope dilution was negligible.

5.3.3. Data Analyses

Depth-integrated data were calculated using a conventional trapezoid method. Statistical analyses were performed using Statistica 6.0 (StatSoft Inc., 1997). The data were \log_{10} -transformed to fit the regression assumptions of normality and homoscedasticity and regression analyses were performed to explore the relationship between EP distribution and biological variables. Data were divided into three basins: Eastern Mediterranean (EM), Western Mediterranean (WM) and Northeast Atlantic (NEA) Ocean.

5.3.3.1. Estimations of the downward EP fluxes

Assuming that the downward flux derived from phytoplankton primary production is the major input of EP into the deep waters, we estimated the EP fluxes at 200 m (EP F_{200}) and 1000 m depth (EP F_{1000}). We first calculated the corresponding POC fluxes at these depths and, then, applied the significant

POC-EP relationship found in this oceanographic survey to obtain the corresponding EP fluxes.

POC fluxes in the Mediterranean Sea were determined from the algorithm of Martin et al. (1987), as described by Yokokawa et al. (2013). First, we calculated the POC fluxes at 100 m depth (F_{100}) with the equation proposed by Berger and Wefer (1990) as a function of primary production (PP):

$$\text{POC } F_{100} \text{ (mg C m}^{-2} \text{ d}^{-1}) = 2 \times \text{PP}^{1/2} \times (\text{PP}/100)$$

where PP is the primary production obtained from satellite estimations. Then, we estimated POC fluxes (F_z) at the selected depths (z) of 200 m and 1000 m depth, using the power function of Martin et al. (1987):

$$\text{POC } F_z \text{ (mg C m}^{-2} \text{ d}^{-1}) = F_{100} \times (z/100)^{-b}$$

where flux attenuation coefficients, b , were obtained from sedimentation tramps by Stavrakakis et al. (2013) in the Eastern Mediterranean Sea ($b = 1.07$) and by Zuñiga et al. (2007) in the Algerian basin ($b = 0.918$) and Sánchez-Vidal et al. (2005) in the Alboran basin ($b = 0.753$) of the Western Mediterranean Sea.

POC fluxes at 200 m and 1000 m depths in the NEA Ocean, however, were estimated from the algorithm proposed by Antia et al. (2001) that relates directly F_z , at a given depth, and PP:

$$\text{POC } F_z \text{ (mg C m}^{-2} \text{ d}^{-1}) = 0.1 \times \text{PP}^{1.77} \times z^{-0.68}$$

5.3.3.2. Transfer efficiency of exopolymer particles (EP TE) between zones

The EP transfer efficiency from epipelagic to mesopelagic waters (EP TE_{epi-meso}) was calculated as:

$$\text{EP TE}_{\text{epi-meso}} = \frac{[\text{EP}]_{\text{meso}}/l_{\text{meso}}}{[\text{EP}]_{\text{SW}}/l_{\text{SW}}} \times 100$$

where $[\text{EP}]_{\text{meso}}$ is the depth-integrated EP concentration in the mesopelagic waters (between 200 to 1000 m depth), l_{meso} the length of the mesopelagic region in meters, $[\text{EP}]_{\text{SW}}$ is the depth-integrated EP concentration between 3 m and the depth below the DCM, l_{SW} is the length of the Surface waters (SW) zone.

Additionally, the EP transfer efficiency from mesopelagic to deep waters (EP TE_{meso-deep}) was calculated as:

$$EP TE_{meso-deep} = \frac{[EP]_{deep} / l_{deep}}{[EP]_{meso} / l_{meso}} \times 100$$

where $[EP]_{deep}$ is the depth-integrated EP concentration in the deep waters, l_{deep} the length of the deep zone, $[EP]_{meso}$ is the depth-integrated EP concentration in the mesopelagic zone, and l_{meso} is the length of the mesopelagic zone in meters.

Finally, the contribution of EP to the total POC fluxes (EP %POC Flux) at the bottom of the surface waters and the mesopelagic zone was calculated as:

$$EP \% POC Flux = (EP Flux / POC Flux) \times 100$$

5.4. Results

5.4.1. Vertical and geographical distribution of exopolymeric particles

Depth-profiles of EP showed consistently higher concentrations in the upper 150 m than in deeper waters (Figure 5.2.). EP concentrations in the upper 150 m ranged ~15-fold, from 5.3 to 81.7 $\mu\text{g XG eq l}^{-1}$, similar to the variability of heterotrophic prokaryote abundance, and with a median value of 30.9 $\mu\text{g XG eq l}^{-1}$ ($n = 121$). By contrast, EP concentrations in deep waters (≥ 200 m depth) showed very constant values, below 35 $\mu\text{g XG eq l}^{-1}$, down to bottom depth (Figure 5.2.).

Considering all the data from 3 m surface waters to the bottom depths, EP concentrations declined with increasing depth. This decline can be described by the exponential fitted regression $\text{EP } (\mu\text{g XG eq l}^{-1}) = 44.54 (\pm 1.53) e^{-6.15 (\pm 0.47) \times \text{depth}^{(\text{km})}}$ ($r^2 = 0.63$ and $p\text{-value} < 0.001$), the power fitted regression $\text{EP } (\mu\text{g XG eq l}^{-1}) = 62.08 (\pm 3.26) \times \text{depth}^{-0.26 (\pm 0.01)}$ with depth expressed in meters ($r^2 = 0.53$ and $p\text{-value} < 0.001$) and the log-log regression $\text{Log}_{10} \text{ EP } (\mu\text{g XG eq l}^{-1}) = -0.38 (\pm 0.02) \text{Log}_{10} \text{ depth (m)} + 1.94 (\pm 0.04)$ ($r^2 = 0.56$ and $p\text{-value} < 0.001$). This log-log slope (-0.38 ± 0.02) was different from the log-log slope of decrease in depth with heterotrophic prokaryotic abundance (-0.50 ± 0.04) and production (-0.52 ± 0.02).

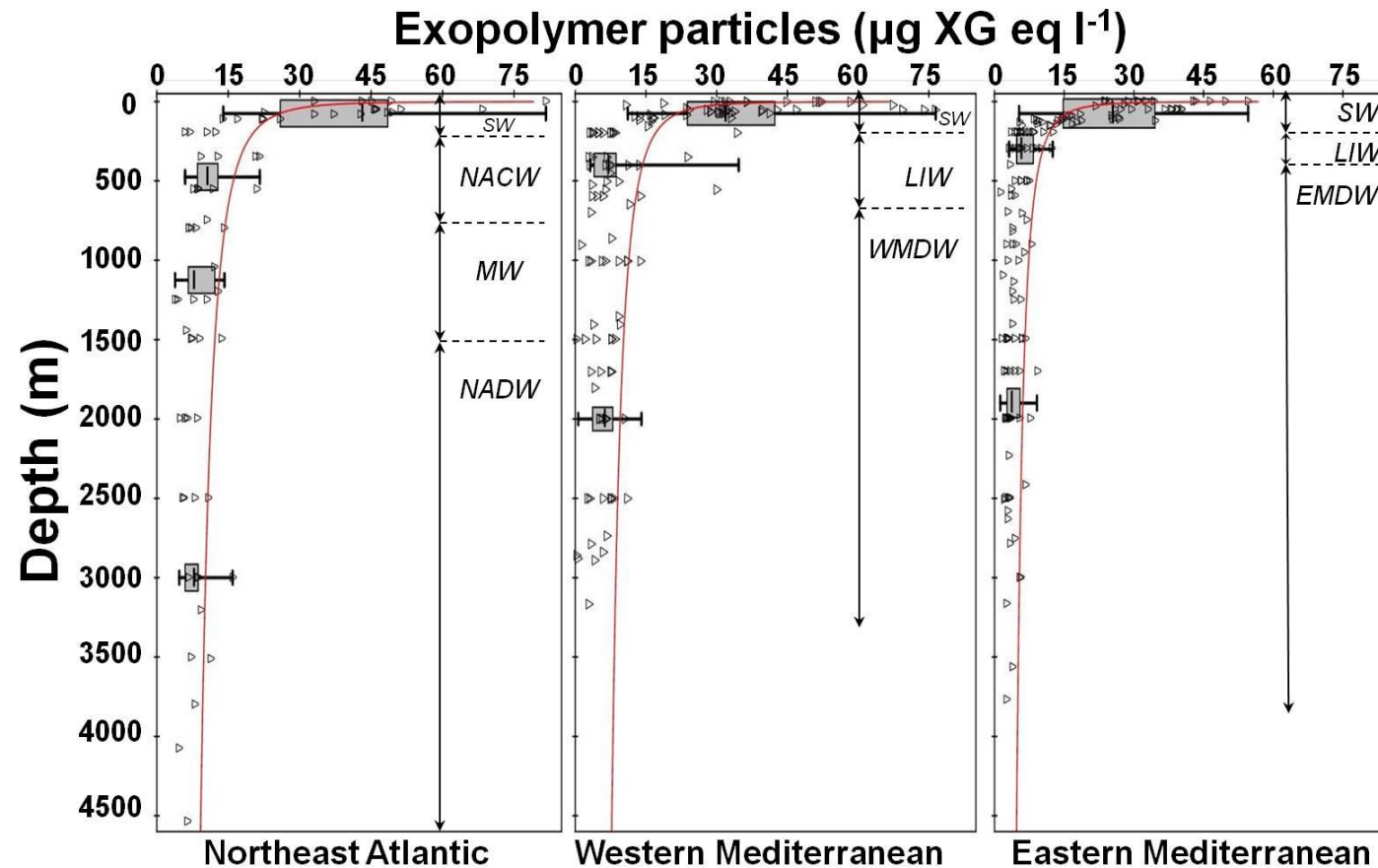


Figure 5. 2. Depth profiles of exopolymer particles in the three basins. Triangles represent the raw data, gray filled boxes and black lines are the 25-75 % percentiles and the median values, respectively. The data were depth-binned in the following water masses: Surface Water (SW, up to 150 m depth), Levantine Intermediate Water (LIW; from 200 to 400 m in the Eastern Mediterranean basin and from 200 to 600 m in the Western Mediterranean), Eastern and Western Mediterranean Deep Water (EMDW and WMDW, respectively), North Atlantic Central Water (NACW; between 200 and 750 m depth), Mediterranean Water (MW; between 750 and 1500 m depth) and North Atlantic Deep Water (NADW). The red lines represent the fitted power decrease with depth at each basin (p -value < 0.05).

EP distribution in surface waters showed generally higher EP concentrations in the WM basin and the NEA Ocean than in the EM basin (Figures 5.2. and 5.3.). The WM and NEA basins also showed shallower DCM depths, exhibiting an inverse relationship between depth-integrated EP in the surface waters (SW-EP) and the DCM depths [n = 29; $\text{Log}_{10} \text{SW-EP} = -0.50 (\pm 0.15) \text{Log}_{10} \text{DCM} + 4.46 (\pm 0.28)$, $r^2 = 0.31$ and p-value = 0.0018]. Maximum EP levels in the surface waters were found in the stations close to the Strait of Gibraltar (Figure 5.3.). EP concentrations in the deep waters reproduced a similar pattern that the observed in the surface waters with high values at intermediate depths and stations close to the Gibraltar Strait (Figure 5.3.).

As a result of this characteristic EP distribution in the water column, depth-integrated EP concentrations in the surface waters were significant and positively correlated to the depth-integrated EP concentration in the mesopelagic zone (from 200 to 1000 m depth, Figure 5.4. A). Similarly, there was a significant relationship between depth-integrated EP in the mesopelagic zone and in waters below 1000 m depth (Figure 5.4. B).

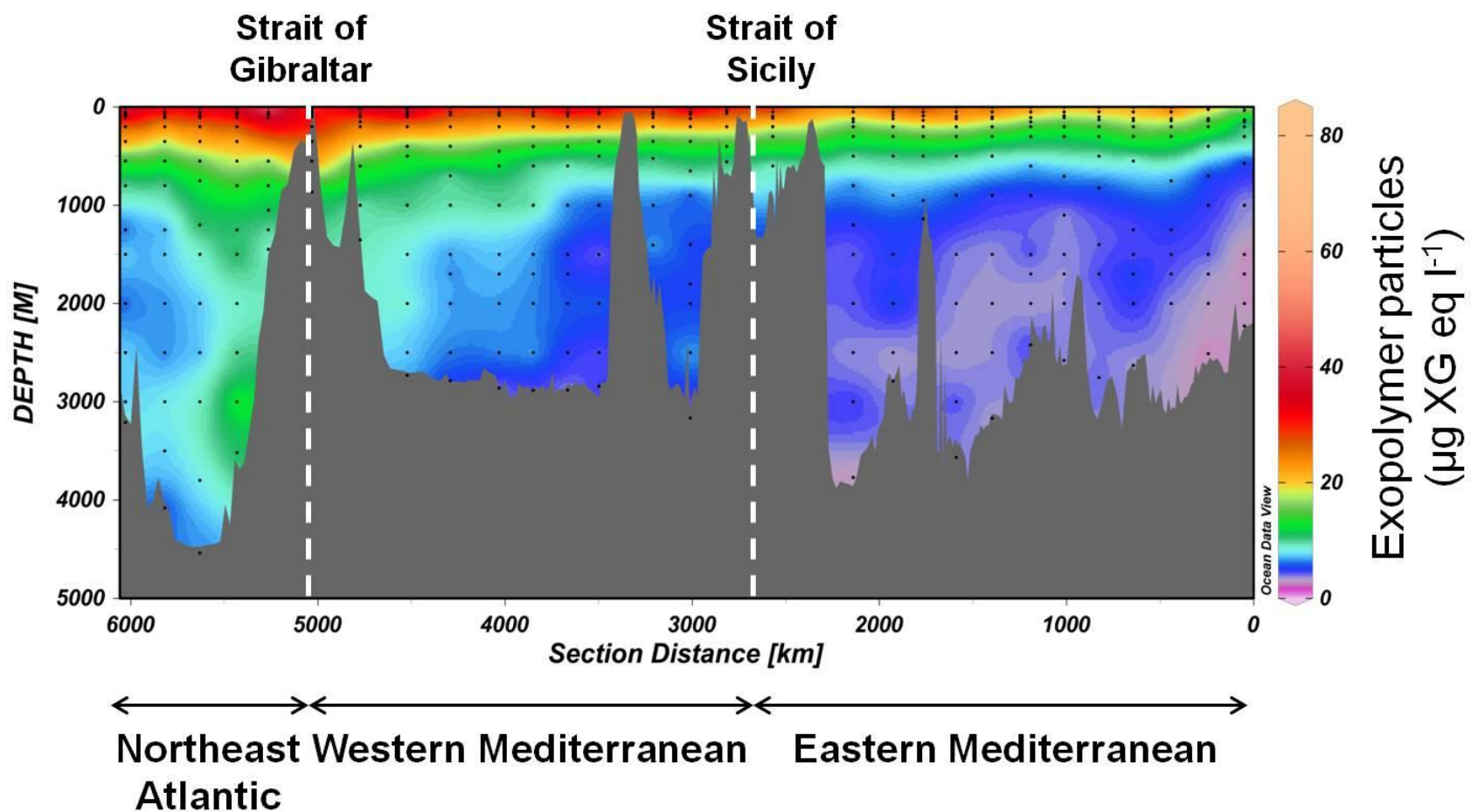


Figure 5. 3. Distribution of exopolymeric particles, in a depth-section from Eastern to Western Mediterranean Sea and Northeast Atlantic Ocean. White dashed lines correspond to the end of each ocean basin.

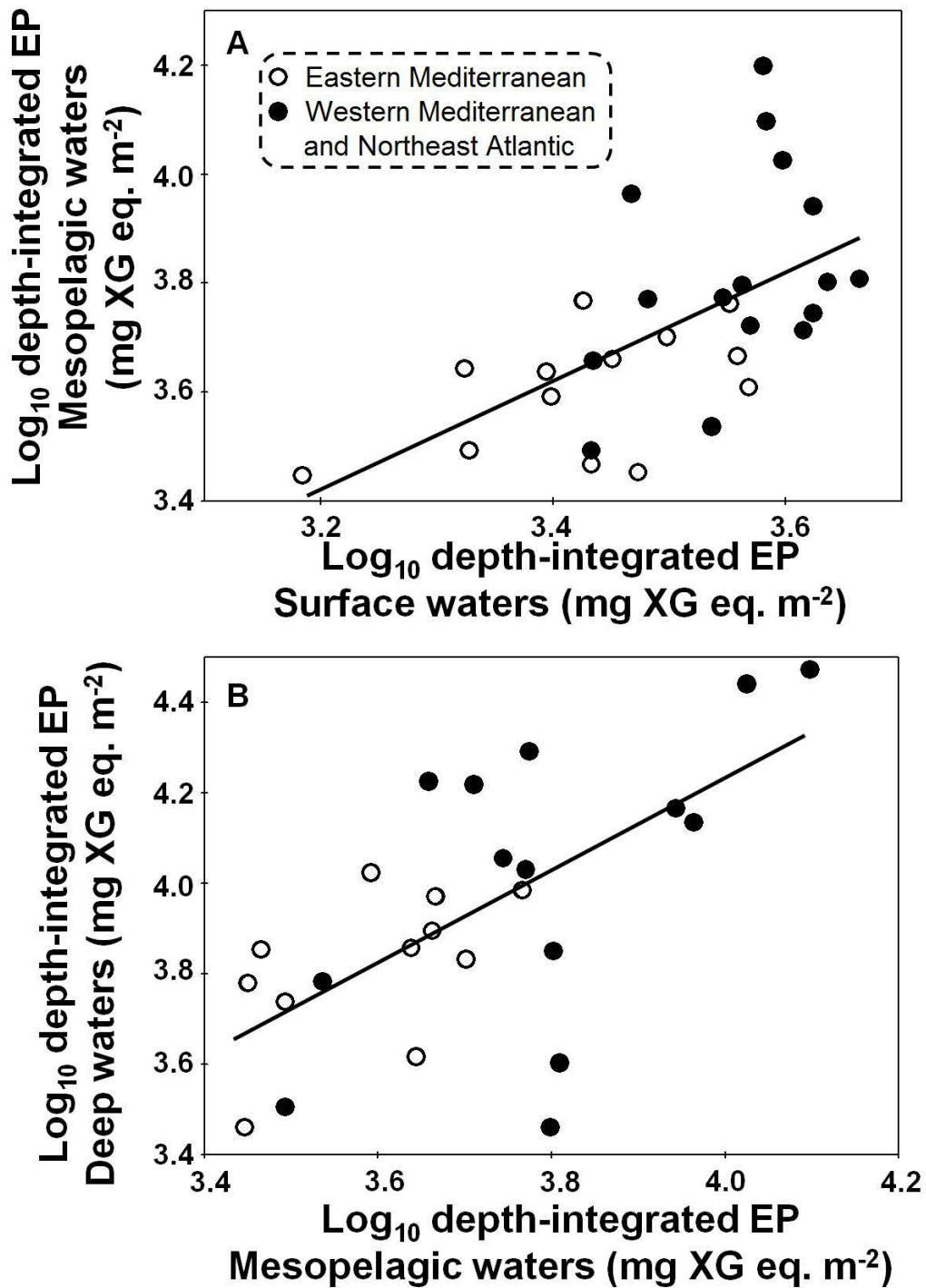


Figure 5. 4. Log-log relationships (A) between depth-integrated EP concentration in the surface waters (SW-EP) and in the mesopelagic waters (Meso-EP) [$n = 29$; Log_{10} Meso-EP = $1.00 (\pm 0.27)$ Log_{10} SW-EP + $0.21 (\pm 0.94)$, $r^2 = 0.34$ and $p\text{-value} = 0.0009$] and (B) between depth-integrated EP in the mesopelagic zone and in deep waters below 1000 m depth (DW-EP)[$n = 25$; Log_{10} DW-EP = $1.02 (\pm 0.26)$ Log_{10} Meso-EP + $0.14 (\pm 0.95)$, $r^2 = 0.41$ and $p\text{-value} = 0.0006$].

5.4.2. EP contribution to particulate organic matter

EP concentrations in the water column were positively and significantly related to particulate organic carbon (POC) and nitrogen (PON) concentrations (Figure 5).

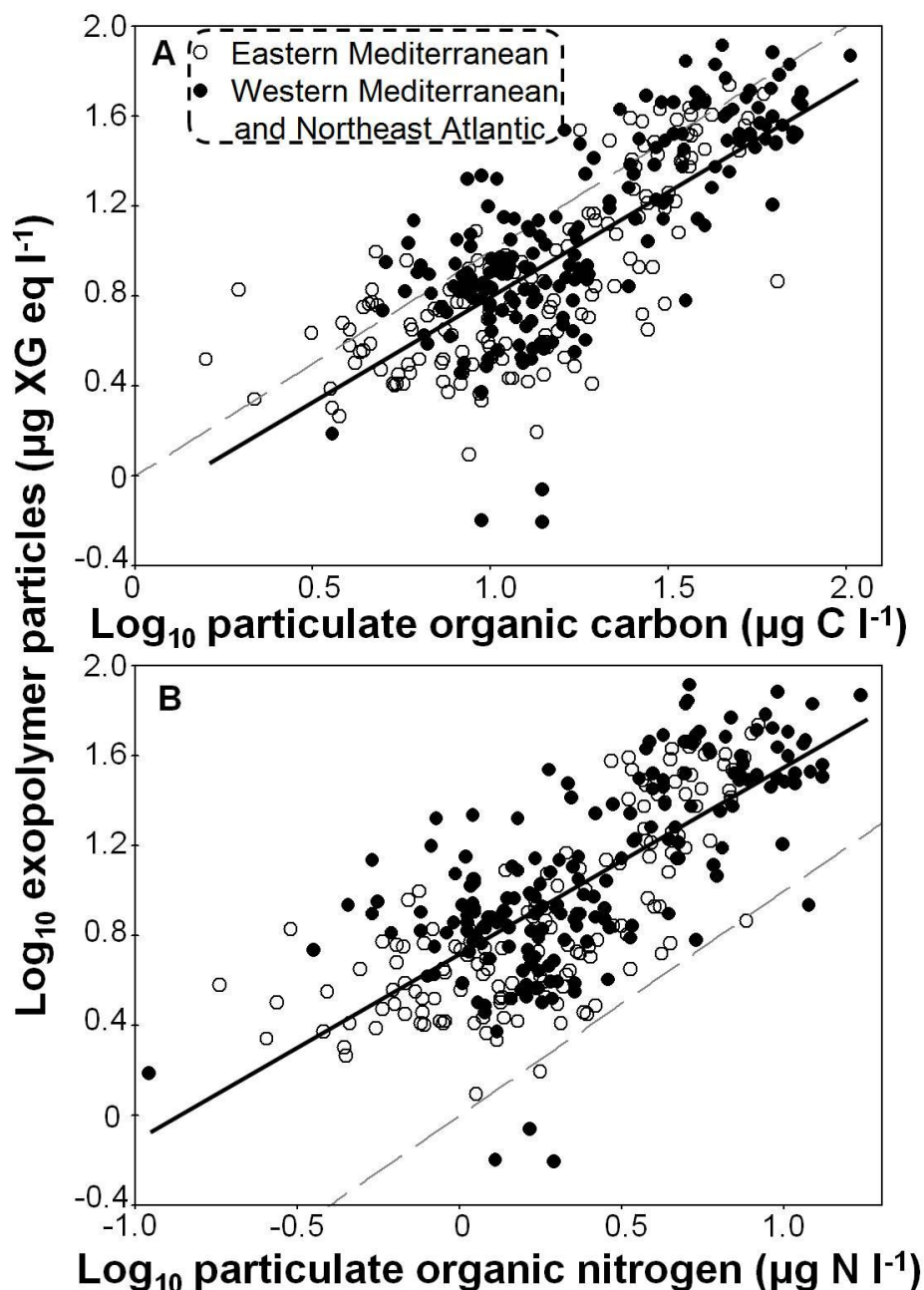


Figure 5. 5. Log-log scatterplot between the EP concentrations and (A) particulate organic carbon (POC) [$n = 336$; Log_{10} EP = $0.95 (\pm 0.04)$ Log_{10} POC - $0.15 (\pm 0.05)$, $r^2 = 0.59$ and p -value < 0.0001] and (B) particulate organic nitrogen (PON) [$n = 334$; Log_{10} EP = $0.83 (\pm 0.04)$ Log_{10} PON + $0.71 (\pm 0.02)$, $r^2 = 0.54$ and p -value < 0.0001]. The dashed gray line corresponds to the 1:1 Line.

EP concentrations were transformed into carbon units (C-EP, $\mu\text{g C l}^{-1}$) to estimate the EP contribution to the total POC pool (%POC) (Table 5.1.). The EP contribution as % of POC was higher in the surface waters (up to 150 m depth) than in the meso- and deep waters. This percentage was particularly high at 3-m surface and subsurface waters (between 3 m and DCM depths) (Table 5.1.). Among basins, %POC values were consistently higher in the Northeast Atlantic than in the Mediterranean Ocean (Table 5.1.).

Table 5. 1. Median and ranges (in brackets) of carbon content (C-EP) of exopolymer particles in the surface, mesopelagic and deep waters (> 1000 m) calculated using the lowest and overall conversion factors of 0.51 and 0.75 $\mu\text{g C per } \mu\text{g XG eq}$ (Engel and Passow, 2001), and their respective percentage of the POC pool [%POC = (C-EP / POC) x 100]. Values of %POC are calculated for the whole data set and for each basin separately.

	Carbon content ($\mu\text{g C l}^{-1}$)				Total		Eastern Med.		Western Med.		Northeast Atlantic	
	0.51		0.75		%POC		%POC		%POC		%POC	
	0.51	0.75	0.51	0.75	0.51	0.75	0.51	0.75	0.51	0.75	0.51	0.51
3-m surface	18.7 (12.0-41.7)	27.5 (17.7-61.3)	45	66	47	69	32	47	60	89		
subsurface	20.1 (5.7-39.0)	29.5 (8.4-57.4)	49	71	48	71	39	57	72	106		
DCM	13.7 (2.7-39.7)	20.2 (4.0-55.7)	35	52	33	48	35	51	49	72		
Below DCM	8.4 (3.1-17.7)	12.4 (4.5-26.0)	32	48	32	47	28	42	44	65		
Epipelagic waters	15.7 (2.7-41.7)	23.1 (4.0- 61.3)	38	56	38	56	34	50	60	89		
Mesopelagic waters	3.4 (0.6-17.7)	5.1 (0.9-26.0)	27	39	27	40	22	32	44	65		
Deep waters	2.7 (0.3-8.1)	4.0 (0.5-11.9)	29	43	25	36	32	48	39	57		

5.4.3. Main biological drivers on the EP distribution

Regression analyses were performed to assess the potential biological drivers regulating the EP concentration in the surface waters (Table 5.2.) or in waters below 200 m depth (Table 5.3.). Chl *a*, as indicator of algal biomass, was not a universal driver of EP concentration. We found inconsistent regressions between chl *a* and EP concentration in volumetric terms (Table 5.2.) and the relationship between depth-integrated chl *a* and epipelagic EP concentrations was not statistically significant. In contrast, the chl *a*:pheo ratios, which provide useful information of the physiological status of the algal community, were consistent and positively correlated with EP distribution. In these regressions, the obtained overall slope of 0.38 (± 0.06) was not significantly different among ocean basins (Table 5.2.). Additionally, satellite-estimated primary production

(PP) was significant and positively correlated to the depth-integrated EP distribution in the surface waters (Figure 5.6).

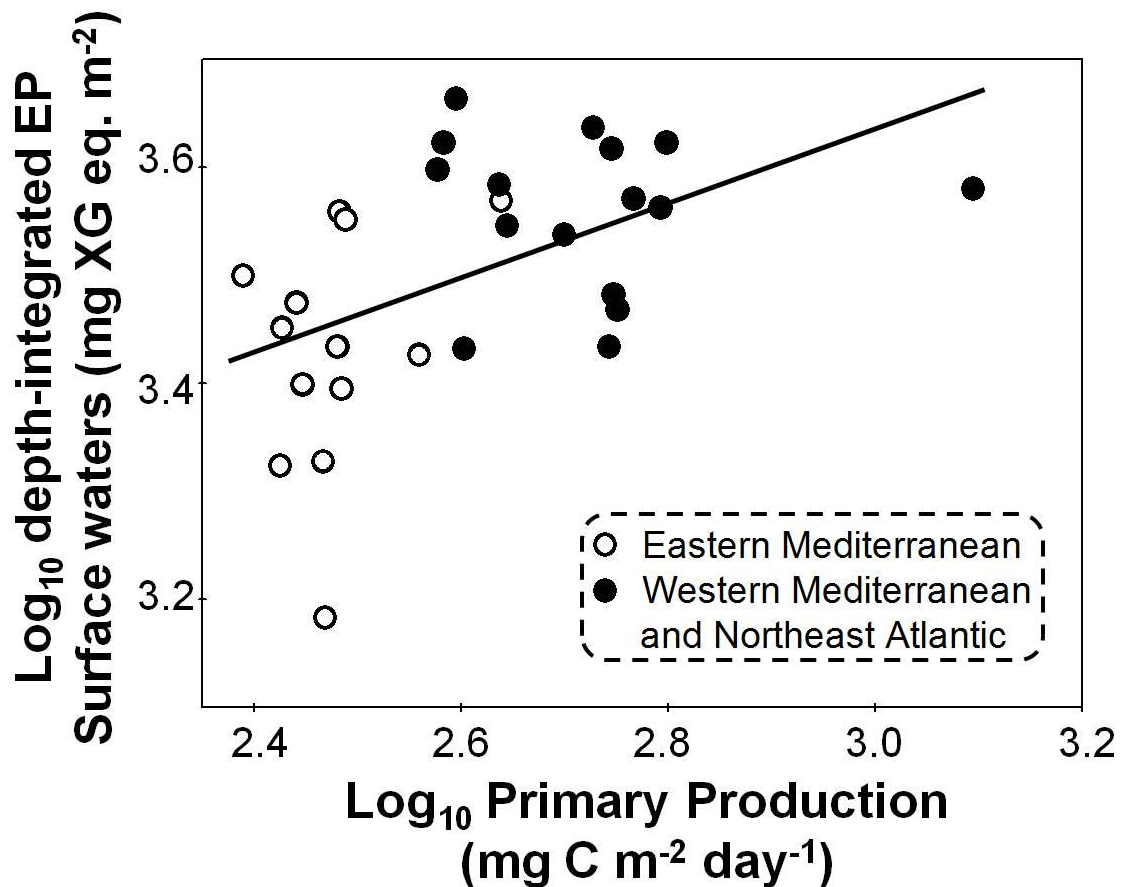


Figure 5. 6. Log-log scatterplot between depth-integrated EP distribution in the surface waters (SW-EP) and primary production (PP) [$\text{Log}_{10} \text{ SW-EP} = 0.35 (\pm 0.12) \text{ Log}_{10} \text{ PP} + 2.60 (\pm 0.30)$; $N = 29$, $r^2 = 0.25$ and $p\text{-value} = 0.0059$].

EP concentrations in surface waters, in volumetric terms, were related to picoeukaryotes and heterotrophic prokaryotes (Table 5.2.). On a basin by basin, EP concentrations in the EM basin had positive relationships with *Synechococcus* sp. and microphytoplankton and a negative relationship with *Prochlorococcus* sp., while picoeukaryotes, nanoeukaryotes and heterotrophic prokaryotes (PHA and PHP) were more robustly correlated to EP concentrations in the WM basin and in the NEA Ocean (Table 5.2.).

Table 5. 2. Results of log-log regression analyses between exopolymer particles and biological drivers in surface waters (upper 150 m). The asterisk means significant regressions (p -value < 0.05) and the abbreviation “n.s.” nonsignificant regressions.

Dependent var.	Independent var.	Geographical region	Slope (\pm SE)	Intercept. (\pm SE)	r ²	p-value	N
Exopolymer particles ($\mu\text{g XG eq l}^{-1}$)	Chlorophyll <i>a</i> ($\mu\text{g L}^{-1}$)	Total	-	-	-	n.s.	121
		EM*	-0.25(\pm 0.08)	1.00 (\pm 0.11)	0.18	< 0.01	52
		WM	-	-	-	n.s.	48
		NEA	-	-	-	n.s.	21
	chl <i>a</i> :pheo ratio	Total*	0.38 (\pm 0.06)	1.33 (\pm 0.02)	0.29	< 0.01	116
		EM*	0.34 (\pm 0.06)	1.26 (\pm 0.03)	0.39	< 0.01	50
		WM*	0.33 (\pm 0.16)	1.38 (\pm 0.06)	0.09	< 0.05	45
		NEA*	0.45 (\pm 0.15)	1.43 (\pm 0.06)	0.32	< 0.01	21
	Picoeukaryotes (cell ml ⁻¹)	Total*	0.20 (\pm 0.05)	0.81 (\pm 0.15)	0.14	< 0.01	121
		EM	-	-	-	n.s.	52
		WM*	1.05 (\pm 0.21)	-4.58 (\pm 1.18)	0.37	< 0.01	48
		NEA*	0.79 (\pm 0.27)	-3.03 (\pm 1.57)	0.31	< 0.01	21
	<i>Synechococcus</i> sp. (cell ml ⁻¹)	Total*	0.17 (\pm 0.03)	0.81 (\pm 0.10)	0.28	< 0.01	121
		EM*	0.14 (\pm 0.04)	0.84 (\pm 0.14)	0.21	< 0.01	52
		WM	-	-	-	n.s.	48
		NEA	-	-	-	n.s.	21
	<i>Prochlorococcus</i> sp. (cell ml ⁻¹)	Total*	-0.06 (\pm 0.03)	1.67 (\pm 0.09)	0.05	< 0.05	121
		EM*	-0.16 (\pm 0.03)	1.94 (\pm 0.11)	0.39	< 0.01	52
		WM	-	-	-	n.s.	48
		NEA	-	-	-	n.s.	21
	Nanoeukaryotes (cell ml ⁻¹)	Total	-	-	-	n.s.	109
		EM	-	-	-	n.s.	40
		WM*	0.18 (\pm 0.03)	0.79 (\pm 0.13)	0.40	< 0.01	48
		NEA*	0.20 (\pm 0.08)	0.85 (\pm 0.28)	0.27	< 0.05	21
	Cryptophytes (cell ml ⁻¹)	Total	-	-	-	n.s.	98
		EM	-	-	-	n.s.	32
		WM*	0.10 (\pm 0.05)	1.35 (\pm 0.07)	0.09	< 0.05	46
		NEA	-	-	-	n.s.	20
Microphytoplankton (cell ml ⁻¹)	Total	-	-	-	n.s.	109	
	EM*	0.39 (\pm 0.13)	0.61 (\pm 0.26)	0.18	< 0.01	40	
	WM	-	-	-	n.s.	48	
	NEA	-	-	-	n.s.	21	
PH Abundance (cell ml ⁻¹)	Total*	0.64 (\pm 0.09)	-2.18 (\pm 0.52)	0.29	< 0.01	121	
	EM	0.46 (\pm 0.24)	-1.15 (\pm 1.32)	0.07	0.064	52	
	WM*	0.73 (\pm 0.20)	-2.43 (\pm 1.08)	0.25	< 0.01	48	
	NEA*	0.79 (\pm 0.27)	-3.03 (\pm 1.57)	0.31	< 0.01	21	
PH Production ($\mu\text{g C l}^{-1} \text{d}^{-1}$)	Total*	0.22 (\pm 0.05)	1.62 (\pm 0.04)	0.17	< 0.01	117	
	EM	-	-	-	n.s.	51	
	WM*	0.25 (\pm 0.05)	1.67 (\pm 0.04)	0.34	< 0.01	45	
	NEA*	0.20 (\pm 0.09)	1.71 (\pm 0.08)	0.20	< 0.05	21	

Interestingly, the depth-integrated EP in surface waters was significant and positively correlated to the depth-integrated picoeukaryotes (Figure 5.7. A) heterotrophic prokaryotes, PHP (Figure 5.7. B) and PHA (Figure 5.7. C).

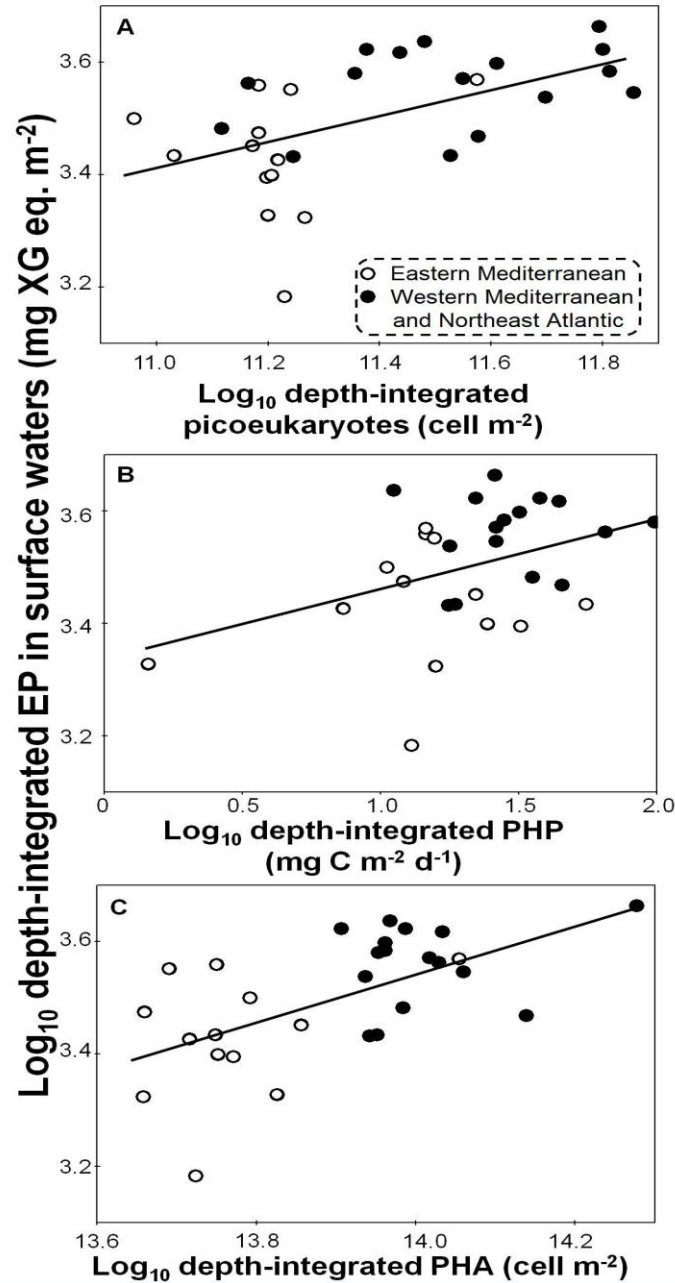


Figure 5. 7. Log-log scatterplot (A) between depth-integrated EP distribution in the surface waters (SW-EP) and pioceukaryote abundances [Log_{10} SW-EP = $0.23 (\pm 0.07) \text{Log}_{10}$ picoeukaryotes + $0.91 (\pm 0.82)$; $n = 29$, $r^2 = 0.27$ and p -value = 0.0036]; (B) between SW-EP and depth-integrated PHP in the surface waters [Log_{10} SW-EP = $0.13 (\pm 0.06) \text{Log}_{10}$ PHP + $3.33 (\pm 0.08)$; $n = 29$, $r^2 = 0.15$ and p -value = 0.035]; and (C) between SW-EP and depth-integrated PHA in the surface waters [Log_{10} SW-EP = $0.43 (\pm 0.11) \text{Log}_{10}$ PHA - $2.51 (\pm 1.53)$; $n = 29$, $r^2 = 0.36$ and p -value = 0.0005].

EP concentrations, in volumetric terms, in waters below the surface zone were poorly correlated to the heterotrophic prokaryotes using either the dataset grouped by water masses (Levantine Intermediate water) or in mesopelagic (between 200 and 1000 m depth) and bathypelagic zone (> 1000 m) (Table 5.3.). Only EP concentrations in the mesopelagic zone were consistently correlated to PHA (Table 5.3.).

Table 5. 3. Results of log-log regression analyses between exopolymeric particles and biological variables in the mesopelagic and in deep waters (> 200 m depth). Regressions in the Levantine Intermediate Waters are also included. Asterisks mean significant regressions (p -value < 0.05) and n.s. = non significant regressions.

Dependent var.	Independent var.	Geographical region	Slope (\pm SE)	Intercept. (\pm SE)	r^2	p -value	N
Mesopelagic Waters (200-1000 m)							
Exopolymeric particles ($\mu\text{g XG eq l}^{-1}$)	HP Abundance (cell ml^{-1})	EM + WM + NEA *	0.48 (\pm 0.10)	-1.62 (\pm 0.49)	0.20	< 0.01	99
		EM*	0.37 (\pm 0.12)	-1.12 (\pm 0.58)	0.19	< 0.01	46
		WM*	0.65 (\pm 0.22)	-2.53 (\pm 1.17)	0.20	< 0.01	35
		NEA	-	-	-	n.s.	18
	PH Production ($\mu\text{g C l}^{-1} \text{d}^{-1}$)	EM + WM + NEA	-	-	-	n.s.	79
		EM	-	-	-	n.s.	33
		WM	-	-	-	n.s.	33
		NEA	-	-	-	n.s.	13
Levantine Intermediate Waters							
Exopolymeric particles ($\mu\text{g XG eq l}^{-1}$)	PH Abundance (cell ml^{-1})	EM + WM*	0.50 (\pm 0.16)	-1.78 (\pm 0.87)	0.14	< 0.01	57
		EM	-	-	-	n.s.	26
		WM*	0.60 (\pm 0.27)	-2.32 (\pm 1.41)	0.15	< 0.05	31
	PH Production ($\mu\text{g C l}^{-1} \text{d}^{-1}$)	EM + WM	-	-	-	n.s.	43
		EM	-	-	-	n.s.	14
		WM	-	-	-	n.s.	29
Deep Waters (> 1000 m)							
Exopolymeric particles ($\mu\text{g XG eq l}^{-1}$)	PH Abundance (cell ml^{-1})	EM + WM + NEA *	0.31 (\pm 0.13)	-0.74 (\pm 0.62)	0.04	< 0.05	124
		EM	-	-	-	n.s.	52
		WM	-	-	-	n.s.	43
		NEA	-	-	-	n.s.	29
	PH Production ($\mu\text{g C l}^{-1} \text{d}^{-1}$)	EM + WM + NEA	-	-	-	n.s.	89
		EM	-	-	-	n.s.	42
		WM	-	-	-	n.s.	34
		NEA	-	-	-	n.s.	13

There were significant and positive relationships between depth-integrated EP concentrations and PHA in the mesopelagic zone (Figure 5.8. A) and in deep waters (>1000 m depth; Figure 5.8. B), but depth-integrated EP and

PHP were not correlated either at mesopelagic depths or in deep waters. In addition, depth-integrated EP in the LIW was positive and significantly related to depth-integrated PHA (Figure 5.9. A) and PHP (Figure 5.9. B).

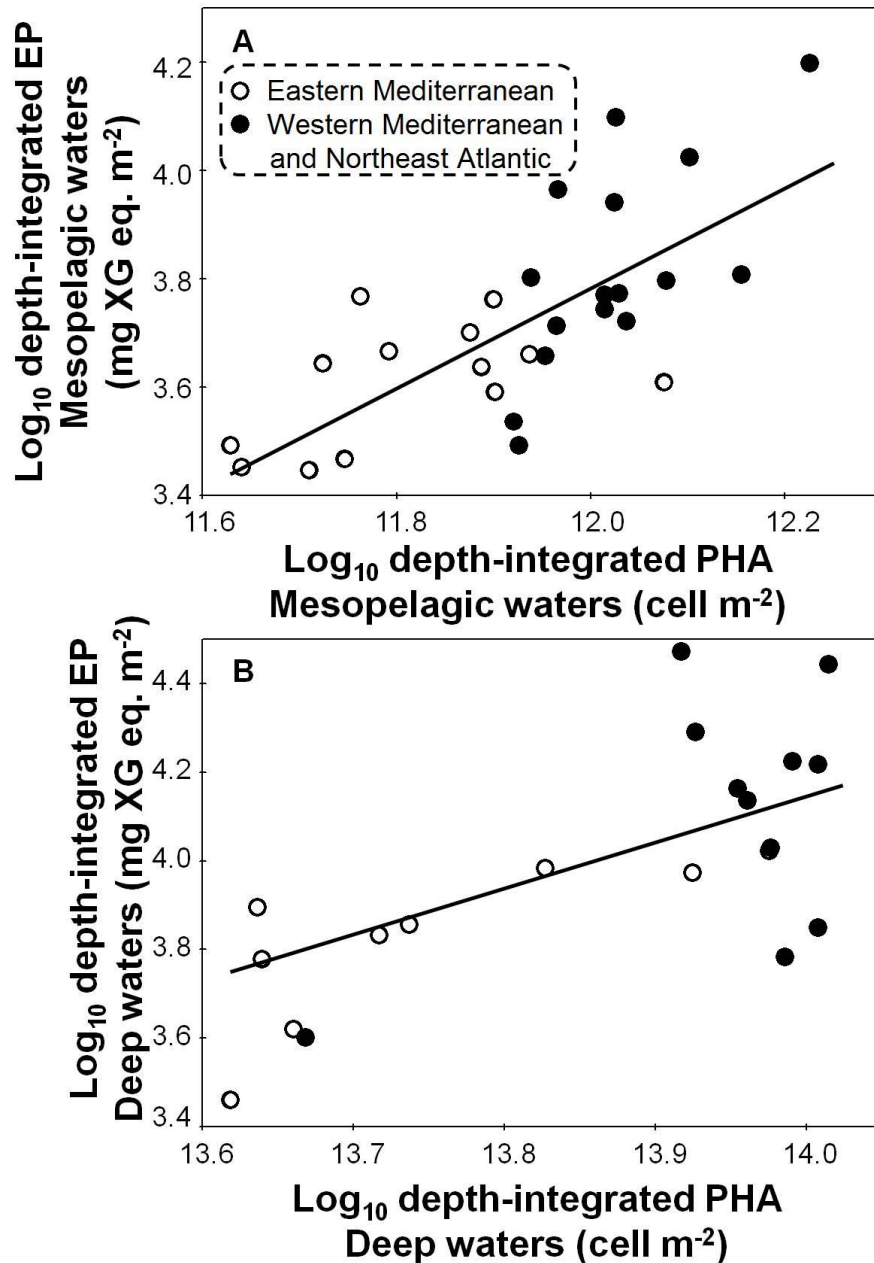


Figure 5. 8. Log-log scatterplot between (A) depth-integrated EP concentration (Meso-EP) and heterotrophic prokaryotic abundance (Meso-PHA) in the mesopelagic waters [$\text{Log}_{10} \text{Meso-EP} = 0.91 (\pm 0.17) \text{Log}_{10} \text{Meso-PHA} - 8.97 (\pm 2.39)$; $N = 29$, $r^2 = 0.51$ and $p\text{-value} < 0.00001$]; and (B) between depth-integrated EP distribution (Deep-EP) and heterotrophic prokaryotic abundance (DW-PHA) in waters below 1000 m depth [$\text{Log}_{10} \text{DW-EP} = 1.02 (\pm 0.18) \text{Log}_{10} \text{Deep-PHA} - 10.16 (\pm 2.52)$; $N = 24$, $r^2 = 0.59$ and $p\text{-value} < 0.00001$].

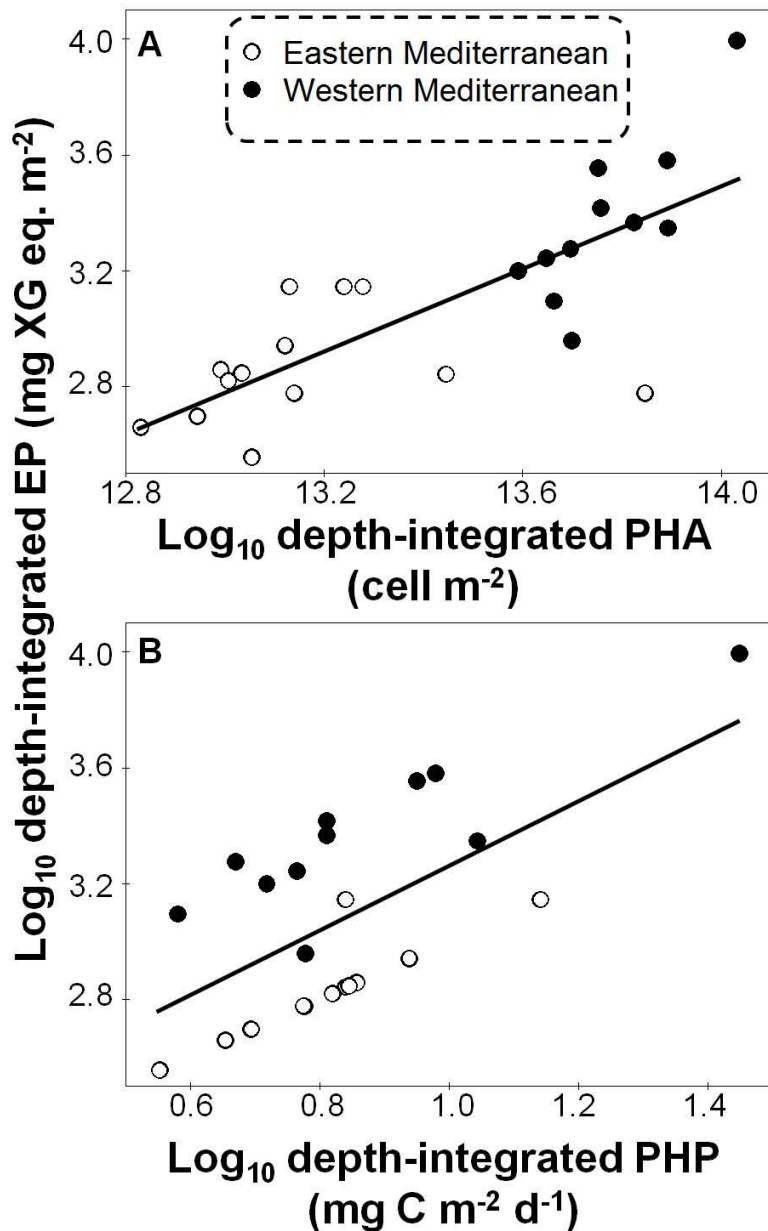


Figure 5. 9. Log-log scatterplot between (A) depth-integrated EP concentration (LIW-EP) and heterotrophic prokaryotic abundance (LIW-PHA) in the Levantine intermediate waters [Log_{10} LIW-EP = $0.71 (\pm 0.13) \text{Log}_{10}$ LIW-PHA - $6.39 (\pm 1.70)$; $N = 24$, $r^2 = 0.58$ and p -value < 0.0001]; and (B) between depth-integrated EP distribution (LIW-EP) and heterotrophic prokaryotic production (LIW-PHP) in the Levantine intermediate waters [Log_{10} LIW-EP = $1.12 (\pm 0.28) \text{Log}_{10}$ LIW-PHP + $2.14 (\pm 0.24)$; $N = 24$, $r^2 = 0.41$ and p -value < 0.001].

5.4.4. EP contribution to POC export

The estimations of EP fluxes at 200 m depth (EP F_{200}) ranged from 11.0 to 137.6 $\text{mg C m}^{-2} \text{d}^{-1}$ with an average of 31.1 $\text{mg C m}^{-2} \text{d}^{-1}$, or from 16.2 to 202.3 $\text{mg C m}^{-2} \text{d}^{-1}$ with an average of 45.7 $\text{mg C m}^{-2} \text{d}^{-1}$, depending on the conversion

factors used (Table 5.4.). EP transfer efficiencies from epipelagic to mesopelagic waters ($EP TE_{\text{epi-meso}}$) indicate that on average approximately half of the epipelagic EP, ~46%, reached mesopelagic waters (Table 5.4.). $EP F_{200}$ and $EP TE_{\text{epi-meso}}$ were higher in the Western Mediterranean and in the Northeast Atlantic basins than in the Eastern Mediterranean basin (Figure 5.10. A and B, respectively). The contribution of EP to the total POC fluxes at 200 m depth ($EP \%POC_{200m}$) averaged ca. 30 or 40 % of the total POC fluxes, with very constant values between basins (Figure 5.10. C).

Depth-integrated EP concentrations in the mesopelagic zone (Meso-EP) were positively related to $EP F_{200}$ [$n = 29$; $\text{Log}_{10} \text{ Meso-EP} = 0.50 (\pm 0.10) \text{ Log}_{10} EP F_{200} + 2.82 (\pm 0.16)$, $r^2 = 0.47$ and $p\text{-value} < 0.001$] (Figure 5.10. D) and $EP TE_{\text{epi-meso}}$ [$n = 29$; $\text{Log}_{10} \text{ Meso-EP} = 0.88 (\pm 0.13) \text{ Log}_{10} EP TE_{\text{epi-meso}} + 2.16 (\pm 0.22)$, $r^2 = 0.61$ and $p\text{-value} < 0.001$] (Figure 5.10. E). However, Meso-EP were inversely related to $EP \%POC_{200m}$ [$n = 29$; $\text{Log}_{10} \text{ Meso-EP} = -9.40 (\pm 1.92) \text{ Log}_{10} EP \%POC_{200m} + 18.89 (\pm 3.12)$, $r^2 = 0.47$ and $p\text{-value} < 0.01$] (Figure 5.10. F).

The estimations of EP fluxes at 1000 m depth ($EP F_{1000}$) ranged from 2.1 to 23.7 $\text{mg C m}^{-2} \text{ d}^{-1}$ with an average of 7.1 $\text{mg C m}^{-2} \text{ d}^{-1}$ or from 3.2 to 34.9 $\text{mg C m}^{-2} \text{ d}^{-1}$ with an average of 10.5 $\text{mg C m}^{-2} \text{ d}^{-1}$, depending on the conversion factors used (Table 5.4.). EP transfer efficiencies from mesopelagic to waters > 1000 m ($EP TE_{\text{meso-deep}}$) ranged from 46 to 201% with an average of 87% (Table 5.4.). The highest estimations for $EP F_{1000}$ were observed in the Northeast Atlantic Ocean, while the highest values for $EP TE_{\text{meso-deep}}$ were found in the Western Mediterranean (Figure 5.11. A and B, respectively). The $EP \%POC_{1000m}$ was very uniform at 1000 m depth (Figure 5.11. C). Unlike the mesopelagic zone, depth-integrated EP concentrations in the deep zone were not dependent on the fluxes at 1000 m ($EP F_{1000}$; Figure 5.11. D), or on the transfer efficiency at this depth ($EP TE_{\text{meso-deep}}$; Figure 5.11. E).

Table 5. 4. Average and range (in brackets) of the fluxes of exopolymer particles (EP) at 200 m and 1000 m (EP F_{200} and EP F_{1000}); the transfer efficiencies (TE) of exopolymer particles (EP) from epipelagic to mesopelagic waters (EP $TE_{epi-meso}$), from mesopelagic to deep waters > 1000 m depth (EP $TE_{meso-deep}$) and the contribution of EP to POC fluxes (EP %POC flux) at 200 m and 1000 m. The conversion factors 0.51 and 0.75 $\mu\text{g C per } \mu\text{g XG eq}$ were used to convert EP in xanthan equivalent into carbon units.

	EP F_{200} ($\text{mg C m}^{-2} \text{ d}^{-1}$)		EP TE epi-meso	EP %POC _{200m} (%)		EP F_{1000} ($\text{mg C m}^{-2} \text{ d}^{-1}$)		EP TE meso-deep	EP %POC _{1000m} (%)	
	0.51	0.75		0.51	0.75	0.51	0.75		0.51	0.75
Global	31.1 (11.0-137.6)	45.7 (16.2-202.3)	46 (24-125)	29 (26-30)	42 (39-44)	7.1 (2.1-23.7)	10.5 (3.2-34.9)	87 (46-201)	31 (29-33)	46 (43-48)
Eastern Med.	15.0 (11.0-25.0)	22.1 (16.2-36.8)	39 (24-55)	30 (29-30)	44 (42-44)	2.9 (2.1-4.9)	4.3 (3.2-7.2)	78 (48-137)	32 (31-33)	48 (46-48)
Western Med.	46.1 (22.9-137.6)	67.7 (33.8-202.3)	52 (25-125)	28 (26-29)	41 (39-43)	9.3 (5.6-16.2)	13.7 (8.3-23.8)	106 (48-201)	30 (30-31)	45 (43-46)
Northeast At.	39.8 (28.6-67.1)	58.5 (42.0-98.7)	55 (35-81)	28 (27-29)	42 (40.42)	14.1 (10.1-23.7)	20.7 (14.9-34.9)	71 (46-111)	30 (29-30)	44 (43-45)

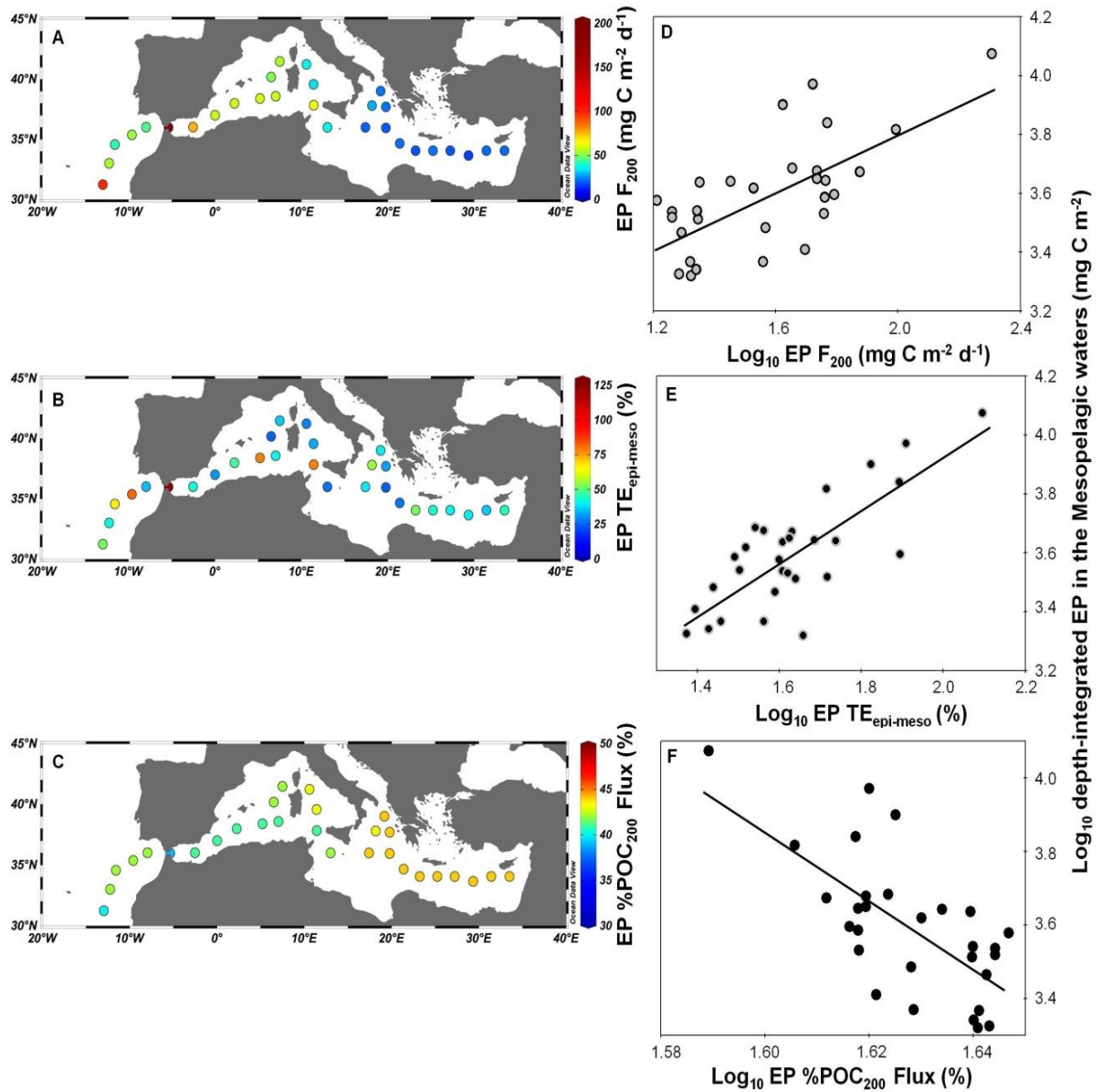


Figure 5. 10. Distribution along the Hotmix cruise track of the fluxes of exopolymer particles (EP) at 200 m ($EP F_{200}$) (A), EP transfer efficiencies from epipelagic to mesopelagic waters ($EP TE_{epi-meso}$) (B) and EP contribution to POC fluxes at 200 m ($EP \%POC_{200m}$) (C). Log-log relationships between depth-integrated EP in the mesopelagic waters and EP fluxes at 200 m (D), EP transfer efficiency from epipelagic to mesopelagic waters (E) and EP contribution to POC fluxes at 200 m (F). $EP F_{200}$ and depth integrated EP concentrations are calculated using the conversion factor of $0.75 \mu\text{g C per } \mu\text{g XG eq}$.

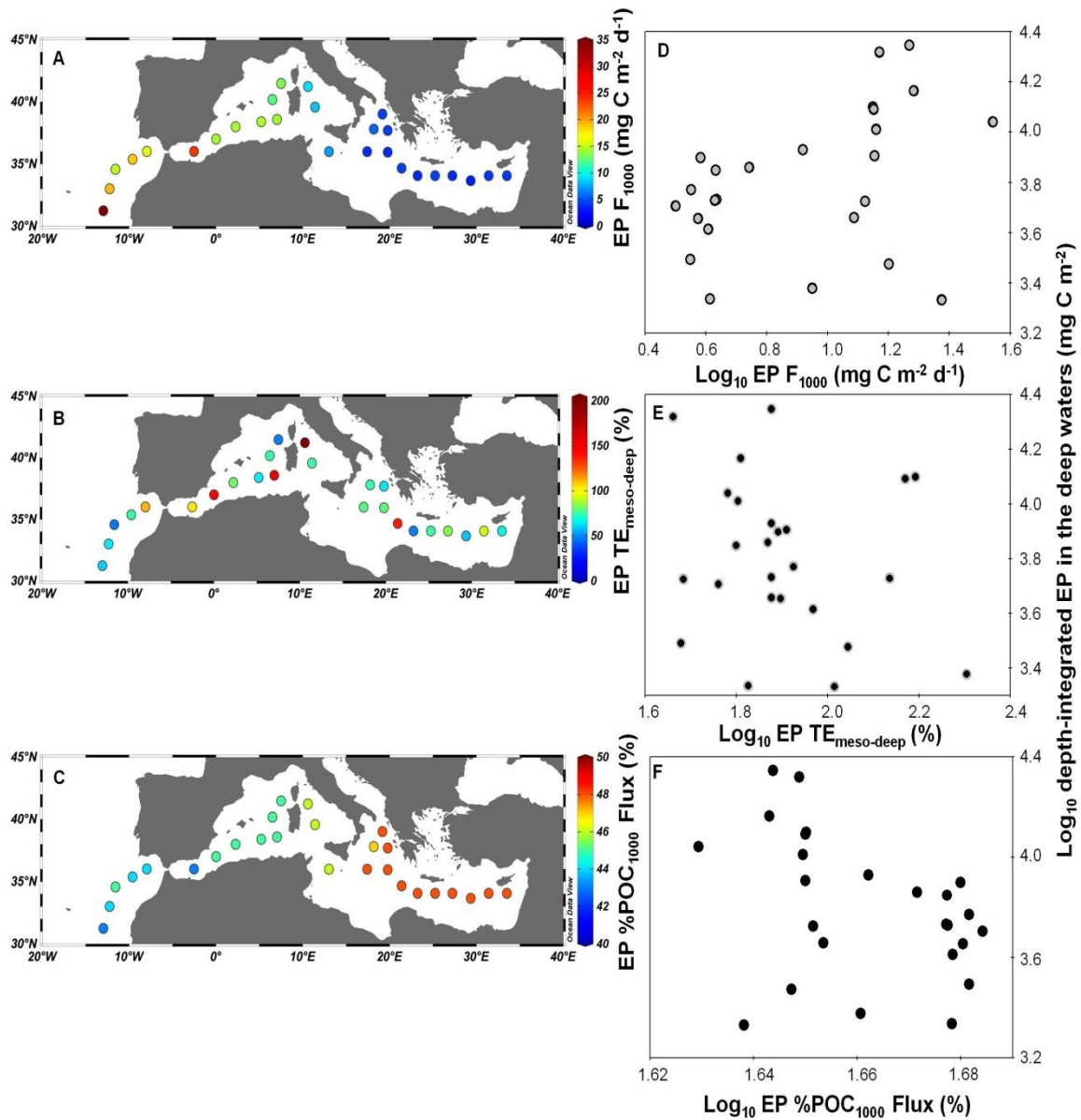


Figure 5. 11. Distribution along the Hotmix cruise track of the fluxes of exopolymer particles (EP) at 1000 m ($EP F_{1000}$) (A), EP transfer efficiencies from mesopelagic to deep (> 1000 m) waters ($EP TE_{meso-deep}$) (B) and EP contribution to POC fluxes at 1000 m ($EP \%POC_{1000m}$) (C). Log-log relationships between depth-integrated EP in the deep waters and the estimated EP fluxes at 1000 m (D), EP transfer efficiency from mesopelagic to deep waters (E) and EP contribution to POC fluxes at 1000 m (F). $EP F_{1000}$ and depth integrated EP concentrations are calculated using the conversion factor of 0.75 $\mu g C$ per $\mu g XG eq$.

5.5. Discussion

We observed very consistent vertical profiles from the surface to the seafloor along the Eastern-Western transect in the Mediterranean sea with higher exopolymer particles (EP) concentrations in the first meters of the water column with maxima just above the DCM depths, and low and very uniform values from 200 m to the bottom (Figures 5.2. and 5.3.). Stations close to the Strait of Gibraltar exhibited the highest EP concentrations both in the surface and deep waters (Figure 5.3.). EP concentrations in the surface waters appeared to be determined by primary producers and heterotrophic prokaryotes. Primary production, the ratio chlorophyll-*a* to pheopigments and, particularly, the picoeukaryote populations explained nearly 40 % of the EP variance depending on the different basins (Table 5.2.). Heterotrophic prokaryotes also affected significantly EP concentrations. Indeed, consistent (similar slopes among basins) and significant relationships between EP concentrations and heterotrophic prokaryotes were observed both in volumetric terms and depth-integrated (Table 5.2. and Figure 5.7.). The depth-integrated EP distribution showed a similar pattern to the surface EP distribution (Figure 5.4.) suggesting that the downward flux was a significant via of EP exports into the deep waters, especially important in the region of the Strait of Gibraltar. In addition, the robust relationships between the EP concentration and depth-integrated prokaryotic heterotrophic abundance (PHA) in the deep waters and, particularly, in the Levantine intermediate waters suggests a predominant particle-attached lifestyle in the deep waters. In addition, the *in situ* EP production in deep waters could explain the values of EP transfer efficiency higher than 100 % between the mesopelagic and the deep waters found in this study (Figure 5.11. B).

5.5.1. Exopolymer particles in surface waters

The range of EP concentrations (5.3 - 81.7 $\mu\text{g XG eq l}^{-1}$) obtained in this study was comparable to the values reported in a similar survey carried out by Ortega-Retuerta et al. (2010) in surface waters of the Mediterranean Sea, in the region of the Strait of Gibraltar (Prieto et al., 2006), at higher latitudes in the Northeast Atlantic Ocean (Engel, 2004; Harlay et al., 2009; Leblanc et al., 2009) in

the oligotrophic western North Pacific Ocean (Kodama et al., 2014), and in the Southern Ocean (Ortega-Retuerta et al., 2009). In contrast, higher epipelagic EP concentrations were reported in other studies conducted in the waters of the Strait of Gibraltar (Garcia et al., 2002), in the ultraoligotrophic eastern Mediterranean basin (Bar-Zeev et al., 2011) and in the Arctic Ocean (Wurl et al., 2011).

The EP profiles in the surface waters of our study showed EP maxima normally above the DCM depths, and particularly at subsurface depths. Several studies in open waters observed similar vertical profiles during the stratification period (Ortega-Retuerta et al., 2010; Prieto et al., 2006; Bar-Zeev et al., 2011; Wurl et al., 2011; Kodama et al., 2014; Mazuecos et al., Chapter 2). These previous studies and our observation thus establish that this vertical pattern is very common at least during thermal stratification.

EP concentrations at epipelagic depths appeared to be mostly related to both phytoplankton production and heterotrophic prokaryotes. Previous works reported that primary production, the photosynthetic production of dissolved and particulate organic carbon, was higher in the upper layer of the epipelagic waters and in the Western Mediterranean basin than in deeper layers below the DCM and in the Eastern Mediterranean basin (Moutin et al., 2002; López-Sandoval et al., 2011). Similarly to our results, Radic et al. (2005) observed that EP distribution could be explained by the ratio chlorophyll-*a* to pheopigments, which is a valuable indicator of the physiological status of the algal community. The higher the ratio, the higher the EP concentration was. The intense incident radiation and the low-nutrient conditions of phytoplankton in the surface waters of the Mediterranean Sea may also have affected the release of dissolved precursors, and consequently, EP production (Beauvais et al., 2003; Berman-Frank et al., 2007; Claquin et al., 2008). In fact, our study showed that EP concentrations were high in the upper layer of the epipelagic zone, commonly above the DCM depths, where the levels of inorganic nutrients were very low.

The EP distribution in the epipelagic waters showed high depth-integrated EP concentrations at stations with shallower DCM depths, normally in

the WM and NEA basins. Prieto et al. (2006) already observed that maximum EP concentrations were associated to regions such as upwellings or fronts with favorable growing conditions for the algal community, where inorganic nutrients input into the photic zone was higher, presenting shallower DCM depths. This phenomenon can thus have affected the net EP accumulation in the epipelagic waters since in regions with high algal biomass, they could exudate more dissolved precursors promoting more EP formation.

In relation to the phytoplankton groups, there were not consistent relationships between EP concentrations and specific phytoplankton groups in the epipelagic waters of all the basins (Table 5.2.), although significant regressions, with depth-integrated values and in volumetric terms, were obtained for picoeukaryotes. It is likely that picoeukaryotes could release significant quantities of dissolved organic precursors in the oligotrophic open ocean (Malinsky-Rushansky and Legrand, 1996) and, then, these precursors would aggregate abiotically producing EP (Arrigo et al., 2007). In fact, Lønborg et al. (2013) experimentally obtained a high EP production from *Micromonas pusilla*, a picoeukaryotic phytoplankter widely distributed in marine waters.

On the other hand, directly or indirectly through the use of phytoplankton exudates, heterotrophic prokaryotes were positive and significantly related to the EP pool, particularly in the Western Mediterranean Sea and North Eastern Atlantic basins (Table 5.2.). Previous studies already highlighted that the EP pool in the surface Mediterranean Sea is highly depended on the prokaryotic assemblages (Radic et al., 2003; Ortega-Retuerta et al., 2010; Bar-Zeev et al., 2011). Indeed, the log-log slopes between EP concentrations and PHA (Table 5.2.) obtained in our study are statistically similar to the slope of 0.48 ± 0.10 found by Ortega-Retuerta et al. (2010). The low explained variances found in this study, however, suggest that other abiotic processes such as turbulence (Pedrotti et al., 2010) or spontaneous assembly (Chin et al., 1998) are likely involved in EP production and storage.

5.5.2. Exopolymer particles in Levantine Intermediate and deep waters

The significant and robust correlations found among the depth-integrated EP values in the epipelagic and mesopelagic waters and deep waters (Figure 5.4.) indicate that, to some extent, there is a high EP proportion in waters below 200 m depth derived from the downward flux of epipelagic waters.

In the deep waters, EP concentrations were very uniform usually below 35 $\mu\text{g XG eq l}^{-1}$. Only a few studies have reported EP concentrations in the deep (> 200 m depth) Mediterranean Sea, sampling the mesopelagic waters in the Strait of Gibraltar (Prieto et al., 2006), the Eastern Mediterranean (Bar-Zeev et al., 2011) and the Northwest Mediterranean (Weinbauer et al., 2013). Only Bar-Zeev et al. (2011) in the Eastern basin observed higher values than the EP range obtained in this study.

EP concentration in the deep waters was predicted by PHA, with depth-integrated data and in volumetric terms, particularly in the Levantine intermediate waters (Table 5.3. and Figure 5.8.). This indicates that heterotrophic prokaryotes in the deep sea might be adapted to a particle-attached lifestyle (Lauro and Bartlett, 2008; Herndl and Reinthaler, 2013). In fact, Weinbauer et al. (2013) in the twilight zone of the Northwestern Mediterranean sea also observed significant relationships between heterotrophic prokaryotes and EP concentrations. Although conditions in the deep waters are less favorable than in the epipelagic zone, prokaryotes in the deep waters may also release gel-forming polysaccharides generating suspended exopolymeric aggregates (Bar-Zeev et al., 2012; Mazuecos et al., Chapter 3 and Chapter 6).

Other processes such as, for instance, the abiotic aggregation and lateral transport could also introduce EP into the deep Mediterranean Sea (Martin et al., 2011; Bar-Zeev et al., 2011; Gogou et al., 2014). However, it is little probable that abiotic aggregation, that is an exopolymer-density dependent process (Verdugo et al., 2008; Burd and Jackson, 2009; Verdugo, 2012), originates great quantities of EP below 200 m depth since EP precursor are likely scant below 100 m depth.

Mineralization of a high fraction of the particulate matter pool would explain the severe decrease of EP during this transit towards the deep waters

(Buesseler et al., 2007). In our study, we calculated, on average, about 46 % transfer efficiency (from epipelagic to mesopelagic waters) of EP in the flux attenuation zone. Despite the limitations related to the used of satellite derived primary production and the attenuation flux coefficients in the functions that predict EP remineralization with depth, our estimated downward EP fluxes are reasonable predictions, similar to those observed in other ocean basins (Yokokawa et al., 2013; Mazuecos et al., Chapter 2). Our estimations are comparable to the measured EP fluxes at different intermediate depths reported in other oceanic regions by Passow (2002) (from 7 to 70 mg C m⁻² d⁻¹), Ramaiah et al. (2005) (from 29 to 62 mg C m⁻² d⁻¹), Waite et al. (2005) (up to 25 mg C m⁻² d⁻¹), Reigstad and Wassmann (2007) (up to 390 mg C m⁻² d⁻¹), Martin et al. (2011) (from undetectable to 120 mg C m⁻² d⁻¹) or Mazuecos et al. (Chapter 2) for the global ocean. We detected the highest EP fluxes in the region of the Strait of Gibraltar suggesting that EP export, and therefore, POC export to deep waters is very significant in this dynamic region.

The estimated EP fluxes at 200 m depth (EP F₂₀₀) significantly predicted the depth-integrated EP concentrations in the mesopelagic waters (Figure 5.10D). By contrast, the estimated EP fluxes at 1000 m (EP F₁₀₀₀) did not predict the *in situ* depth-integrated EP concentrations in the deep waters (Figure 5.11D). This fact and the elevated transfer efficiencies (punctually > 100 %) from mesopelagic to deep waters suggest that other alternative sources would introduce EP into the deep Mediterranean Sea. Lateral EP inputs at different depths, caused by the proximity of continental margins and boundary currents in this semi-enclosed sea (Gogou et al., 2014), and *de novo* EP synthesis by heterotrophic prokaryotes (Mazuecos et al., Chapter 3 and Chapter 6) would mostly explain this imbalance found in our study for the deep waters. The absence of relationship might also be produced by intermittent downward fluxes caused by the dynamics of the pycnocline. Martin and Miquel (2010), in the Northwest Mediterranean Sea, observed an intense downward flux of mucilaginous aggregates after a strong stratification period. This flux was preceded by a very sharp increase of sea surface temperature accumulating high quantities of EP-enriched aggregates

over the pycnocline, and when the stratification was broken by a storm, there was a massive downward flux of these mucous particles to the deep waters. This process might thus be repetitive in the stations sampled in our study and the downward EP flux would occur when the pycnocline relaxed (as in mixing periods).

Assuming constant rates over the year and with the most conservative conversion factor ($0.51 \mu\text{g C per } \mu\text{g XG eq}$), the annual global rates of EP F_{200} and EP F_{1000} in our study would be lower in the EM basin (on average, 5.5 and $1.1 \text{ g C m}^{-2} \text{ yr}^{-1}$, respectively) than in the WM basin (16.8 and $3.4 \text{ g C m}^{-2} \text{ yr}^{-1}$, respectively) or in the NEA Ocean (14.5 and $5.1 \text{ g C m}^{-2} \text{ yr}^{-1}$, respectively). Similarly, Gogou et al. (2014) observed approximately one order of magnitude lower POC fluxes in the EM basin than in the WM basin. The differences of EP fluxes among ocean basins may be attributed to the contrasting planktonic community structure in the ocean basins. Planktonic communities dominated by picoautotrophs, as in the ultraoligotrophic EM basin, would not be subjected to direct sedimentation, and grazing by nano- and microzooplankton or organic matter mineralization by heterotrophic organisms in the microbial food web, would ultimately retain carbon in surface layers (Boyd and Trull, 2007; Buesseler and Boyd, 2009).

Other environmental parameters, such as water temperature in the attenuation flux zone, would affect the downward EP fluxes decreasing them in the warmer stations (Martín-Cuadrado et al., 2007; Marsay et al., 2015; Mazuecos et al., 2015). We observed that warmer stations (considering the median temperature in the upper 200 m and 1000 m) were located in the EM basin and inverse correlations between downward EP fluxes (EP F_{200} and F_{1000}) and median temperatures were observed (Figure 5.12.). This suggests that the EP downward transit would be greater in colder stations of the WM basin and NEA Ocean than in the EM basin.

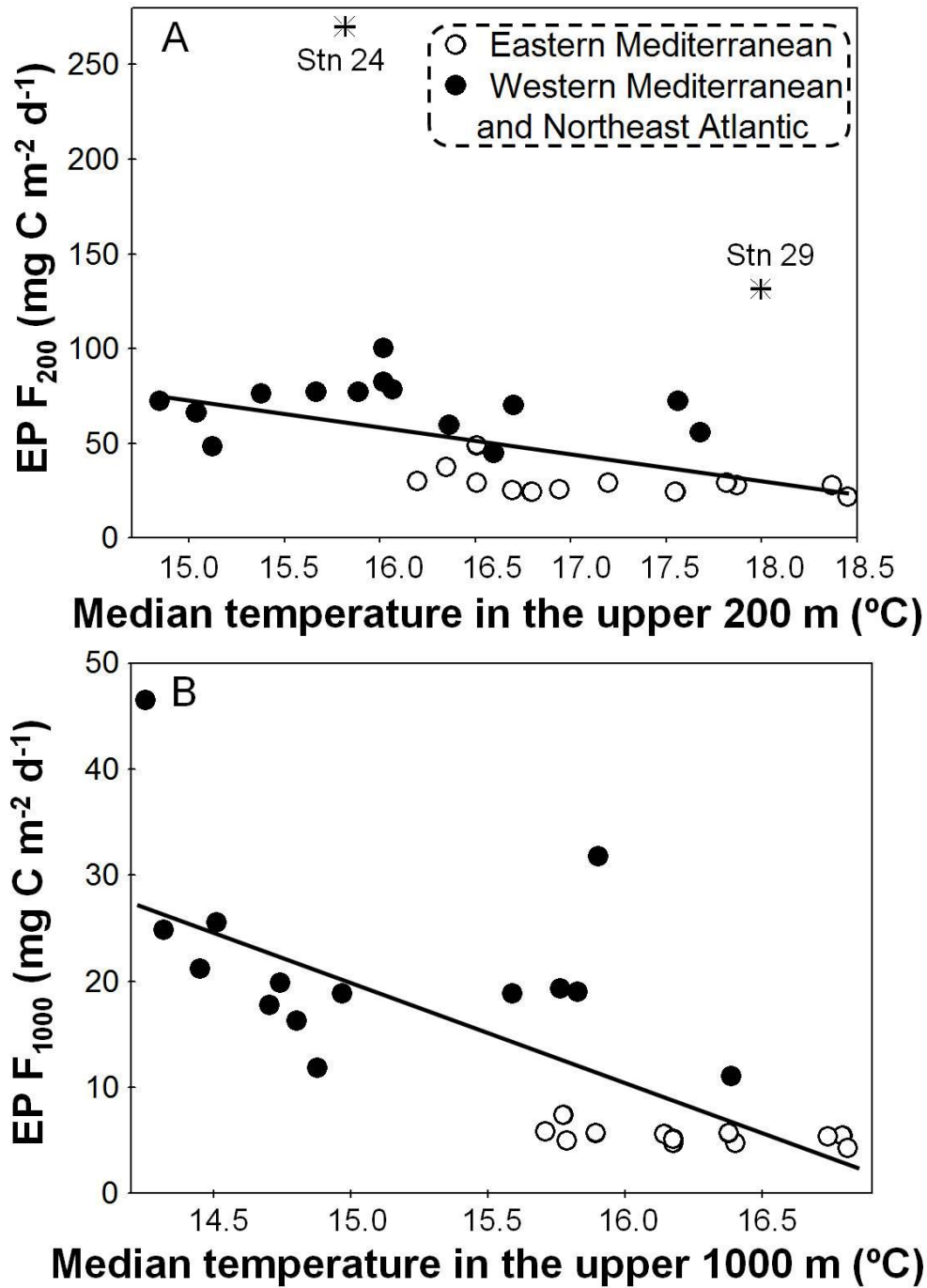


Figure 5. 12. Log-log scatterplot between (A) median temperature in the upper 200 m depth and fluxes of exopolymer particles at 200 m depth ($EP F_{200}$), solid line correspond to the significant regression excluding stations (stn) 24 and 29 (asterisks): $EP F_{200} = -14.34 (\pm 3.86) \text{ Temperature} + 288.53 (\pm 64.20)$; $N = 27$, $r^2 = 0.36$ and $p\text{-value} < 0.01$; and between (B) median temperature in the upper 1000 m depth and fluxes of exopolymer particles at 1000 m depth ($EP F_{1000}$): $EP F_{1000} = -9.29 (\pm 1.83) \text{ Temperature} + 159.13 (\pm 28.64)$; $N = 26$, $r^2 = 0.52$ and $p\text{-value} < 0.0001$.

Finally, our estimations (using the most conservative conversion factor of 0.51) led to an overall EP contribution of, on average, ~30 % to the POC fluxes at 200 and 1000 m depths (Table 5.4.), which is in accordance with the overall estimation of 30 % in relation to the total POC flux predicted by Passow et al. (2002) and the percentages (on average, ~22% at 200 m depth and ~39% at 1000 m) reported by Mazuecos et al (Chapter 2) for the global ocean.

Acknowledgements

This research work is a contribution to the coordinated project HOTMIX (CTM2011-30010-C02/MAR). We thank our scientific colleagues as well as the technical staff and crew members on board the B/O Sarmiento de Gamboa, for their support in the field sampling during the cruise. IPM was supported by a JAE Pre-doc fellowship, from the Spanish National Research Council (CSIC) and the BBVA Foundation, Spain.

5.6. References

- Allredge A. L., Passow U., Logan B. E. 1993. The abundance and significance of a class of large, transparent organic particles in the ocean. *Deep-Sea Research I*, 40 (6): 1131 – 1140.
- Antia, A. N., Koeve W., Fischer G., Blanz T., Schulz-Bull D., Jan Scholten T. M., Neuer S., Kremling K., Kuss J., Rolf Peinert T. M., Hebbeln D., Bathmann U., Conte M., Fehner U., Zeitzsche B. 2001. Basin-wide particulate carbon flux in the Atlantic Ocean: Regional export patterns and potential for atmospheric carbon sequestration, *Global Biogeochemical Cycles*, 15: 845 – 862.
- Arrigo K. R. 2007. Carbon cycle: Marine manipulations. *Nature*, 450: 491 – 492.
- Azetsu-Scott K., Passow U. 2004. Ascending marine particles: Significance of transparent exopolymer particles (TEP) in the upper ocean. *Limnology and Oceanography*, 49(3): 741 – 748.
- Bar-Zeev E., Berman T., Rahav E., Dishon G., Herut B., Kress N. and Berman-Frank I. 2011. Transparent exopolymer particle (TEP) dynamics in the eastern Mediterranean sea. *Marine Ecology Progress Series*, 431: 107 – 118.
- Bar-Zeev E., Berman-Frank I., Stambler N., Vazquez E. D., Zohary T., Capuzzos E., Meeder E., Suggests D. J., Iluz D., Dishon G. and Berman T. 2009. Transparent exopolymer particles (TEP) link phytoplankton and bacterial production in the Gulf of Aqaba. *Aquatic Microbial Ecology*, 56: 217 – 225.
- Bar-Zeev E., Berman-Frank I., Girshevitz O., Berman T. 2012. Revised paradigm of aquatic biofilm formation facilitated by microgel transparent exopolymer particles. *PNAS*, 109 (23): 9119 – 9124.
- Beauvais S., Pedrotti M. L., Villa E., Lemeé. 2003. Transparent exopolymer particle (TEP) dynamics in relation to trophic and hydrological conditions in the NW Mediterranean Sea. *Marine Ecology Progress Series*, 262: 97 - 109.
- Berger W. H., Wefer G. 1990. Export production: Seasonality and intermittency, and paleoceanographic implications. *Paleogeogr. Paleoclimatol. Paleocol.* 89: 245 – 254. doi:10.1016/0031-0182(90)90065-F
- Berman-Frank I., Rosenberg G., Levitan O., Haramaty L., Mari X. 2007. Coupling between autocatalytic cell death and transparent exopolymeric particle production in the marine cyanobacterium *Trichodesmium*. *Environmental Microbiology*, 9(6): 1415 – 1422.
- Boyd P. W., Trull T. W. 2007. Understanding the export of biogenic particles in oceanic waters: is there consensus? *Prog. Oceanogr.* 72: 276 – 312.
- Burd A. B., Jackson G. A. 2009. Particle Aggregation. *Annual review of Marine Science*, 1: 65-90.
- Buesseler K. O., Boyd P. W. 2009. Shedding light on processes that control particle export and flux attenuation in the twilight zone of the open ocean. *Limnol. Oceanogr.*, 54 (4): 1210 – 1232.
- Buesseler, K. O., Lamborg C. H., Boyd P. W., Lam P J., Trull T. W., Bidigare R. R., Bishop K. B., Casciotti K. L., Dehairs F., Elskens M., Honda M., Karl D. M., Siegel D. A., Silver M. W., Steinberg D. K., Valdes J., Van Mooy B., Wilson S. 2007. Revisiting carbon flux through the ocean's twilight zone. *Science*, 316: 567 – 570.
- Chin W.-C., Orellana M. V., Verdugo P. 1998. Spontaneous assembly of marine dissolved organic matter into polymer gels. *Nature*, 391: 568 – 572.
- Claquin P., Probert I., Lefebvre S., Veron B. 2008. Effects of temperature on photosynthetic parameters and TEP production in eight species of marine microalgae. *Aquatic Microbial Ecology*, 51: 1 – 11.
- Corzo A., Morillo J. A., Rodríguez S. 2000. Production of transparent exopolymer particles (TEP) in cultures of *Chaetoceros calcitrans* under nitrogen limitation. *Aquatic Microbial Ecology*, 23: 63 – 72.
- Danovaro R., Umani S. F., Pusceddu A. 2009. Climate Change and the Potential Spreading of Marine Mucilage and Microbial Pathogens in the Mediterranean Sea. *Plos One*, 4(9): e7006.
- Engel A. 2000. The role of transparent exopolymer particles (TEP) in the increase in apparent particle stickiness (a) during the decline of a diatom bloom. *Journal of Plankton Research*, 22 (3): 485 – 497.

- Engel A. 2004. Distribution of transparent exopolymer particles (TEP) in the northeast Atlantic Ocean and their potential significance for aggregation processes. *Deep-Sea Research I*, 51: 83 – 92.
- Engel A., Passow U. 2001. Carbon and nitrogen content of transparent exopolymer particles (TEP) in relation to their Alcian Blue adsorption. *Marine Ecology Progress Series*, 219: 1 – 10.
- Gasol J. M., del Giorgio P. A. 2000. Using flow cytometry for counting natural planktonic bacteria and understanding the structure of planktonic bacterial communities. *Scientia Marina*, 64: 197 – 224.
- Gascard J.C., Richez C. Water masses and circulation in the Western Alboran Sea and in the Straits of Gibraltar. *Prog. Oceanogr.* 1985;15:157–216. doi: 10.1016/0079-6611(85)90031-X.
- García C. M., Prieto L., Vargas M., Echevarría F., García-LaFuente J., Ruíz J., Rubín J. P. 2002. Hydrodynamics and the spatial distribution of plankton and TEP in the Gulf of Cadiz. (SW Iberian Peninsula). *Journal of Plankton Research*, 24: 817 – 833.
- Gogou A., Sanchez-Vidal A., de Madron X. D., Stavrakakis S., Calafat A. M., Stabholz M., Psarra S., Canals M., Heussner S., Stavrakaki I., Papathanassiou E. 2014. Carbon flux to the deep in three open sites of the Southern European Seas (SES). *Journal of Marine Systems*, 135: 170-179.
- Harlay J., De Bodt C., Engel A., Jansen S., d’Hoop Q., Piontek J., Van Oostende N., Groomd S., Sabbe K., Chou L. 2009. Abundance and size distribution of transparent exopolymer particles (TEP) in a coccolithophorid bloom in the northern Bay of Biscay. *Deep-Sea Research I*, 56: 1251 – 1265.
- Herndl G. J., Reinthaler T. 2013. Microbial control of the dark end of the biological pump. *Nature Geoscience*, 6 (9): 718–724.
- Hong Y., Smith W. O., White A.-M. 1997. Studies of transparent exopolymer particles (TEP) produced in the Ross Sea (Antarctica) and by *Phaeocystis antarctica* (Prymnesiophyceae). *Journal of Phycology*, 33: 368 – 376.
- Kirchman D. L., Kneess E., Hodson R. E. 1985. Leucine incorporation and its potential as a measure of protein synthesis by bacteria in natural aquatic systems. *Applied Environmental Microbiology*, 49: 599 - 607.
- Kodama T., Kurogi H., Okazaki M., Jinbo T., Chow S., Tomoda T., Ichikawa T. and Watanabe T. 2014. Vertical distribution of transparent exopolymer particle (TEP) concentration in the oligotrophic western tropical North Pacific. *Marine Ecology Progress Series*, 513: 29-37.
- Lacombe H., Richez C. The Regime of the Strait of Gibraltar. In: Nihoul J.C.J., editor. *Hydrodynamics of Semi-Enclosed Seas*. Elsevier Scientific; Amsterdam, The Netherlands: 1982. pp. 13–73.
- Lampitt R. S., Achterberg E. P., Anderson T. R., Hughes J. A., Iglesias-Rodriguez M. D., Kelly-Guerreyn B. A., Lucas M., Popova E. E., Sanders R., Shepherd J. G., Smythe-Wright D. and Yool A. 2008. Ocean fertilization: a potential means of geoengineering? *Phil. Trans. R. Soc. A*, 366: 3919 – 3945.
- Lauro M. F., Barlett D. H. 2008. Prokaryotic lifestyles in deep sea habitats. *Extremophiles*, 12:15–25.
- Leblanc K., Hare C. E., Feng Y., Berg G. M., DiTullio G. R., Neeley A., Benner I., Sprengel C., Beck A., Sanudo-Wilhelmy S. A., Passow U., Klinck K., Rowe J. M., Wilhelm S. W., Brown C. W., Hutchins D. A. 2009. Distribution of calcifying and silicifying phytoplankton in relation to environmental and biogeochemical parameters during the late stages of the 2005 North East Atlantic Spring Bloom. *Biogeosciences*, 6: 2155 – 2179.
- Lopez-Sandoval D. C., Fernández A., Marañón E. 2011. Dissolved and particulate primary production along a longitudinal gradient in the Mediterranean Sea. *Biogeosciences*, 8: 815 – 825.
- Lønborg C., Middelboe M. and Brussaard C. P. D. 2013. Viral lysis of *Micromonas pusilla*: impacts on dissolved organic matter production and composition. *Biogeochemistry*, DOI 10.1007/s10533-013-9853-1.
- Malinsky-Rushansky N. Z., Legrand. C. 1996. Excretion of dissolved organic carbon by phytoplankton of different sizes and subsequent bacterial uptake. *Marine Ecology Progress Series* 132: 249 - 255.

- Mari X., Kjørboe T. 1996. Abundance, size distribution and bacterial colonization of transparent exopolymeric particles (TEP) during spring in the Kattegat. *Journal of plankton Research*, 18(6): 969-986.
- Marsay C. M., Sanders R. J., Henson S. A., Pabortsava K., Achterberg E. P., Lampitt R. S. 2015. Attenuation of sinking particulate organic carbon flux through the mesopelagic ocean. *PNAS*, 112(4): 1089 – 1094.
- Martín-Cuadrado A.-B., López-García P., Alba J.-C., Moreira D., Monticelli L., Strttmatter A., Gottschalk G., Rodríguez-Valera. 2007. Metagenomics of the Deep Mediterranean, a Warm Bathypelagic Habitat. *PLoS ONE*, 2(9): e914. doi:10.1371/journal.pone.0000914
- Martin J., Miquel J.-C. 2010. High downward flux of mucilaginous aggregates in the Ligurian Sea during summer 2002: similarities with the mucilage phenomenon in the Adriatic Sea. *Marine ecology*, 31 (3): 393 - 406.
- Martin J. H., Knauer G. A., Karl D. M., Broenkow W. W. 1987. Vertex-carbon cycling in the Northeast Pacific. *Deep-Sea Research*, 34: 267-285.
- Martin P., Lampitt R. S., Perry M. J., Sanders R., Lee C., D'Asaro E. 2011. Export and mesopelagic particle flux during a North Atlantic spring diatom bloom. *Deep-Sea Research I*, 58: 338 – 349.
- Moutin T., Raimbault P. 2002. Primary production, carbon export and nutrients availability in western and eastern Mediterranean Sea in early summer 1996 (MINOS cruise). *J. Marine Syst.*, 33– 34: 273 – 288.
- Mazuecos I. P., Arístegu J., Vázquez-Domínguez E., Ortega-retuerta E., Gasol J. M., Reche I. 2015. Temperature control of microbial respiration and growth efficiency in the mesopelagic zone of the South Atlantic and Indian Oceans. *Deep Sea Research I*, 95: 131 – 138.
- Ortega-Retuerta E., Duarte C. M., Reche I. 2010. Significance of Bacterial Activity for the distribution and dynamics of transparent exopolymer particles in the Mediterranean sea. *Microbial Ecology*, 59: 808 – 818.
- Ortega-Retuerta E., Reche I., Pulido-Villena E., Agusti S., Duarte C. M. 2009. Uncoupled distributions of transparent exopolymer particles (TEP) and dissolved carbohydrates in the Southern Ocean. *Marine Chemistry*, 115: 59-65
- Parsons T. R., Maita Y., Lalli C. M. 1984. *A Manual of Chemical and Biological Methods for Seawater Analysis*. Pergamon Press, Oxford, p.p 173.
- Passow U. 2002. Transparent exopolymer particles (TEP) in aquatic environments. *Progress in Oceanography*, 55: 287 – 333.
- Passow U., Alldredge A. L. 1995. A die-binding assay for the spectrophotometric measurement of transparent exopolymer particles (TEP). *Limnology and Oceanography*, 40 (7): 1326 - 1335.
- Passow U., Carlson C. A. 2012. The biological pump in a high CO₂ world. *Marine Ecology Progress Series*, 470: 249 – 271.
- Pedrotti M.L., Peters F., Beauvais S., Vidal M., Egge J., Jacobsen A., Marrasé C. 2010. Effects of nutrients and turbulence on the production of transparent exopolymer particles: a mesocosm study. *Marine ecology Progress Series*, 419: 57-69.
- Prieto L., Navarro G., Cózar A., Echebarría F., García C. M. 2006. Distribution of TEP in the euphotic and upper mesopelagic zones of the Southern Iberian coasts. *Deep-Sea Research II*, 53: 1314 – 1328.
- Radic T., Kraus R., Fuks D., Radic J., Pecar O. 2005. Transparent exopolymeric particles' distribution in the northern Adriatic and their relation to microphytoplankton biomass and composition. *Science of the Total Environment*, 353: 151 -161.
- Radic T., Radic J., Najdek M., Fuks D., Blazina M. 2003. Potential of the northern Adriatic bacterioplankton for the reduction of transparent exopolymer particles. *Periodicum Biologorum*, 105(4): 381 - 387.
- Ramaiah N., Takeda S., Furuya K., Yoshimura T., Nishioka J., Aono T., NOjiri Y., Imai K., Kudo I., Saito H., Tsuda A. 2005. Effect of iron enrichment on the dynamics of transparent exopolymer particles in the western subarctic Pacific. *Progress in Oceanography*, 64: 253 – 261.
- Reigstad M., Wassmann P. 2007. Does *Phaeocystis* spp. contribute significantly to vertical export of organic carbon? *Biogeochemistry*, 83: 217 – 234.

- Sanchez-Vidal A., Calafat A., Canals M., Frigola J., Fabres J. 2005. Particle fluxes and organic carbon balance across the Eastern Alboran Sea (SW Mediterranean Sea). *Cont. Shelf Res.* 25: 609–628.
- Simon M., Azam F. 1989. Protein content and protein synthesis rates of planktonic marine bacteria. *Marine Ecology-Progress Series*, 51: 201–213.
- Smith D. C., Azam F. 1992. A simple economical method for measuring bacterial protein synthesis rates in seawater using ^3H leucine. *Marine Microbial Food Webs*, 6: 107–114.
- Stavarakakis, S., Gogou, A., Krasakopoulou, E., Karageorgis, A.P., Kontoyiannis, H., Rousakis, G., Velaoras, D., Perivoliotis, L., Kambouri, G., Stavrakaki, I., Lykousis, V., 2013. Downward fluxes of sinking particulate matter in the deep Ionian Sea (NESTOR site), Eastern Mediterranean: seasonal and interannual variability. *Biogeosci. Discuss.* 10: 591–641.
- Thingstad T. F., Krom M. D., Mantoura R. F. C., Flaten G. A. F., Groom S., Herut B., Kress N., Law C. S., Pasternak A., Pitta P., Psarra S., Rassoulzadegan F., Tanaka T., Tselepides A., Wassman P., Woodward E. M. S., Wexels Riser C., Zodiatis G., Zohary T. 2005.
- Verdugo P. 2012. Marine Microgels. *Annual Review of Marine Science*, 4: 375–400.
- Verdugo P., Orellana M. V., Chin W.-C., Petersen T. W., van den Eng G., Benner R., Hedges J. I. 2008. Marine biopolymer self-assembly: implications for carbon cycling in the ocean. *Faraday Discussions*, 139: 393–398.
- Verdugo P., Alldredge A. L., Aam F., Kirchman D. L., Passow U., Santschi P. H. 2004. The oceanic gel phase: a bridge in the DOM-POM continuum. *Marine Chemistry*, 92: 67–85.
- Weinbauer M. G., Liu J., Motegi C., Maier C., Pedrotti M. L., Dai M., Gattuso J. P. 2013. Seasonal variability of microbial respiration and bacterial and archaeal community composition in the upper twilight zone. *Aquatic Microbial Ecology*, 71: 99–115.
- Wurl O., Miller L., Svein S. 2011. Production and fate of transparent exopolymer particles in the ocean. *Journal of Geophysical Research*, 116: 1–16.
- Yentsch C. S., Menzel D. W. 1963. A method for the determination of phytoplankton chlorophyll and phaeophytin by fluorescence. *Deep-Sea Research*, 10: 221–231.
- Yokokawa T., Yang Y., Motegi C., Nagata T. 2013. Large-scale geographical variation in prokaryotic abundance and production in meso- and bathypelagic zones of the central Pacific and Southern Ocean. *Limnology and Oceanography*, 58 (1): 61–73.
- Zúñiga, D., Calafat, A., Sanchez-Vidal, A., Canals, M., Price, B., Heussner, S., Miserocchi, S., 2007. Particulate organic carbon budget in the open Algero-Balearic Basin (Western Mediterranean): assessment from a one-year sediment trap experiment. *Deep-Sea Research I*, 54: 1530–1548.

Chapter 6:

*High heterotrophic production of
exopolymer particles in the Levantine
Intermediate Waters of the
Mediterranean Sea*



Abbreviated title: **Prokaryotic EP production in the Mediterranean Sea**

6.1. Abstract

Heterotrophic prokaryotes are known to have a relevant role in exopolymer particle (EP) formation, as promoters of recurrent mucilage events, particularly in the Mediterranean Sea. We experimentally tested the influence of inorganic and organic nutrients on EP prokaryotic production using seawater from different depths obtained from the Western (WM) and Eastern Mediterranean (EM) basins. A total of four experiments were performed, one with surface waters of the EM (EM-SW), two experiments with Levantine Intermediate Waters (LIW): one in the EM basin (EM-LIW) and another in the WM basin (WM-LIW), and another one with deep waters of the WM (WM-DW). Each experiment included a control, without nutrient additions, and treatments with organic (glucose) and/or inorganic (phosphorous and nitrogen) nutrient additions. The EP production rates in the EM-SW experiment ranged from 7.7 to 48.9 $\mu\text{g XG eq. L}^{-1} \text{ day}^{-1}$ and between 0.7 and 56.2 $\mu\text{g XG eq. L}^{-1} \text{ day}^{-1}$ in the WM-DW experiment, yet the highest values were measured in the LIW experiments, varying from 16.4 to 177.6 $\mu\text{g XG eq. L}^{-1} \text{ day}^{-1}$ in the EM-LIW experiment and from 122.7 to 232.2 $\mu\text{g XG eq. L}^{-1} \text{ day}^{-1}$ in the WM-LIW. In general, EP production was higher in treatments with nutrient additions, particularly with glucose addition, except in the WM-LIW experiment. These experiments suggest that the bioavailability of nutrients, particularly highly labile organic substrates, regulates prokaryotic EP production in the environment. The *in situ* EP production was estimated using the experimental rates and the *in situ* heterotrophic prokaryotic abundance. These *in situ* rates were consistently higher in the WM basin than in the EM basin leading to shorter EP residence times. It is noteworthy that the residence times calculated for the LIW (between 230 and 240 days) were the shortest values indicating that the EP pool in this layer is highly dynamic.

6.2. Introduction

Heterotrophic prokaryotes release extracellular polymers during their growth, producing mucous capsules (Decho et al., 1990), and modify the stickiness properties of the organic matter in the environment (Rochelle-Newall et al., 2010; Van Oostende et al., 2013), contributing to POM formation. In the POM pool, exopolymer particles (EP) are a class of mucous POM generated by autotrophic and heterotrophic microorganisms, actively involved in aggregation processes (Passow, 2002). EP provide the interstitial matrix for formation of larger ballasted-aggregates (known as “*marine snow*”) that fuel carbon export to the seafloor (De La Rocha and Passow, 2007; Passow and Carlson, 2012).

Environmental parameters, such as nutrient availability, affect the structure and growth of heterotrophic prokaryotic assemblages (Church, 2008), which in turn determine the contribution of prokaryotes to POM, including EP, formation. In surface waters, inorganic nutrient limitation might result in enhanced EP accumulation since autotrophic and heterotrophic planktonic communities are both affected. It is known that algal secretion of fresh exudates increases under nutrient limitation or light stress (Berman-Frank and Dubinsky, 1999; Corzo et al., 2000; Pedrotti et al., 2010). In addition, the availability of fresh exudates for heterotrophic microbial growth can promote the persistence of the EP pool either modifying the stickiness properties of the algal exudates (Rochelle-Newall et al., 2010; Van Oostende et al., 2013) or reducing the efficiency of organic matter decomposition, including that of the particulate material, which is observed under inorganic nutrient limitation (Obernosterer and Herndl, 1995; del Giorgio and Cole, 1998; Zoppini et al., 1998; Kritzberg et al., 2010). In contrast to surface waters, there is no information on the role of heterotrophic prokaryotes on EP formation in the dark ocean (Mazuecos et al. Chapters 2 and 5). The deep waters are enriched in inorganic nutrients but the microbial metabolism is highly dependent on the downward flux of organic carbon from surface waters (Aristegui et al., 2009). Mesopelagic prokaryotes (living between 200 and 1000 m depth) are apparently well adapted to a particle-attached lifestyle (Baltar et al., 2009; Herndl and Reinthaler, 2013). As for planktonic communities in surface or

coastal waters, changes in element stoichiometry (Radic et al., 2006; Engel et al., 2015) or the nature of the available organic matter (Ogawa et al., 2001; Koch et al., 2014) are known to affect the prokaryotic production of POM and EP, but a clear model of how this is regulated has not been presented. Therefore, it is necessary to understand the regulating mechanisms that govern prokaryotic generation of EP, both in surface and deep waters, due to their potential role in the formation of large aggregates that could act as hotspots of microbial activity (Azam 1998).

Prokaryotic assemblages in surface waters of the Mediterranean Sea have been reported to play a significant role in EP production and dynamics (Radic et al., 2003; Ortega-Retuerta et al., 2010; Bar-Zeev et al., 2011). The massive formation of large aggregates (known as *mucilage events*), which are preceded by high EP concentrations, is an increasingly common phenomenon in the Mediterranean Sea (Radic et al., 2005; Danovaro et al., 2009; Giani et al., 2012). Although the large scale formation of aggregates is not well understood, changes from east to west in the Levantine intermediate waters could influence the aggregate production (Innamorati et al., 2001; Moutin and Raimbault, 2002) because of the contrasting inorganic nutrient content in the surface waters of the basins that could enhance aggregates formation, including EP.

With the objective of understanding the underlying mechanisms in the formation of gelatinous aggregates in the Mediterranean Sea, we performed experiments to assess the effects of additions of inorganic nutrients (nitrogen and phosphorous) and labile organic carbon (glucose) on prokaryotic EP production in different water masses at different depths in the well-contrasted eastern and western Mediterranean basins.

6.3. Material and methods

6.3.1. Study area and sampling

Sampling was carried out along the Mediterranean Sea on board of R/V *Sarmiento de Gamboa* in the framework of the *Hotmix* project. Water samples were collected at different depths and sampling stations were located in the open waters of the Eastern (EM) and Western Mediterranean (WM) basins (Figure 6.1. and Table 6.1.). Data on environmental conditions at the time of sampling are reported in Table 6.1. We used a rosette sampler with 24 Niskin bottles (12 l) coupled to a conductivity and temperature–pressure (CTD) probe (Seabird SBE911).

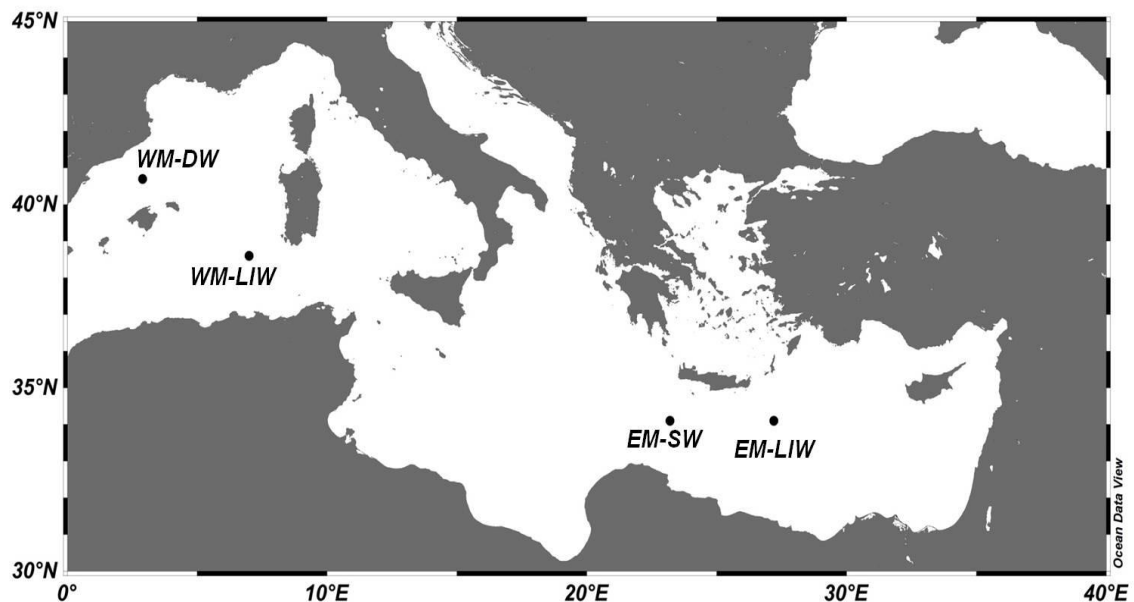


Figure 6. 1. Location of the stations where water was collected for the experiments. The nomenclature of every sampling station is given in the Table 6.1.

6.3.2. Experimental set-up

The effects of organic or inorganic nutrient additions on production of exopolymeric particles (EP) by heterotrophic prokaryotes were measured using re-growth cultures. A total of four experiments were performed and incubated using 2L Nalgene bottles, for 6 days, in a temperature-controlled chamber under *in situ* temperature and in the dark. All used material was acid-washed and rinsed with ultrapure water prior to its use.

Water samples were pre-filtered through 1 μm filters (using 0.1N HCl pre-washed Preflow capsule filters, Pall Corporation), to remove large particles and grazers, and were used as inoculum of natural microbial populations. Then, the water samples were subsequently filtered by 0.2 μm (using sterile Whatman Polycap cartridge filters). These fractions were mixed, and homogenized, with 75% of 0.2 μm filtered seawater + 25% of microbial inocula.

The effects of nutrient addition were monitored after the addition of solutions of labile organic carbon, D-glucose (Sigma; 150 μM final concentration), and/or inorganic nutrients, NH_4Cl and KH_2PO_4 (Sigma; 6.2 and 0.1 μM final concentration, respectively). The initial experiment WM-DW consisted of two treatments in triplicate: no nutrient additions (control) and glucose + inorganic nutrient additions (+GPN treatment). The other three experiments (EM-SW, EM-LIW and WM-LIW) consisted of three treatments in triplicate: no nutrient additions (control), with glucose addition (+Glucose treatment), with inorganic nutrient additions (+PN treatment).

Heterotrophic prokaryotic abundance (PHA) and production (PHP) were monitored during the course of the experiments. The concentration of exopolymer particles (EP), dissolved inorganic nutrients, dissolved and particulate organic carbon were determined at the onset and end of the experiments.

6.3.3. Biological and chemical analyses

6.3.3.1. Determination of exopolymeric particles

EP concentrations were measured by using the colorimetric alcian blue method (Passow and Alldredge, 1995). Three or four replicate samples (25 - 500 ml) were gently filtered through 0.4 μm polycarbonate filters. EP retained on the filters were stained (fully covered) with 0.5 ml of a 0.02% solution of alcian Blue (Sigma) in 0.06% acetic acid (pH 2.5) and frozen at -80°C until analysis. Three or four blanks (with ultrapure water) were also performed in each batch of samples (stained and frozen in parallel). The alcian blue was extracted, from the unfrozen filters, adding 5 ml of 80% sulfuric acid for 2 - 3 hours and absorbance was read at 787 nm in 1 cm path disposable polystyrene cuvettes against ultrapure water

Prokaryotic EP production in the Mediterranean Sea

as blank. EP concentration is expressed as micrograms of xanthan gum equivalents per liter ($\mu\text{g XG eq l}^{-1}$) after performing a calibration curve with increasing volumes of a xanthan gum (XG) solution (25 mg l^{-1}). The coefficient of variation of replicates was, on average, 17%.

6.3.3.2. Total Dissolved Nitrogen and Phosphorous

Samples for total dissolved nitrogen (TDN) and phosphorous (TDP) were initially pre-filtered through $0.4 \mu\text{m}$ polycarbonate filters (Sartorius) and stored in 250 ml sterile polypropylene bottles at $-20 \text{ }^\circ\text{C}$ until analysis. Concentrations (in $\mu\text{mol L}^{-1}$) of TDN and TDP were determined after oxidation ($120 \text{ }^\circ\text{C}$ and 30 min.) with potassium persulfate as reported by Valderrama (1981), in which all chemical forms of nitrogen and phosphorous are hydrolyzed to inorganic compounds (nitrate and orthophosphate, respectively). TDP was analyzed according to the modified method of Murphy and Riley (1962). Under alkaline conditions, the mixed reagent (composed of sulphuric acid, ammonium molybdate, ascorbic acid and potassium antimony tartrate) is added and absorbance read at 885 nm. Dilutions (from 0.01 to 0.5 mg L^{-1}) of a phosphate standard solution (KH_2PO_4 , 1000 mg L^{-1}) were used as a calibration standard. TDN was analyzed by the ultraviolet spectrophotometric method proposed by Rice et al. (2012), reading the absorbance at 220 nm and corrected at 275 nm. Dilutions ($0.1\text{-}2.5 \text{ mg L}^{-1}$) of a standard solution of potassium nitrate (KNO_3 , 1000 mg L^{-1}) were also used for calibration. All material used in the nutrient analysis was acid-washed and rinsed previously. The limits of detection (twice the standard deviation of the blanks) were $0.1 \mu\text{M}$ for TDN and $0.02 \mu\text{M}$ for TDP.

6.3.3.3. Organic carbon

TOC and DOC (previously filtered by $0.4 \mu\text{m}$) samples were collected into pre-combusted glass bottles, acidified with phosphoric acid (final $\text{pH} < 2$), sealed and stored at 4°C until analysis. These samples were analyzed by high-temperature catalytic oxidation on a Shimadzu TOC-V CSH total organic carbon analyzer. Standards of potassium hydrogen phthalate (with concentrations from 10 to $100 \mu\text{M}$) were used in each batch of samples to assess the accuracy of the measurements and determine the DOC concentrations. Particulate organic

carbon (POC) was determined by the difference between TOC and DOC measurements.

6.3.3.4. Prokaryotic heterotrophic abundance and production

Prokaryotic heterotrophic abundance (PHA) and production (PHP) were directly determined collecting an aliquot from the Niskin bottles or at different times during the incubation experiments.

PHA was measured by flow cytometry (Gasol and del Giorgio, 2000). 1.5 ml aliquots were fixed with 1% of paraformaldehyde + 0.05 % glutaraldehyde, deep-frozen in liquid nitrogen and stored at -80 °C until analysis. Samples were stained with SybrGreen I and run through a FACSCalibur cytometer fitted with a laser emitting at 488 nm. Cells were enumerated in a bivariate plot of 90° light scatter and green fluorescence. Molecular Probes latex beads (1 µm) were used as internal standards. Prokaryotic biomass (PB; mg m⁻³) was calculated by transforming relative light side scatter (SSC) to cell diameter, using the linear regression model of Calvo-Díaz and Morán (2006) after staining the samples with SybrGreen I. A spherical shape was assumed to derive cellular volumes, which were later converted to biomass with the allometric equation of Gundersen et al. (2002). The net specific growth rate (SGR, day⁻¹) was calculated as $\text{Ln}(PB_{T_f}/PB_{T_0})/T_f$, where T_f and T_0 are final and initial incubation times (days), respectively.

PHP rates were measured by ³H-Leucine (specific activities = 112 Ci mmol⁻¹) incorporation into proteins (Kirchman et al., 1985) and using the microcentrifugation protocol proposed by Smith and Azam (1992). Three replicates (1.2 ml) and two trichloroacetic acid (TCA)-killed blanks in microcentrifuge tubes were added L-[4, 5-³H] leucine at 20 nM. Samples and blanks were incubated (for 3 to 15 h) at *in situ* temperatures. Incubations were stopped by adding 50% TCA. Subsequently, the samples were centrifuged twice (10 min. and 14000 r.p.m.) and rinsed with 5% TCA. Scintillation cocktail (1 ml Optisafe HiSafe) was added, and after 24 h, the samples were counted in a liquid scintillation counter. Leucine incorporation rates (pmol Leu l⁻¹ h⁻¹) were converted into carbon (µg C l⁻¹ d⁻¹) by using a theoretical factor of 1.55 kg C mol

Prokaryotic EP production in the Mediterranean Sea

Leu⁻¹ (Simon and Azam, 1989), assuming that isotope dilution was negligible under this saturating concentration of 20 nM of ³H-Leucine.

6.3.4. Data analysis

PHP rates were integrated (PHP_{int}) during the experiments from the initial to the final time and expressed as µg C L⁻¹ day⁻¹. Daily rates of change for EP (ΔEP), DOC (ΔDOC), POC (ΔPOC) and PHA (ΔPHA) were calculated using the expression:

$$\Delta_x = (X_{t_f} - X_{t_0}) / t$$

where X_{t_f} and X_{t_0} are the variables at final (t_f) and initial times (t_0), respectively, and t ($t_f - t_0$) is the elapsed time in days.

The efficiency with which heterotrophic prokaryotes convert DOC into POC ($E_{\text{DOC} \rightarrow \text{POC}}$), assuming that all POC generated in experiments is exclusively derived from prokaryotic growth, was estimated as

$$E_{\text{DOC} \rightarrow \text{POC}} (\%) = [\Delta\text{POC} / (\Delta\text{POC} - \Delta\text{DOC})] \times 100$$

where ΔPOC is the POC generated at the end of the experiments and ΔDOC is the total DOC consumed.

We explored the relationship between the daily increase rate of EP (ΔEP) and the other variables with regression analysis. All variables were log-transformed to fit the required assumptions of normality and homocedasticity.

The slopes of the regressions between ΔEP and ΔPHA gave experimental estimates of intrinsic EP production rates (i.e. the quantity of EP produced per day normalized by PHA). We used these experimental EP production rates to calculate *in situ* EP production rates by heterotrophic prokaryotes using the PHA data obtained in the natural environment. The EP residence time (days) was estimated by dividing the *in situ* EP concentration by the *in situ* EP production rate.

Differences among treatments and incubation times were tested with Tukey HSD tests with significance set at a p-value < 0.05. Statistical analyses were performed using Statistica 6.0 (StatSoft Inc., 1997).

6.4. Results

6.4.1. Changes in the heterotrophic prokaryotes in the experiments

The Table 6.1. shows the initial values (T_0) of PHA and PHP, which were, on average, 34% lower than most of the *in situ* values (except for PHP T_0 of the EM-LIW experiment) because of the initial filtration + dilution.

Table 6. 1. Sample information, *in situ* environmental conditions of the water samples and prokaryotic parameters and nutrients at the onset of the time-series experiments (T_0). The acronym “SW” corresponds to experiments performed with surface waters, the acronym “LIW” corresponds to Levantine intermediate waters and “DW” corresponds to experiments performed with deep waters (below the LIW depths). Standard deviation in brackets.

Sampling data					
Ocean basin		Western Mediterranean (WM)		Eastern Mediterranean (EM)	
Latitude		40.7°N	38.6°N	34.1°N	34.1°N
Longitude		2.9°E	7.0°E	23.2°E	27.2°E
Date (day/month/year)		02/10/2013	17/05/2014	04/05/2014	02/05/2014
Sampling depth (m)		2000	400	90	200
Parameters <i>in situ</i> ¹					
Temperature (°C)		13.2	13.2	15.9	16.2
Salinity		38.49	38.55	39.02	39.12
[O ₂] (μmol kg ⁻¹)		-	150	196	205
Chl <i>a</i> (μg l ⁻¹)		-	-	0.20	-
Phosphate (μM)		-	0.42	0.03	0.04
Nitrate (μM)		-	9.7	1.1	1.0
EP (μg eq XG L ⁻¹)		12.3	7.5	16.2	5.5
PHA (x 10 ⁵ cell ml ⁻¹)		0.64	1.5	3.5	2.3
PHP (ng C l ⁻¹ h ⁻¹)		-	2.67	4.65	0.55
Experimental data ¹					
Experiment codes		WM-DW	WM-LIW	EM-SW	EM-LIW
PHA T_0 (x 10 ⁵ cell ml ⁻¹)		0.21(0.04)	0.41 (0.02)	1.57 (0.12)	0.63 (0.05)
PHP T_0 (ng C l ⁻¹ h ⁻¹)		-	1.24 (0.33)	1.36 (0.42)	2.47 (0.64)
DOC T_0 (μM)	Control	47 (7)	87 (10)	53 (3)	46 (4)
	+Glucose/+CPN	165 (3)	398 (15)	202 (3)	154 (5)
TDN T_0 (μM)	Control	10.1 (0.2)	11.2 (0.4)	1.5 (0.1)	1.1 (0.3)
	+PN/+CPN	14.7 (0.6)	16.4 (1.0)	5.2 (0.5)	5.7 (0.1)
TDP T_0 (μM)	Control	0.40 (0.03)	0.36 (0.04)	0.04 (0)	0.06 (0.01)
	+PN/+CPN	0.49 (0.02)	0.42 (0.03)	0.10 (0.02)	0.13 (0.01)

¹[O₂] = dissolved oxygen concentration; Chl *a* = chlorophyll *a* concentration; EP = exopolymer particle concentration; PHA = heterotrophic prokaryotic abundance; PHP = prokaryotic heterotrophic production; DOC = dissolved organic carbon; TDN = total dissolved nitrogen; TDP = total dissolved phosphorous.

Prokaryotic EP production in the Mediterranean Sea

In the WM-DW experiment, prokaryotic heterotrophic abundance (PHA) increased ~3-fold in the control and ~212 fold in the +GPN treatment (Figure 6.2.). The increase in PHA (Δ PHA) was from 0.59×10^7 cells L⁻¹ day⁻¹ in the control treatment and 71.97×10^7 cells L⁻¹ day⁻¹ in +GPN treatment (Table 6.2.). Similarly, the specific growth rate (SGR) was higher in the +GPN treatment than in the controls (Table 6.2.).

Table 6. 2. Microbial parameters in the different experiments. Average, and standard deviation (in brackets), of the daily increments in prokaryotic heterotrophic abundance (Δ PHA), the integrated heterotrophic prokaryotic production (PHP_{int}) and the specific growth rate (SGR).

Experiment	Treatment	Δ PHA (x 10 ⁷ cells L ⁻¹ day ⁻¹)	PHP _{int} (μ g C L ⁻¹ day ⁻¹)	SGR (day ⁻¹)
WM-DW	Control	0.59 (\pm 0.07)	-	0.13
	+GPN	71.97 (\pm 0.98)	-	0.84
WM-LIW	Control	57.05 (\pm 0.25)	14.14	0.71
	+Glucose	36.88 (\pm 1.63)	18.06	0.64
	+PN	32.65 (\pm 0.57)	21.42	0.62
EM-SW	Control	3.43 (\pm 0.26)	8.97	0.17
	+Glucose	9.39 (\pm 0.70)	16.22	0.29
	+PN	5.73 (\pm 0.30)	13.13	0.23
EM-LIW	Control	9.81 (\pm 0.71)	8.71	0.69
	+Glucose	9.13 (\pm 0.67)	9.68	0.70
	+PN	7.90 (\pm 0.29)	12.33	0.66

In the WM-LIW experiments, PHA in all treatments increased considerably after six days of incubation, although surprisingly (only after incubation 6 days) more in the control treatments (~85-fold above the initial PHA) than in the +Glucose and +PN treatments (~50-fold) (Figure 6.2.). Δ PHA was $> 50 \times 10^7$ cells L⁻¹ day⁻¹ in the control and around 35×10^7 cells L⁻¹ day⁻¹ in the +Glucose and +PN treatments (Table 6.2.). Integrated PHP (PHP_{int}) ranged between 14.1 (in the control) and 21.4 μ g C L⁻¹ day⁻¹ (in +PN treatment), while SGR between 0.62 (in +PN treatment) and 0.71 day⁻¹ (in control) (Table 6.2.).

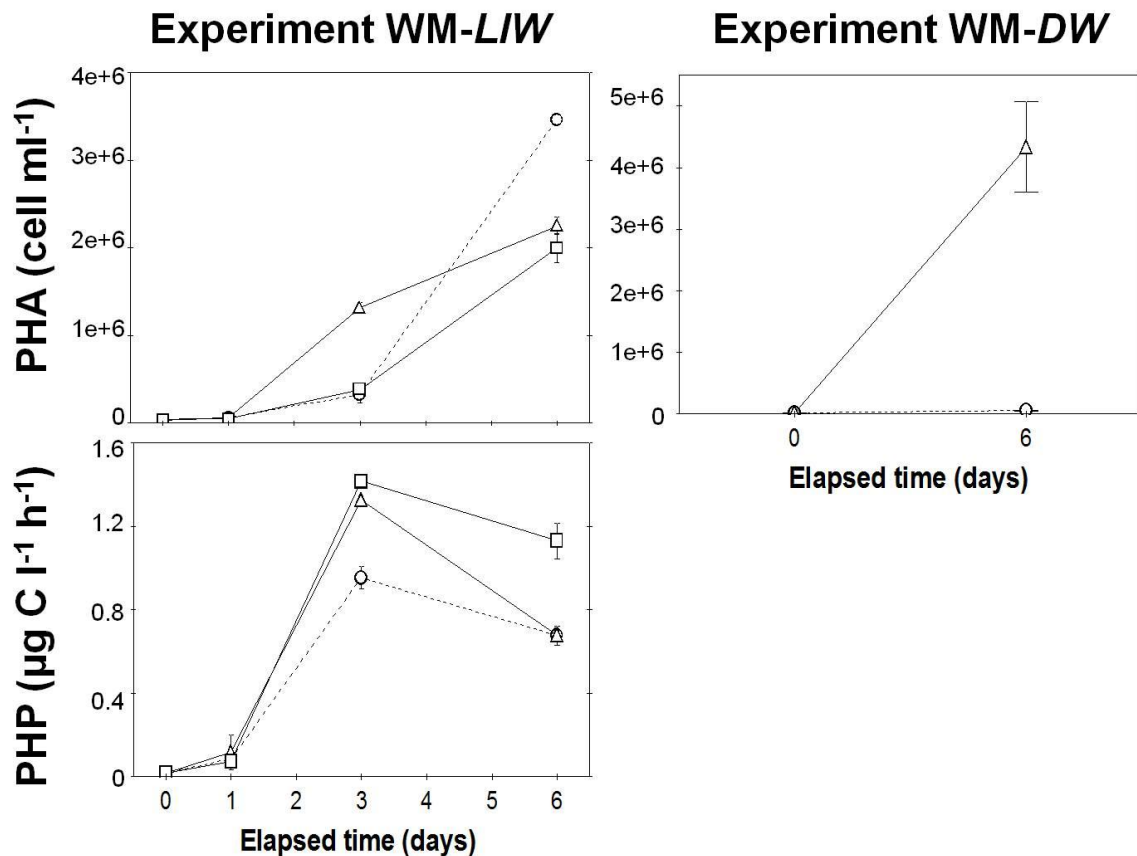


Figure 6. 2. Time evolution of prokaryotic heterotrophic abundance (PHA) and production (PHP) for the experiments conducted with Levantine Intermediate Water (WM-LIW) and Deep Water (WM-DW) in the Western Mediterranean Sea. Each value represents the average of triplicates \pm standard deviation (SD). When no error bars are shown, the SD is smaller than the symbol. Circles: controls; Triangles: +Glucose treatments; Squares: +GNP treatment in the WM-DW and +PN treatment in the WM-LIW.

In the EM-SW experiment, PHA increased in all the seawater cultures, but more in +Glucose treatment (\sim 5-fold above the initial values) than in the +PN (\sim 3-fold) and control treatments (two-fold) (Figure 6.3.). Δ PHA was 3.43×10^7 cells L^{-1} day $^{-1}$ in control, 9.39×10^7 cells L^{-1} day $^{-1}$ in +Glucose treatment and 5.73×10^7 cells L^{-1} day $^{-1}$ in +PN treatment (Table 6.2.). PHP increased over time in both treatments and reached the plateau after three days of incubation (Figure 6.3.). PHP_{int} and SGR were consistently higher in the +Glucose treatments than in the +PN treatments and controls (Table 6.2.).

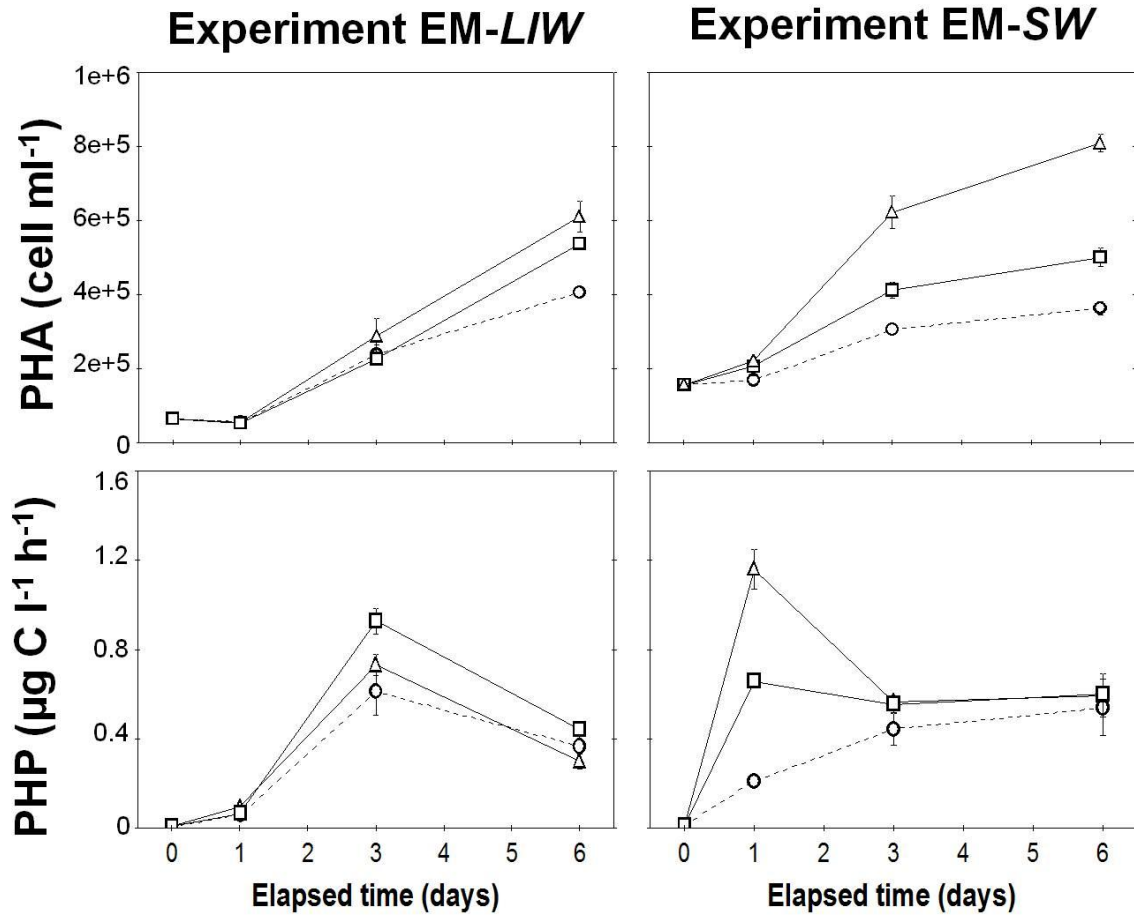


Figure 6. 3. Time evolution of prokaryotic heterotrophic abundance (PHA) and production (PHP) for the EM-SW and EM-LIW experiments. The information symbols and abbreviations are given in detail in Figure 6.2. When no error bars are shown, the SD is smaller than the symbol.

In the EM-LIW experiment, PHA increased also in all treatments, about 10-fold above the initial values in the +Glucose and control treatments, but with a slightly lower increase in the +PN treatment (9-fold) (Figure 6.3.). Δ PHA was $> 9 \times 10^7$ cells L^{-1} day $^{-1}$ in +Glucose and control treatments, while this increment for +PN treatment was about 8×10^7 cells L^{-1} day $^{-1}$ (Table 6.2.). PHP increased progressively until the third day of incubation, and then, decreased at the end of the incubations (Figure 6.3.). PHP_{int} was more elevated in the +PN treatments and SGR in the +Glucose treatments (Table 6.2.).

6.4.2. Changes of organic matter and inorganic nutrients in the experiments

At the onset of the experiments, DOC was logically higher in the +Glucose or +GPN (in case of the experiment *WM-DW*) treatments than in controls and +PN treatments (Table 6.1.). Concentrations of total dissolved nitrogen (TDN) and phosphorous (TDP) were as expected also higher in the +GNP or +PN treatments than in control or +Glucose treatments (Table 6.1.).

At the end of the experiments, the variability of DOC and POC (Δ DOC and Δ POC) was normally higher in the +Glucose or +GPN treatments than in controls and +PN treatments, with exception of POC in the experiment *WM-LIW* (Table 6.3.). The prokaryotic efficiencies to convert DOC into POC ($E_{\text{DOC} \rightarrow \text{POC}}$) in the + Glucose treatments were normally the smallest ones, although the addition of inorganic and organic nutrients in the experiment *WM-DW* increased the $E_{\text{DOC} \rightarrow \text{POC}}$ (Table 6.3.). TDN and TDP concentrations decreased usually more in the *WM-LIW* experiment, but there were no clear differences among treatments (Table 6.3.).

Table 6. 3. Average \pm SD (in brackets) of the daily increments of dissolved organic carbon (Δ DOC), particulate organic carbon (Δ POC) and exopolymer particles concentrations (Δ EP). Changes of total dissolved nitrogen (Δ TDN) and total dissolved phosphorous (Δ TDP). Prokaryotic efficiency to convert DOC into POC ($E_{\text{DOC}\rightarrow\text{POC}}$) is also presented.

Experiment	Treatment	Δ DOC ($\mu\text{mol L}^{-1} \text{day}^{-1}$)	Δ POC ($\mu\text{mol L}^{-1} \text{day}^{-1}$)	$E_{\text{DOC}\rightarrow\text{POC}}$ (%)	Δ TDN ($\mu\text{mol L}^{-1}$)	Δ TDP ($\mu\text{mol L}^{-1}$)	Δ EP ($\mu\text{g XG eq. L}^{-1} \text{day}^{-1}$)
WM-DW	Control	0	-	-	0	0	0.7 (\pm 0.1)
	+GNP	-13 (\pm 3)	4 (\pm 1)	23	-0.7	-0.5	56.2 (\pm 15.2)
WM-LIW	Control	-6 (\pm 2)	7 (\pm 3)	54	-1.6	-0.08	232.2 (\pm 14.6)
	+Glucose	-26 (\pm 5)	5 (\pm 1)	16	-0.8	-0.10	122.7 (\pm 34.7)
	+PN	-8 (\pm 4)	5 (\pm 2)	38	-1.2	-0.14	140.1 (\pm 7.4)
EM-SW	Control	-1 (\pm 0)	< 1	25	0.2	0	7.7 (\pm 3.0)
	+Glucose	-9 (\pm 2)	2 (\pm 1)	18	-0.5	-0.04	48.9 (\pm 10.7)
	+PN	-2 (\pm 1)	1 (\pm 0)	33	-0.4	-0.02	21.1 (\pm 1.4)
EM-LIW	Control	-2 (\pm 1)	1 (\pm 0)	33	0.3	-0.06	16.4 (\pm 5.0)
	+Glucose	-11 (\pm 4)	5 (\pm 3)	31	-0.4	-0.06	177.6 (\pm 19.1)
	+PN	-2 (\pm 1)	1 (\pm 2)	33	-0.4	-0.09	21.9 (\pm 11.7)

The EP concentrations in the experiments carried out in the WM basin increased consistently in all treatments (Figure 6.4.). However, the increment of EP concentrations (ΔEP) was different between control and treatments with nutrient additions (+GPN, +PN and +Glucose). ΔEP in the experiment *WM-DW* increased significantly in +GPN treatment relative to the control, but ΔEP in the experiment *WM-LIW* EP production was lower in the treatment with addition of nutrients (+Glucose or +PN than in the control treatment (Figure 6.4 and Table 6.3). Interestingly, the cell-specific EP production in the *WM-LIW* experiment was not significantly different among treatments, while in the *WM-DW* experiment the cell-specific EP production in the +GPN treatment was significantly lower than the EP production in the control treatment (Figure 6.4.).

Prokaryotic EP production in the Mediterranean Sea

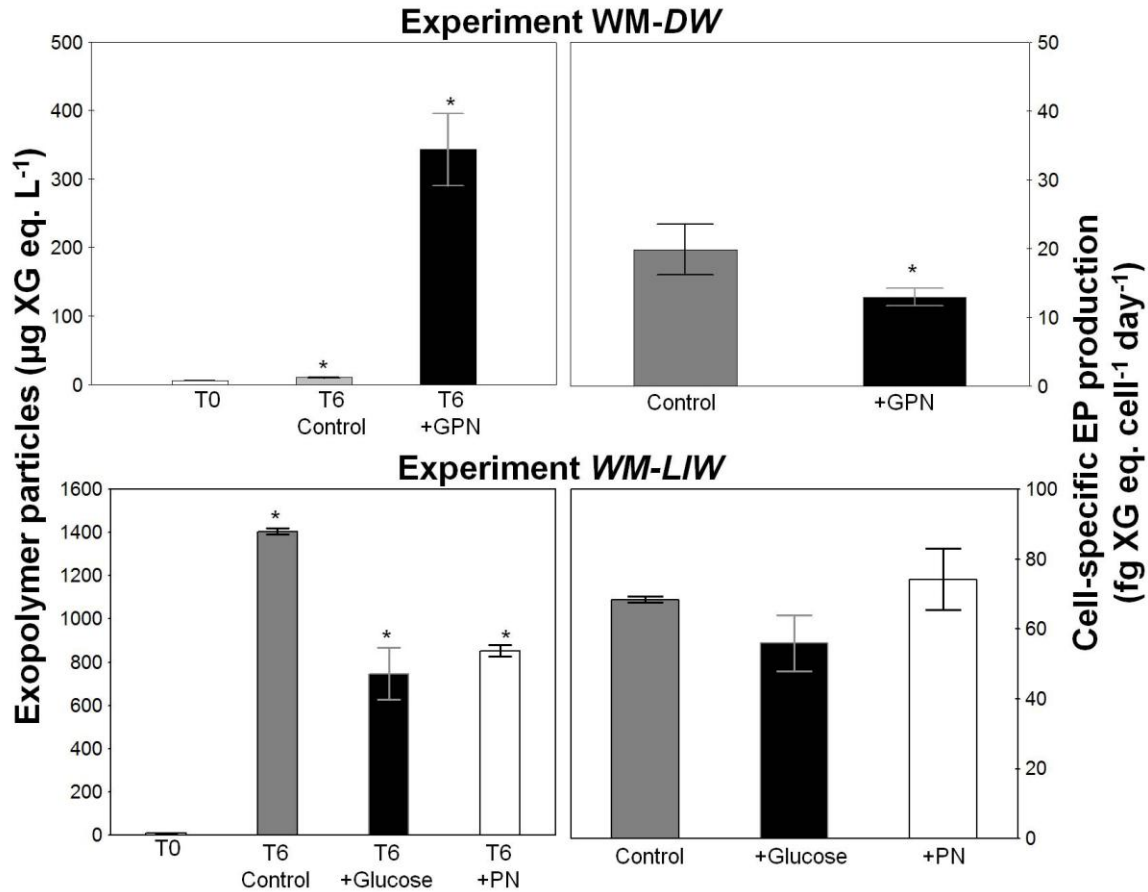


Figure 6. 4. Changes in EP concentrations (left) and cell-specific EP production (right) in the experiments conducted with waters of the Western Mediterranean basin (WM-DW and WM-LIW). Asterisks indicate statistically significant differences in comparison with the initial time in the EP concentrations, and in comparison to the controls in the cell-specific EP production (Tukey HSD's test, p -value < 0.05).

EP concentrations in the experiments conducted in the EM basin (*EM-SW* and *EM-LIW*) increased consistently at the end of the incubation time (Figure 6.5). The highest values of EP production and cell-specific EP production were found in the +Glucose treatments, followed by the +PN treatments and the lower values corresponded to the control treatments (Figure 6.5. and Table 6.3.).

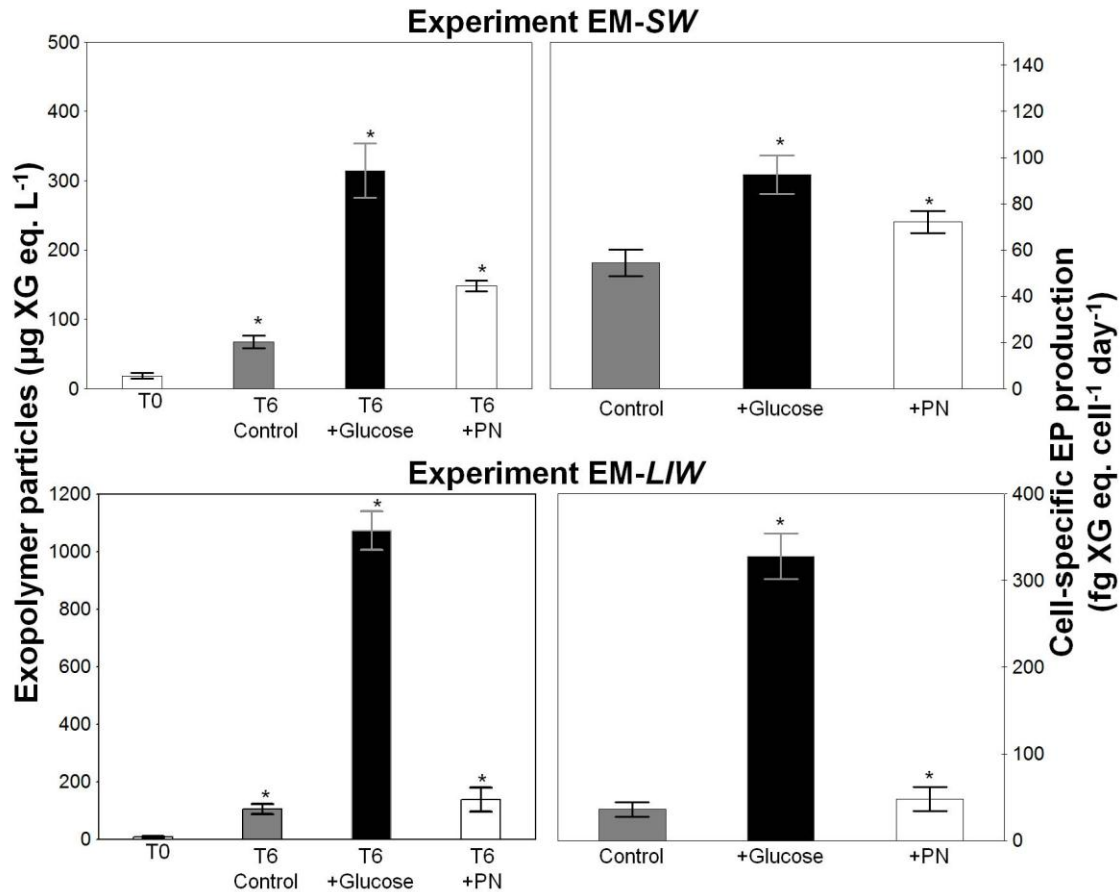


Figure 6. 5. Changes in EP concentrations (left) and cell-specific EP production (right) in the experiments conducted with waters of the Eastern Mediterranean basin (EM-SW and EM-LIW). Asterisks indicate statistically significant differences comparing with the EP concentrations at the initial time, and comparing with the control treatments in the cell-specific EP production (Tukey HSD's test, p -value < 0.05).

EP production rates (ΔEP) were significant and positively related to heterotrophic prokaryotic abundance ΔPHA [$n = 11$; $r^2 = 0.75$ and p -value < 0.001; $\text{Log}_{10} \Delta EP = 1.05 (\pm 0.20) \text{Log}_{10} \Delta PHA - 6.95 (\pm 1.63)$] (Figure 6.6. A) and to the specific growth rate (SGR) [$n = 11$; $r^2 = 0.60$ and p -value < 0.01; $\text{Log}_{10} \Delta EP = 1.96 (\pm 0.53) \text{Log}_{10} \text{SGR} + 2.24 (\pm 0.24)$] (Figure 6.6. B), but there was not relationship with PHP_{int} (Figure 6.6. C).

Prokaryotic EP production in the Mediterranean Sea

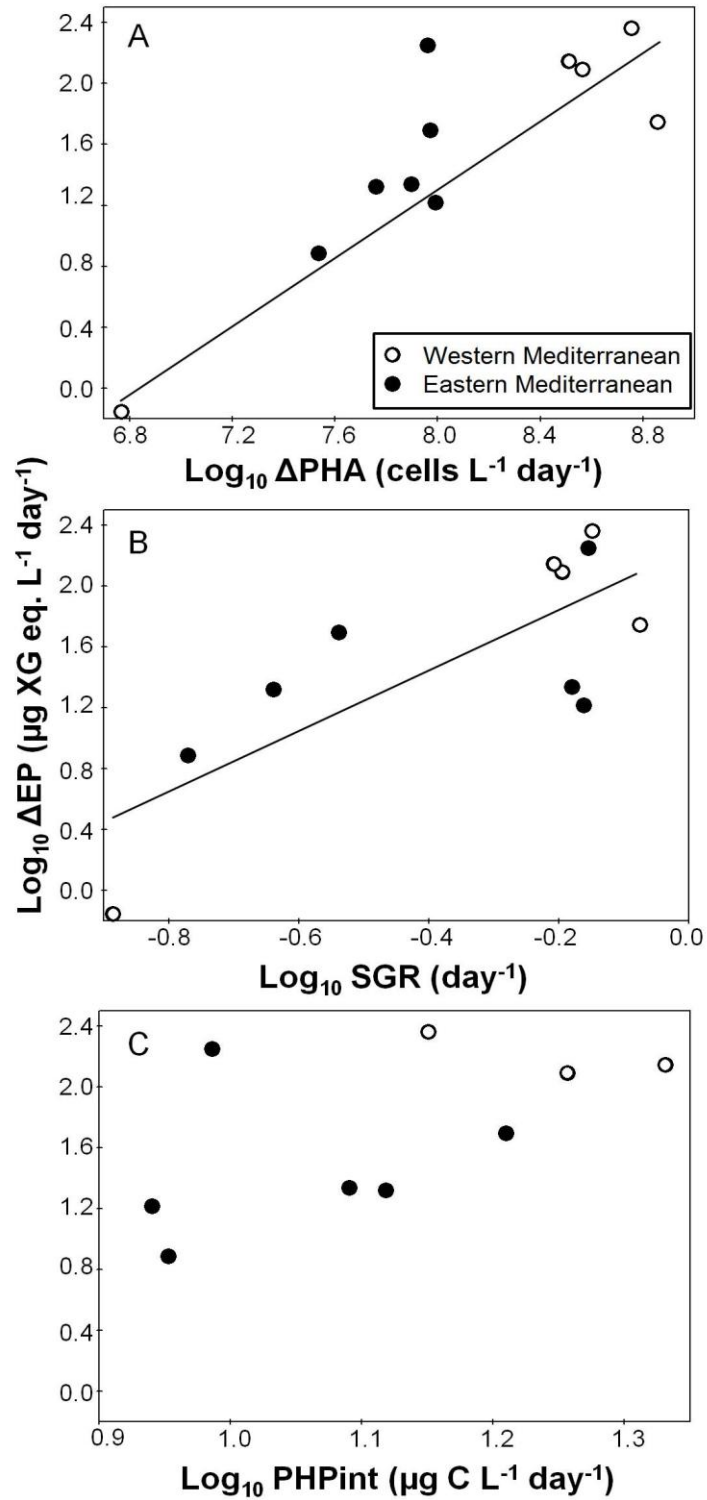


Figure 6. 6. Log-Log relationships between ΔEP and ΔPHA (A), SGR (B) and PHP_{int} (C).

We observed that ΔEP was positive and tightly correlated to ΔPOC [$n = 10$; $r^2 = 0.95$ and $p\text{-value} < 0.0001$: $\Delta EP = 1.11 (\pm 0.09) \Delta POC + 1.33 (\pm 0.05)$] (Figure 6.7). However, there were not significant relationships with ΔDOC and $E_{DOC \rightarrow POC}$ ($p\text{-value} > 0.05$). In relation to the inorganic nutrients, TDN concentration was inversely related to ΔEP [$n = 11$; $r^2 = 0.65$ and $p\text{-value} < 0.01$: $\Delta EP = -111.3 (\pm 27.4) \Delta TDN + 21.2 (\pm 20.2)$] and there were not significant relationships with TDP, C:N or N:P ratios.

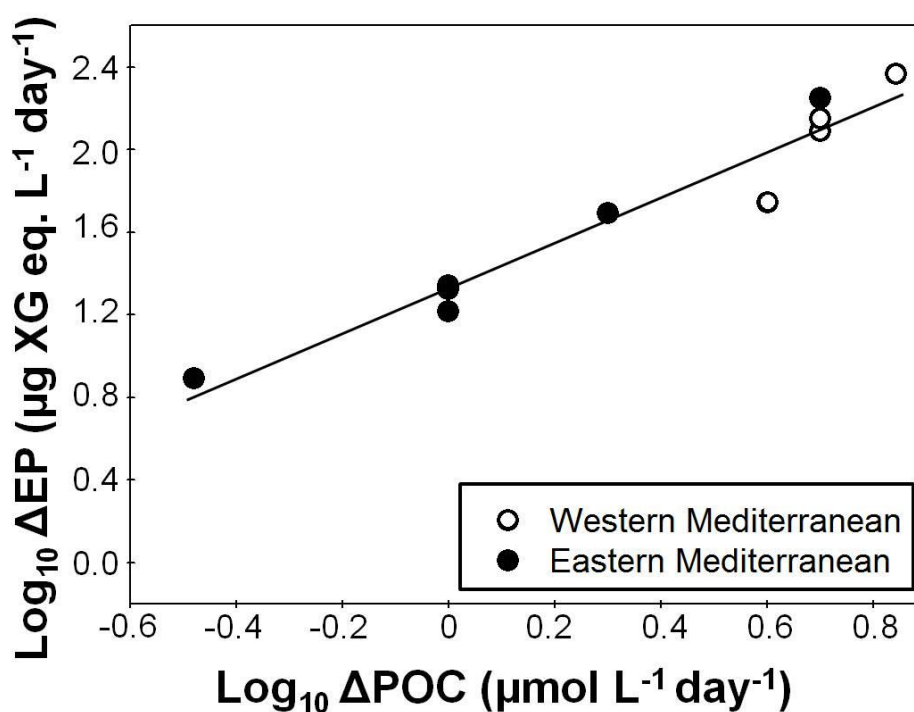


Figure 6. 7. Log-Log relationship between ΔPOC and ΔEP .

Prokaryotic EP production in the Mediterranean Sea

6.4.3. The *in situ* EP production rates and the residence times

We used the *in situ* values of prokaryotic heterotrophic abundance to calculate the *in situ* EP production using the regression model between Δ PHA and Δ EP obtained experimentally (Figure 6.6. A). The estimated *in situ* generation rates in the WM basin were higher than these values in the EM basin, while the EP residence times in the WM basin were consistently lower than those in the EM basin (Table 6.4.). The residence times in the Levantine Intermediate Water in both ocean basins were shorter than those estimated for the surface and deep layers.

Table 6. 4. Estimated *in situ* EP generation rates and residence times at the depth of the experiments; calculated mean and ranges (in brackets) in the Eastern and Western Mediterranean basins sampled in the surface waters (SW), Levantine intermediate waters (LIW) and deep waters (DW; below the LIW).

Experiments	Western Mediterranean		Eastern Mediterranean	
	<i>in situ</i> EP generation rates ($\mu\text{g XG eq. L}^{-1} \text{ day}^{-1}$)	EP residence times (days)	<i>in situ</i> EP generation rates ($\mu\text{g XG eq. L}^{-1} \text{ day}^{-1}$)	EP residence times (days)
SW	-	-	0.074	219
LIW	0.030	247	0.047	117
DW	0.012	985	-	-
marine region				
SW	0.133 (0.063-0.247)	265 (126-704)	0.068 (0.025-0.187)	401 (89-1001)
LIW	0.40 (0.19-0.080)	232 (56-743)	0.030 (0.013-0.062)	240 (81-506)
DW	0.011 (0.005-0.026)	604 (54-1649)	0.008 (0.003-0.024)	619 (116-2060)

6.5. Discussion

Our study experimentally demonstrates that heterotrophic prokaryotes are sources of EP not just in the surface waters, but also in deeper water masses such as the Levantine Intermediate Waters (LIW) and the Deep Mediterranean Waters. Nutrient additions, mainly glucose, stimulated EP production in the experiments performed in the Eastern Mediterranean (EM) basin (Figure 6.5.). This stimulus was not observed in the Western Mediterranean (WM) basin, where EP production was even lower under glucose additions. Interestingly, the EP pool in the WM basin, and particularly in the LIW, exhibited relatively short residence times suggesting a high prokaryotic EP production, although the removal processes would also be elevated maintaining these low residence times.

6.5.1. EP production in the surface, Levantine intermediate and deep waters

In the *LIW* experiments, EP production in absolute terms (from 16.4 to 232.2 $\mu\text{g XG eq. L}^{-1} \text{ day}^{-1}$) was consistently higher than the rates obtained in the experiments with *SW* (7.7-48.9 $\mu\text{g XG eq. L}^{-1} \text{ day}^{-1}$) or *DW* (0.7-56.2 $\mu\text{g XG eq. L}^{-1} \text{ day}^{-1}$). The rates in our study are within the range found in the literature, from undetectable to 267 $\mu\text{g XG eq. L}^{-1} \text{ day}^{-1}$, in surface waters of the open Mediterranean Sea (Ortega-Retuerta et al., 2010) or the coastal waters (Stoderegger and Herndl, 1999; Prieto et al., 2002; Sugimoto et al., 2007). The higher rates are also comparable to the rates observed for some algal groups (Sugimoto et al., 2007), emphasizing the significant contribution of prokaryotes to the EP pool (Passow, 2002). In fact, in our study the ΔPHA was the best predictor of ΔEP (Figure 6.7. A). Previous studies have also reported robust regressions between both parameters (Sugimoto et al., 2007; Ortega-Retuerta et al., 2010). The higher the ΔPHA , the higher the EP production was.

In relation to control treatments, the *WM-LIW* experiments showed the highest EP absolute production values ($232.2 \pm 14.6 \mu\text{g XG eq. L}^{-1} \text{ day}^{-1}$) and the highest per cell EP production ($68.4 \pm 1.5 \text{ fg XG eq. cell}^{-1} \text{ day}^{-1}$), as well as the highest efficiency of conversion of DOC into POC (54%) (Table 6.3.). This fact and a

Prokaryotic EP production in the Mediterranean Sea

higher estimated *in situ* EP generation rates in the WM (Table 6.4.) emphasize that prokaryotes (when growing in optimal conditions) can have a significant role in the generation of the EP pool, and ultimately, in the proliferation of mucilage events in the Mediterranean Sea (Innamorati et al., 2001).

However, the short EP residence times in the LIW, around 200 days, in relation to the values estimated for the SW and DW layers (Table 6.4.) contrast with the EP production role, being part of the semi-labile organic carbon fraction (with residence times of months to years; Carlson, 2002). In other words, the EP removal mechanisms must be very active since EP concentrations at LIW depths are consistently low (Chapter 5). These EP residence times are more than an order of magnitude higher than the values (0.8 - 17.5 days) obtained by Ortega-Retuerta et al. (2010) in the surface waters of the Mediterranean Sea. However, the observed *in situ* EP also come from other sources besides the heterotrophic prokaryotes, such as the autotrophic plankton, and are exported vertically or horizontally, so very likely, the EP pool in the different compartments of the Mediterranean Sea would have shorter residence times than those we have estimated, which only consider the heterotrophic prokaryotic role.

6.5.2. EP production promoted by nutrient additions

Environmental variability, such as temperature, solar radiation and nutrient availability may differently affect prokaryotic EP production (Piontek et al., 2009; Ortega-Retuerta et al. 2009; Koch et al., 2014). In this sense, the Mediterranean Sea presents two basins (Eastern and Western Mediterranean) with well contrasted environmental parameters (Pujo-Pay et al., 2011).

In the EM basin, with high phosphorous deficiency, the addition of glucose resulted in high EP production per cell and in absolute terms (Table 6.3. and Figure 6.6.). Koch et al. (2014) in experimental additions of diverse organic sources observed also the highest prokaryotic EP production when adding glucose. In a phosphorus limited environment, prokaryotes hydrolyze organic matter incompletely, leaving behind refractory polymers in excess (Obenosterer and

Herndl, 1995; Azam et al., 1999), and a considerable fraction of these polymers may become EP. This would explain that the highest cell-specific EP productions were detected when glucose was added in the EM-LIW experiment. The addition of inorganic nutrients also slightly increased prokaryotic EP production (Table 6.3. and Figure 6.5.). The increase of phosphorous concentrations promoted microbial growth leading a higher prokaryotic EP production (see Table 6.2.). Other possible explanation might be that a departure of the N:P ratio, as it occurs in +PN treatments, could trigger a high release of dissolved EP precursors by prokaryotes (Radic et al., 2006). Bar-Zeev et al. (2011), in the mesopelagic zone of the Levantine region (EM basin), also observed higher values of EP concentrations than observed in other regions of the Mediterranean Sea (Prieto et al., 2006). Therefore, heterotrophic prokaryotes in the ultraoligotrophic Eastern Mediterranean Sea might be a significant source of EP, potentially affecting the aggregation processes and efficiency of the carbon exports.

In the WM basin, without extreme phosphorus limitation, the addition of nutrients resulted only in high prokaryotic EP production, relative to no-addition controls, in the experiment WM-DW. The cell-specific EP production did not increase significantly with nutrient additions, and even decreased in the experiment WM-DW. A previous experimental work observed that the glucose addition in regrowth prokaryotic cultures yielded higher EP production than in the cultures with algal exudates (Koch et al., 2014). This would explain the different prokaryotic EP production among treatments, particularly between +Glucose and control treatments.

The lowest values in the efficiencies of prokaryotic transformation from DOM to POM (Table 6.3.) were observed consistently in the treatments with glucose additions. Koch et al. (2014) similarly detected a decrease in prokaryotic growth efficiency when glucose was added to prokaryotic regrowth cultures. Our results are in agreement with what has been observed when highly oxidized and nitrogen-poor labile substrates (Vallino et al., 1996; del Giorgio and Cole, 1998).

Prokaryotic EP production in the Mediterranean Sea

Low efficiencies of incorporation of DOM to the particulate phase are then expected in extreme oligotrophic marine environments, as a result of the energy cost of maintaining active transport systems and basic metabolic machinery (del Giorgio and Cole, 1998). Additionally, we observed that these efficiencies slightly increased (in relation to controls) in the EM-SW experiment when inorganic nutrients were added (Table 6.3.). This fact indicates that inorganic nutrient also controlled the prokaryotic efficiencies to convert DOM into POM (del Giorgio and Cole, 1998).

Acknowledgements

This research work is a contribution to the Hotmix project (CTM2011-30010-C02/MAR). We thank our scientific colleagues as well as the technical staff and crew members on board the B/O Sarmiento de Gamboa, for their support in the field sampling during the cruise. IPM was supported by a JAE Pre-doc fellowship, from the Spanish National Research Council (CSIC) and the BBVA Foundation, Spain.

6.6. References

- Arístegui J., Gasol J. M., Duarte C. M., Herndl G. J. 2009. Microbial oceanography of the dark ocean's pelagic realm. *Limnology and Oceanography*, 54(5): 1501 – 1529.
- Azam F. Microbial control of oceanic carbon flux: The plot thickens. *Science*, 280:694 - 96.
- Azam F., Umani S. F., Funari E. 1999 Significance of bacteria in the mucilage phenomenon in the northern Adriatic Sea. *Ann Ist Super Sanità*, 35: 411–419.
- Baltar F., Arístegui J., Gasol J. M., Sintés E., Herndl G. J. 2009. Evidence of prokaryotic metabolism on suspended particulate organic matter in the dark waters of the subtropical North Atlantic. *Limnology and Oceanography*, 54(1): 182–193.
- Bar-Zeev E., Berman T., Rahav E., Dishon G., Herut B., Kress N. and Berman-Frank I. 2011. Transparent exopolymer particle (TEP) dynamics in the eastern Mediterranean sea. *Marine Ecology Progress Series*, 431: 107 – 118.
- Berman-Frank I., Dubinsky Z. 1999. Balanced Growth in Aquatic Plants: Myth or Reality? *BioScience*, 49: 29 - 37.
- Calvo-Díaz A., Morán X. A. G. 2006. Seasonal dynamics of picoplankton in shelf waters of the southern Bay of Biscay. *Aquatic Microbial Ecology*, 42: 159.
- Carlson C. A. 2002. Production and removal processes. In: Hansell D. A., Carlson C. A. (Eds.), *Biogeochemistry of Marine Dissolved Organic Matter*. Elsevier, San Diego, p. p. 91–151.
- Church M. J. 2008. Resource control of bacterial dynamics in the sea. In: Kirchman D. L. (Ed.), *Microbial Ecology of the Oceans*. second ed., p. p. 335 – 383.
- Corzo A., Morillo J. A., Rodríguez S. 2000. Production of transparent exopolymer particles (TEP) in cultures of *Chaetoceros calcitrans* under nitrogen limitation. *Aquatic Microbial Ecology*, 23: 63 – 72.
- Danovaro R., Umani S. F., Pudescu A. 2009. Climate Change and the Potential Spreading of Marine Mucilage and Microbial Pathogens in the Mediterranean Sea. *PLoS ONE*, 4(9): e7006. doi:10.1371/journal.pone.0007006
- Decho A. W. 1990. Microbial exopolymer secretions in ocean environments: their role(s) in food webs and marine processes. *Oceanogr. Mar. Biol. Annu. Rev.*, 28: 73 – 153.
- De la Rocha C., Passow U. 2007. Factors influencing the sinking of POC and the efficiency of the biological carbon pump. *Deep-Sea Research II*, 54: 639 – 658.
- del Giorgio P. A., Cole J. J. 1998. Bacterial Growth Efficiency in Natural Aquatic Systems. *Annual Reviews of Ecology Systems*, 29: 503 – 541.
- Engel A., Borchard C., Loginova A., Meyer J., Hauss H., Kiko R. 2015. Effects of varied nitrate and phosphate supply on polysaccharidic and proteinaceous gel particles production during tropical phytoplankton bloom experiments. *Biogeosciences Discuss.*, 12: 6589 – 6635.
- Gasol J. M., del Giorgio P. A. 2000. Using flow cytometry for counting natural planktonic bacteria and understanding the structure of planktonic bacterial communities. *Scientia Marina*, 64: 197 – 224.
- Gundersen K., Heldal M., Norland S., Purdie D. A., Knap A. H. 2002. Elemental C, N, and P cell content of individual bacteria collected at the Bermuda Atlantic Time-Series Study (BATS) site. *Limnol. Oceanogr.*, 47: 1525–1530.
- Giani M., Sist P., Berto D., Serrazanetti G. P., Ventrella V., Urbani R. 2012. The organic matrix of pelagic mucilaginous aggregates in the Tyrrhenian Sea (Mediterranean Sea). *Marine Chemistry*, 132-133: 83 - 94.
- Herndl G. J., Reinthaler T. 2013. Microbial control of the dark end of the biological pump. *Nature Geoscience* 6 (9), 718–724.
- Innamorati, M., Nuccio, C., Massi, L., Mori, G., Melley, A., 2001. Mucilages and climatic changes in the Tyrrhenian Sea. *Aquat. Conserv. Mar. Freshw. Ecosyst.* 11: 289–298.
- Kirchman D. L., K'nees E., Hodson R. E. 1985. Leucine incorporation and its potential as a measure of protein synthesis by bacteria in natural aquatic systems. *Applied Environmental Microbiology*, 49: 599 - 607.

- Koch B. P., Kattner G., Witt M., Passow U. 2014. Molecular insights into the microbial formation of marine dissolved organic matter: recalcitrant or labile? *Biogeosciences*, 11: 4173 – 4190.
- Kritzberg E. S., Arrieta J. M., Duarte C. M. 2010. Temperature and phosphorus regulating carbon flux through bacteria in a coastal marine system. *Aquatic Microbial Ecology*, 58: 141 – 151.
- Moutin T., Raimbault P. 2002. Primary production, carbon export and nutrients availability in western and eastern Mediterranean Sea in early summer 1996 (MINOS cruise). *Journal of Marine Systems* 33– 34: 273– 288.
- Murphy J., Riley J. P. 1962. A modified single solution method for the determination of phosphate in natural waters. *Analytica Chimica Acta*, 27: 31 – 36.
- Obernosterer I., Herndl G. J. 1995. Phytoplankton extracellular release and bacterial growth: dependence on the inorganic N:P ratio. *Mar. Ecol. Prog. Ser.*, 116: 247 - 257.
- Ogawa H., Amagai Y., Koike I., Kaiser K., Benner R. 2001. Production of Refractory Dissolved Organic Matter by Bacteria. *Science*, 242: 917 – 920.
- Ortega-Retuerta E., Passow U., Duarte C. M., Reche I. 2009. Effects of Ultraviolet B radiation on (not so) Transparent Exopolymer Particles *Biogeosciences*, 6: 3071–3080
- Ortega-Retuerta E., Duarte C. M., Reche I. 2010. Significance of Bacterial Activity for the distribution and dynamics transparent exopolymer particles in the Mediterranean sea. *Microbial Ecology*, 59: 808 – 818.
- Passow U. 2002. Transparent exopolymer particles (TEP) in aquatic environments. *Progress in Oceanography*, 55: 287 – 333.
- Passow U., Alldredge A. L. 1995. A die-binding assay for the spectrophotometric measurement of transparent exopolymer particles (TEP). *Limnology and Oceanography*, 40 (7): 1326 - 1335.
- Passow U., Carlson C. A. 2012. The biological pump in a high CO₂ world. *Marine Ecology Progress Series*, 470: 249 – 271.
- Pedrotti M. L., Peters F., Beauvais S., Vidal M., Egge J., Jacobsen A., Marrasé C. 2010. Effects of nutrients and turbulence on the production of transparent exopolymer particles: a mesocosm study. *Marine ecology Progress Series*, 419: 57 – 69.
- Piontek J., Händel N., Langer G., Wohlers J., Riesebell U., Engel A. 2009. Effects of rising temperature on the formation and microbial degradation of marine diatom aggregates. *Aquatic Microbial Ecology*, 54: 305 – 318.
- Prieto L., Navarro G., Cózar A., Echebarria F., García C. M. 2006. Distribution of TEP in the euphotic and upper mesopelagic zones of the Southern Iberian coasts. *Deep-Sea Research II*, 53: 1314 – 1328.
- Prieto L., Ruiz J., Echevarria F., Garcia C. M., Bartual A., Galvez J. A., Corzo A., Macias D. 2002. Scales and processes in the aggregation of diatom blooms: high time resolution and wide size range records in a mesocosm study. *Deep-Sea Res. I*, 49: 1233 – 1253.
- Pujo-Pay M., Conan P., Oriol L., Cornet-Barthaux V., Falco C., Ghiglione J.-F., Goyet C., Moutin T., Prieur L. 2011. Integrated survey of elemental stoichiometry (C, N, P) from the western to eastern Mediterranean Sea. *Biogeosciences*, 8: 883 – 899.
- Radic T., Kraus R., Fuks D., Radic J., Pecar O. 2005. Transparent exopolymeric particles' distribution in the northern Adriatic and their relation to microphytoplankton biomass and composition. *Science of the Total Environment*, 353: 151 -161.
- Radic T., Ivancic I., Fuks D., Radic J. 2006. Marine bacterioplankton production of polysaccharidic and proteinaceous particles under different nutrient regimes. *FEMS Microbiol. Ecol.*, 58: 333 – 342.
- Radic T., Radic J., Nadjek M., Fuks D., Blazina M. 2003. Potential of the Northern Adriatic bacterioplankton for the production of the transparent exopolymer particles. *Periodicum Biologorum*, 105(4): 381-387.
- Rice E. W., Baird R. B., Eaton A. D., Clesceri L. S. 2012. *Standard Methods for the Examination of Water and Wastewater*, 22nd Edition. 4500-Ultraviolet Spectrophotometric Screening Method. APHA, AWWA, WEF.

Prokaryotic EP production in the Mediterranean Sea

- Robinson C., Steinberg D. K., Anderson T. R., Arístegui J., Carlson C. A., Frost J. R., Ghiglione J.-F., Hernández-León S., Jackson J. A., Koppelman R., Quéguiner B., Ragueneau O., Rassoulzadegan F., Robison B. H., Tamburini C., Tanaka T., Wishner K. F., Zhang J. 2010. Mesopelagic zone ecology and biogeochemistry - a synthesis. *Deep-Sea Research II*, 57: 1504 - 1518.
- Rochelle-Newall E. J., Mari X., Pringault O. 2010. Sticking properties of transparent exopolymeric particles (TEP) during aging and biodegradation. *Journal of Plankton Research*, 32(10): 1433 - 1442.
- Sempéré R., Charriere B., Van Wambeke F., Cauwet G. 2000. Carbon inputs of the Rhone River to the Mediterranean Sea: Biogeochemical implications. *Global Biogeochemical Cycles*, 14: 669-681.
- Simon M., Azam F. 1989. Protein content and protein synthesis rates of planktonic marine bacteria. *Marine Ecology Progress Series*, 51: 201 - 213.
- Smith D. C., Azam F. 1992. A simple, economical method for measuring bacterial protein synthesis rates in seawater using ³H-leucine. *Marine Microbial Food Webs*, 6: 107 - 114.
- StatSoft Inc., 1997. *Statistica for Windows (Computer Program Manual)*. Tulsa, Oklahoma, USA.
- Stoderegger K., Herndl G. J. 1999. Production of exopolymer particles by marine bacterioplankton under contrasting turbulence conditions. *Marine Ecology Progress Series*, 189: 9 - 16.
- Sugimoto K., Fukuda H., Baki M. A., Koike I. 2007. Bacterial contributions to formation of transparent exopolymer particles (TEP) and seasonal trends in coastal waters of Sagami Bay, Japan. *Aquatic Microbial Ecology*, 46: 31 - 41.
- Valderrama J. C. 1981. The simultaneous analysis of total Nitrogen and total phosphorus in natural waters. *Marine chemistry*, 10: 109 - 122.
- Vallino J. J., Hopkinson C. S., Hobbie, J. E. 1996. Modeling bacterial utilization of dissolved organic matter: Optimization replaces Monod growth kinetics, *Limnol. Oceanogr.*, 41, 1591- 1609.
- Van Oostende N., Moerdijk-Poortvliet T. C. W., Boschker H. T. S., Vyverman W. and Sabbe K. 2013. Release of dissolved carbohydrates by *Emiliania huxleyi* and formation of transparent exopolymers particles depend on algal life cycle and bacterial activity. *Environmental Microbiology*, 15(5): 1514- 1531.
- Zoppini A., Bacci C., Fazi S., Pettine N., Tandoi V. 1998. Bacterial utilization of different DOC size classes and demand for inorganic nutrients in the Northern Adriatic Sea. *Fresenius Env. Bull.*, 7: 42 - 50.

Conclusions/Conclusiones (In Spanish)



CONCLUSIONES

1. En el océano global, las concentraciones más elevadas de partículas exopoliméricas las encontramos en las aguas superficiales, normalmente por encima de la profundidad del máximo de clorofila, y a nivel regional en las zonas de surgencias como la de Benguela, el Domo de Costa Rica, o las divergencias ecuatoriales.
2. A escala global, entre las variables biológicas consideradas, la producción primaria integrada fue la variable que explica una mayor parte de la varianza en la concentración de partículas exopoliméricas en el océano superficial.
3. El patrón espacial global observado en el océano superficial se repite en el océano mesopelágico y batipelágico, subrayando la importancia del flujo descendente de partículas exopoliméricas en la distribución global de las mismas. Este flujo descendente se estima que puede suponer entre un 25% y un 40 % de las exportaciones de material orgánico particulado hacia el océano profundo, contribuyendo significativamente con ello a la bomba biológica.
4. La eficiencia de transferencia de partículas exopoliméricas entre el océano superficial y el mesopelágico está alrededor del 35% y entre éste y el batipelágico en torno al 97%, superando puntualmente el 100%. Estas estimas sugieren una elevada atenuación del transporte dentro de la zona mesopelágica y sugieren la existencia de otras entradas de partículas exopoliméricas, diferentes del flujo descendente mayoritariamente fotosintético, en el océano profundo. De hecho, existe en la zona mesopelágica una relación significativa entre la producción heterotrófica procariota integrada y la concentración de partículas exopoliméricas integrada indicando la existencia de síntesis de novo por parte de los procariotas heterotróficos.
5. La producción de partículas exopoliméricas por procariotas heterotróficos ocurre tanto en las aguas superficiales (por encima de la profundidad de exportación) como en las aguas profundas (por debajo de la profundidad de secuestro de carbono). Las tasas de producción de partículas exopoliméricas en términos absolutos fueron más elevadas en el océano superficial, mientras que las tasas de producción específicas (por célula) fueron mayores en el océano profundo a pesar de unas condiciones ambientales mucho más adversas (baja temperatura y disponibilidad de recursos orgánicos). Las estimas del tiempo

de residencia de las partículas exopoliméricas varía desde días en superficie a años en profundidad.

6. La eliminación/disminución del efecto de los virus sobre los procariotas heterotróficos produjo una mayor tasa de producción de partículas exopoliméricas únicamente en las aguas superficiales.
 7. Las eficiencias de crecimiento de los procariotas heterotróficos en la zona mesopelágica de los océanos Atlántico Sur e Índico fueron muy bajas (entre el 0.3 y 3.7%) indicando que la mayor parte de los substratos orgánicos incorporados por los procariotas son mineralizados en esta zona, contribuyendo a la atenuación del flujo de carbono exportado desde las aguas superficiales. Tanto la respiración como la eficiencia de crecimiento de los procariotas heterotróficos estuvo regulada por la temperatura.
 8. En el mar Mediterráneo se observó un patrón vertical similar al de los grandes océanos, con máximos de concentración de partículas exopoliméricas en las aguas superficiales, justo por encima de las profundidades del máximo de clorofila-*a*. Espacialmente, las concentraciones fueron menores en la cuenca oriental que en la occidental o el Atlántico nororiental, destacando máximos alrededor del estrecho de Gibraltar. La distribución espacial en profundidad reflejó en cierta medida el patrón espacial superficial siendo el flujo descendente de partículas exopoliméricas mayor en la cuenca occidental que en la oriental.
 9. Al igual que en el océano global, la producción primaria es uno de los principales predictores de la concentración de partículas exopoliméricas en la superficie del mar Mediterráneo. Sin embargo, en este sistema la contribución de los procariotas heterotróficos es también relevante.
 10. En el mar Mediterráneo, las mayores tasas de producción de partículas exopoliméricas por procariotas heterotróficos se obtuvieron en las aguas levantinas intermedias. Estas producciones pueden verse afectadas por la disponibilidad de nutrientes, especialmente de carbono orgánico de naturaleza lábil.
-

ANNEXES/ANEXOS



ANNEX I/ANEXO I: Abbreviation Index/Índice de Abreviaturas

AB: Great Australian Bight
 A_{blank} : absorption of the blank
 A_{sample} : absorption at 787 nm of the sample
 At: Atlantic
 Bathy-EP= bathypelagic depth-integrated EP concentration
 BOD: biological oxygen demand
 C-EP: carbon content of EP
 chl *a*: chlorophyll *a*
 CTD: conductivity, temperature and depth
 dAPS: dissolved acidic polysaccharides
 Da: Daltons
 DCM: deep chlorophyll maximum
 DMCHO: dissolved neutral monosaccharides
 DNA: deoxyribonucleic acid
 DOA: dissolved oxygen analyzer
 DOC: dissolved organic carbon
 DOM: dissolved organic matter
 DPCHO: dissolved neutral polysaccharides
 DTCHO: dissolved total neutral carbohydrates
 EA: Equatorial Atlantic
 E_a : activation energy
 EM: Eastern Mediterranean
 EMDW = Eastern Mediterranean Deep Water
 EP: exopolymer particles
 EPA: Equatorial Pacific
 EP F_{200} : exopolymer particles flux at 200 m depth
 EP F_{1000} : exopolymer particles flux at 1000 m depth
 Epi-EP= epipelagic depth-integrated EP concentration
 EP $TE_{\text{epi-meso}}$: transfer efficiency of exopolymer particles from epipelagic to mesopelagic waters
 EP $TE_{\text{meso-bathy}}$: transfer efficiency of exopolymer particles from mesopelagic to bathypelagic waters
 EP-TE meso-deep = transfer efficiency of exopolymer particles from mesopelagic to deep waters
 ExpW = water from export depth (above 200 m)
 $E_{\text{DOC} \rightarrow \text{POC}}$ = efficiency to convert DOC into POC
 ETS = electron transport system
 Pg C: petagrams of carbon
 PHA: prokaryotic heterotrophic abundance
 Ind: Indian Ocean
 K: degrees Kelvin

LDOM: labile dissolved organic matter
 LIW = Levantine Intermediate Waters
 Meso-EP= mesopelagic depth-integrated EP concentration
 MLD: mixed layer depth
 MW = Mediterranean Water
 NA: North Atlantic
 NADW = North Atlantic Deep Water
 NEA: Northeast Atlantic
 NP: North Pacific
 MTE: metabolic theory of ecology
 Pac: Pacific
 PAR: photosynthetically active radiation
 PGE: prokaryotic growth efficiency
 PHP: prokaryotic heterotrophic production
 PHP_{int}: integrated prokaryotic heterotrophic production
 PB: prokaryotic biomass
 POC: particulate organic carbon
 %POC: percentage of exopolymer particles in relation to particulate organic carbon
 %POCFlux: percentage of exopolymer particle flux in relation to particulate organic carbon flux
 POM: particulate organic matter
 PON = particulate organic nitrogen
 PP = primary production
 Q₁₀: Q₁₀ temperature coefficient
 PP: primary production
 R: respiration
 r: gases constant
 R_a: fluorescence of the acetone blank
 R_{int}: integrated R in the experiments
 R_s: fluorescence of the sample
 R_{int}: integrated respiration in the experiments
 RDOM: refractory dissolved organic matter
 SA: South Atlantic
 SeqW: water from sequestration depth (below 1000 m depth)
 SLDOM: semilabile organic matter
 SCM: subsurface chlorophyll maximum
 SGR = net specific growth rate
 SW = surface waters
 T: temperature
 TCA: trichloroacetic acid
 T₀: initial incubation time in experiments
 T_f: final incubation time in experiments
 TDN = total dissolved nitrogen

TDP = total dissolved phosphorous
TOC: total organic carbon
TPP: total primary production
VA: viral abundance
WM: Western Mediterranean
WMDW = Western Mediterranean Deep Water
XG: xanthan gum

ANNEX II/ANEXO II: Figure Index/Índice de Figuras

Figure 1. 1. Simplified depiction of the organic carbon fate through three major prokaryotic metabolic pathways: respiration, organic exudation and new biomass production.....	24
Figure 1. 2. Illustration indicating the global estimates for organic matter reservoirs and DOM and prokaryotic mineralization, new biomass generation and growth efficiencies in the epipelagic (from surface to 200 m depth), mesopelagic (200 – 1000 m depth) and deep ocean (> 1000 m).	26
Figure 1. 3. Size continuum of marine organic matter from dissolved to particulate organic matter.	28
Figure 1. 4. Schematic depiction showing the organisms and routes involved in the EP formation and described in the literature. Additionally, the fate of EP in the oceanic water column is also illustrated: mineralization mostly by heterotrophic microbes, sinking down to the deep ocean as ballasted aggregates, persistence in the water column as suspended particles or ascending to the surface as buoyant particles..	30
Figure 1. 5. Map of the Malaspina 2010 cruise showing the stations (where the samples were collected for both the epipelagic and the deep ocean).....	32
Figure 1. 6. Launching of a 24 Niskin bottles rosette coupled to a CTD sensor (at the bottom) from on board the oceanographic R/V Hespérides.	33
Figure 1. 7. Map of the Hotmix cruise showing the sampling stations.	34
Figure 1. 8. Scheme of the used chemical and biological analysis for this dissertation.	37
<hr/>	
Figure 2. 1. Map of the circumnavigation expedition Malaspina 2010 showing the 125 sampling stations distributed in seven legs.....	50
Figure 2. 2. Laboratory procedure to determinate EP concentrations by the colorimetric alcian blue technique.	52
Figure 2. 3. Calibration curve used to relate the absorbance of alcian blue dye at 787 nm with the weight of Xanthan Gum.....	53
Figure 2. 4. Vertical profiles of exopolymer particles in different oceanic basins	62
Figure 2. 5. Geographical distribution of the concentration of exopolymer particles in the epipelagic zone (A) and in the deep ocean (B).....	63
Figure 2. 6. Log-log relationships between depth-integrated EP (A) in the epipelagic and mesopelagic waters and (B) between depth-integrated EP in mesopelagic waters and depth-integrated EP in the bathypelagic waters.	64
Figure 2. 7. Log-log relationship between exopolymer particles and particulate organic carbon including all epipelagic and mesopelagic samples available from this global study.....	65
Figure 2. 8. Log-log relationship between depth-integrated exopolymer particles concentration and depth-integrated primary production in the epipelagic zone.	68
Figure 2. 9. Log-log relationship between depth-integrated EP concentrations and PHP in the mesopelagic zone.	71
Figure 2. 10. Distribution along the circumnavigation Malaspina 2010 of the exopolymer particles fluxes at 200 m (A), EP transfer efficiency to mesopelagic waters (B) and EP contribution to total POC (C). Log-log relationships between depth-integrated EP in the mesopelagic waters and the estimated EP fluxes at 200 m (D), EP transfer efficiency from epipelagic to mesopelagic waters (E) and EP contribution to the total POC fluxes at 200 m (F).	75
Figure 2. 11. Distribution along the circumnavigation Malaspina 2010 of the exopolymer particles fluxes at 1000 m (A), EP transfer efficiency to bathypelagic waters (B) and EP contribution to total POC (C). Log-log relationships between depth-integrated EP in the bathypelagic waters and the estimated EP fluxes at 1000 m (D), EP transfer efficiency from mesopelagic to bathypelagic waters (E) and EP contribution to the total POC fluxes at 1000 m (F)..	76
<hr/>	
Figure 3. 1. Scheme of the experimental set-up and the different sequential filtrations.	101

Figure 3. 2. Time changes of the virus abundance, prokaryotic heterotrophic abundance and production in control treatments and in the treatments with a manipulation of the viral load for the three experiments conducted with waters located above the export depths in the Atlantic, Indian and Pacific Oceans.	107
Figure 3. 3. Time changes of the virus abundance, prokaryotic heterotrophic abundance and production in control treatments and in the treatments with a manipulation of the viral load for the three experiments conducted with waters located below the sequestration depths in the Atlantic, Indian and Pacific Oceans. ...	110
Figure 3. 4. Changes of EP concentrations throughout incubation time in the experiments conducted with waters from above the export depths.	111
Figure 3. 5. Changes of the cell-specific EP production throughout incubation time in the experiments conducted with waters from above the export depths.	112
Figure 3. 6. Changes of EP concentrations throughout incubation time in the experiments conducted with waters from below the sequestration depths.	113
Figure 3. 7. Changes of the cell-specific EP production throughout incubation time in the experiments conducted with waters from below the sequestration depths.	114
Figure 3. 8. Log-log relationships between integrated PHP and (A) production of neutral polysaccharides, (B) production of dissolved acidic polysaccharides and (C) production of exopolymer particles.	115

Figure 4. 1. Location of the stations selected for the respiration experiments.	140
Figure 4. 2. Process of O ₂ fixation in BOD bottles and titration with the Dissolved Oxygen Analyzer DOA SiS® titrator.	144
Figure 4. 3. Representative example of the changes in the leucine incorporation rate and the O ₂ concentration along the experiment performed at station I1 located in the Indian Ocean at 430 m depth.	146
Figure 4. 4. Log-log relationship between integrated prokaryotic heterotrophic production and integrated community respiration in the in vitro experiments.	148
Figure 4. 5. Relationships between temperature and respiration rates and prokaryotic growth efficiencies in the in vitro experiments.	150
Figure 4. 6. Arrhenius plot showing the effect of temperature on the deep ocean R data found in the literature, including also this study data.	151
Figure 4. 7. Scatterplot of prokaryotic growth efficiencies, derived from direct estimates of R and PHP, as function of temperature for deep ocean prokaryotes found in the literature including this study.	154

Figure 5. 1. Map showing the sampling stations during the Hotmix cruise.	172
Figure 5. 2. Depth profiles of exopolymer particles in the three basins.	179
Figure 5. 3. Distribution of exopolymeric particles, in a depth-section from Eastern to Western Mediterranean Sea and Northeast Atlantic Ocean.	181
Figure 5. 4. Log-log relationships (A) between depth-integrated EP concentration in the surface waters and in the mesopelagic waters and (B) between depth-integrated EP in the mesopelagic zone and in deep waters below 1000 m depth.	182
Figure 5. 5. Log-log scatterplot between the EP concentrations and (A) particulate organic carbon and (B) particulate organic nitrogen.	183
Figure 5. 6. Log-log scatterplot between depth-integrated EP distribution in the surface waters and primary production.	185
Figure 5. 7. Log-log scatterplot (A) between depth-integrated EP distribution in the surface waters (SW-EP) and picocaryote abundances; (B) between SW-EP and depth-integrated PHP in the surface waters and (C) between SW-EP and depth-integrated PHA in the surface waters.	187
Figure 5. 8. Log-log scatterplot between (A) depth-integrated EP concentration and heterotrophic prokaryotic abundance (Meso-PHA) in the mesopelagic waters; and (B) between depth-integrated EP distribution (Deep-EP) and heterotrophic prokaryotic abundance in waters below 1000 m depth.	189

Figure 5. 9. Log-log scatterplot between (A) depth-integrated EP concentration and heterotrophic prokaryotic abundance in the Levantine intermediate waters; and (B) between depth-integrated EP distribution and heterotrophic prokaryotic production in the Levantine intermediate waters.....	190
Figure 5. 10. Distribution along the Hotmix cruise track of the fluxes of exopolymer particles at 200 m (A), EP transfer efficiencies from epipelagic to mesopelagic waters (B) and EP contribution to POC fluxes at 200 m (C). Log-log relationships between depth-integrated EP in the mesopelagic waters and EP fluxes at 200 m (D), EP transfer efficiency from epipelagic to mesopelagic waters (E) and EP contribution to POC fluxes at 200 m (F).....	193
Figure 5. 11. Distribution along the Hotmix cruise track of the fluxes of exopolymer particles at 1000 m (A), EP transfer efficiencies from mesopelagic to deep (> 1000 m) waters (B) and EP contribution to POC fluxes at 1000 m (C). Log-log relationships between depth-integrated EP in the deep waters and the estimated EP fluxes at 1000 m (D), EP transfer efficiency from mesopelagic to deep waters (E) and EP contribution to POC fluxes at 1000 m (F)..	194
Figure 5. 12. Log-log scatterplot between (A) median temperature in the upper 200 m depth and fluxes of exopolymer particles at 200 m depth and between (B) median temperature in the upper 1000 m depth and fluxes of exopolymer particles at 1000 m depth.....	201
<hr style="border-top: 1px dashed black;"/>	
Figure 6. 1. Location of the stations where water was collected for the experiments..	215
Figure 6. 2. Time evolution of prokaryotic heterotrophic abundance and production for the experiments conducted with Levantine Intermediate Water and Deep Water in the Western Mediterranean Sea..	222
Figure 6. 3. Time evolution of prokaryotic heterotrophic abundance and production for the EM-SW and EM-LIW experiments.	223
Figure 6. 4. Changes in EP concentrations and cell-specific EP production in the experiments conducted with waters of the Western Mediterranean basin.....	227
Figure 6. 5. Changes in EP concentrations and cell-specific EP production in the experiments conducted with waters of the Eastern Mediterranean basin.....	228
Figure 6. 6. Log-Log relationships between ΔEP and ΔPHA (A), SGR (B) and PHP_{int} (C).....	229
Figure 6. 7. Log-Log relationship between ΔPOC and ΔEP	230

ANNEX III/ANEXO III: Table Index/Índice de Tablas

Table 2. 1. Carbon content of the exopolymer particles in the epipelagic, mesopelagic and bathypelagic waters and their corresponding percentage of the POC pool	66
Table 2. 2. Results of the log-log regression analyses in the epipelagic waters between exopolymer particles and phytoplankton.....	69
Table 2. 3. Results of the log-log regression analyses in the epipelagic waters between exopolymer particles and heterotrophic prokaryotes and viruses.....	70
Table 2. 4. Results of the log-log regression analyses in the mesopelagic waters between exopolymer particles and biological variables.....	71
Table 2. 5. Transfer efficiencies of exopolymer particles from epipelagic to mesopelagic waters and from mesopelagic to bathypelagic waters, as well as the estimated EP fluxes and their percentages relative to the total POC fluxes at 200 m and 1000 m depths,	74
Table 2. 6. Compilation of the exopolymer particles concentrations reported from the literature.....	81
<hr/>	
Table 3. 1. Location of the sampling stations, environmental conditions of the water collected to perform the experiments and conditions at the onset of experiments	106
Table 3. 2. Mean values of the daily increments in viral abundance, prokaryotic heterotrophic abundance, integrated prokaryotic heterotrophic production, dissolved acidic polysaccharides, dissolved neutral carbohydrates, exopolymer particles and VA:PHA ratios in the experiments.	108
Table 3. 3. Results of ANOVAs in the experiments to determine if the differences in EP concentrations over time and between treatments.....	117
Table 3. 4. Results of ANOVAs in the experiments to determine if the differences in the cell-specific EP concentrations over time and between treatments	118
Table 3. 5. Estimations of in situ EP production rates and residence times at the depths of the different experiments and in the different ocean basins.....	119
<hr/>	
Table 4. 1. Stations' location in the South Atlantic and Indian Oceans and water mass properties at the sampling depths where time-series experiments were performed.....	141
Table 4. 2. Integrated community respiration rate and prokaryotic heterotrophic production estimated over the incubation times in the experiments. The prokaryotic growth efficiencies are also included. T = Incubation Temperature.....	147
Table 4. 3. Prokaryotic heterotrophic abundance and production, prokaryotic biomass, turnover time, back-scaled respiration rates and resulting growth efficiencies corresponding to the in situ conditions.	149
Table 4. 4. Reported prokaryotic growth efficiencies in the dark ocean, derived from direct measurements of both prokaryotic heterotrophic production and respiration, indicating the different approaches.....	152
Table 4. 5. The slopes of the regression and the parameters of the Arrhenius plot between Ln of respiration rate and inverse of temperature, $\text{Ln}(R) = a - b(1/kT)$, for in situ data in this study and all data in the literature. The Q_{10} temperature coefficients are also shown.....	153
<hr/>	
Table 5. 1. Median and ranges of carbon content of exopolymer particles in the surface, mesopelagic and deep waters (> 1000 m) and their respective percentage of the POC pool.	184
Table 5. 2. Results of log-log regression analyses between exopolymer particles and biological drivers in surface waters (upper 150 m).....	186
Table 5. 3. Results of log-log regression analyses between exopolymeric particles and biological variables in the mesopelagic and in deep waters (> 200 m depth). Regressions in the Levantine Intermediate Waters are also included.....	188
Table 5. 4. Fluxes of exopolymer particles at 200 m and 1000 m; the transfer efficiencies of exopolymer particles (EP) from epipelagic to mesopelagic waters, from mesopelagic to deep waters > 1000 m depth and the contribution of EP to POC fluxes at 200 m and 1000 m.	192

Table 6. 1. <i>Sample information, in situ environmental conditions of the water samples and prokaryotic parameters and nutrients at the onset of the time-series experiments.....</i>	220
Table 6. 2. <i>Microbial parameters in the different experiments.....</i>	221
Table 6. 3. <i>Daily increments of dissolved organic carbon, particulate organic carbon and exopolymer particles concentrations. Changes of total dissolved nitrogen and total dissolved phosphorous. Prokaryotic efficiency to convert DOC into POC is also presented.</i>	225
Table 6. 4. <i>Estimated in situ EP generation rates and residence times at the depth of the experiments and in the Eastern and Western Mediterranean basins</i>	231

ANNEX IV/ANEXO IV: LIBRO BLANCO DE MÉTODOS Y TÉCNICAS DE TRABAJO OCEANOGRÁFICO.

- 1) Mazuecos I. P., Ortega-Retuerta E., Reche I. 2012. Medida de Partículas Exopoliméricas Transparentes (TEP) en agua marina, in: *EXPEDICIÓN DE CIRCUNNAVEGACIÓN MALASPINA 2010: CAMBIO GLOBAL Y EXPLORACIÓN DE LA BIODIVERSIDAD DEL OCÉANO GLOBAL. LIBRO BLANCO DE MÉTODOS Y TÉCNICAS DE TRABAJO OCEANOGRÁFICO*. CSIC, Enrique Moreno-Ostos (eds.), p. p. 515 - 520.

 - 2) Arístegui J., Mazuecos I. P., Vázquez-Domínguez E. 2012. Medida de la respiración mediante cambios *in vitro* de la concentración de O₂, in: *EXPEDICIÓN DE CIRCUNNAVEGACIÓN MALASPINA 2010: CAMBIO GLOBAL Y EXPLORACIÓN DE LA BIODIVERSIDAD DEL OCÉANO GLOBAL. LIBRO BLANCO DE MÉTODOS Y TÉCNICAS DE TRABAJO OCEANOGRÁFICO*. CSIC, Enrique Moreno-Ostos (eds.), p. p. 565 - 573.
-

Medida de Partículas Exopoliméricas Transparentes (TEP) en agua marina

¹Mazuecos, I. P.; ²Ortega-Retuerta, E.; ¹Reche, I.

¹ *Departamento de Ecología, Universidad de Granada*

² *Laboratoire d'Océanographie Microbienne, Banyuls sur mer, France.*

Finalidad. Campo de aplicación

Protocolo de recogida de muestras de agua marina para el análisis de TEP. Las concentraciones de TEP se determinarán usando el método colorimétrico propuesto por Passow y Alldredge (1995). Los TEP se analizarán en muestras *in vivo*, aunque también pueden ser analizados en muestras fijadas con formol (~ 1% final).

Conceptos generales

Dentro de las sustancias exopoliméricas, las partículas exopoliméricas transparentes (TEP) son partículas de naturaleza adhesiva, y susceptibles de ser teñidas con azul alcian (Alldredge et ál. 1993). Estas partículas se forman predominantemente por la polimerización abiótica de precursores disueltos, principalmente mono- y polisacáridos de naturaleza ácida. Las TEP son excretadas por microorganismos y tradicionalmente se han asociado a *blooms* de fitoplancton (Passow y Alldredge, 1994; Passow, 2000). Sin embargo, las bacterias también producen TEP, aunque a su vez pueden consumirlas.

De este modo, las TEP contribuyen de forma significativa al flujo descendente de materia orgánica en sistemas marinos, ya que debido a su alta adhesividad actúan como una matriz intersticial generando agregados macroscópicos, formados por compuestos orgánicos e inorgánicos que son conocidos como *nieve marina*. La formación y sedimentación de nieve marina es una ruta principal de retirada de carbono de la superficie del océano hacia aguas profundas (Alldredge et ál. 1993, Passow et ál. 2001; Passow, 2002).

Equipamiento necesario

- Tubo de silicona.
- Botellas Nalgene 2 l (de polipropileno).
- Bomba de vacío.
- Rampa de filtración.
- Kitasato de seguridad (de polipropileno) con tapón perforado para conectar a la bomba.
- Filtros de policarbonato de 0.4 μm de tamaño de poro (\varnothing 25 mm).
- Pinzas para filtros.
- Pipetas de 1 y 5 ml.
- Botes de vidrio de 20 ml o algo similar para la extracción.
- Espectrofotómetro.
- Cubetas desechables de 1 cm.
- Botes de polipropileno para preparar disoluciones de azul alcian.
- Balanza de alta precisión para la preparación de la curva de calibración (precisión de 0.0001 mg).
- Ionizador.
- Vasos de precipitado 500 ml.
- Probeta de 200-500 ml.
- Filtros de jeringa de 0.2 μm de tamaño de poro.
- Jeringas (10 y 20 ml).
- Frasco lavador para el agua ultrapura (Milli-Q).
- Guantes.
- Viales para introducir los filtros.
- Cajas de plástico para almacenar los viales en el congelador.
- Estadillo de recogida de muestras.
- Material de papelería (rotuladores, bolígrafos, lápices...).
- Bandeja.
- Homogeneizador de tejidos para preparar la solución de calibración de goma de xantano.

Reactivos u otro material fungible

- a) *Tinción*: las TEP se tiñen con azul alcian (conjunto de colorantes básicos polivalentes derivados de la "ftalocianina" que son solubles en agua). En una solución con ácido acético (pH = 2.5), el azul alcian tiñe a los grupos carboxílicos y éster-sulfato de los mucopolisacáridos ácidos, para los cuales es uno de los colorantes catiónicos más ampliamente usado. Las partes teñidas son de color azulado debido a la presencia de cobre en la molécula.

Reactivos:

- Solución de azul alcian para la tinción de TEP:
 - a. Azul alcian (0.02 %).
 - b. Ácido acético (0.06 %).

Preparación de la solución stock de azul alcian para 50 ml de esta solución: en botes de polipropileno (PET) añadir 0.5 g de azul alcian, seguidamente 1,5 ml de ácido acético y el resto se completa con agua ultrapura hasta 50 ml.

Preparación de la solución de trabajo de azul alcian: se diluye la solución anterior 1: 50. Ejemplo: 20 ml de stock + 980 ml de agua ultrapura. Finalmente, con una jeringuilla a través de filtros de 0.2 μm desechables se filtrará la solución de trabajo.

b) *Extracción del azul alcian de los filtros teñidos:***Reactivos:**

- Ácido sulfúrico (80%).

c) *Solución patrón para realizar la curva de calibración:***Reactivos:**

- Goma de xantano (0.1 mg ml⁻¹) o ácido algínico, ya que generan partículas similares a las TEP y dan buenos resultados colorimétricos.

Preparación de la solución de goma de xantano: pesar aproximadamente 15 – 20 mg de goma de xantano y añadir 200 ml de agua ultrapura. A continuación se pasa la solución por el homogeneizador (con tres o cuatro pasadas de pistón se obtendrá una disolución homogénea de la goma de xantano). Se deja reposar a ~ 4 °C, y se vuelve a pasar otra vez por el homogeneizador.

Calibración

Curva de calibración de goma de xantano (y/o ácido algínico): Con la solución de goma de xantano (y/o ácido algínico) se calculará la concentración exacta filtrando volúmenes conocidos (e. g. 1, 2, 4, y 8 ml) a través de filtros de policarbonato de 0.4 μm de tamaño de poro, que se pesarán antes y después (al menos 3 veces) de la filtración. De igual modo, se filtrarán volúmenes semejantes (e. g. 1, 2, 4, y 8 ml) de solución patrón de goma de xantano para teñir los filtros con azul alcian y se leerá la absorbancia del extracto obtenido a 787 nm. Por último, con la relación de la ab-

sorbancia a 787 nm y los μg de goma de xantano (obtenidos con la diferencia de pesadas antes y después de filtrar) se realizará la curva de calibración.

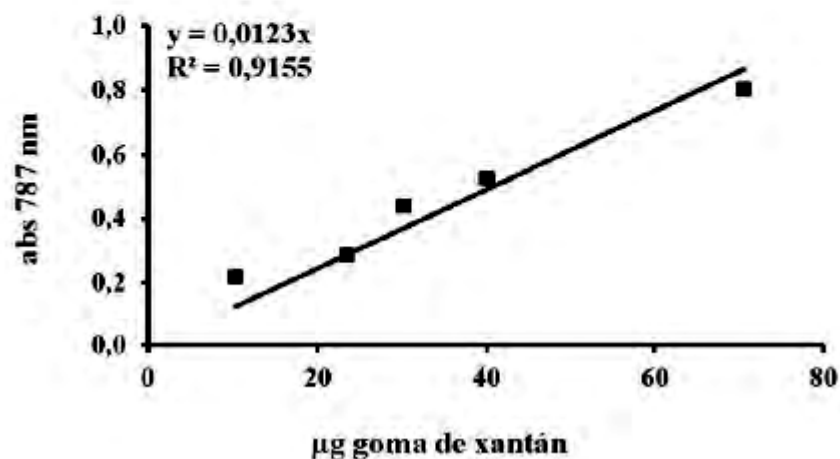


Figura 1. Ejemplo de curva de calibración absorbancia 787 nm vs μg de goma de xantano.

Descripción de la técnica

Pasos a seguir:

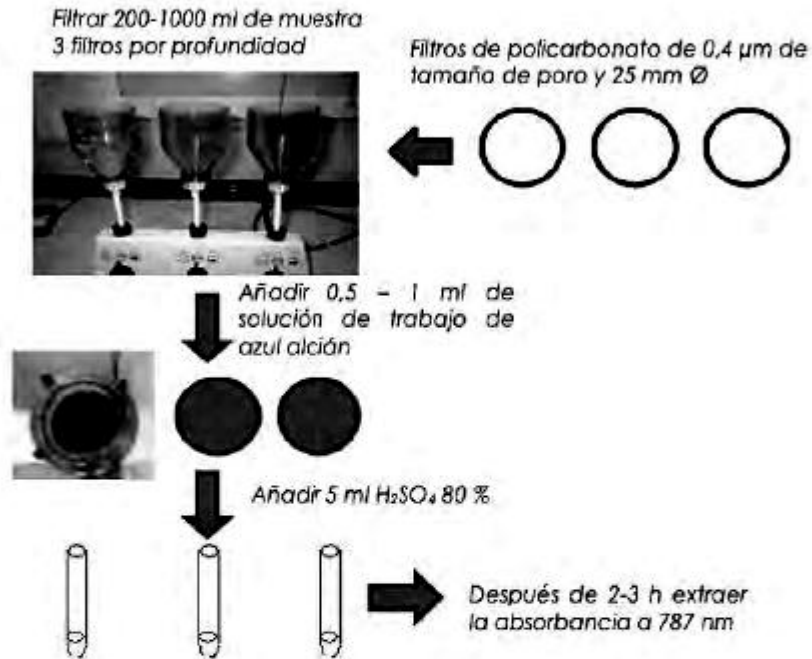
- Preparación de solución de trabajo de azul alcian.
- Recoger el agua en botellas Nalgene de 2 l para cada muestra.
- Filtrar 200-1000 ml de muestra (según saturación del filtro) a través de filtros de policarbonato de $0,4 \mu\text{m}$ de tamaño de poro. Tres filtros (réplicas) por profundidad. Usar una presión no muy alta ($\sim 150 \text{ mm}$ de Hg) con ritmo constante.
- Tinción: Teñir el filtro con $0,5 - 1 \text{ ml}$ de solución de trabajo de azul alcian (que lo cubra completamente). Dejar unos 5 segundos. Filtrar la solución de azul alcian y enjuagar con agua ultrapura filtrada por $0,2 \mu\text{m}$.

Nota: en este paso los filtros podrían ser congelados durante más de 6 meses a $-20 \text{ }^\circ\text{C}$ o $-80 \text{ }^\circ\text{C}$ (Passow y Alldredge, 1995).

Por último, los filtros teñidos con azul alcian se colocarán en tubos de ensayo y se añadirá 5 ml de H_2SO_4 al 80% para la extracción. El extracto se agitará al menos un par de veces para facilitar la extracción. Y después de 2-3 h se leerá la absorbancia de dicho extracto a 787 nm usando cubetas desechables.

Esquema y cuadro sinóptico de la técnica

Filtración y tinción de TEP



Cálculo de los resultados

La curva de calibración nos permite calcular el factor de calibración (que es la inversa de la pendiente de la curva que obtuvimos en el apartado de calibración). Con este factor de calibración junto con el volumen (L) filtrado de muestra y los datos de absorbancia (a 787 nm) obtenidos anteriormente podremos calcular la concentración de partículas exopoliméricas transparentes (C_{TEP}) expresadas como µg de equivalentes de goma de xantano (XG) por litro (µg XG eq L⁻¹):

$$C_{TEP} = (A_{muestra} - A_{blanco}) V^{-1} F$$

Donde A_{muestra} es la absorbancia de la muestra, A_{blanco} es la absorbancia del blanco, V el volumen filtrado de muestra y F es el factor de calibración. El factor de calibración F se calcula de la siguiente forma:

$$F = W \times [(A_{787} - C_{787}) \times V^{-1}]^{-1}$$

Donde F es el factor de calibración, W es la concentración de la solución de goma de xantano en $\mu\text{g l}^{-1}$, A_{787} es la absorbancia del extracto a 787 nm, C_{787} es la absorbancia del blanco y V es el volumen filtrado en l.

Control de calidad

Al inicio de cada grupo de muestras hacer un blanco filtrando agua ultrapura y tiñendo igual que el resto de las muestras. El valor de absorbancia (787 nm) de los blancos será sustraído al valor total de la absorbancia de las muestras, para eliminar la capacidad del azul alcian de teñir el filtro vacío. Después de un mes de uso de la solución de azul alcian, preparar otra solución nueva debido a que podría haber perdido parte de su capacidad de tinción. El límite de detección del método es de $2.2 \mu\text{g XG eq l}^{-1}$ y el coeficiente de variación es de 13 %.

Referencias

- ALLDREDGE, A. L., U. PASSOW, B. E. LOGAN. 1993. «The abundance and significance of a class of large, transparent organic particles in the ocean». *Deep-sea Res. I.* 40: 1131-1140.
- PASSOW, U., A. L. ALLDREDGE. 1995. «A dye-binding assay for the spectrophotometric measurement of transparent exopolymer particles (TEP)». *Limnol. Oceanogr.* 40: 1326-1335.
- PASSOW, U., A. L. ALLDREDGE. 1994. «Distribution, size and bacterial colonization of transparent exopolymer particles (TEP) in the ocean». *Mar. Ecol. Progr. Ser.* 113: 185-198.
- PASSOW, U. 2000. Formation of transparent exopolymer particles, TEP, from dissolved precursor material. *Mar. Ecol. Progr. Ser.* 192: 1-11.
- PASSOW, U. 2002a. Production of transparent exopolymer particles (TEP) by phyto- and bacterioplankton. *Mar. Ecol. Progr. Ser.* 236: 1-12.
- PASSOW, U. 2002b. Transparent exopolymer particles (TEP) in aquatic environments. *Progr. Oceanogr.* 55: 287-333.
- PASSOW, U., R. F. SHIPE, A. MURRAY, D. K. PAK, M. A. BRZEZINSKI, A. L. ALLDREDGE. 2001. «The origin of transparent exopolymer particles (TEP) and their role in the sedimentation of particulate matter». *Cont. Shelf Res.* 21: 327-346.

Medida de la respiración mediante cambios *in vitro* de la concentración de O₂

¹Aristegui, J.; P. Mazuecos², I.; Vázquez-Domínguez^{3,4}, E.

¹*Instituto de Oceanografía y Cambio Global, Universidad de Las Palmas de Gran Canarias*

²*Departamento de Ecología Facultad de ciencias, Universidad de Granada*

³*Departamento de Biología Marina y Oceanografía, Institut de Ciències del Mar (CSIC)*

⁴*C.O. Gijón. Instituto Español de Oceanografía*

Finalidad. Campo de aplicación

Determinación de la respiración en el océano profundo mediante cambios en la concentración de oxígeno disuelto dentro de botellas, utilizando el método Winkler.

El oxígeno es un elemento directamente relacionado con el metabolismo aeróbico de los organismos vivos. Se produce en reacciones anabólicas tales como la fotosíntesis y se consume en reacciones catabólicas como la respiración. Por tanto, la determinación de su concentración en medio acuático proporciona información muy valiosa sobre los procesos biológicos y balances metabólicos en ecosistemas acuáticos.

Aunque la determinación química de oxígeno disuelto en muestras de agua fue descrita por primera vez en el siglo XIX (Winkler, 1888), las medidas de metabolismo planctónico basadas en cambios en la concentración de oxígeno no fueron introducidas hasta el inicio del siglo XX por Gardner y Gran (1927). El método Winkler está basado en que el oxígeno de las muestras de agua marina oxida el ión yoduro a yodo y la cantidad de yodo generado es determinado mediante titración con una solución de concentración conocida de tiosulfato sódico. La cantidad de oxígeno disuelto se calcula a partir del volumen de tiosulfato añadido durante la titración hasta alcanzar el punto final. Este método ha sido uno de los más usados, no solo por su simplicidad, sino también debido a su precisión; sobre todo gracias al desarrollo de sistemas automatizados con detección del punto final de la valoración, bien potenciométrica o colorimétrica, que han aumentado considerablemente la sensibilidad del método.

Conceptos generales

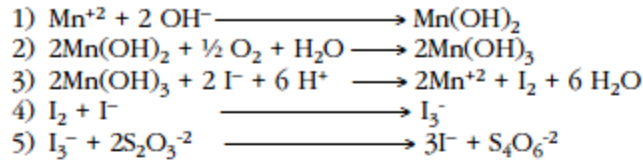
La técnica que se describe en este protocolo está basada en la incubación de muestras de agua de mar en botellas DBO (Demanda Biológica de Oxígeno) de c.a. 100 ml de capacidad. Varias de estas botellas son usadas para establecer la concentración inicial de oxígeno (Botellas iniciales; Bi), mientras que otra serie de botellas se incuban en oscuridad a temperatura in situ ($\pm 0,1$ °C) durante aproximadamente 24-72 h (Botellas oscuras: Bo). La respiración se obtiene, bien mediante la diferencia en la concentración de oxígeno entre el tiempo inicial y final del experimento, o como la pendiente de la recta de regresión debida a la disminución de oxígeno a lo largo del tiempo (e. g. Arístegui et ál. 2005).

Para evitar problemas de interacción entre la fase acuosa y la atmósfera es muy importante que las botellas estén completamente sumergidas en agua (por encima del tapón) durante la incubación, incluso una vez que se han fijado las muestras y hasta el momento de ser valoradas. Si no, podría haber intercambio de gases entre el aire y el agua de las botellas (por diferencias en la presión parcial de los gases), creándose burbujas de aire que alterarían la concentración de oxígeno o el volumen real de líquido a valorar.

Para la preparación y dosificación de los reactivos que se añaden al agua de mar para fijar la muestra, se siguieron las recomendaciones hechas por Carpenter (1965) y Carrit y Carpenter (1966). La detección del punto final de la valoración Winkler se llevará a cabo espectrofotométricamente, mediante un sistema comercial (DOA SiS) automatizado, controlado por un microprocesador, basado en el sistema descrito por Williams y Jenkinson (1982).

Las reacciones que tienen lugar para la determinación de la concentración de oxígeno disuelto son las siguientes:

Una vez añadidos el reactivo 1 –sulfato de manganeso (MnSO_4)– y el reactivo 2 –solución alcalina de yoduro e hidróxido sódico ($\text{NaOH} + \text{NaI}$ –, las botellas son cerradas cuidadosamente (evitando la aparición de burbujas) y agitadas vigorosamente (para facilitar la reacción). El oxígeno disuelto químicamente reacciona con $\text{Mn}(\text{OH})_2$ en un fuerte medio alcalino resultando en un precipitado marrón de $\text{Mn}(\text{OH})_3$. Después de la fijación y precipitación completa del oxígeno, las botellas permanecen en reposo (bajo el agua) unas horas antes de su análisis. Previamente al análisis, la muestra es acidificada a pH 2.5 – 1.0, provocando que los hidróxidos precipitados sean disueltos, liberando Mn^{+3} . Los iones Mn^{+3} oxidan el yoduro (I^-) a yodo (I_2). El yodo forma un complejo con el exceso de los iones yoduro, siendo determinado mediante titración con tiosulfato ($\text{S}_2\text{O}_3^{2-}$) que es oxidado a tetrionato ($\text{S}_4\text{O}_6^{2-}$).



La fijación de oxígeno es una reacción muy rápida debido a la inestabilidad del Mn^{+2} en medio alcalino.

El método está descrito en detalle en Strickland y Parsons (1977).

Equipamiento necesario

- Analizador de oxígeno disuelto (DOA) de "Sensoren Instruments Systems" compuesto por:
 - Bureta Dosimat (Methrom) para dosificar el tiosulfato.
 - Soporte para botella con agitador magnético.
 - Espectrofotómetro con lámparas y fotomultiplicador.
 - Unidad de control e interfaz A/D.
 - Ordenador PC con "software DOA SiS" para controlar automáticamente la valoración.
- Botellas de borosilicato DBO.
- Baño termostatzado / refrigerado con cubeta para incubar las muestras.
- Agitadores magnéticos (recubiertos de cristal) y varilla para recogerlos.
- Pipetas automáticas de repetición eppendorf (con cánulas de 12.5 ml) para dispensar los reactivos 1 y 2 (o bien dosificadores de precisión de 1 ml).
- Pipeta automática (y puntas) de 1 ml para dosificar el ácido.
- Bureta Dosimat (Methrom) para dosificar el yodato potásico.
- Botes Pyrex para almacenar reactivos. El reactivo 2 es fotosensible, la botella debe ser ámbar (opaca) o recubierta con papel de aluminio.
- Tubos de silicona para llenar las botellas DBO.
- Ácido clorhídrico y barreño con tapa para lavar las botellas DBO.
- Barreño para mantener las botellas sumergidas en agua antes de valorarlas.
- Termómetro.
- Guantes.
- Bata y gafas de seguridad.
- Botellas para residuos de reactivos (p. e. tiosulfato sódico).

Reactivos u otro material fungible

Reactivos:

- *Reactivo 1* (para fijar el O₂ de las muestras): Sulfato de manganeso (MnSO₄ · 4 H₂O).
- *Reactivo 2* (para fijar el O₂ de las muestras): Solución alcalina compuesta por hidróxido sódico (NaOH) y yoduro sódico (NaI).
- Ácido sulfúrico (H₂SO₄), para acidificar la muestra previa a su valoración.
- Tiosulfato sódico (Na₂S₂O₃ · 5 H₂O), para la valoración del O₂.
- Yodato potásico (KIO₃), para la estandarización del tiosulfato.

Preparación de reactivos:

Los reactivos deben mantenerse en el frigorífico (~ 4 °C) mientras no se usen.

Reactivo 1: Disolver 450 g de sulfato de manganeso MnSO₄ · 4H₂O en 500 ml de agua destilada en una botella de 1 l. Aforar a 1 l con agua destilada y almacenar en una botella de cristal con tapón a rosca (Pyrex).

Reactivo 2: (NaI+NaOH, solución alcalina de yoduro sódico): disolver 320 g de NaOH en 400 ml de agua destilada en una botella de 2 l. Esperar a que se enfríe y entonces añadir 600 g de NaI (mezclar muy bien para disolver). Una vez fría, la solución es transferida a un matraz aforado de 1 l y rellenada con agua destilada. Almacenar en botella de cristal con tapón de plástico a rosca (Pyrex).

Ácido sulfúrico H₂SO₄ 5 M: 280 ml de ácido sulfúrico en 500 ml de agua destilada en una botella de 1 l. La solución es almacenada fría y entonces llevada a 1 l con agua destilada.

Nota: si este reactivo toma un color extraño, debe ser preparado de nuevo.

Solución de tiosulfato sódico 0.25 M: disolver 62.04 g Na₂S₂O₃ · 5H₂O en un 1 l de agua destilada. La solución es almacenada en una botella ámbar con el tapón a rosca.

Estándar de yodato potásico, 0.001666 M: secar ~ 0.5 g KIO₃ a 105 °C durante 1 h. Esperar a que se enfríe y pesar exactamente 0.3567 g de KIO₃. Disolver en 100 ml de agua destilada y llevar a 1 l con agua destilada.

Nota: En el caso de que se use un estándar certificado 0.1 N de KIO₃, concentración final de una ampolla de 100 ml [titrisol Merck] es llevada hasta 1 l con agua ultrapura (Milli-Q). Esta solución es diluida a 0.01 N con agua ultrapura antes de usarla como estándar.

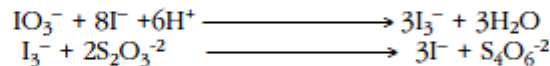
Calibración

Calibración del volumen de las botellas DBO

Para determinar el volumen exacto de las botellas de borosilicato DBO, se deben pesar vacías y llenas de agua ultrapura (controlando la temperatura del agua) en una balanza de alta precisión ($300 \pm 0.0001\text{g}$). El volumen se determina a partir de la diferencia de ambos pesos, corrigiendo para el coeficiente de expansión de borosilicato, obtenido a partir de la densidad del agua (Kell, 1975). La calibración del volumen de las botellas DBO debe ser realizado de forma muy precisa, ya que la precisión del método depende de ello.

Estandarización del tiosulfato

El tiosulfato puede variar su molaridad por diversos motivos (e. g. cambios bruscos de temperatura), por lo que es conveniente estandarizarlo frecuentemente, y siempre una vez que se preparan reactivos nuevos. Para ello se utiliza una solución estándar de yodato potásico (KIO_3). Bajo condiciones ácidas el yodato reacciona con los iones yoduro hacia yodo, el cual es titrado con tiosulfato.



Para la estandarización se añaden los reactivos en orden inverso: Primero añadir 1 ml de H_2SO_4 , seguido por 1 ml de solución alcalina (reactivo 2) y por último 1 ml de sulfato de manganeso (reactivo 1) sobre 80-100 ml de agua ultrapura o agua marina contenida dentro de una botella BDO. Después se añaden 10 ml de la solución estándar de yodato potásico con una bureta Dosimat (o similar) con una precisión superior a $1 \mu\text{l}$. Es muy importante agitar y mezclar bien la muestra entre dosificaciones. El yodo se valora con la solución de tiosulfato apropiada y la molaridad se calcula como sigue:

$$M_t = (V_1 \times M_1 \times 6) / V_t$$

Donde M_t : molaridad del tiosulfato (M), V_t : volumen de tiosulfato añadido (l), V_1 : volumen de estándar de yodato potásico añadido (ml) y M_1 : molaridad del estándar del yodato (M).

Blancos

Para probar que los reactivos están en buenas condiciones, se deben llevar a cabo controles esporádicos, añadiendo los reactivos de forma inversa; similar al proceso de estandarización, pero sin añadir el yodato potásico. Si el resultado del proceso produce color en los reactivos (debe de estar totalmente transparente) habría que cambiar de reactivos.

Descripción de la técnica

Toma de muestras y preparación de incubaciones

Las muestras de agua de mar se recogen mediante botellas Niskin y se vierten a una garrafa de plástico (20 l). Para evitar problemas de subsaturación, la garrafa se agita suavemente antes de dispensar el agua con una manguera de silicona, de forma homogénea, en las botellas para DBO. El extremo del tubo de silicona se coloca en el fondo de la botella para eliminar las burbujas de aire que podrían permanecer dentro. Las botellas deben ser llenadas dispensando al menos 2 veces su volumen de agua, y de forma aleatoria. Una vez llenadas, las botellas se colocan en el incubador (baño termostatzado) para comenzar el experimento de respiración. El proceso de llenado debe realizarse en una zona fresca / fría y en penumbra, evitando la luz directa en las garrafas y las botellas.

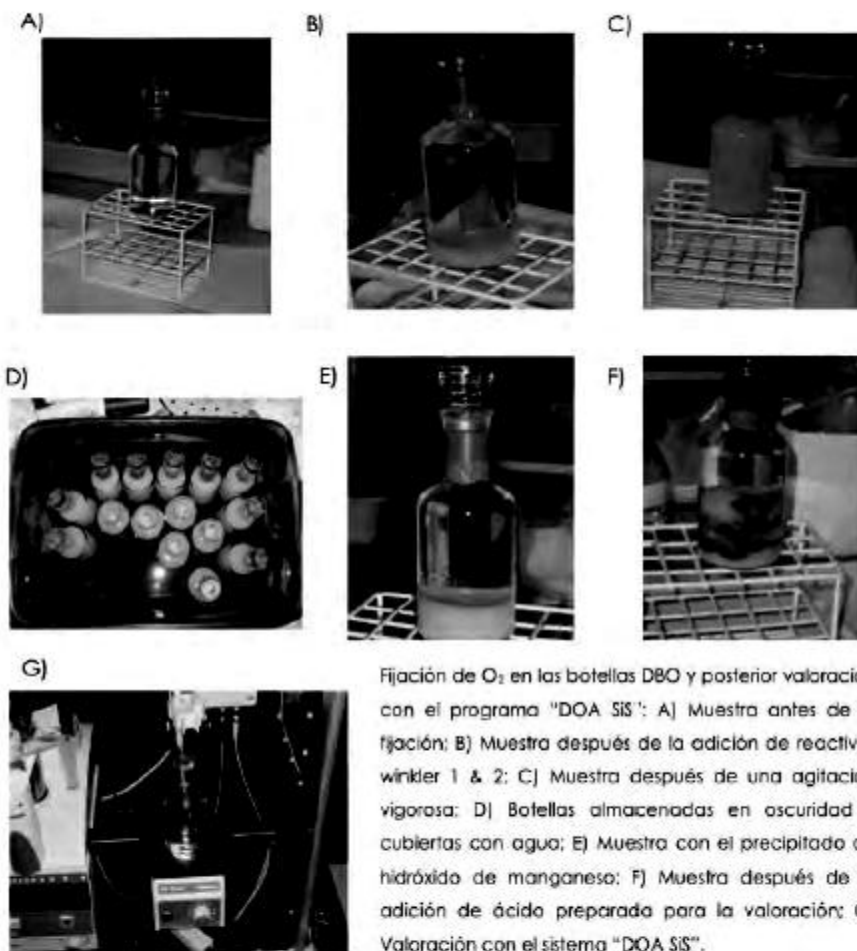
Fijación de O₂

Las muestras (de 4 a 6 replicados por tiempo) se fijan a intervalos establecidos (e. g. 0h, 12h, 24h, 36h, 48h, 72h) tal y como se ha explicado en el apartado 5, añadiendo los reactivos 1 y 2 sucesivamente. Las botellas deben agitarse vigorosamente al menos dos veces, con un intervalo de unos 5 minutos, para que se forme bien el precipitado, y mantenerlas sumergidas en agua hasta su valoración. Para fijar las botellas iniciales (T0) se debe esperar al menos unas 2 h de incubación para que la temperatura dentro de todas las botellas sea exactamente la misma que la del agua del incubador.

Valoración de las muestras

Cuando el precipitado esté sedimentado (aproximadamente entre 8 y 24 horas; ver Figura E), y nunca después de 48h, se deben valorar las muestras. Retirar el tapón de la botella con cuidado de que no entre agua en el interior y añadir 1 ml de H₂SO₄ (inclinando la botella). Insertar la mosca magnética en el fondo de la botella con la varilla, sin provocar burbujas. Colocar la botella sobre el soporte del DOA con el agitador y comenzar la valoración automática con tiosulfato sódico. Al final de la titración, el programa genera una copia de los detalles de la muestra y del proceso de valoración, junto con las estimas de la concentración de oxígeno y porcentajes de saturación.

Cuadro sinóptico de la técnica



Cálculo de los resultados

Debe calcularse el valor medio (en $\mu\text{mol O}_2 \text{ l}^{-1}$), coeficiente de variación y error estándar de cada grupo de replicados de botellas. Como estimación de referencia, la precisión de los replicados debe ser $\text{CV} < 0.5\%$ para poder detectar cambios significativos en la respiración. En cualquier caso, debería de comprobarse que la diferencia entre valores medios (con sus errores estándar) de grupos de replicados son significativas.

Control de calidad y errores experimentales

A pesar de la precisión del método, las tasas respiratorias que se miden en el océano oscuro son tan bajas ($<1 \mu\text{mol O}_2 \text{ l}^{-1} \text{ d}^{-1}$) que conviene tener en cuenta algunos aspectos metodológicos importantes que pueden condicionar la estima correcta de estas tasas.

1. Tanto la detección fotométrica como espectrofotométrica del punto final de la valoración son muy precisas, pero a menudo el método potenciométrico implica retirar una alícuota de la botella sobre la que se inserta el electrodo y se hacen las mediciones. En este proceso se puede perder precisión por dos causas: (i) Pérdida por volatilización de I_3^- en el proceso de manipular la alícuota, y (ii) control menos preciso en el volumen de la alícuota con respecto a la calibración más exacta del volumen total de la botella
2. El volumen de las botellas debe de ser determinado con una precisión de milésima de gramo, ya que la precisión del método depende en gran medida de lo bien calibradas que estén las botellas
3. Es crítico el control de la temperatura durante todo el proceso de incubación. Generalmente los cambios de oxígeno por procesos físicos (e. g. variación de $> 0.5 \text{ }^\circ\text{C}$) son mucho más acusados que los que se producen por el metabolismo microbiano.
4. Es importante controlar que no se produzca ninguna burbuja ni durante la incubación ni tras haber fijado la muestra con los reactivos 1 y 2 y una vez puesto el tapón. Cualquier botella con burbuja (por pequeña que sea) debe ser desechada.
5. Comprobar frecuentemente la molaridad (M) del tiosulfato. Dosificar con mucha precisión ($< 1 \mu\text{L}$) el yodato, con el fin de obtener una buena replicabilidad en las estimas de M.

Referencias

- ARÍSTEGUI, J., C. M. DUARTE, J. M. GASOL, L. ALONSO-SÁEZ L. 2005. «Active mesopelagic prokaryotes support high respiration in the subtropical northeast Atlantic Ocean». *Geophys. Res. Lett.* Vol. 32, L03608, 4 pp.
- CARRIT, D. E., J. H. CARPENTER. 1966. «Comparison and evaluation of currently employed modification of the winkler method for determining dissolved oxygen in sea-water». *J. Mar. Res.* 24: 286-318.
- CARPENTER, J. H. 1965. «The Chesapeake Bay Institute. Technique for the winkler oxygen method». *Limnol. Oceanogr.* 10: 141-143.
- GRASSHOFF, K., M. EHRHARDT, K. KREMLING. 1983. «Methods of Seawater Analysis». Eds Verlag Chemie GmbH. 419 pp.
- KELL, G. S. 1975. «Density, Thermal Expansivity, and Compressibility of Liquid Water from 0° to 150 °C: Correlations and Tables for Atmospheric

- Pressure and Saturation Reviewed and Expressed on 1968 Temperature Scale». *J. Chem. Eng. Data.* 21: 91-105.
- STRICKLAND, J. D. H., T. R. PARSONS. 1968. «Determination of dissolved oxygen in A Practical Handbook of Seawater Analysis». *J. Fish. Res. Board.* 167: 71-75.
- WEAST, R. C. 1973. «Handbook of chemistry and physics». 59th Ed. CRC Press. pp. 1978 -1979.
- WILLIAMS, P. J. LEB., N. W. JENKINSON. 1982. «A transportable microprocessor-controlled precise Winkler titration suitable for field station and siph-board use». *Limnol. Oceanogr.* 27 (3): 2843 -2855.
- WINKLER, L. W. 1888. «Die Bestimmung des in Wasser gelösten Sauerstoffes». *Ber. Dtsch. Chem. Ges.* 21: 2843-2855.

ANNEX V/ANEXO V: artículo en Deep-Sea Research I

Ignacio P. Mazuecos, Javier Arístegui, Evaristo Vázquez-Domínguez, Eva Ortega-Retuerta, Josep M Gasol, Isabel Reche. 2015. Temperature control of microbial respiration and growth efficiency in the mesopelagic zone of the South Atlantic and Indian Oceans. *Deep-Sea Research I*, 95: 131-138.



ELSEVIER

Contents lists available at ScienceDirect

Deep-Sea Research I

journal homepage: www.elsevier.com/locate/dsri

Temperature control of microbial respiration and growth efficiency in the mesopelagic zone of the South Atlantic and Indian Oceans



Ignacio P. Mazuecos^{a,c,*}, Javier Arístegui^b, Evaristo Vázquez-Domínguez^{c,d},
Eva Ortega-Retuerta^c, Josep M. Gasol^c, Isabel Reche^a

^a Departamento de Ecología, Instituto del Agua, Universidad de Granada, Granada, Spain

^b Instituto de Oceanografía y Cambio Global (IOCAG), Universidad de Las Palmas de Gran Canaria, Las Palmas de Gran Canaria, Spain

^c Departament de Biologia Marina i Oceanografia, Institut de Ciències del Mar, CSIC, Barcelona, Catalunya, Spain

^d Instituto Español de Oceanografía (IEO), Centro Oceanográfico de Gijón, Gijón, Spain

ARTICLE INFO

Article history:

Received 18 July 2014

Received in revised form

28 October 2014

Accepted 30 October 2014

Available online 13 November 2014

Keywords:

Mesopelagic zone

Microbial respiration

Prokaryotic growth efficiency

Temperature

Indian Ocean

South Atlantic Ocean

ABSTRACT

We have measured both prokaryotic heterotrophic production (PHP) and respiration (R), then providing direct estimates of prokaryotic growth efficiencies (PGE), in the upper mesopelagic zone (300–600 m) of the South Atlantic and Indian Oceans. Our results show that in situ R ranged 3-fold, from 87 to 238 $\mu\text{mol C m}^{-3} \text{d}^{-1}$. In situ PHP rates were much lower but also more variable than R (ranging from 0.3 to 9.1 $\mu\text{mol C m}^{-3} \text{d}^{-1}$). The derived in situ PGE values were on average $\sim 1.4\%$ (from 0.3% to 3.7%), indicating that most of the organic substrates incorporated by prokaryotes were respired instead of being used for growth. Together with the few previous studies on PGE published before for the Atlantic Ocean and Mediterranean Sea, our findings support the hypothesis that the global mesopelagic zone represents a key remineralization site for export production in the open ocean. We also found a strong correlation between R and PGE with temperature across a gradient ranging from 8.7 to 14.9 °C. The derived Q_{10} value of 3.7 suggests that temperature variability in the mesopelagic zone plays a significant role in the remineralization of organic matter.

© 2014 Elsevier Ltd. All rights reserved.

1. Introduction

Prokaryotes thriving in the mesopelagic zone (200–1000 m depth) are known to play a key role in the mineralization of organic matter transported to the deep ocean (Arístegui et al., 2009; Anderson and Tang, 2010; Giering et al., 2014). Nevertheless, there is still a great lack of information on the regional variability in the percentage of organic matter that is either mineralized as CO_2 (respiration, R) or used by prokaryotes for growth (prokaryotic heterotrophic production; PHP) in the global ocean mesopelagic zone. This metabolic balance is frequently expressed as “prokaryotic growth efficiency” ($\text{PGE} = \text{PHP}/(\text{PHP} + R)$), a term that provides a proxy of the efficiency in the recycling of organic matter by prokaryotes. Direct estimations of R in the dark ocean, by monitoring oxygen changes inside bottles incubated at in situ temperatures,

are cumbersome, due to the low microbial rates and the much lower sensitivity of the R methodology, compared with the tracer technique used for PHP. Thus, few studies have provided simultaneous direct estimates of both dark ocean R and PHP, being most of them carried out in waters from the North Atlantic Ocean (Biddanda and Benner, 1997; Arístegui et al., 2005b; Reinthaler et al., 2006; Baltar et al., 2010).

Despite the lack of data of actual R across the world oceans, it has been estimated that mesopelagic microorganisms mineralize up to 90% of the organic matter exported from the photic zone (Robinson et al., 2010), yielding high R at these depths (del Giorgio and Duarte, 2002). This hypothesis is supported by indirect estimates (mostly derived from enzymatic respiratory activities) of global mesopelagic R , ranging between 0.6 and 1.4 pmol C y^{-1} (Arístegui et al., 2003; Arístegui et al., 2005a), that would contribute 9–12% of the global ocean respiration (del Giorgio and Williams, 2005). Arístegui et al. (2009) compiled a large data set on metabolic activities from the dark ocean and found that the decrease in PHP with depth was higher than the decrease in R inferred from ETS activity, leading to a decreasing trend in PGE as the -0.3 power of depth. Assuming a mean PGE in the epipelagic zone of 15% (del Giorgio and Cole, 2000), the predicted PGE in the deep ocean would thus be $\sim 4\%$. Similarly low PGE (on average $\sim 2\%$) derived from

Abbreviations: MTE, metabolic theory of ecology; PA, prokaryotic abundance; PB, prokaryotic biomass; PGE, prokaryotic growth efficiency; PHP, prokaryotic heterotrophic production; R , respiration rate

* Corresponding author at: Departamento de Ecología, Facultad de Ciencias, Universidad de Granada, Campus Fuentenueva s/n, 18071 Granada, Spain. Tel.: +34 958 241000x20018.

E-mail address: igperez@ugr.es (I.P. Mazuecos).

<http://dx.doi.org/10.1016/j.dsr.2014.10.014>

0967-0637/© 2014 Elsevier Ltd. All rights reserved.

direct R estimates were obtained in the meso- and bathypelagic waters of the central North Atlantic (Reinthal et al., 2006), although higher PGE values have been reported also from the North Atlantic dark ocean (e.g. Arístegui et al., 2005b; Baltar et al., 2010). Nevertheless, in spite of the importance of measuring simultaneously R and PHP for addressing the balance between source and sinks of carbon in the water column, there are still very few PGE estimates using direct R measurements to corroborate the above prediction across the world oceans.

The metabolism of all organisms is affected by many environmental factors, being temperature a key parameter (Brown et al., 2004). In this sense, marine heterotrophic prokaryotes are not an exception (i. e. Pomeroy and Wiebe, 2001; Vázquez-Domínguez et al., 2007; Sarmento et al., 2010) and temperature changes have been reported to have direct implications for the microbial degradation of organic matter in the surface ocean by modifying PGE (Rivkin and Legendre, 2001; López-Urrutia and Morán, 2007; Vázquez-Domínguez et al., 2007; Wohlers et al., 2009; Kritzberg et al., 2010a, 2010b). As it occurs in the surface ocean, temperature variability in the upper mesopelagic zone would affect the activity of marine microorganisms. Depending on the way in which PGE is modified by temperature in the mesopelagic zone the microbial food web could shift the flow of organic carbon by circulating more C through higher trophic levels or by remineralizing the C as CO_2 . Understanding the effects of temperature on PGE and R in the mesopelagic zone would thus help to predict future changes on

carbon biogeochemistry in a warmer dark ocean, a region poorly investigated until now (Nagata et al., 2001; Arístegui et al., 2009).

In this study, we provide direct estimates of both R and PHP, and derived PGE values, from the upper mesopelagic zone of two largely unexplored ocean basins: the South Atlantic and the Indian Oceans. We hypothesized that, as reported from the North-Atlantic Ocean (Arístegui et al., 2005b; Reinthal et al., 2006; Baltar et al., 2010; Giering et al., 2014), the prokaryotic assemblages in the upper mesopelagic of these two oceans represent active nodes of remineralization of organic matter. We also tested the temperature dependence of R and PGE in our in situ data derived from temperature-controlled experiments. Finally, we compiled the existing literature from direct estimates of R and PGE to explore the temperature sensitivity of the dark ocean carbon metabolism.

2. Material and methods

2.1. Study site and sampling

The study was conducted on board the “R/V Hesperides” across the South Atlantic and Indian Oceans (Fig. 1 and Table 1), during part of the Malaspina 2010 Expedition (www.expedicionmalaspina.es) from January to March 2011. A total of 12 stations were sampled crossing the two ocean basins (Fig. 1). Water samples for metabolism experiments, as well as for in situ measurements, were collected at

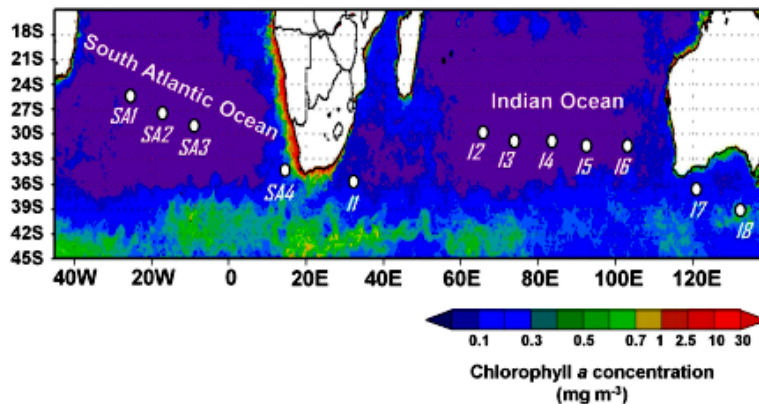


Fig. 1. Location of the stations selected for the respiration experiments (white dots), superimposed to a Moderate Resolution Imaging Spectroradiometer (MODIS) image of chlorophyll *a* averaged for the sampling period (from January to March 2011).

Source: <http://modis.gsfc.nasa.gov/>.

Table 1

Stations' location in the South Atlantic (SA) and Indian (I) Oceans and water mass properties at the sampling depths where time-series experiments were performed. AOU=apparent oxygen utilization.

Stations	Date (d/m/y)	Latitude	Longitude	Depth (m)	Temperature (°C)	Salinity (psu)	O ₂ concentration (μmol kg ⁻¹)	AOU (μmol kg ⁻¹)
SA1	22/01/2011	25.9°S	27.6°W	550	9.8	34.78	185.62	94.15
SA2	24/01/2011	27.0°S	21.4°W	450	11.8	35.02	195.81	70.29
SA3	27/01/2011	28.7°S	11.8°W	585	8.7	34.66	178.83	108.43
SA4	04/02/2011	32.8°S	12.8°E	330	11.4	34.95	201.98	64.97
I1	15/02/2011	34.4°S	31.1°E	430	14.9	35.42	189.63	58.16
I2	25/02/2011	28.0°S	63.3°E	450	12.5	35.15	213.54	46.18
I3	28/02/2011	29.6°S	72.4°E	450	11.7	35.03	214.26	50.65
I4	03/03/2011	29.8°S	82.6°E	450	10.9	34.91	222.47	47.23
I5	06/03/2011	29.6°S	93.0°E	450	10.5	34.83	225.67	46.61
I6	09/03/2011	30.3°S	103.3°E	450	9.5	34.71	220.63	57.63
I7	19/03/2011	36.6°S	120.9°E	470	9.5	34.68	227.93	50.85
I8	24/03/2011	39.2°S	135.1°E	400	9.6	34.71	226.81	52.23

the same depths in the upper mesopelagic zone (from 330 to 585 m, Table 1) using a rosette sampler (provided with 24 12 L-Niskin bottles), implemented with a Conductivity–Temperature–Depth (CTD) instrument (Seabird SBE 9). Before setting up the experiments, water from the Niskin bottle was drawn into a carboy (without any pre-filtration), gently mixed, and left for 2 h inside a temperature-controlled chamber to reach in situ temperature. Following, the water was homogeneously distributed into 28 BOD bottles; 7 for each time sampling interval (0, 24, 48 and 72 h) of the experiment. From these, six bottles were used as replicates for oxygen consumption measurement and one bottle for prokaryotic heterotrophic production.

2.2. Prokaryotic abundance

In situ prokaryotic abundances (PA) were measured by flow cytometry (Gasol and del Giorgio, 2000), using a FACScalibur Becton Dickinson cytometer equipped with a laser emitting at 488 nm. Samples were obtained from the same Niskin bottles where water was collected for experiments. A 1.5 ml aliquot was fixed with 1% of paraformaldehyde+0.05% glutaraldehyde (final concentrations), deep-frozen in liquid nitrogen and stored at -80°C until analysis (less than 1 week after collection). Prokaryotic biomass (PB; mg C m^{-3}) was calculated by transforming relative light side scatter (SSC) to cell diameter, using the linear regression model of Calvo-Díaz and Morán (2006) after staining the samples with SybrGreen I. A spherical shape was assumed to derive cellular volumes, which were later converted to biomass with the allometric equation of Gundersen et al. (2002).

2.3. Prokaryotic heterotrophic production

Samples for prokaryotic heterotrophic production (PHP) were obtained both directly from the Niskin bottles (in situ PHP) and from the BOD bottles used in the time-series experiments at different incubation times (0, 24, 48 and 72 h). PHP was measured by ^3H -leucine (specific activity = $144.2 \text{ Ci mmol}^{-1}$) incorporation into proteins (Kirchman et al., 1985), according to the microcentrifugation protocol proposed by Smith and Azam (1992). Four replicates (1.2 ml) and two trichloroacetic acid (TCA)-killed blanks in microcentrifuge tubes were added to ^3H -leucine at 20 nM. Samples and blanks for experiments and Niskin bottles were incubated (for 2–8 h) at in situ temperature. Incubations were stopped by adding 50% TCA, centrifuged (10 min and 14,000 r.p.m.) and again rinsed with 5% TCA and centrifuged. Scintillation cocktail (1 ml Optisafe HiSafe, PerkinElmer) was added and, after 24 h, the emitted radioactivity was counted on board in a liquid scintillation counter (Wallac-PerkinElmer). Leucine incorporation rates ($\text{pmol Leu l}^{-1} \text{ h}^{-1}$) were converted into carbon by using a theoretical factor of $1.55 \text{ kg C mol Leu}^{-1}$ (Simon and Azam, 1989), assuming that isotope dilution was negligible under this saturating concentration of 20 nM of ^3H -leucine. PHP rates (average coefficient of variation $\sim 4\%$) were integrated during the experiments as the area obtained from time 0 to the final time (Fig. 2), and expressed as daily rates ($\mu\text{mol C m}^{-3} \text{ d}^{-1}$). Prokaryotic biomass turnover times (days) were estimated as PB/PHP for in situ samples.

2.4. Respiration

Water samples for the respiration experiments were homogeneously siphoned into 24 biological oxygen demand (BOD) bottles (nominal volume 125 ml), that were kept in the dark inside temperature-controlled water baths ($\pm 0.1^{\circ}\text{C}$). Six BOD bottles were fixed immediately with Winkler reagents, and left immersed together with the rest of bottles inside the water baths during the dark incubation steps. Other six replicate bottles were fixed at 24, 48

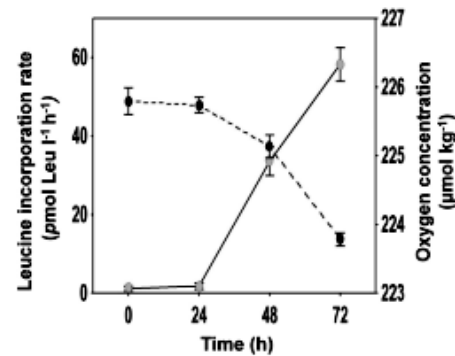


Fig. 2. Representative example of the changes in the leucine incorporation rate ($\text{pmol Leu l}^{-1} \text{ h}^{-1}$, gray dots) and the O_2 concentration ($\mu\text{mol O}_2 \text{ kg}^{-1}$, black dots) along the experiment performed at station 11 located in the Indian Ocean at 430 m depth. Bars represent the standard error of 6 replicates.

and 72 h. Community respiration was measured at each time series interval (0–24, 24–48 and 48–72 h) from changes in O_2 concentration in the bottles. Finally, like with PHP, integrated respiration rates (R) were estimated as the area obtained from t_0 to final time and expressed as daily rates ($\mu\text{mol C m}^{-3} \text{ d}^{-1}$). Dissolved oxygen measurements were carried out by automated microWinkler titrations using a Dissolved Oxygen Analyser (DOA; SiS[®]) with photometric end-point detection (Williams and Jenkinson, 1982). The coefficient of variation of oxygen concentration among replicated bottles was always $< 1\%$. A respiratory quotient of 1 was used to convert oxygen consumption into carbon respiration (del Giorgio et al., 2006). To minimize the potential effect of growing prokaryotes inside the BOD bottles along the incubations, experimental R was back-scaled to in situ conditions using the power fit obtained between experimentally derived PHP and R , knowing in situ PHP (see details Section 3). For this, we assumed that prokaryotic assemblages were responsible for the whole community respiration. In situ specific R rates were obtained as the ratio between in situ R and the prokaryotic biomass (R/PB).

2.5. Influence of temperature on respiration

The dependence of R on temperature was tested using the Metabolic Theory of Ecology (MTE) (Brown et al., 2004), assuming that metabolic processes at community-level or ecosystem level depend on ambient temperature (Sarmiento et al., 2010). This temperature dependence was examined in our in situ back-scaled R values and also compared to all R data available, derived from direct O_2 consumption, found in the literature

$$\ln \text{ metabolic rate } (R) = a - b(1/kT),$$

where k is Boltzmann's constant $8.62 \cdot 10^{-5} \text{ eV K}^{-1}$ and T is the absolute water temperature in K. The negative slope (b) in the Arrhenius plot corresponds to the activation energy (E_a , eV). E_a was further transformed to Q_{10} (the change in metabolic rate for a 10°C temperature increase) using the algorithm proposed by Raven and Geider (1988), $Q_{10} = \text{Exp}(10E_a/RT^2)$, where R is the gas constant ($8.314472 \text{ mol}^{-1} \text{ K}^{-1}$) and T is the mean absolute temperature (K) across the range over which Q_{10} was measured. E_a was converted to J mol^{-1} using the conversion factor of $96,486.9 \text{ J eV}^{-1} \text{ mol}^{-1}$.

2.6. Statistical analyses

Statistical analyses were performed using Statistica 6.0 (StatSoft Inc, 1997). The dataset were log-transformed to fit the assumptions

of normality and homoscedasticity before performing the regression analysis.

3. Results

3.1. Respiration, prokaryotic production and growth efficiency in the experiments

In all the experiments ^3H -leucine incorporation rates increased and O_2 concentrations decreased over time (e.g. Fig. 2). Integrated PHP in the experiments ranged from 1.7 to $96.1 \mu\text{mol C m}^{-3} \text{d}^{-1}$, while R varied from 131 to $467 \mu\text{mol C m}^{-3} \text{d}^{-1}$ (Table 2), being R and PHP strongly correlated ($N=10$, $r^2=0.79$ and $p\text{-value}=0.001$). The calculated PGE values from R and PHP in the experiments were low on average ($\sim 5.9\%$), although variable, ranging from 1.3% to 17.1% (Table 2).

3.2. In situ prokaryotic assemblages and metabolism in the upper mesopelagic environment

In situ prokaryotic abundance (PA) and heterotrophic production (PHP) varied 20-fold (from 0.5 to $11.0 \times 10^5 \text{ cell ml}^{-1}$) and 30-fold (from 0.3 to $9.1 \mu\text{mol C m}^{-3} \text{d}^{-1}$), respectively (Table 3). The highest in situ PA and PHP were found in the western Indian Ocean (stations I1 and I2). However, the highest biomass turnover times were located in the eastern Indian Ocean (stations I6, I7 and I8).

Table 2
Integrated community respiration rate (R) and prokaryotic heterotrophic production (PHP) estimated over the incubation times (Time, h) in the experiments (see Section 2). The prokaryotic growth efficiencies (PGE) derived from both integrated PHP and R are also included. Temp.=Incubation temperature.

Experiment	Time (h)	Temp. ($^{\circ}\text{C}$)	PHP ($\mu\text{mol C m}^{-3} \text{d}^{-1}$)	R ($\mu\text{mol C m}^{-3} \text{d}^{-1}$)	PGE (%)
SA1	72	9.3	24.2	255	8.7
SA2 ^a	72	9.2	16.9	-	-
SA3	72	9.0	17.7	254	6.5
SA4	24	10.2	7.2	203	3.4
I1	72	15.1	96.1	467	17.1
I2	72	12.6	28.0	340	7.6
I3	72	11.7	12.4	349	3.4
I4	72	11.2	15.4	274	5.3
I5	72	10.6	8.2	297	2.7
I6	72	9.6	4.1	145	2.7
I7 ^a	72	8.6	1.7	-	-
I8	72	8.6	1.7	131	1.3

^a R and consequently PGE estimates were not determined in these experiments.

Table 3
Prokaryotic abundance (PA), biomass (PB), heterotrophic production (PHP), turnover time, back-scaled respiration rates (R) and resulting growth efficiencies (PGE) corresponding to the in situ conditions.

Stations	PA ($\times 10^5 \text{ cell ml}^{-1}$)	PB (mg C m^{-3})	PHP ($\mu\text{mol C m}^{-3} \text{d}^{-1}$)	Turnover time (days)	R ($\mu\text{mol C m}^{-3} \text{d}^{-1}$)	PGE (%)
SA1	0.5	0.30	1.0	24	129	0.8
SA2	0.8	0.47	4.4	9	194	2.2
SA3	0.8	0.44	2.8	13	170	1.6
SA4	3.0	1.62	2.8	48	170	1.6
I1	11.0	6.67	9.1	61	238	3.7
I2	6.0	0.92	6.6	11	218	3.0
I3	1.4	0.86	0.9	80	123	0.7
I4	1.7	0.85	0.8	93	118	0.6
I5	1.7	0.88	1.0	70	129	0.8
I6	1.7	0.88	0.3	278	87	0.3
I7	2.3	1.20	0.3	288	94	0.4
I8	3.0	1.50	1.0	125	127	0.8

In situ R was estimated by back-scaling experimental R to in situ PHP, using the power relationship observed between the integrated experimental PHP and R (Fig. 3); where $R=127.24 (\pm 22.52) \times \text{PHP}^{0.283} (\pm 0.053)$ ($N=10$, $r^2=0.78$ and $p\text{-value}=0.0007$). Back-scaled in situ R ranged between 87 and $238 \mu\text{mol C m}^{-3} \text{d}^{-1}$ (Table 3), and represented, on average, about two-fifth, of in vitro experimentally-derived values. However, both in situ and experimental PHP were significantly correlated ($N=12$, slope= 7.65 ± 1.59 , $r^2=0.70$ and $p\text{-value}=0.0007$) and then in situ PHP can be used to scale in situ R . The in situ R in the studied stations showed a similar geographical pattern as the experimental R estimates, with the highest values in the western Indian Ocean (stations I1 and I2).

The estimated in situ PGE values (derived from back-scaled R and in situ PHP) were low in all the study stations, but ranged one order of magnitude, from 0.3% to 3.7% (Table 3), and averaged about 1.4%. The geographic pattern of in situ PGE was similar to PHP and R , being the highest observed PGE values in stations I1 and I2.

3.3. Temperature control on R and PGE

Experimental R was strongly correlated with temperature during the incubations (Fig. 4; $N=10$, $r^2=0.79$ and $p\text{-value}=0.0004$). Fig. 5 plots the Arrhenius trend for all deep ocean data (derived from O_2

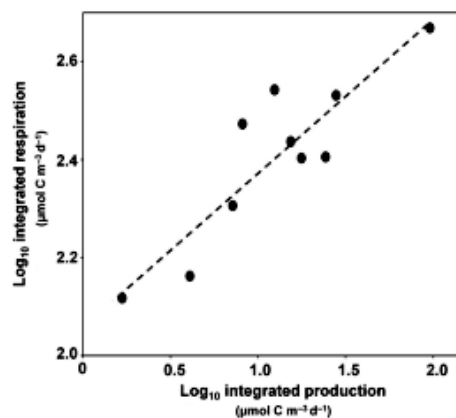


Fig. 3. Relationship between integrated prokaryotic heterotrophic production (PHP) and integrated community respiration (R) in the in vitro experiments. The dashed regression line represents the log-log linear transformation of the fitted power function $R=127.24 (\pm 22.52) \times \text{PHP}^{0.283} (\pm 0.053)$ ($r^2=0.78$ and $p\text{-value}=0.0007$).

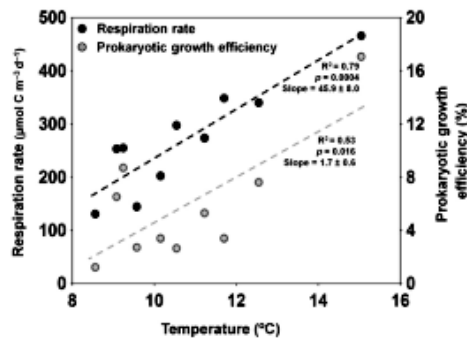


Fig. 4. Relationships between temperature and respiration rates (black dots) and prokaryotic growth efficiencies (gray dots) in the *in vitro* experiments. The dashed regression lines plot significant relationships (p -values < 0.05).

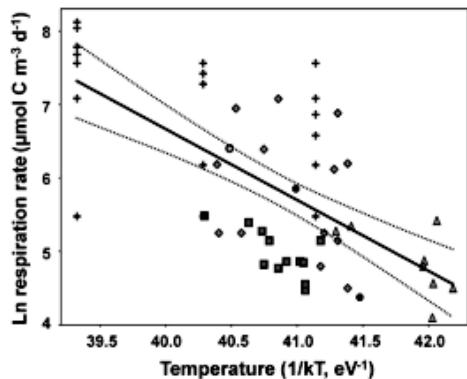


Fig. 5. Arrhenius plot showing the effect of temperature ($1/KT$) on dark ocean R data (derived from O_2 consumption) found in the literature, including also this study data. The black line represents the significant linear relationship (p -value = 0.000001); dashed lines are the 95% confidence interval of the slope. Biddanda and Benner (1997) (crosses), Reinthaler et al. (2006) (triangles), Baltar et al. (2010) (diamonds), Aristegui et al. (2005b) (black circles), Weinbauer et al. (2013) (gray circles) and this study (squares).

consumption in BOD bottles) found in the literature (see also Table 4) showing a significant temperature dependence ($N=57$ and p -value = 0.000001) on R across different marine regions. Table 5 also shows the results of the Arrhenius plots and Q_{10} values corresponding to this study and all data in the literature. The estimated activation energy (E_a) and fitted Q_{10} value for this study ($E_a = 0.90 \pm 0.29$ eV and $Q_{10} = 3.65$) were consistent with the calculated values from the literature ($E_a = 0.98 \pm 0.16$ eV and $Q_{10} = 4.07$). However, the specific rates of the *in situ* R values (R/PB) were not significantly related to temperature (p -value = 0.418).

PGE derived from experimental PHP and R was positive and significantly correlated to temperature ($N=10$, $r^2=0.53$ and p -value = 0.016) (Fig. 4), as well as considering the *in situ* conditions ($N=12$, $r^2=0.58$ and p -value = 0.004). However, including all the data found in the literature, we did not obtain a significant relationship between PGE and temperature (p -value > 0.05 ; Fig. 6).

4. Discussion

Direct determination of R from O_2 consumption during *in vitro* incubations in the dark ocean requires, in most cases, long-term incubations (> 24 h) to detect significant changes in O_2

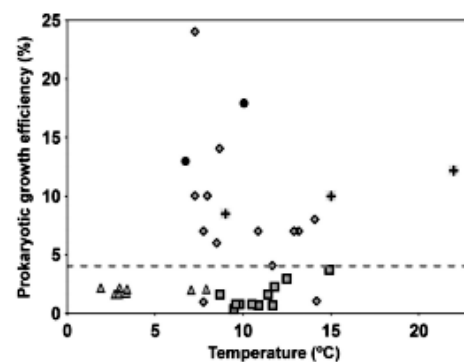


Fig. 6. Scatterplot of prokaryotic growth efficiencies (PGE), derived from direct estimates of R and PHP, as function of temperature for deep ocean prokaryotes found in the literature including this study. The gray dashed line represents $PGE=4\%$. The symbols correspond to Biddanda and Benner (1997) (crosses), Reinthaler et al. (2006) (triangles), Baltar et al. (2010) (diamonds), Aristegui et al. (2005b) (circles) and this study (squares).

concentration. This may lead to the generation of artifacts as consequence of the confinement of microbial populations inside bottles, favoring cell growth after 1–2 days and increasing metabolism. In addition, changes in community structure may also take place during the incubations, shifting the community towards opportunistic populations (Massana et al., 2001). Nevertheless, some studies have shown that, in spite of these changes in community structure during daily incubations, metabolic rates can be maintained constant or directly correlated to the increases in biomass (e.g. Baltar et al., 2012). Despite these drawbacks, some previous studies derived *in situ* R directly from oxygen consumption in *in vitro* incubations (Reinthaler et al., 2006; Baltar et al., 2010). Aristegui et al. (2005b) demonstrated, however, that when long incubations (> 24 h) are necessary to obtain significant changes in oxygen consumption, the back-scaling of the experimental results to the *in situ* conditions is likely the most accurate approach to infer R in the dark ocean. Therefore, experimental R can be back-scaled to *in situ* conditions when a strong relationship between microbial respiration and production (or biomass) is obtained along the experiment, as it happened in this study (Fig. 3).

Few studies have addressed the effect of hydrostatic pressure on prokaryotic metabolism. In spite of the limited information currently available, Tamburini et al. (2013) reviewed these studies, concluding that decompression of deep-water samples underestimates *in situ* activity. This conclusion, however, is based on prokaryotic piezophilic populations from the deep ocean (> 1000 m depth), adapted to live under high pressures, low temperatures and very low organic matter concentrations, a situation far different to the mesopelagic realm with lower hydrostatic pressure and higher organic matter content.

To date, the few available estimates of dark R obtained from oxygen consumption have been mostly determined for the North Atlantic Ocean and the Mediterranean Sea (Biddanda and Benner, 1997; Aristegui et al., 2005b; Reinthaler et al., 2006; Baltar et al., 2010; Weinbauer et al., 2013). Our back-scaled *in situ* values of R (ranging from 87 to 238 $\mu\text{mol C m}^{-3} \text{d}^{-1}$) are comparable to the back-scaled R estimates determined by Aristegui et al. (2005b) in the Canary Current region ($220 \pm 50 \mu\text{mol C m}^{-3} \text{d}^{-1}$). On the other hand, the experimental R values in this study (from 131 to 467 $\mu\text{mol C m}^{-3} \text{d}^{-1}$) are more similar to other studies (Biddanda and Benner, 1997; Reinthaler et al., 2006; Baltar et al., 2010; Weinbauer et al., 2013) where the back-scaling approach was not applied.

The largest data set of respiration in the global dark ocean is, however, based on potential respiratory activity derived from

enzymatic electron transport system (ETS) measurements. A global average R of $10 \mu\text{mol C m}^{-3} \text{d}^{-1}$ was estimated by Aristegui et al. (2003) for the mesopelagic zone assuming a conservative R/ETS ratio of 0.1, characteristic of bacterial populations in senescent state (Christensen et al., 1980). This global rate represents, however, a lower threshold since prokaryotic communities in the mesopelagic zone can be far from being senescent, presenting R/ETS ratios closer to 1 (Aristegui et al., 2005b), typical of bacterial assemblages in exponential growth phase (Christensen et al., 1980). If so the ETS-derived R (using R/ETS of 1) would be in the range of the back-scaled R obtained in this study.

There are also very few studies in the literature reporting PGE in the dark ocean derived from direct measurements of R and PHP (Table 4). In situ PGE in our study were on average $\sim 1.4\%$. These low PGE are in accordance with estimates reported by Reintaler et al. (2006) in the meso- and bathypelagic region of the North Atlantic Ocean ($\sim 2\%$), but without any back-scaling procedure in the direct R estimates. Dumont et al. (2011) found similar low PGE in the South of Tasmania using the equation proposed by del Giorgio and Cole (1998) to predict PGE from PHP. Other studies have estimated the prokaryotic consumption from empirical equations, which had been generated from surface ocean samples (Carlson et al., 2004; Tanaka and Rassoulzadegan, 2004), resulting in higher PGE estimates (5–13% and 19–39%, respectively). Zaccone et al. (2003) and Biddanda and Benner (1997) also found high PGE between 6–11% and 8–12%, respectively. The methodology used in these later reports, however, could have affected the estimation of in situ R . Zaccone et al. used indirect R measurements from ETS activity and Biddanda and Benner only considered 50% of the measured respiration in the experiments to estimate PGE. Baltar et al. (2010) obtained a wide range of PGE (< 1 –24%) from a variety of approaches to estimate PGE from in vitro experiments, similar to our experimental range of PGE (1.7–17.1%). Only Aristegui et al. (2005b) used a similar back-scaling procedure to our study to derive R , although PHP was estimated by averaging leucine and thymidine incorporation rates. These authors obtained higher PGE (13–18%), which they attributed, based also on other molecular and metabolic prokaryotic proxies, to the larger organic

carbon supply from the continental margins, which likely translated into a more efficient use of carbon for growth in the mesopelagic zone. The low in situ PGE in our study confirm the hypothesis that most of the organic matter transported to the mesopelagic zone in open ocean waters is mineralized, ending up as CO_2 ; yet more studies reporting direct R estimates are essential for a better knowledge of the regional variability in prokaryotic carbon use throughout the dark ocean.

We observed a strong correlation between water temperature and in situ R , suggesting a significant temperature dependence on prokaryotic metabolism also in the mesopelagic ocean. There are several studies describing the influence of temperature on R and PGE. Nagata et al. (2001), in the mesopelagic waters of the subarctic Pacific, observed temperature dependence of prokaryotic growth, reporting positive significant linear regressions in the upper part of the mesopelagic zone. Bendtsen et al. (2002), based on a model of the microbial food web, postulated that the gradient of dissolved organic carbon in the deep North Atlantic could be explained by the temperature dependence of bacterial metabolism. Iversen and Ploug (2013) used results obtained in laboratory experiments to hypothesize that the carbon flux into deep waters would be reduced in warmer environments due to increased remineralization rates. Our results and all these studies suggest that prokaryotic metabolism in the dark ocean would be affected by rising temperatures. Nevertheless, the influence would be different depending on whether the temperature affects more growth (new biomass generation), being carbon channeled through higher trophic levels, or respiration, being carbon recycled as CO_2 (e.g. Vázquez-Domínguez et al., 2007). The temperature dependence of mineralization rates does not preclude however that the concentration and quality of organic matter might also affect oxygen consumption rates in the dark ocean. Indeed, Nagata et al. (2001) concluded that organic matter was more important than temperature in determining the growth of heterotrophic prokaryotes in the upper mesopelagic zone of the Subarctic Pacific.

The metabolic theory of ecology (MTE) establishes an increment of the organisms' metabolism with increasing temperatures (Brown et al., 2004), as it has been observed in planktonic

Table 4
Reported prokaryotic growth efficiencies (PGE) in the dark ocean, derived from prokaryotic heterotrophic production (PHP) and direct respiration (R) measurements, indicating the different approaches to estimate PHP and R .

Location	Depth (m)	PHP approach	R approach	PGE (%)	Reference
Subtropical North Atlantic Ocean	350–1000	In situ leucine incorporation and prokaryotic biomass yield in experiments	Difference in O_2 concentration in experiments	< 1 –24	Baltar et al. (2010)
Subtropical North Atlantic Ocean	600–1000	Average of in situ thymidine and leucine incorporation	Difference in O_2 concentration in experiments. Back-scaling to in situ conditions	13–18	Aristegui et al. (2005b)
North Atlantic Ocean	100–4000	In situ leucine incorporation	Difference in O_2 concentration in experiments	~ 2	Reintaler et al. (2006)
Gulf of Mexico	100–500	In situ leucine incorporation	Linear regression between time and O_2 concentration in experiments	8–12	Biddanda and Benner (1997)
South Atlantic Ocean and Indian Ocean	300–600	In situ leucine incorporation	Difference in O_2 concentration in experiments. Back-scaling to in situ conditions	< 1 –17	This study

Table 5
The slopes of the regression (τ activation energy, eV) and the parameters of the Arrhenius plot between \ln of respiration rate (R , $\mu\text{mol C m}^{-3} \text{d}^{-1}$) and inverse of temperature ($1/K$), $\ln(R) = a - b(1/KT)$, for in situ data in this study and all data in the literature (Fig. 5). The Q_{10} temperature coefficients are also shown.

	Temperature range ($^{\circ}\text{C}$)	Rate	Intercept \pm SE	Slope \pm SE	R^2	p-Value	N	Q_{10}
This study	8.7–14.9	R	41.86 ± 11.98	-0.90 ± 0.29	0.49	0.012	12	3.65
Literature	1.9–22.0	R	45.89 ± 6.33	-0.98 ± 0.16	0.42	0.000001	57	4.07

communities of the surface ocean (López-Urrutia and Morán, 2007; Regaudie-de-Gioux and Duarte, 2012). Our results also show a significant in situ R dependence on temperature in the range of 8.7–14.9 °C. This temperature dependence is also obtained considering all R data previously reported from the dark ocean (Table 5). In contrast to the expected increase of cell-based metabolism in a warmer environment, we observe in our study a lack of correlation between temperature and specific R (R/PB). Likely a variable fraction of in situ prokaryotes was metabolically inactive (Gasol et al., 1995) and, consequently, specific R in our study was not a good proxy to detect temperature changes. The R activation energy value estimated in this study (E_a of 0.90 ± 0.29 eV) was higher than those reported by López-Urrutia and Morán (2007) for specific R in the surface ocean ($E_a=0.589$ eV), by Yvon-Durocher et al. (2012) for microbial populations in the global ocean ($E_a=0.57$ eV) or by Aristegui and Montero (1995) for microplankton R derived from ETS activity ($E_a=0.70$ eV). However, Regaudie-de-Gioux and Duarte (2012) reported comparable E_a values for R in the Atlantic Ocean ($E_a=0.92 \pm 0.11$ eV). The Q_{10} values determined in this study (Table 5) were also higher than the Q_{10} range of 1–3 for R reported by Church (2008).

Recent forecasts consider a global warming rate per decade between 0.015 and 0.11 °C in the upper 700 m (Intergovernmental Panel on Climate Change (Rhein et al., 2013)), which could lead to an increase of R of about 4% according to our calculations. Since the global-warming slowdown detected in surface ocean during the 21st century is partially a consequence of the heat transfer to deeper depths (Chen and Tung, 2014), prokaryotic mineralization rates at the mesopelagic zone could be influenced by increasing temperatures in the dark ocean. Therefore, R vs. temperature reported in this study could help to predict future scenarios in the mesopelagic zone.

The positive relationship between PGE and temperature in the experiments (Fig. 4) is not consistent with previous studies that report a decrease of PGE as temperature increases (Rivkin and Legendre, 2001; Kritzberg et al., 2010a, 2010b). Rivkin and Legendre (2001), in a data compilation study, found a negative relationship between these two parameters for a wide range of temperatures (–1.4 to 29 °C). Likewise, Kritzberg et al. (2010a and 2010b) showed a stronger response of respiration to temperature than production, both in an oligotrophic coastal marine system (with a temperature range of 14.4–28 °C) and in Arctic waters (with a temperature range of –0.6 to 5.8 °C). On the contrary, Wohlers et al. (2009) observed in in-door mesocosms' experiments carried out with water from the Baltic Sea, under a gradient of low temperatures (2.5–8.5 °C), that bacterial production was stimulated by temperature increases but community respiration (< 3 μm) remained apparently unaffected; then, BGE increasing with rising temperatures. Reinthaler and Herndl (2005) also found higher PGE during the warmer spring and summer periods than during the cooler winter time in the southern North Sea. Other studies, however, had suggested that R and PHP would respond similarly to temperature changes (López-Urrutia and Morán, 2007; Vázquez-Domínguez et al., 2007), suggesting that differences in the response of PHP and R to environmental factors (and consequently to BGE) would be related to the bioavailability of organic resources (López-Urrutia and Morán, 2007) or, as discussed above, to the co-variation effect between temperature and organic matter.

5. Conclusions

Our study supports previous hypotheses (del Giorgio and Duarte, 2002; Aristegui et al., 2009) formulating that organic matter exported to the deep ocean is mostly respired by prokaryotic communities in the mesopelagic zone, instead of being used for

growth. Moreover, in addition to the effects of organic matter composition and lability on prokaryotic R , our results suggest that the variability of dark ocean respiration is also dependent on temperature gradients. More effort should be dedicated to explore the effects of temperature variations on metabolic processes (growth and respiration) in the dark ocean, in order to understand how the flow of carbon would be affected by the rising temperatures in the deep ocean.

Acknowledgments

We thank our scientific colleagues and C. M. Duarte for the coordination of Malaspina 2010 expedition, as well as the technical staff and crew members on board the BIO Hespérides, for their support in the field sampling during the different legs of the cruise, and particularly A. Gomes and X.A.G. Morán for providing the in situ PHP data. This paper is a contribution to the INGENIO 2010 CONSOLIDER program (CDS2008-00077). IPM was supported by a JAE Pre-doc fellowship, from the Spanish National Research Council (CSIC) and the BBVA Foundation, Spain. IPM, JA and JMG were partly supported by Project HotMix (CTM2011-30010-C02/MAR).

References

- Anderson, T.R., Tang, K.W., 2010. Carbon cycling and POC turnover in the mesopelagic zone of the ocean: insights from a simple model. *Deep Sea Res.* II 57, 1581–1592.
- Aristegui, J., Agustí, S., Duarte, C.M., 2003. Respiration in the dark ocean. *Geophys. Res. Lett.* 30 (2), 1041. <http://dx.doi.org/10.1029/2002GL016227>.
- Aristegui, J., Agustí, S., Middelburg, J.J., Duarte, C.M., 2005a. Respiration in the mesopelagic and bathypelagic zones of the ocean. In: del Giorgio, P.A., et al. (Eds.), *Respiration in Aquatic Ecosystems*, pp. 181–205.
- Aristegui, J., Duarte, C.M., Gasol, J.M., Alonso-Sáez, L., 2005b. Active mesopelagic prokaryotes support high respiration in the subtropical northeast Atlantic Ocean. *Geophys. Res. Lett.* 32, L03608. <http://dx.doi.org/10.1029/2004GL021863>.
- Aristegui, J., Gasol, J.M., Duarte, C.M., Herndl, G.J., 2009. Microbial oceanography of the dark ocean's pelagic realm. *Limnol. Oceanogr.* 54 (5), 1501–1529.
- Aristegui, J., Montero, M.F., 1995. The relationship between community respiration and ETS activity in the ocean. *J. Plankton Res.* 17, 1563–1571.
- Baltar, F., Aristegui, J., Gasol, J.M., Herndl, G.J., 2010. Prokaryotic carbon utilization in the dark ocean: growth efficiency, leucine-to-carbon conversion factors, and their relation. *Aquat. Microb. Ecol.* 60, 227–232. <http://dx.doi.org/10.3354/ame01422>.
- Baltar, F., Lindh, M.V., Parparov, A., Berman, T., Pinhassi, J., 2012. Prokaryotic community structure and respiration during long-term incubations. *Microbiologyopen* 1 (2), 214–224.
- Bendtsen, J., Lundsgaard, C., Middelboe, M., Acher, D., 2002. Influence of bacterial uptake on deep-ocean dissolved organic carbon. *Glob. Biochem. Cycles* 16 (4), 1127.
- Biddanda, B., Benner, R., 1997. Major contribution from mesopelagic plankton to heterotrophic metabolism in the upper ocean. *Deep Sea Res.* I 44 (12), 2069–2085.
- Brown, J.H., Gillooly, J.F., Allen, A.P., Savage, V.M., West, G.B., 2004. Toward a metabolic theory of ecology. *Ecology* 85, 1771–1789.
- Calvo-Díaz, A., Morán, X.A.G., 2006. Seasonal dynamics of picoplankton in shelf waters of the southern Bay of Biscay. *Aquat. Microb. Ecol.* 42, 159.
- Carlson, C.A., Giovannoni, S.J., Hansell, D.A., Goldberg, S.J., Parsons, R., Vergin, K., 2004. Interactions among dissolved organic carbon, microbial processes, and community structure in the mesopelagic zone of the northwestern Sargasso Sea. *Limnol. Oceanogr.* 49, 1073–1083.
- Chen, X., Tung, K.-K., 2014. Varying planetary heat sink led to global-warming slowdown and acceleration. *Science* 345 (6199), 897–903.
- Christensen, J.P., Owens, T.G., Devol, A.H., Packard, T.T., 1980. Respiration and physiological state in marine bacteria. *Mar. Biol.* 55, 267–276.
- Church, M.J., 2008. Resource control of bacterial dynamics in the sea. In: Kirchman, D.L. (Ed.), *Microbial Ecology of the Oceans*, pp. 335–382.
- Dumont, I., Schoemann, V., Jacquet, S.H.M., Masson, F., Becquevort, S., 2011. Bacterial abundance and production in epipelagic and mesopelagic waters in the Subantarctic and Polar Front zones south of Tasmania. *Deep Sea Res.* II 58, 2212–2221.
- del Giorgio, P.A., Cole, J.J., 2000. Bacterial energetics and growth efficiency. In: Kirchman, D.L. (Ed.), *Microbial Ecology of the Oceans*. Wiley, Liss, pp. 289–325.
- del Giorgio, P.A., Cole, J.J., 1998. Bacterial growth efficiency in natural aquatic systems. *Annu. Rev. Ecol. Syst.* 29, 503–541.
- del Giorgio, P.A., Duarte, C.M., 2002. Respiration in the open ocean. *Nature* 420, 379–384.

- del Giorgio, P.A., Pace, M.L., Fischer, D., 2006. Relationship of bacterial growth efficiency to spatial variation in bacterial activity in the Hudson River. *Aquat. Microb. Ecol.* 45, 55–67.
- del Giorgio, P.A., Williams, P.J.B., 2005. Chapter 14: The global significance of respiration in aquatic ecosystems: from single cells to the biosphere. In: *Respiration in Aquatic Ecosystems*. Oxford University Press, New York, NY, pp. 267–303.
- Gasol, J.M., del Giorgio, P.A., 2000. Using flow cytometry for counting natural planktonic bacteria and understanding the structure of planktonic bacterial communities. *Sci. Mar.* 64, 197–224.
- Gasol, J.M., del Giorgio, P.A., Massana, R., Duarte, C.D., 1995. Active versus inactive bacteria: size-dependence in a coastal marine plankton community. *Mar. Ecol. Prog. Ser.* 128, 91–97.
- Giering, S.L., Sanders, R., Lampitt, R.S., Anderson, T.R., Tamburini, C., Boutrif, M., Zubkov, M.V., Marsay, C.M., Henson, S.A., Saw, K., Cook, K., Mayor, D.J., 2014. Reconciliation of the carbon budget in the ocean's twilight zone. *Nature* 507, 480–483.
- Gundersen, K., Heldal, M., Norland, S., Purdie, D.A., Knap, A.H., 2002. Elemental C, N, and P cell content of individual bacteria collected at the Bermuda Atlantic time-series study (BATS) site. *Limnol. Oceanogr.* 47 (5), 1525–1530.
- Iversen, M.H., Ploug, H., 2013. Temperature effects on carbon-specific respiration rate and sinking velocity of diatom aggregates—potential implications for deep ocean export processes. *Biogeosciences* 10, 4073–4085.
- Kirchman, D.L., Kneess, E., Hodson, R.E., 1985. Leucine incorporation and its potential as a measure of protein synthesis by bacteria in natural aquatic systems. *Appl. Environ. Microbiol.* 49, 599–607.
- Kritzberg, E.S., Arrieta, J.M., Duarte, C.M., 2010a. Temperature and phosphorus regulating carbon flux through bacteria in a coastal marine system. *Aquat. Microb. Ecol.* 58, 141–151.
- Kritzberg, E.S., Duarte, C.M., Wassmann, P., 2010b. Changes in Arctic marine bacterial carbon metabolism in response to increasing temperature. *Polar Biol.* 33, 1673–1682.
- López-Urrutia, A., Morán, X.A.G., 2007. Resource limitation of bacterial production distorts the temperature dependence of oceanic carbon cycle. *Ecology* 88 (4), 817–822.
- Massana, R., Pedrós-Alió, C., Casamayor, E.O., Gasol, J.M., 2001. Changes in marine bacterioplankton phylogenetic composition during incubations designed to measure biogeochemically significant parameters. *Limnol. Oceanogr.* 46, 1181–1188.
- Nagata, T., Fukuda, R., Fukuda, H., Koike, I., 2001. Basin-scale geographic patterns of bacterioplankton biomass and production in the Subarctic Pacific, July–September 1997. *J. Oceanogr.* 57, 301–313.
- Pomeroy, L.R., Wiebe, W.J., 2001. Temperature and substrates as interactive limiting factors for marine heterotrophic bacteria. *Aquat. Microb. Ecol.* 23, 187–204.
- Raven, J.A., Geider, R.J., 1988. Temperature and algal growth. *New Phytol.* 110, 441–461.
- Regaudie-de-Gioux, A., Duarte, C.M., 2012. Temperature dependence of planktonic metabolism in the ocean. *Glob. Biogeochem. Cycles* 26, GB1015.
- Rhein, M., Rintoul, S.R., Aoki, S., Campos, E., Chambers, D., Feely, R.A., Gulev, S., Johnson, G.C., Josey, S.A., Kostianoy, A., Mauritzen, C., Roemmich, D., Talley, L.D., Wang, F., 2013. Observations: ocean (Contribution of Working Group I to the Fifth Assessment Report of the Intergovernmental Panel on Climate Change). In: Stocker, T.F., Qin, D., Plattner, G.-K., Tignor, M., Allen, S.K., Boschung, J., Nauels, A., Xia, Y., Bex, V., Midgley, P.M. (Eds.), *Climate Change 2013: The Physical Science Basis*. Cambridge University Press, Cambridge, United Kingdom and New York, NY, USA.
- Reinthal, T., Herndl, G.J., 2005. Seasonal dynamics of bacterial growth efficiencies in relation to phytoplankton in the southern North Sea. *Aquat. Microb. Ecol.* 39, 7–16.
- Reinthal, T., van Aken, H., Veth, C., Aristegui, J., Robinson, C., Williams, P.J.B., Lebaron, P., Herndl, G.J., 2006. Prokaryotic respiration and production in the meso- and bathypelagic realm of the eastern and western North Atlantic basin. *Limnol. Oceanogr.* 51 (3), 1262–1273.
- Rivkin, R.B., Legendre, L., 2001. Biogenic carbon cycling in the upper ocean: effects of microbial respiration. *Science* 291, 2398–2400.
- Robinson, C., Steinberg, D.K., Anderson, T.R., Aristegui, J., Carlson, C.A., Frost, J.R., Ghiglione, J.-F., Hernández-León, S., Jackson, J.A., Koppelman, R., Quéguiner, B., Ragueneau, O., Rassoulzadegan, F., Robison, B.H., Tamburini, C., Tanaka, T., Wishner, K.F., Zhang, J., 2010. Mesopelagic zone ecology and biogeochemistry—a synthesis. *Deep Sea Res. II* 57, 1504–1518.
- Sarmiento, H., Montoya, J.M., Vázquez-Domínguez, E., Vaqué, D., Gasol, J.M., 2010. Warming effects on marine microbial food web processes: how far can we go when it comes to predictions? *Philos. Trans. R. Soc. B* 365, 2137–2149.
- Simon, M., Azam, F., 1989. Protein content and protein synthesis rates of planktonic marine bacteria. *Mar. Ecol. Prog. Ser.* 51, 201–213.
- Smith, D.C., Azam, F., 1992. A simple, economical method for measuring bacterial protein synthesis rates in seawater using ³H-leucine. *Mar. Microb. Food Webs* 6, 107–114.
- StatSoft Inc, 1997. *Statistica for Windows (Computer Program Manual)*. Tulsa, Oklahoma, USA.
- Tamburini, C., Boutrif, M., Gareil, M., Colwell, R.R., Deming, J.W., 2013. Prokaryotic responses to hydrostatic pressure in the ocean—a review. *Environ. Microbiol.* 15 (5), 1262–1274.
- Tanaka, T., Rassoulzadegan, F., 2004. Vertical and seasonal variations of bacterial abundance and production in the mesopelagic layer of the NW Mediterranean Sea: bottom-up and top-down controls. *Deep Sea Res. I* 51, 531–544.
- Vázquez-Domínguez, E., Vaqué, D., Gasol, J.M., 2007. Ocean warming enhances respiration and carbon demand of coastal microbial plankton. *Glob. Change Biol.* 13, 1327–1334.
- Weinbauer, M.G., Liu, J., Motegi, C., Maier, C., Pedrotti, M.L., Dai, M., Gattuso, J.P., 2013. Seasonal variability of microbial respiration and bacterial and archaeal community composition in the upper twilight zone. *Aquat. Microb. Ecol.* 71, 99–115.
- Williams, P.J.B., Jenkinson, N.W., 1982. A transportable microprocessor-controlled precise Winkler titration suitable for field station and siphonboard use. *Limnol. Oceanogr.* 27 (3), 2843–2855.
- Wohlers, J., Engel, A., Zöllner, E., Breithaupt, P., Jurgens, K., Kans-Georg, H., Sommer, U., Riebesell, 2009. Changes in biogenic carbon flow in response to sea surface warming. *Proc. Natl. Acad. Sci. USA* 106, 7067–7072.
- Yvon-Durocher, G., Caffrey, J.M., Cescatti, A., Dossena, M., del Giorgio, P., Gasol, J.M., Montoya, J.M., Pampayan, J., Staehr, P.A., Trimmer, M., Woodward, G., Allen, A.P., 2012. Reconciling the temperature dependence of respiration across timescales and ecosystem types. *Nature* 487, 472–476.
- Zaccaro, R., Monticelli, L.S., Seritti, A., Santinelli, C., Azzaro, M., Boldrin, A., La Ferla, R., Ribera, M.D., 2003. Bacterial processes in the intermediate and deep layers of the Ionian Sea in winter 1999: vertical profiles and their relationship to the different water masses. *J. Geophys. Res.* 108, 8117–8128.

